

University of Alberta

Novel intracellular role of matrix metalloproteinase-2 in cardiac cell injury

by

Mohammad Abdel-Motaal Mohammad Ali

A thesis submitted to the Faculty of Graduate Studies and Research in partial fulfillment
of the requirements for the degree of

Doctor of Philosophy

Department of Pharmacology

©Mohammad Abdel-Motaal Mohammad Ali

Fall 2012

Edmonton, Alberta

Permission is hereby granted to the University of Alberta Libraries to reproduce single copies of this thesis and to lend or sell such copies for private, scholarly or scientific research purposes only. Where the thesis is converted to, or otherwise made available in digital form, the University of Alberta will advise potential users of the thesis of these terms.

The author reserves all other publication and other rights in association with the copyright in the thesis and, except as herein before provided, neither the thesis nor any substantial portion thereof may be printed or otherwise reproduced in any material form whatsoever without the author's prior written permission.

To those who sacrificed their lives for the sake of pure freedom, justice and human dignity.

To our martyrs in Egypt, Tunisia, Libya, Yemen, Syria, Bahrain and every place on earth and to their families' hearts that suffer the pain of separation.

ABSTRACT

Despite originally being described as a secreted protease, matrix metalloproteinase-2 (MMP-2) was recently revealed to have targets within cardiomyocytes. The biological mechanism(s) that describes the intracellular localization of MMP-2 is unknown and is thus the subject of this thesis. Additionally, activation and inhibition of MMP-2 as well as novel intracellular target(s) of it that are involved in cardiomyocyte injury were investigated.

The cytosolic targeting of MMP-2 was examined and it was found that the signal sequence of MMP-2 led to its incomplete targeting to the endoplasmic reticulum for secretion. Moreover, an MMP-2 splice variant which lacks the signal sequence and is enriched in the cytosol was discovered. Thus, intracellular MMP-2 is explained by the expression of a splice variant and by the inefficient targeting of canonical MMP-2 to the secretory pathway.

Intracellular MMP-2 was found to play a pathological role in myocardial ischemia/reperfusion injury by proteolyzing the giant sarcomeric protein, titin. Discrete co-localization between MMP-2 and titin was found at the sarcomeric Z-disc region. Isolated rat hearts subjected to ischemia/reperfusion injury showed cleavage of titin, whereas inhibition of MMP-2 prevented titin proteolysis and improved the contractile function.

To explore whether oxidative stress affects intracellular MMP-2 activity, isolated cardiomyocytes were treated with various concentrations of hydrogen peroxide. Treatment with 200 μ M hydrogen peroxide led to elevated MMP-2 level/activity in cardiomyocyte lysates. Hydrogen peroxide primarily caused necrotic and not apoptotic

cell death, however, pretreatment with selective MMP inhibitors did not protect against necrosis.

In myocardial ischemia/reperfusion injury, MMP-2 or calpain inhibitors were shown to improve the myocardial contractile function. In order to investigate whether calpain inhibitors target intracellular MMP-2, the inhibitory effect of some calpain inhibitors on MMP-2 activity was tested. The IC_{50} values of calpain inhibitors, PD-150606 and ALLN, against MMP-2 were determined to be 9.3 and 21.9 μM , respectively, revealing that some calpain inhibitors have significant pharmacological activity as inhibitors of MMP-2.

In summary, these studies describe a set of mechanisms that cells utilize to equilibrate MMP-2 in both extracellular and intracellular locations. These results suggest that MMP-2 inhibitors should be rigorously tested as a therapeutic strategy to alleviate myocardial ischemia/reperfusion injury.

ACKNOWLEDGMENTS

I would like to thank my supervisor, Dr. Richard Schulz without whom this work would not have been a reality. I want to express my gratitude to him for inspiration, patience and positive mentoring during this period of my research. I am extremely thankful and grateful for this mentorship.

My next appreciation goes to my supervisory committee members, Dr. Thomas Simmen for teaching me molecular biology techniques and giving me an example of how to be a good scientist. Thanks to Dr. Alexander Clanachan and Dr. Simonetta Sipione for their kindness, guidance, support, and valuable suggestions.

My gratitude also goes to all members in Dr. Schulz's lab for their help during this study and Dr. Granzier's lab for helping in titin studies. I would like to thank Dawne Colwell for help in illustrations and Alberta Heritage Foundation for Medical Research for funding.

I am thankful to my parents, Mr. Abdel-Motaal and Mrs. Ekhlas, and my siblings for their ongoing prayers, support and encouragement. I thank all my friends who stood behind me in times of hardship. My thanks are to my beloved wife, Omnia, for being by my side and to my kids Nadine and Kareem. Finally, all the praises and thanks are to Allah, the Lord of all that exists.

TABLE OF CONTENTS

CHAPTER 1

Introduction

1.1: Matrix metalloproteinases	2
1.1.1: Classification	2
1.1.2: Structure	3
1.2: Regulation of MMPs activity	4
1.2.1: Transcriptional regulation	5
1.2.2: RNA alternative splicing	5
1.2.3: Post-transcriptional regulation	6
1.2.4: Post-translational regulation	7
1.2.5: Compartmentalization	9
1.2.6: Tissue inhibitors of metalloproteinases (TIMPs)	10
1.3: MMPs in cardiac physiology	12
1.4: MMPs involvement in cardiac pathology	13
1.4.1: The role of MMPs in ischemia-reperfusion injury	13
1.4.2: The role of MMPs in inflammatory heart diseases	16
1.4.3: The possible role of MMPs in cardiac cell death	17
1.5: Intracellular localization of MMP-2 in cardiomyocytes	19
1.5.1: Localization of MMP-2 to the sarcomere	19
1.5.2: Localization of MMP-2 to the cytoskeleton	20
1.5.3: Localization of MMP-2 to the nucleus	21
1.5.4: Localization of MMP-2 to mitochondria	22
1.6: Reactive oxygen species: cellular generation and hormone-like action	22
1.7: Overall Hypothesis	25
1.8: Thesis objectives	25
1.8.1: Mechanism of cytosolic targeting of matrix metalloproteinase-2 (Chapter 2)	25
1.8.2: Hydrogen peroxide-induced necrotic cell death in cardiomyocytes is independent of matrix metalloproteinase-2 (Chapter 3)	26

1.8.3:	Calpain inhibitors exhibit MMP-2 inhibitory activity (Chapter 4)	26
1.8.4:	Titin is a target of matrix metalloproteinase-2: Implications in ischemia/reperfusion injury (Chapter 5)	26
1.9:	Conclusions	27
1.10:	References	36

CHAPTER 2

Mechanisms of cytosolic targeting of matrix metalloproteinase-2

2.1:	Introduction	57
2.2:	Materials and methods	58
2.2.1:	Quantitative RT-PCR	58
2.2.2:	Construction of expression vectors harbouring different MMP-2 variants or mutants	60
2.2.3:	Cell culture, transfection and subcellular fractionation...	61
2.2.4:	MG-132 or bafilomycin A1 treatment	62
2.2.5:	Protein assay	63
2.2.6:	Immunocytochemistry and confocal microscopy	63
2.2.7:	Western blotting	63
2.2.8:	Neonatal rat cardiomyocytes	64
2.2.9:	Lentiviral vector production and transduction of cardiomyocytes	65
2.2.10:	Hypoxia-reoxygenation protocol	66
2.2.11:	Statistical analysis	66
2.3:	Results	67
2.3.1:	Presence of MMP-2 in the cytosol and distribution MMP-2 splicing variants	67
2.3.2:	Strength of the MMP-2 signal sequence	69
2.3.3:	MMP-2 targeting determines troponin I cleavage in neonatal cardiomyocytes	71
2.4:	Discussion	73
2.5:	References	109

CHAPTER 3

Hydrogen peroxide-induced necrotic cell death in cardiomyocytes is independent of matrix metalloproteinase-2

3.1:	Introduction	115
3.2:	Materials and methods	117
3.2.1:	Neonatal rat cardiomyocytes culture	117
3.2.2:	Hydrogen peroxide and MMP inhibitor treatments	118
3.2.3:	Lactate dehydrogenase leakage assay	118
3.2.4:	Western blotting	118
3.2.5:	Gelatin zymography	119
3.2.6:	Caspase-3 activity assay	120
3.2.7:	Statistical analysis	120
3.3:	Results	120
3.3.1:	Hydrogen peroxide treatment increases MMP-2 level and activity in neonatal cardiomyocytes	120
3.3.2:	Hydrogen peroxide induces necrotic but not apoptotic cell death in neonatal cardiomyocytes	121
3.3.3:	MMP inhibitors do not prevent increased MMP-2 level induced by hydrogen peroxide	122
3.3.4:	MMP inhibitors do not prevent hydrogen peroxide-induced necrotic cell death	122
3.4:	Discussion	122
3.5:	References	134

CHAPTER 4

Calpain inhibitors exhibit matrix metalloproteinase-2 inhibitory activity

4.1:	Introduction	141
4.2:	Materials and methods	143
4.2.1:	Gelatin zymography	143
4.2.2:	TnI degradation assay	144
4.2.3:	OmniMMP kinetic assay	145
4.3:	Results	145

4.3.1:	Calpain inhibitors, but not ONO-4817, inhibit calpain-1-induced TnI cleavage	145
4.3.2:	Calpain inhibitors decrease the gelatinolytic activity of MMP-2	146
4.3.3:	Inhibition of MMP-2 catalytic activity by calpain inhibitors	146
4.3.4:	Determination of IC ₅₀ of calpain and MMP inhibitors on MMP-2 activity using OmniMMP assay	147
4.4:	Discussion	147
4.5:	References	160

CHAPTER 5

Titin is a target of matrix metalloproteinase-2: implications in myocardial ischemia/reperfusion injury

5.1:	Introduction	167
5.2:	Materials and methods	169
5.2.1:	Titin isolation and purification	169
5.2.2:	Skinned cardiomyocyte isolation	169
5.2.3:	In silico analysis	170
5.2.4:	Cleavage of native titin in skinned cardiomyocytes	171
5.2.5:	In vitro degradation of titin	171
5.2.6:	Isolated working rat heart- ex vivo model of I/R	172
5.2.7:	In vivo model of I/R	173
5.2.8:	Analysis of titin by gel electrophoresis	173
5.2.9:	Immunohistochemistry and confocal microscopy	174
	5.2.9.1: Co-localization of titin and MMP-2	174
	5.2.9.2: Titin 9D10 immunostaining	175
	5.2.9.3: Three dimensional surface rendered image construction	176
5.2.10:	Overlay assay to determine MMP-2 binding to titin	176
5.2.11:	Statistical analysis	177
5.3:	Results	178
5.3.1:	Co-localization of MMP-2 and titin near the Z disc region of the cardiac sarcomere	178
5.3.2:	MMP-2 binds and cleaves titin in a concentration-dependent manner	178
5.3.3:	Effect of ONO-4817 on functional recovery of I/R hearts	179

5.3.4: Myocardial I/R causes titin cleavage, an effect diminished by an MMP inhibitor	180
5.3.5: Titin degradation is reduced in hearts from MMP-2 knockout mice subjected to I/R injury in vivo	180
5.3.6: MMP-2 localizes near the Z-disc region of titin in the human heart	181
5.4: Discussion	181
5.5: References	206

CHAPTER 6

Conclusions

6.1: Conclusions	216
6.2: Limitations	221
6.3: Future directions	225
6.4: Final words	227
6.5: References	230

APPENDIX

A.1: Introduction	234
A.2: Methods	234
A.2.1: In vitro cleavage assays	234
A.2.2: Cytochrome c release	235
A.3: Results	235
A.3.1: MMP-2 cleaves full length Bid into a 15 kD fragment	235
A.3.2: MMP-2-cleaved Bid induces cytochrome c release from isolated mitochondria.	236
A.4: Discussion	236
A.5: References	237

LIST OF TABLES

Table 2.1:	The PCR primers used for the indicated chimeras	106
Table 2.2:	Primary antibodies used in the study	107
Table 2.3:	Comparison of signal sequences	108

LIST OF FIGURES

Figure 1.1:	MMP domain structure	28
Figure 1.2:	Post-translational modification of MMP-2	30
Figure 1.3:	Schematic showing the sequence of pathophysiological events in myocardial I/R injury	32
Figure 1.4:	Intracellular targets of MMP-2 in the cardiac sarcomere	34
Figure 2.1:	Schematic diagram of chimeric proteins used in the study	78
Figure 2.2:	Subcellular distribution of endogenous MMP-2 in HEK 293 cells.	80
Figure 2.3:	Canonical and splice variant MMP-2.	82
Figure 2.4:	Titration of expression levels of HA-tagged canonical MMP-2	84
Figure 2.5:	Effect of proteasomal inhibition (using MG132) or lysosomal inhibition (using bafilomycin A1) on the level of canonical and splice variant MMP-2 in HEK 293 cells	86
Figure 2.6:	Proteolysis of splice variant MMP-2 by proteinase K	88
Figure 2.7:	Assaying secreted vs. intracellular MMP-2	90
Figure 2.8:	Comparison of signal sequence efficiencies of MMP-2 chimeras	92
Figure 2.9:	MMP-2 signal sequence reduces targeting of BiP to the endoplasmic reticulum	94
Figure 2.10:	ER localization of MMP-2 chimeras	96
Figure 2.11:	Differential distributions of MMP-2 chimeras in cardiomyocytes	98
Figure 2.12:	Relative expression levels of endogenous MMP-2 to expressed canonical or splice variant MMP-2 in cardiomyocytes	100
Figure 2.13:	Splice variant MMP-2 increases intracellular substrate cleavage during cell stress	102
Figure 2.14:	Troponin I (TnI) cleavage is reduced by either pharmacologic or biologic inhibition of MMP-2	104

Figure 3.1:	Hydrogen peroxide increases MMP-2 protein level and activity in neonatal cardiomyocytes	126
Figure 3.2:	Hydrogen peroxide induces necrotic but not apoptotic cell death in neonatal cardiomyocytes	128
Figure 3.3:	Effect of MMP inhibitors on hydrogen peroxide-induced MMP-2 elevation.	130
Figure 3.4:	MMP inhibitors do not protect against hydrogen peroxide-induced necrosis in cardiomyocytes	132
Figure 4.1:	Chemical structures of the calpain inhibitors in comparison with the selective MMP inhibitor ONO-4817	150
Figure 4.2:	Calpain inhibitors, but not the selective MMP inhibitor ONO-4817, inhibit calpain-1 activity	152
Figure 4.3:	Calpain inhibitors inhibit MMP-2 gelatinolytic activity	154
Figure 4.4:	Some calpain inhibitors exhibit MMP-2 inhibitory activity as assessed by TnI degradation assay	156
Figure 4.5:	Concentration-dependent inhibitory effects of calpain inhibitors and a selective MMP inhibitor (ONO-4817) on MMP-2 activity as measured by fluorogenic substrate (OmniMMP) kinetic assay	158
Figure 5.1:	Schematic representation of titin	186
Figure 5.2:	Co-localization of MMP-2 and titin at the Z disc region	188
Figure 5.3:	Possible MMP-2 cleavage sites within mouse and human N2B titin	190
Figure 5.4:	MMP-2 binds titin in vitro	192
Figure 5.5:	In vitro degradation (60 min, 37°C) of rabbit longissimus dorsi titin by MMP-2	194
Figure 5.6:	In vitro incubation (60 min, 37°C) of skinned cardiomyocytes with MMP-2	196
Figure 5.7:	Mechanical recovery of isolated perfused working rat hearts subjected to 25 min global, no-flow ischemia followed by 60 min reperfusion	198
Figure 5.8:	Titin degradation in ischemic-reperfused rat hearts	200

Figure 5.9:	Titin degradation in MMP-2 knockout and wild type mouse hearts subjected to I/R in vivo	202
Figure 5.10:	Co-localization of MMP-2 and titin near the Z-disc in diseased human heart	204
Figure 6.1:	Cytosolic targeting and post-translational modifications of MMP-2 in the cardiac myocyte	228
Figure A.1:	In vitro cleavage of Bid by MMP-2	239
Figure A.2:	MMP inhibitors prevent Bid cleavage by MMP-2	241
Figure A.3:	MMP-2-cleaved Bid induces cytochrome c release from isolated mitochondria preparation	243

LIST OF NON-STANDARD ABBREVIATIONS

AP-1	activated protein-1
BCS	bovine calf serum
BH	Bcl-2 homology
Cav-1	caveolin-1
eGFP	enhanced green fluorescence protein
ER	endoplasmic reticulum
GSK-3 β	glycogen synthase kinase-3 β
HA	hemagglutinin
IL-1 β	interleukin-1 β
I/R	ischemia/reperfusion
MHC	myosin heavy chain
MLC-1	myosin light chain-1
MMP	matrix metalloproteinase
MT-MMP	membrane type-matrix metalloproteinase
ONOO ⁻	peroxynitrite
PEVK domain	proline-glutamate-valine-lysine domain
shRNAmir	micro-RNA adapted short-hairpin RNA
TIMP	tissue inhibitor of metalloproteinase
TNF- α	tumor necrosis factor- α
TnI	troponin I

CHAPTER 1

INTRODUCTION

Portions of this chapter have been published in the following reviews:

Ali MA, Schulz R. (2009): Activation of MMP-2 as a key event in oxidative stress injury to the heart. *Front Biosci.* 1:699-716

Kandasamy A, Chow AK, Ali MA, Schulz R. (2009): Matrix metalloproteinase-2 and myocardial oxidative stress injury: beyond the matrix. *Cardiovasc Res.* 85: 413-423.

1.1: Matrix metalloproteinases

Matrix metalloproteinases (MMPs) are a family of zinc-dependent neutral endopeptidases that are collectively capable of degrading the components of the extracellular matrix. It was recognized, from their first description in amphibian metamorphosis ¹, that they play an active role in remodeling the extracellular matrix accompanying both physiological and pathological processes, such as embryogenesis, wound healing, uterine involution, bone resorption, metastasis, arthritis, and heart failure. Although most research has focused on the extracellular role of MMPs over long term remodeling processes, it has more recently been recognized that MMPs may also act on non-extracellular matrix substrates both outside ² and inside the cell ^{3,4}, and on time scale of seconds to minutes and not hours-days which occurs in so many of the extracellular matrix actions of MMPs.

1.1.1: Classification

MMPs belong to a family of structurally related enzymes. In humans there are 24 MMP genes but only 23 MMP proteins because MMP-23 is coded by two identical genes ⁵. The MMPs can be subgrouped, based on their primary structure, substrate specificity and subcellular localization into five classes: collagenases (MMP-1, MMP-8, and MMP-13), gelatinases (MMP-2 and MMP-9), stromelysins (MMP-3, MMP-10, MMP-11, and MMP-12), matrilysins (MMP-7, MMP-26) and membrane type (MT)-MMPs (MT1-MMP, MT2-MMP, MT3-MMP, MT4-MMP, MT5-MMP, and MT6-MMP) ⁶. This original classification of MMPs was made only from the perspective of their action on extracellular matrix proteins. It is, however, becoming increasingly apparent that this classification scheme is imperfect, particularly as previously classified MMPs have been shown to proteolyze other substrates in addition to the ones for which

they were originally named. Moreover, the addition of matrix to metalloproteinase is contested by the findings that these enzymes contribute also to various non-matrix substrates processing including cytokines, chemokines and hormones ⁷.

1.1.2: Structure

In general most secreted proteins including MMPs are encoded with a short removable N-terminal motif called the 'signal sequence' that targets them for export out of the cell (Figure 1.1). It was shown that signal sequences are recognized by dedicated factors that catalyze the transport of newly synthesized secretory proteins into the endoplasmic reticulum (ER) lumen for subsequent secretion. The key molecules in this pathway in eukaryotic cells include a cytosolic targeting factor called the signal recognition particle, the ER membrane-bound receptor for the signal recognition particle, an integral ER membrane protein conducting channel called the Sec61p complex and a membrane-bound peptidase that removes signal sequences from secretory proteins on the luminal face of the ER ⁸.

Originally, it was predicted that all signal sequences would share a distinctive sequence motif. However, the absence of any consensus quickly became apparent when several secretory proteins were sequenced. An early comparative sequence analysis showed that signal sequences have a typical chain length of 20-30 amino acid residues and a recognizable three-domain structure (a basic domain, a hydrophobic domain and a slightly polar domain), but otherwise lack any significant homology ⁹. Although signal sequences vary widely in primary structure, they all share certain features such as hydrophobicity which allows for efficient targeting to the ER ¹⁰. Recent evidence, however, suggest that variations amongst signal sequences have various functional consequences including altered secretion efficiencies and subcellular localizations of certain proteins (e.g. calreticulin ¹⁰, prion ¹¹ and apolipoprotein E ¹²) and there is growing

appreciation that such signal sequence diversity may be biologically meaningful (for review see ¹³). A seminal study by Levine et al ¹⁴ provided proof-of concept that a signal sequence-containing protein can reside and function in the cytosol as a consequence of inefficient translocation into the ER.

Next to MMP signal sequence is a hydrophobic propeptide domain which shields the neighboring zinc-containing catalytic domain. The catalytic domain contains a highly conserved zinc-binding site and consists of five stranded beta sheets and three alpha helices. This fold forms the substrate binding pocket, coordinates with the catalytic zinc ion, and also binds two calcium ions ¹⁵. In its zymogen form, the catalytic zinc is coordinated to a cysteinyl thiol group on the propeptide domain and is rendered inactive. Finally, at the C-terminus there is a haemopexin-like domain that is linked to the catalytic domain by a hinge region. In addition, MMP-2 and MMP-9 contain fibronectin type II inserts within the catalytic domain, and MT-MMPs (MT-1, MT-2, MT-3, and MT-5 MMP) contain a transmembrane domain at the C-terminal end of the haemopexin-like domain, whereas MT-4 and MT-6 MMP are bound to the membrane via glycosylphosphatidylinositol moiety. The haemopexin domain is absent in the matrilysins (MMP-7, MMP-26) ⁴.

1.2: Regulation of MMPs activity

In general, MMPs are tightly regulated via many mechanisms at every step of their induction to their ultimate inhibition and clearance ¹⁶. These several levels at which MMPs are regulated include transcriptional, post-transcriptional, and post-translational levels. In addition, MMPs are controlled via their endogenous inhibitors, tissue inhibitors of metalloproteinases (TIMPs), and their intra/extra-cellular localization.

1.2.1: Transcriptional regulation

MMPs are closely regulated at the level of transcription. In contrast to original observations that MMP-2 may be a “constitutive” enzyme, MMP-2 was also found to be regulated at the transcriptional level and its expression can be upregulated in cardiac cells in response to many factors including hypoxia, angiotensin II, endothelin-1 or interleukin-1beta^{17, 18}. Generally, MMP gene expression is regulated through the interaction of transcription factors, co-activators and co-repressor proteins with specific elements in the promoter region of MMP genes¹⁹. Transcriptional activation can be stimulated by a variety of inflammatory cytokines, hormones, and growth factors, such as interleukin-1beta, interleukin-6, tumor necrosis factor-alpha, epidermal growth factor, platelet-derived growth factor, basic fibroblast growth factor and angiotensin II²⁰⁻²⁴. Prolonged hypoxia, greater than 24 h, has been shown to increase MMP-2 expression whereas shorter durations decrease its expression. However, re-oxygenation, after short periods of hypoxia, upregulates MMP-2 and MT1-MMP expression²⁵. Bergman *et al.*¹⁷ demonstrated that MMP-2 transcription in hypoxic cardiomyocytes and fibroblasts is driven by the functional activating protein-1 (AP-1) components FosB and JunB. The same group further revealed that the AP-1-binding site on the intrinsic genomic MMP-2 promoter was specifically occupied by FosB and JunB and that ischemia-reperfusion injury increased the occupancy of the AP-1 site¹⁸.

1.2.2: RNA alternative splicing

RNA splicing or the removal of introns from pre-mRNAs resulting in mature mRNA, is an essential step in eukaryotic gene expression. The enzyme complex responsible for this process is the spliceosome, which carries out both the excision of introns and exons ligation. The spliceosome is an extraordinarily complex, 2000–3000

kD machine composed of five small nuclear RNAs and a set of ~100 proteins ²⁶. RNA splicing occurs in a multi-step complex pathway. In brief, the small nuclear RNAs and a subset of associated proteins form stable particles called small nuclear ribonucleoproteins that constitute the largest building blocks of the spliceosome. Aided by a plethora of more loosely associated proteins called splicing factors, the small nuclear ribonucleoproteins interact with pre-mRNA to complete a round of splicing via a dynamic process which includes intron excision, exon ligation, spliced product (mature mRNA) release and finally dissociation of the spliceosome.

Alternative splicing is a process by which the exons of the pre-mRNA can be reconnected in multiple ways during RNA splicing. The resulting different mature mRNA transcripts are translated into different protein isoforms, thus, a single gene may code for multiple protein isoforms with different activity, tissue distributions or subcellular localizations ²⁷. Different transcript variants have been reported in the MMP family including MMP-13 ²⁸, MMP-16 ²⁹, MMP-24 ³⁰ and MMP-28 ³¹. Interestingly, Hu et al identified a splice variant of MMP-8 lacking a secretory signal sequence and thus is not targeted to the secretory pathway ³².

1.2.3: Post-transcriptional regulation

Regulation of MMPs can also occur at posttranscriptional level in which mRNA transcripts are stabilized and/or destabilized by various exogenous and endogenous factors. For example, mRNA transcripts that encode MMP-1 and MMP-3 in fibroblasts are stabilized by phorbol esters and epidermal growth factor, whereas in osteoblasts MMP-13 transcripts are stabilized by platelet derived growth factor and glucocorticoids and destabilized by transforming growth factor-beta ^{33, 34}. In rats, it was found that

androgen ablation by castration increased the steady-state mRNA levels of MMP-2 and MMP-9 in the prostate³⁵. In addition, a soluble and proteolytically active form of MT3-MMP is generated by alternative mRNA splicing rather than membrane shedding³⁶. Different transcript variants have been reported in the MMP family including MMP-8³², MMP-13²⁸, MMP-24³⁰ and MMP-28³¹.

1.2.4: Post-translational regulation

Since MMPs are initially synthesized with the propeptide domain shielding the catalytic domain, they must be activated to expose the catalytic zinc ion. The most commonly recognized mechanism of MMPs activation involves post-translational proteolytic removal of the propeptide domain, which can be achieved by a range of endogenous proteases³⁷. However, several studies have indicated that MMPs could also be regulated via nonproteolytic modulation of the full length zymogen form including S-glutathiolation³⁸, S-nitrosylation³⁹, and phosphorylation⁴⁰.

Proteolytic activation of MMPs can occur extracellularly, pericellularly, and intracellularly. In the extracellular activation process, another protease (such as plasmin, trypsin, elastase, or one of the MMPs) cleaves at a susceptible loop region in the propeptide domain. Upon cleavage, the prodomain's shielding of the catalytic cleft is withdrawn. Alternatively, MMP-2 is activated at the cell surface through a unique multi-step pathway involving MT1-MMP and TIMP-2⁴¹. MMP-11 and MT-MMPs can also be activated intracellularly by furin-like proprotein convertases^{42, 43}. After intracellular activation, the active MMP is transported to the cell membrane for insertion or secretion. In this regard, it is worth noting that the intracellular activation of these MMPs does not result in their intracellular proteolytic activity, in contrast to MMP-2 as will be discussed later in this chapter.

In addition to proteolytic activation mechanisms, activation of MMPs can also occur by non-proteolytic pathways. It was demonstrated that MMP-1, -8 and -9 can be activated by the pro-oxidant species peroxynitrite (ONOO^-) without requiring the removal of the inhibitory propeptide domain^{38,44}. In the presence of cellular glutathione, low concentrations of ONOO^- (1 to 10 μM) cause the S-glutathiolation of the cysteine containing the PRCGVDP sequence within the propeptide domain which then results in an increase in proteolytic activity³⁸. As all members of the MMP family contain this highly conserved sequence in their propeptide domain, it is likely that S-glutathiolation may play a role in the regulation of the activities of other MMPs in the presence of ONOO^- . Glutathiolation is an increasingly recognized mechanism of post-translational control of protein activity^{45,46}. Higher concentrations of ONOO^- (> 100 μM) have, in contrast, been shown to inactivate MMPs⁴⁷, possibly via the nitration of tyrosine residues⁴⁸. Likewise, it was shown that full length human recombinant MMP-2 (72 kD) is activated by low levels of ONOO^- (0.3-10 μM , peak at approximately 1 μM) but concentrations in excess of 100 μM inactivate it⁴⁹. This suggests, therefore, that commonly used nomenclature which labels an MMP as being an inactive “proMMP” only by virtue of its higher molecular weight in SDS-PAGE is inaccurate and misleading. Such nomenclature does not take into account the potential for the higher molecular weight form of MMPs to be enzymatically active during conditions of oxidative stress, a condition common to several cardiovascular pathologies and perhaps even occurring under physiological levels of reactive oxygen species which are increasingly being appreciated as important in cell signalling⁵⁰.

Another post-translational modification which may play a significant role in the regulation of MMP activity is phosphorylation. MMP-2, expressed in human cells, is phosphorylated on S32, S160, S365, T250, and Y271. Phosphorylation of MMP-2 greatly

reduces its enzymatic activity⁴⁰. *In silico* analysis of the MMP-2 protein sequence shows that several kinases, including protein kinase A, protein kinase C, and glycogen synthase kinase-3 are potentially able to phosphorylate MMP-2 and consequently modulate its activity. The protein kinases and phosphatases responsible for changing MMP-2 phosphorylation status *in vivo* are yet to be discovered. Likewise, MT1-MMP is phosphorylated in human fibrosarcoma cells and this modification is associated with enhanced cell migration and invasion^{51, 52}. Although the role of phosphorylated MMP-2 in the heart is not yet known, these data underscore the notion that MMPs (and MMP-2 in particular) can act as intracellular proteases regulated by various post-translational modifications³. Figure 1.2 depicts some of the possible proteolytic and non-proteolytic post-translational modifications of MMP-2 as described above.

1.2.5: Compartmentalization

An important concept in MMPs regulation is their intra/extra-cellular localization. The canonical view is that MMPs are secreted and/or anchored to the cell membrane, thereby targeting their catalytic activity to specific substrates within the extracellular/pericellular space. Specific cell-MMP interactions have been reported in recent years, such as the binding of MMP-2 to the integrin $\alpha\beta3$ ⁵³, binding of MMP-9 to CD44⁵⁴, and binding of MMP-7 to surface proteoglycans⁵⁵. As mentioned before, 72 kD MMP-2 also interacts with TIMP-2 and MT1-MMP on the cell surface, and this trimeric complex is an intermediate in the extracellular activation of this gelatinase⁴¹. It is likely that other MMPs are also attached to cells via specific interactions with membrane proteins, and determining the identity of these anchors will lead to identification of additional activation mechanisms and pericellular substrates.

Many recent studies have revealed that MMP-2 is also localized to various intracellular sites such as the thin and thick myofilaments of the sarcomere of

cardiomyocytes,^{56, 57} the nucleus,^{58, 59} and within cell membrane caveolae^{60, 61}. Caveolae are small cell membrane invaginations which play important roles in regulating the activity of signaling proteins and are also involved in macromolecular transport⁶². Caveolins are integral membrane proteins found within lipid rafts. Caveolin-1 (Cav-1), which is crucial for the formation of caveolae, binds to and regulates the function of a number of proteins including endothelial NOS⁶³. MMP-2 was found to be localized to the caveolae of endothelial cells⁶⁰. Moreover, it was shown that chemical disruption of caveolae activates MMP-2 in fibrosarcoma cells⁶⁴ while Cav-1 overexpression in tumor cells decreases MMP-2 activity⁶⁵. Furthermore, our laboratory presented evidence that MMP-2 co-localizes with Cav-1 in the mouse heart. Hearts of mice deficient in Cav-1 have increased MMP-2 activity. Purified caveolin scaffolding domain (the domain of Cav-1 which binds and negatively regulates several proteins which interact with Cav-1) inhibited MMP-2 activity in a concentration dependent manner as assessed using an *in vitro* degradation assay⁶¹. This study sheds some light on the possible participation of Cav-1 in the intracellular localization and/or regulation of MMP-2 which by its turn may act as an intracellular signaling molecule. Providing that oxidative stress was shown to cause the translocation of Cav-1 from the plasma membrane to the Golgi apparatus⁶⁶, decrease Cav-1 mRNA expression⁶⁷, and inhibit the trafficking of Cav-1 to the membrane lipid raft domains⁶⁸, this may speculatively provide an additional link by which oxidative stress enhances the intracellular activity of MMPs.

1.2.6: Tissue inhibitors of metalloproteinases (TIMPs)

TIMPs are the major endogenous inhibitors of the MMPs, exhibiting varying efficacies against different MMPs, as well as differing tissue expression patterns and modes of regulation. The TIMP family is composed of four members, TIMP-1 through TIMP-4, all of which have been found in the heart and cardiomyocytes⁶⁹. The TIMPs

have molecular weights of ~20 kD and are variably glycosylated. Structurally, TIMPs are two domain molecules, having an N-terminal MMP inhibiting domain and a smaller C-terminal domain. They are cysteine-rich proteins containing three disulfide bonds that stabilize each of these domains. In general, TIMPs bind to various MMPs in a 1:1 stoichiometric ratio ⁷⁰. Although all TIMPs are expressed in the heart ⁷¹, human TIMP-4 appears to be expressed abundantly in heart tissues and only at very low levels in other tissues ⁷². Interestingly, TIMP-4 is found to be localized to the sarcomere within cardiomyocytes in a similar pattern to MMP-2, implying a protective effect of TIMP-4 against potential detrimental actions of intracellular MMP-2 upon oxidative stress injury ⁷³. On the other hand, TIMP-3 in the heart is tightly bound to the extracellular matrix where it is exclusively localized ⁷⁴. TIMP-3 knock-out mice develop dilated cardiomyopathy through excessive extracellular matrix degradation and inflammatory cytokine activation ⁷⁵.

Apart from their MMP inhibitory activities, TIMPs seem to have various other biological functions. TIMP-1 and TIMP-2 have a growth-factor-like activity that stimulates the growth of erythroid precursors by a mechanism independent of MMP inhibition ^{76, 77}. TIMP-3, on contrary, has been found to play an important role in inhibiting angiogenesis by acting as a vascular endothelial growth factor receptor antagonist ⁷⁸. Likewise, this effect is independent of its MMP inhibitory activity, since other TIMPs could not inhibit binding of the growth factor to its receptor ⁷⁸. Future studies need to uncover the mechanism of these novel biological actions for TIMPs which appear to be independent of their MMP inhibitory action.

1.3: MMPs in cardiac physiology

Despite that more than 50 years have passed since their first discovery, very little is known regarding the role of MMPs in cardiac physiology. However, the presence of MMPs in the heart has been implicated in early heart development. Of particular significance is the role of MMP-2 in heart tube formation. In chick embryos an MMP-2 neutralizing antibody or a selective MMP inhibitor were shown to inhibit MMP-2 activity and produce severe heart defects, including cardia bifida, abnormal left-right patterning and a disruption in the looping direction ⁷⁹. Moreover, extensive MMP-2 activity is observed in areas of the developing heart where migration of neural crest cells and formation of the tunica media for the great vessels requires remodeling of the extracellular matrix ⁸⁰.

MMP-2 has also been shown to play important roles in angiogenesis ⁸¹ and heart valve development ⁸². Blockade of MMP activity with GM-6001 blocks cell invasion necessary for normal heart valve development ⁸³. Furthermore, introduction of MMP-2 antisense morpholino oligonucleotides into zebrafish severely disrupts their embryonic development ⁸⁴. In contrast, MMP-2 deficient mice are viable at birth although upon closer examination, they have a number of problems that distinguish them from their wild-type littermates. For example MMP-2 knockout mice display significantly retarded growth compared with their wild-type controls ⁸⁵. MMP-2 knockout mice also display impaired neovascularization in a hindlimb ischemia model when compared with controls ⁸⁶. Generally, the MMP-2 knockout phenotype is relatively benign in mice when compared to zebrafish which could be as a result of additional compensatory mechanisms in the more complex mammalian system.

1.4: MMPs involvement in cardiac pathology

1.4.1: The role of MMPs in ischemia-reperfusion injury

The exact mechanism of myocardial ischemia-reperfusion (I/R) injury has yet to be fully elucidated. However, it is known that a burst of reactive oxygen and nitrogen species, including ONOO^- , is generated in the myocardium in the first seconds of reperfusion which plays a central role in the pathogenesis of reperfusion injury^{87, 88}. The generation of ONOO^- not only activates MMPs^{38, 44, 49} but also inactivates TIMPs^{89, 90}, emphasizing potential roles of MMPs in I/R injury. Cheung et al were the first to demonstrate that both 72 and 64 kD MMP-2 are released at a basal rate into the perfusate of normal, aerobically perfused rat hearts, whereas there was a marked increase in this release during the first minutes of reperfusion following ischemia⁹¹. Two years later, another report found a positive correlation between increasing duration of ischemia, enhanced release of MMP-2 at reperfusion, and a reduction in cardiac mechanical function during reperfusion⁹². Interestingly, treatment with MMP inhibitors such as o-phenanthroline, doxycycline or a neutralizing MMP-2 antibody functionally protected hearts from I/R injury⁹¹.

An imbalance between TIMPs and MMPs in the heart may be one of the contributing factors to acute I/R injury. In a Langendorff rat model of I/R, TIMP-4 was also found to be acutely released into the perfusate during the initial reperfusion phase. Though it is released in conjunction with MMP-2, there is an overall shift towards enhanced proteolytic activity in the heart tissue as revealed by *in situ* zymography⁷³. The export of MMP-2 during reperfusion may likely be a protective mechanism of the heart to diminish the net cellular proteolytic activity by reducing the myocardial MMP/TIMP ratio³. Levels of both MMP-9 and TIMP-1 are increased in the plasma of patients following myocardial infarction⁹³. Likewise, right atrial biopsies from patients

undergoing cardiopulmonary bypass for coronary artery bypass grafting, obtained within ten minutes of aortic cross-clamp release (a mild form of reperfusion injury), show a dramatic increase in both MMP-2 and MMP-9 activities and a decrease in TIMP-1 during reperfusion⁹⁴. The increase in MMP-2 and -9 activities positively correlates with the duration of cross clamp and inversely with cardiac mechanical function 3 h after cross clamp release. In contrast TIMP-1 levels correlated positively with cardiac mechanical function at this time and correlated negatively with the duration of cross clamp placement. Plasma activities of both MMP-2 and MMP-9 were also seen to be elevated one minute following release of the aortic cross clamp⁹⁴.

It is likely that the alteration in MMP activities is a result of the increased oxidative stress which occurs most evidently during reperfusion following ischemia. During the first minute of reperfusion, cardiotoxic levels of ONOO⁻ are generated in the heart^{87, 88} and this is then followed by the rapid release of MMP-2⁹¹ (Figure 1.3). Direct infusion of ONOO⁻ into aerobically perfused isolated rat hearts caused a time-dependent loss in cardiac mechanical function which was preceded by evidence of MMP-2 activation (its release into the perfusate). The loss in contractile function was prevented by an MMP inhibitor⁹⁵. At these levels ONOO⁻ is likely capable of activating MMP-2 within the cardiomyocyte without proteolytic removal of the propeptide domain⁴⁹. Furthermore, exposure of isolated adult rat cardiomyocytes to ONOO⁻ resulted in a time and concentration dependent loss of contractile function which can be abrogated in the presence of the MMP inhibitors doxycycline or PD-166793⁹⁶.

David Lovett's group has investigated the transcriptional activation of MMP-2 as a result of I/R injury of the heart. They found that there is a rapid activation of the MMP-2 promoter as early as 30 min of reperfusion following global ischemia in hearts

isolated from transgenic mice containing the MMP-2 promoter linked to a β -galactosidase reporter ¹⁸. This result was observed in cardiac myocytes, fibroblasts and endothelial cells. The transcription factors JunB-FosB bind to a distinct, functional AP-1 site which activates the MMP-2 promoter in this setting ^{17, 18}. Using these same mice in a myocardial infarct model, as well as mice to which the MMP-9 promoter was linked to β -galactosidase, revealed that the MMP-2 promoter was induced within one day of infarct whereas the MMP-9 promoter was first detected after three days and peaked seven days after myocardial infarct ⁹⁷. Given the rapid activation of MMP-2 in the acute reperfusion phase following ischemia by ONOO⁻, resulting in its activation and release within minutes, it is not surprising that these measures would then occur to replenish MMP-2 levels in the myocardium. However, this underscores the unknown reason as to why MMP-2 is expressed in the normal heart.

Cardiac specific overexpression of a catalytically active mutant of MMP-2 in transgenic mice also highlights the role of MMP-2 in cardiac I/R injury. In this constitutively active MMP-2 mutant, valine at position 107 is replaced by glycine resulting in the unfolding of the propeptide domain from the catalytic site ⁹⁸. In fact, four month old MMP-2 transgenic mice that are not exposed to insult already display cardiac myocyte abnormalities, including disruption of sarcomere architecture, disintegration of Z bands and myofilament lysis ⁹⁹. When compared with their controls, six month old heterozygous MMP-2 transgenic mice display larger infarct size and greater functional impairment following 30 min of ischemia followed by 30 min of reperfusion in a Langendorff model ¹⁰⁰.

1.4.2: The role of MMPs in inflammatory heart diseases

MMPs are implicated in the pathogenesis of myocardial inflammation (myocarditis) which is a characteristic feature of a number of diseases including rheumatic heart fever and bacterial or viral myocarditis. Acute inflammation of the heart may lead to structural alterations and marked impairment of its contractile function. One common pathway by which MMPs are stimulated in these inflammatory diseases is through the production of pro-inflammatory cytokines. Both tumor necrosis factor- α (TNF- α) and interleukin-1 β (IL-1 β) have been shown to affect the expression and activity of MMPs. IL-1 β and TNF- α both regulate the expression of collagenase in human fibroblasts via an AP-1 responsive element of the gene¹⁰¹. Similarly, IL-1 β stimulates the expression and enhanced activity of MMP-2, but not MMP-9, in cardiac fibroblasts²¹ and microvascular endothelial cells¹⁰².

Acute viral myocarditis can occur in young and otherwise healthy patients, resulting in dilated cardiomyopathy with no effective treatment besides supportive therapy. Patients can develop viral myocarditis following infection with Coxsackie virus B3 and both direct infection of the cardiomyocyte by the virus, or immune reaction following infection can lead to impaired heart function¹⁰³. In a mouse model of Coxsackie virus B3-induced myocarditis, it was shown that MMP-2, -9 and -12 transcription and translation, as well as activities were increased during acute myocarditis in cardiac ventricles and this was accompanied by a significant reduction in the mRNA levels of TIMP-3 and -4¹⁰⁴. Interestingly, in the same year another group demonstrated that inhibition of both MMP-2 and MMP-9 activities in the same model of Coxsackie virus B3-induced myocarditis significantly prevented cardiac injury and dysfunction¹⁰⁵. Recently, however, targeted deletion of MMP-2 gene in mice subjected to viral myocarditis was associated with less degradation of the chemokine, monocyte

chemotactic protein-3, by MMP-2 which then increased the inflammatory response and impaired cardiac function during Coxsackie virus B3-induced myocarditis ¹⁰⁶.

The majority of the research in acute myocarditis has focused on the role of MMPs acting on extracellular proteins of the heart, however, this does not preclude a possible intracellular role of MMPs in the pathogenesis of inflammatory heart disease. In this regard, our group exposed isolated working rat hearts to proinflammatory cytokines and revealed that MMP-2 activation was accompanied by the loss of TIMP-4 from hearts. This MMP-2 activation was associated with cardiac contractile dysfunction as well as reduction in troponin I (TnI) levels (see section 1.5.1 for sarcomeric proteins targeted by MMP-2), an effect reversed by selective MMP inhibitors ¹⁰⁷.

1.4.3: The possible role of MMPs in cardiac cell death

Cell death pathways are triggered in the heart as a result of enhanced oxidative stress as seen in reperfusion injury ¹⁰⁸. *In vivo*, cardiac cell death (apoptosis and/or necrosis) occurs during myocardial ischemia ¹⁰⁹, and especially when followed by reperfusion ¹⁰⁸. Studies by Menon et al. ^{110, 111}, suggest that the pro-apoptotic role of MMP-2 in adult rat cardiomyocyte apoptosis occurs via stimulation of β -adrenergic receptors. MMP-2 inhibition abrogated isoproterenol-stimulated increases in cytochrome c release and restored the mitochondrial membrane potential in adult rat ventricular myocytes. Interestingly, using the same experimental model, purified MMP-2 also increases GSK-3 β activity in rat cardiomyocytes through its interference with the β 1-integrin-mediated survival signal and inhibition of MMP-2 prevented the β -adrenoceptor mediated increase in GSK-3 β activity ¹¹². Considering the essential role played by GSK-3 β in various cellular processes including metabolism, cell growth and death, MMP-2 mediated regulation of GSK-3 β is potentially important. A recent finding from our lab suggests a direct interaction between MMP-2 and GSK-3 β . MMP-2 was found to cleave

the N-terminal region of GSK-3 β , leading to its increased kinase activity. H9c2 cardiomyoblasts exposed to oxidative stress showed evidence of increased MMP-2 activity, GSK-3 β cleavage and increased GSK-3 β activity, all of which were abrogated with MMP inhibitors ¹¹³.

A recent study has also linked the activation of MMP-2 by oxidative stress in lung endothelial cells and the subsequent apoptotic events ⁵⁹. Moreover, Shen et al reported a contribution of MMP-2 in TNF- α -induced apoptosis in cultured cardiomyocytes ¹¹⁴. They showed that inhibiting MMP-2 prior to TNF- α treatment decreased myocardial MMP-2 activity and reduced the TUNEL-positive myocytes and DNA fragmentation. Moreover, MMP-2 inhibition was associated with a reduction in Bax expression and caspase-3 activity and a subsequent reduction in myocardial apoptosis, with increased Bcl-2 expression ¹¹⁴. On the other hand, addition of 64 kD MMP-2 to cultured endothelial cells showed a concentration-dependent induction of apoptosis with no influence on the level of active caspase-3 ¹¹⁵, suggesting that MMP-2 may act downstream of caspases. Consistent with this latter observation, Yarbrough et al (2010) showed increased MMP-2 activity after treatment of heart homogenates with active caspase-3 and generation of the 64 kD MMP-2 by an active caspase cocktail ¹¹⁶.

It is worth noting that cardiac-specific expression of active MMP-2 in transgenic mice caused abnormalities in cardiac mitochondria ultrastructure, impaired mitochondrial respiration, increased lipid peroxidation and myocardial cell necrosis all of which contributed to reduced recovery of contractile performance during post-ischemic reperfusion ¹⁰⁰.

1.5: Intracellular localization of MMP-2 in cardiomyocytes

In accordance with the abundant evidence linking MMPs with extracellular matrix remodelling in chronic cardiovascular diseases, most researchers have focused on the long term effects of MMPs on extracellular matrix proteins^{117, 118}. However, emerging evidence has shown that MMP-2 is closely associated with intracellular compartments within human and rat cardiomyocytes including the sarcomere^{56, 119, 120}. Moreover, MMP-2 was found to contribute to acute cardiac mechanical dysfunction before the development of changes in collagen matrix^{91, 107}. Although a few other MMPs have been localized in different intracellular compartments of various cells (for review see⁴), I will focus herein on the intracellular localizations of MMP-2 in cardiomyocytes.

1.5.1: Localization of MMP-2 to the sarcomere

Degradation or loss of myofilament regulatory proteins as well as structural and cytoskeletal proteins is known to accompany I/R injury of the heart^{121, 122}. However, the proteases responsible for these actions have not been fully elucidated. The Schulz lab was the first to show that MMP-2 is localized within cardiac myocytes at the sarcomere and is responsible for the rapid degradation of TnI, a regulatory protein of actin-myosin interaction found in the thin myofilaments, in acute myocardial I/R injury^{56, 91}. Different experimental approaches provided compelling evidence for the localization of MMP-2 to the sarcomere which included: (a) immunogold electron microscopy with anti-MMP-2 showed a distinct sarcomeric staining pattern; (b) highly purified preparations of thin myofilaments (which include TnI) prepared from these hearts showed both 72 and 64 kD MMP-2 gelatinolytic activities as well as MMP-2 protein; (c) TnI immunoprecipitated from I/R heart homogenates included gelatinolytic activities by zymographic analysis revealing both 72 and 64 kD MMP-2 activities; and (d) confocal microscopy showed the colocalization of MMP-2 with TnI. Not only MMP-2 was found to co-localize with TnI,

but it is also responsible for its degradation⁵⁶. The study also showed that: (a) TnI is very susceptible to proteolysis by MMP-2 which occurs at a low enzyme to substrate ratio *in vitro* within 20 min of incubation at 37°C; (b) proteolytic activity susceptible to MMP inhibition was found in rat heart extracts immunoprecipitated with anti-TnI and was capable of cleaving TnI in the same sample. Finally the conditions of I/R were such that there was no significant myocardial necrosis, as TnI or its degradation products were not found in the coronary effluent. This result was the first evidence showing the biological action of a MMP via its intracellular action and targeting to a novel intracellular substrate, TnI⁵⁶.

Using a combined pharmaco-proteomics approach, our lab discovered another intracellular target of MMP-2 in I/R hearts, myosin light chain-1 (MLC-1)⁵⁷. MLC-1 was found to undergo proteolytic degradation in hearts subjected to I/R injury¹²³. MMP-2 activity was found in preparations of thick myofilaments (which contain MLC-1) prepared from rat hearts; immunogold microscopy localized MMP-2 to the sarcomere in a pattern consistent with the known distribution of MLC-1, and purified MLC-1 was susceptible to proteolysis by MMP-2 (but not MMP-9) *in vitro*. Mass spectrometric analysis of degradation products of MLC-1 from I/R hearts identified a cleavage site of MLC-1 by MMP-2 at an accessible portion of the C-terminus between Y189 and E190⁵⁷. These studies reveal that MMP-2 may be a crucial protease which targets specific sarcomeric proteins as a result of oxidative stress injury to the heart (Figure 1.4).

1.5.2: Localization of MMP-2 to the cytoskeleton

Matsumura et. al. reported that guinea pig hearts subjected to I/R injury *in vitro* showed evidence for the degradation of cytoskeletal proteins desmin, spectrin, and α -actinin¹²², although the protease(s) responsible for this was not identified. α -Actinin is known to connect actin filaments of adjacent sarcomeres and plays a substantial role in

transmitting force generated by actin-myosin interaction. Interestingly, MMP-2 was found to colocalize with α -actinin in cardiac myocytes^{124, 125}. Sung et. al. found that not only α -actinin and desmin (but not spectrin) were susceptible to degradation by MMP-2 *in vitro* but also infusion of ONOO⁻ into isolated, perfused rat hearts caused activation of MMP-2 with concomitant loss of myocardial α -actinin content, which was prevented by a selective MMP inhibitor, PD-166793¹²⁵.

1.5.3: Localization of MMP-2 to the nucleus

MMP-2^{56, 58, 126}, MMP-3¹²⁷ and MMP-9¹²⁶ were found to either localize or translocate to the nucleus of various cell types including cardiomyocytes. Interestingly, the nucleus has a matrix that resembles the extracellular matrix and provides structural and organizational support for various nuclear processes¹²⁸. Various biological processes such as apoptosis¹²⁹, cell cycle regulation¹³⁰, and nuclear matrix degradation¹³¹ involve proteolytic processing of nuclear proteins. MMP-2 was found in the nucleus of human cardiomyocytes and rat liver⁵⁸. Indeed MMP-2 and other MMPs were found to carry a putative nuclear localization sequence^{58, 127}. Our laboratory found that MMP-2 was able to proteolyze the nuclear DNA repair enzyme, poly (ADP-ribose) polymerase *in vitro*⁵⁸. Consistent with this observation, a recent report showed that cerebral I/R injury in rats was associated with increased intranuclear MMP-2 activity as well as poly (ADP-ribose) polymerase degradation¹²⁶. Furthermore, treatment with MMP inhibitor attenuated ischemia-induced poly (ADP-ribose) polymerase cleavage suggesting a novel role of nuclear MMP-2 in neuronal apoptosis seen in many ischemic brain injuries¹²⁶.

Si-Tayeb et. al. reported that a truncated yet active fragment of MMP-3 was localized to the nucleus of several human cancer cell lines¹²⁷. Pro-MMP-3 remained cytosolic, whereas the active form translocated to the nucleus and a nuclear localization sequence was demonstrated to be essential for this translocation. Moreover, they found

that nuclear MMP-3 induces apoptosis in Chinese hamster ovary cells via its MMP activity¹²⁷.

1.5.4: Localization of MMP-2 to mitochondria

Although the precise nature of mitochondrial MMP-2, its substrates and functions in mitochondria are not yet understood, the Schulz lab was the first to report evidence for the presence of MMP-2 in cardiac mitochondria⁵⁶. Subsequently, others have detected increased mitochondrial MMP activity during cardiac injury and linked the increased level of mitochondrial MMP-9 to cardiac mechanical dysfunction in hyperhomocysteinemia¹³². Moreover, another MMP e.g. MMP-1, was found associated with the mitochondrial membrane in corneal fibroblasts and retinal pigment epithelial cells¹³³. Interestingly, mitochondrial MMP-1, via an unknown mechanism, confers resistance to lamin A/C (a nuclear envelope protein) degradation during apoptosis in a human Muller glial cell line, MIO-M1¹³³.

1.6: Reactive oxygen species: cellular generation and hormone-like action

Free radicals are chemically defined as atoms or molecules that exist with one or more unpaired electrons. Biologically relevant free radicals are a subset of reactive, pro-oxidant molecules which are classified as both reactive oxygen species and reactive nitrogen species. Since all of the biologically relevant reactive nitrogen species contain oxygen, I will henceforth only use the term reactive oxygen species. The forms of reactive oxygen species that are most relevant in biological systems include superoxide anion, peroxy radical, hydroxyl radical, hydrogen peroxide, nitric oxide (NO), and ONOO⁻^{50,134}.

Superoxide is produced as a result of the addition of an electron to molecular oxygen which itself is a diradical, thus leaving a molecule with one unpaired electron and

a net charge of -1¹³⁵. This reductive process is accomplished by a variety of enzymatic reactions, including xanthine oxidase, NADPH oxidases, and as a byproduct of oxidative phosphorylation in mitochondria. For instance, xanthine oxidase can produce both superoxide and hydrogen peroxide during reoxidation of the enzyme¹³⁶.

Hydrogen peroxide is generated via dismutation of superoxide by the enzyme, superoxide dismutase. Under physiological condition, peroxisomes are known to produce hydrogen peroxide as well. Peroxisomes are major sites of oxygen consumption in the cell and participate in several metabolic functions that use oxygen e.g. beta-oxidation of long chain fatty acids¹³⁷. Oxygen consumption in the peroxisome leads to hydrogen peroxide production, which is then used to oxidize a variety of molecules including FADH₂. The organelle also contains catalase, which decomposes hydrogen peroxide into water and presumably prevents accumulation of this toxic compound. Thus, the peroxisome maintains an exquisite balance with respect to the relative activities of these enzymes to ensure a controlled level of reactive oxygen species. When peroxisomes are damaged and their hydrogen peroxide consuming enzymes are downregulated, hydrogen peroxide is released into the cytosol and significantly contributes to oxidative stress¹³⁸.

NO is formed primarily by a family of enzymes known as NO synthases which oxidize L-arginine to form NO and L-citrulline¹³⁹. There are three NO synthase isoforms, each with specific localizations and functions. NO synthase-1 (neuronal NO synthase) and NO synthase-3 (endothelial NO synthase) are found in a variety of cell types and are regulated by calcium and calmodulin binding. In contrast, NO synthase-2 (inducible NO synthase) has a very high baseline affinity for calcium and calmodulin; therefore, its activity is effectively independent of calcium concentration¹³⁴.

Peroxynitrite (ONOO^-) is a product of the extremely fast, diffusion rate-limited reaction of NO with superoxide. At physiological pH, ONOO^- is protonated to form peroxynitrous acid, a highly unstable intermediate species with a very short half-life. This spontaneously undergoes either homolytic or heterolytic cleavage and these breakdown products of peroxynitrous acid, including nitrogen dioxide and hydroxyl radical, are able to react with DNA, proteins, and lipids, causing cellular damage and cytotoxicity¹⁴⁰. The hydroxyl radical is one of most highly reactive of all reactive oxygen species with a very short half-life *in vivo*¹⁴¹. Thus when produced hydroxyl radical reacts close to its site of formation (i.e. within the distance of a carbon-carbon bond). Tyrosine nitration by ONOO^- has been demonstrated both *in vitro* and *in vivo* and has long been suspected to be a mechanism of protein inactivation¹⁴². However, the post-translational modifications of proteins caused by ONOO^- are many, and it can target several amino acids, cysteine and tyrosine residues in particular¹⁴³. The type of these post-translational modifications range from subtle oxidation of cysteine residues (resulting in their S-glutathiolation or S-nitrosylation) to a direct nitration of tyrosine residues as a result of higher concentration and/or longer duration of exposure to ONOO^- . Although the majority of research has shown that a high concentration of ONOO^- can generally inactivate enzymes (i.e. $\geq 100 \mu\text{M}$), an increasing number of reports show that low concentrations of ONOO^- (i.e. 0.1-10 μM) can even stimulate enzyme activity^{38, 49, 144}. For example, ONOO^- activates SERCA¹⁴⁴ and MMPs as described above via S-glutathiolation and/or S-nitrosylation of cysteine residues^{38, 49, 145}.

Reactive oxygen species play an important role in cell signaling and their effects depend on the precise location, amount, and the duration of their production¹⁴⁶. They are not intrinsically destructive, on the contrary, increasing evidence shows that they play

necessary roles in normal signal transduction and cellular function ⁵⁰. Interestingly, hydrogen peroxide was shown to stimulate a number of insulin-like effects in adipocytes including activation of glucose transport, enhancement of glucose oxidation, glycogenesis and lipogenesis ¹⁴⁷. The activity of NADPH oxidase, a superoxide-producing enzyme, was increased in insulin-stimulated adipocytes and insulin was shown to stimulate intracellular hydrogen peroxide production ¹⁴⁸. These studies suggest that insulin-stimulated hydrogen peroxide production mediates some of the effect of insulin and thus hydrogen peroxide is a possible second messenger downstream of the insulin receptor.

1.7: Overall Hypothesis

MMP-2 is an intracellular protease and the signal sequence of MMP-2 as well as alternative splicing of its transcript could account for the intracellular presence of the enzyme in addition to its secretion from cells. Other hypotheses tested include: 1) reactive oxygen species increase intracellular level/activity of MMP-2 to stimulate cell death pathway, 2) calpain inhibitors can also inhibit intracellular MMP-2 activity, and 3) MMP-2 localizes to and cleaves titin, a giant sarcomeric protein, upon myocardial I/R injury.

1.8: Thesis Objectives

1.8.1: Mechanism of cytosolic targeting of matrix metalloproteinase-2 (Chapter 2)

In general, MMPs are originally defined as secreted proteases. They possess a signal sequence targeting the synthesized protein to the endoplasmic reticulum membrane, thus allowing entry into the secretory pathway. However, recent evidence from our laboratory has revealed novel intracellular actions of MMP-2 in the cardiomyocyte. In these cells MMP-2 co-localizes with sarcomeric and cytoskeletal proteins and proteolyzes susceptible intracellular substrates in the context of oxidative stress injury. These observations beg the question as to how this “secreted” protease

comes to reside within the intracellular compartment. The objective of Chapter 2 is to examine possible mechanisms of cytosolic targeting of MMP-2.

1.8.2: Hydrogen peroxide-induced necrotic cell death in cardiomyocytes is independent of matrix metalloproteinase-2 (Chapter 3)

Reactive oxygen species including hydrogen peroxide can induce cardiomyocyte death by apoptosis or necrosis. MMP-2 expression and/or activity are increased in cardiac cells after hydrogen peroxide treatment. This chapter examines the contribution of MMP-2 in hydrogen peroxide mediated cardiomyocyte death pathways.

1.8.3: Calpain inhibitors exhibit MMP-2 inhibitory activity (Chapter 4)

MMP-2 plays a fundamental role in oxidative stress-induced injury to the heart. Intracellular cleavage targets of MMP-2 mediating this injury include the sarcomeric proteins TnI, MLC-1 and α -actinin; some of these substrates are also targeted by calpains, calcium-dependant cysteine proteases. Cleavage of these sarcomeric proteins rapidly impairs cardiac contractile function. In myocardial I/R injury, inhibitors of MMP-2 as well as some calpain inhibitors were shown to improve the recovery of myocardial contractile function. The objective of Chapter 4 is to determine whether the protective effects of some calpain inhibitors is due in part to their ability to inhibit MMP-2 activity.

1.8.4: Titin is a target of matrix metalloproteinase-2: Implications in ischemia/reperfusion injury (Chapter 5)

Titin, the largest known mammalian protein (~3000 kD), plays a central role as a backbone of the cardiac sarcomere. One molecule of titin spans half the length of the sarcomere acting as a molecular spring and thus is an important determinant of both systolic and diastolic function of the heart. Although loss of titin in ischemic hearts has

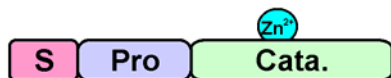
been reported, the mechanism of titin degradation has not been extensively studied. MMP-2 is localized to the cardiac sarcomere and proteolyzes various myofilament proteins in I/R injury. The objective of Chapter 5 is to determine whether titin is an intracellular substrate for MMP-2 and its degradation as a result of I/R injury contributes to cardiac dysfunction.

1.9 Conclusions

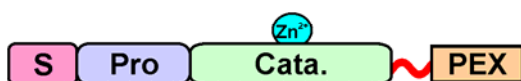
MMP-2 plays novel roles in cardiac oxidative stress-induced injury via proteolyzing intracellular substrates. Cardiac titin is a very crucial molecule in sarcomere structure and contractile function and unravelling the mechanism of titin degradation seen in ischemic heart diseases is essential to investigate new pharmacologic agents for treatment or prevention of such conditions. Moreover, providing mechanism(s) of intracellular targeting of MMP-2 will not only bridge a gap in our knowledge in the MMP biology field, but also stimulate MMP biologists to broaden their horizons as to where MMP-2, and likely also other MMPs, can have biological actions both in extra- as well as intra-cellular domains.

Figure 1.1 MMP domain structure. MMPs possess a general common domain structure. The N-terminus typically contains a signal sequence which dictates their entry into the secretory pathway for secretion from the cell. MMPs are synthesized in a zymogen form with a propeptide domain that shields the catalytic zinc in the adjacent catalytic domain. The catalytic domain of the gelatinases (MMP-2 and -9) is unique in that it has three fibronectin II repeats. MMPs contain a flexible hinge region that attaches the catalytic domain to the C-terminus hemopexin domain (with exception for the matrilysins MMP-7 and -26). MT-MMPs are anchored to the cell membrane via a C-terminus transmembrane domain or glycosylphosphatidylinositol moiety.

Matrilysins
(MMP-7, 26)



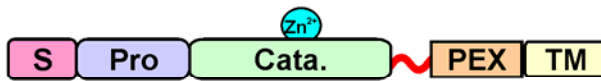
Collagenases
(MMP-1, 8, 13)
Stromelysins
(MMP-3, 10, 11, 12)



Gelatinases
(MMP-2, 9)



Membrane-type
(MT-MMP 1, 2, 3, 5)



Membrane-type
(MT-MMP 4, 6)

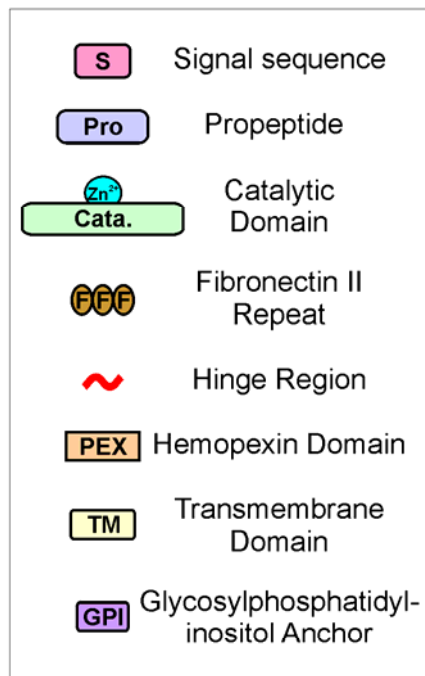
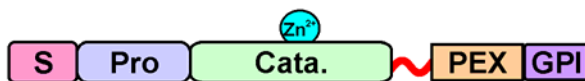


Figure 1.2 Post-translational modification of MMP-2. The 72 kD form of MMP-2 can be activated extracellularly by MT1-MMP in the presence of TIMP-2, or by other proteases (e.g. plasminogen) via cleavage of its propeptide domain to yield the 64 kD form. 72 kD MMP-2 can also be activated by S-glutathiolation when exposed to ONOO^- (as caused by I/R injury) in the presence of cellular glutathione without losing the propeptide domain. The S-glutathiolation of MMP-2 results in a molecular weight gain of 305 Dalton which is too small to be resolved by SDS-PAGE. MMP-2 is also a phosphoprotein with several identified phosphorylation sites and whose activity is further modulated by its phosphorylation status. The kinases and phosphatases involved in its regulation in vivo are yet to be discovered.

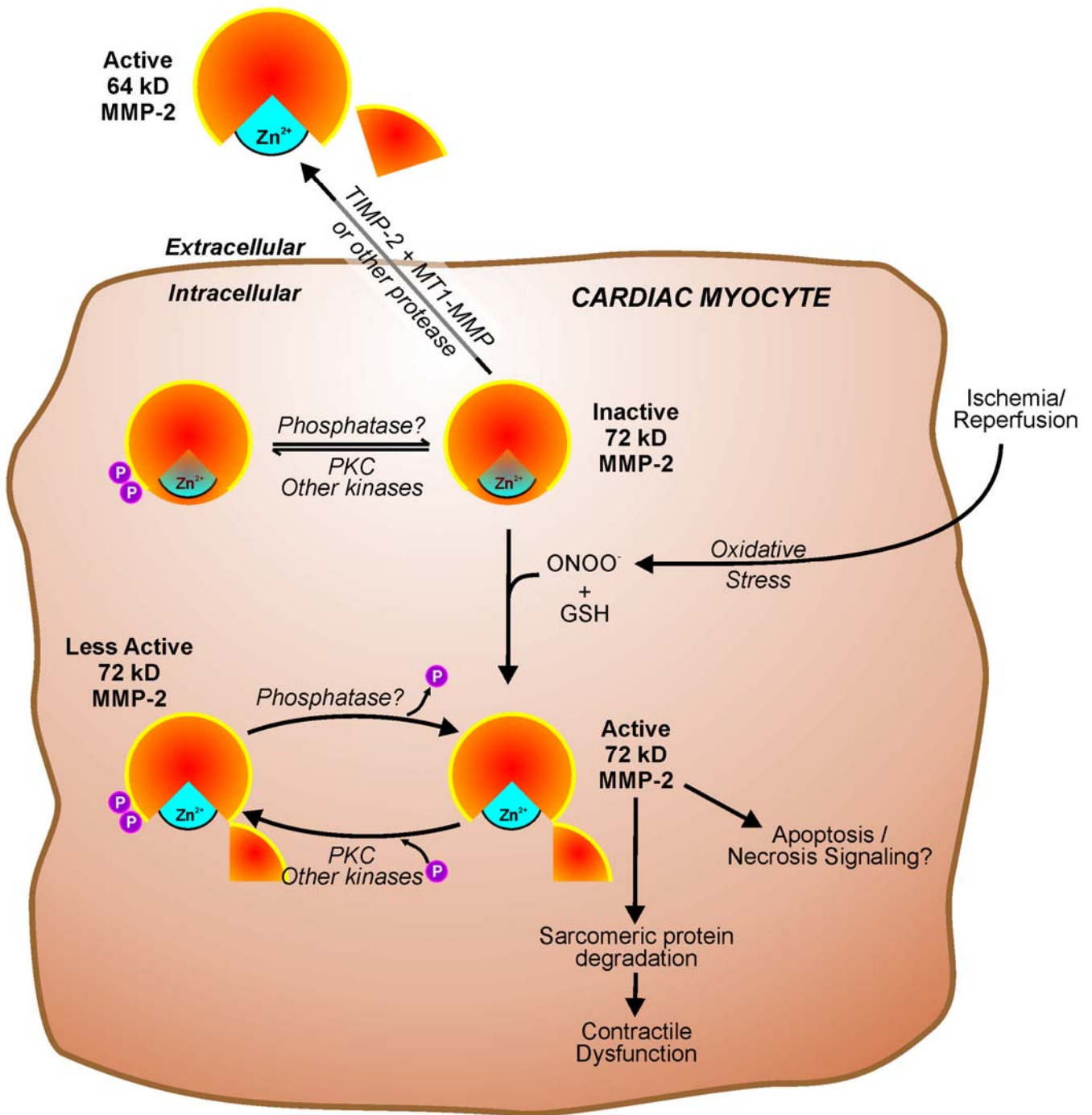


Figure 1.3 Schematic showing the sequence of pathophysiological events in myocardial I/R injury. ONOO⁻ biosynthesis peaks during the first minute of reperfusion following ischemia and is followed by rapid activation and release of MMP-2 (which peaks 2-5 minutes during reperfusion). Those effects contribute to the acute loss in myocardial contractile function seen in reperfusion which can be ameliorated by pharmacological inhibition of MMP activity.

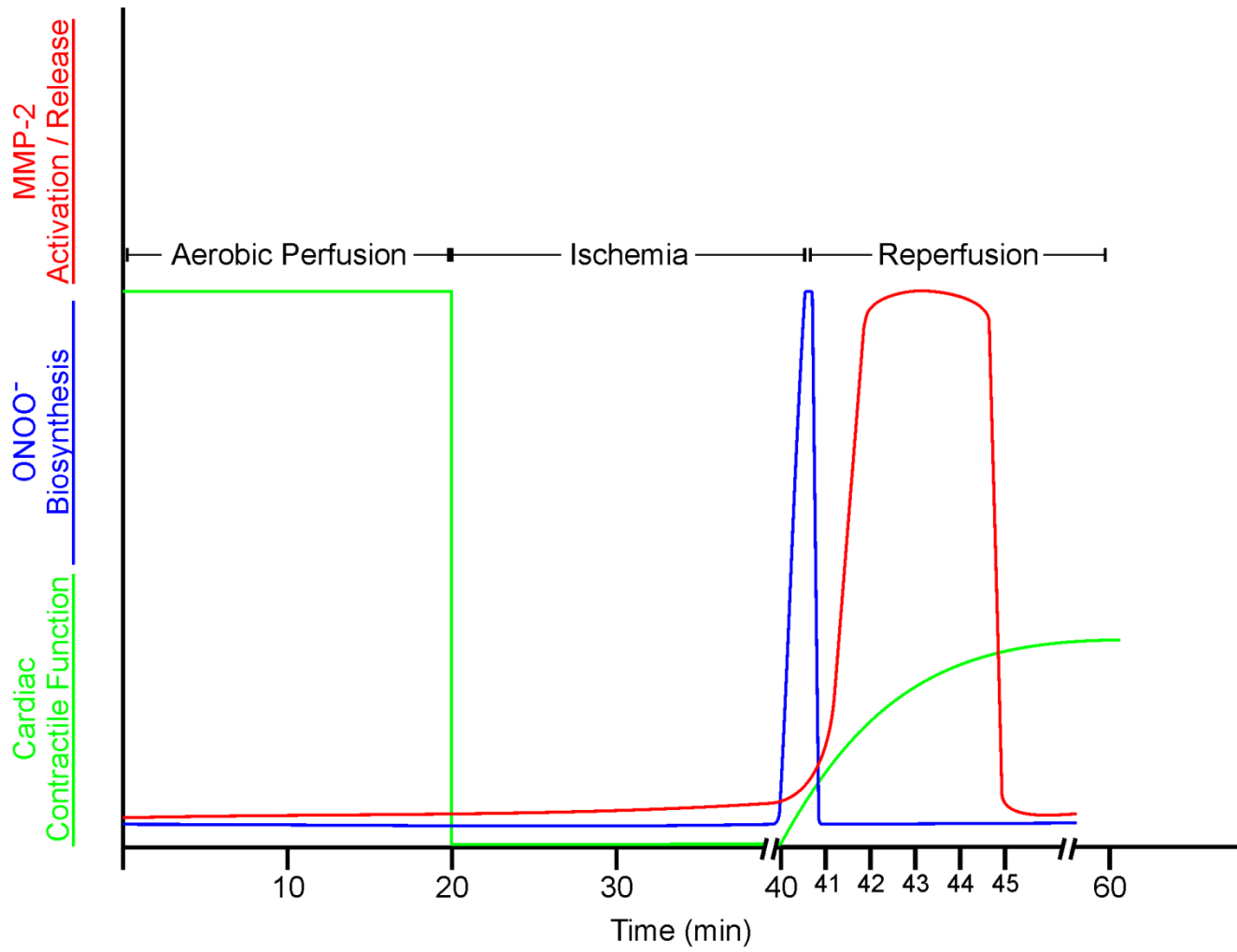
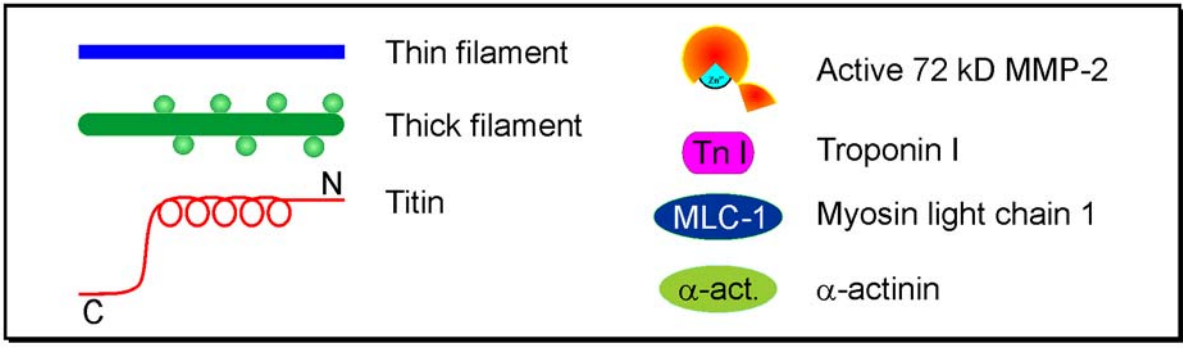
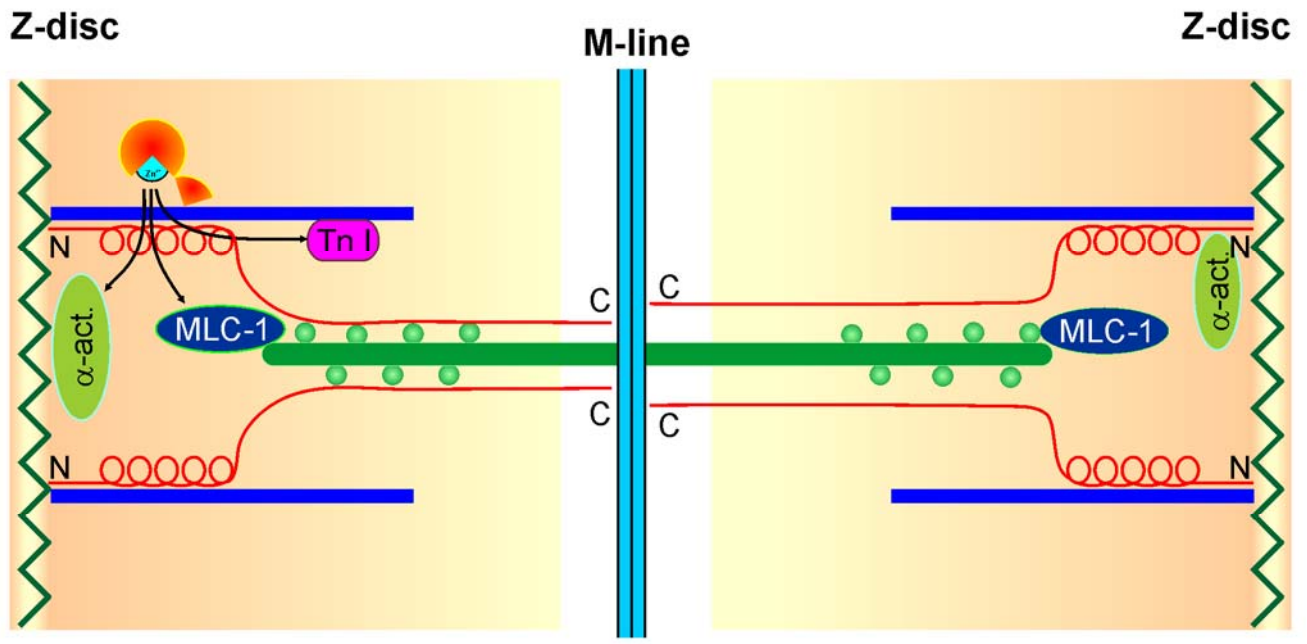


Figure 1.4 Intracellular targets of MMP-2 in the cardiac sarcomere. MMP-2 is co-localized and able to proteolyze sarcomeric proteins during I/R injury including TnI in thin filament, MLC-1 in the thick filament as well as the cytoskeletal protein α -actinin found in the Z-disc. One molecule of titin spans half the length of sarcomere from the Z-disc to the M-line. N; N-terminus of titin, C; C-terminus of titin.



1.10 References

1. Gross J, Lapiere CM. Collagenolytic activity in amphibian tissues: a tissue culture assay. *Proc Natl Acad Sci U S A*. 1962; 48: 1014-1022.
2. McCawley LJ, Matrisian LM. Matrix metalloproteinases: they're not just for matrix anymore! *Curr Opin Cell Biol*. 2001; 13: 534-540.
3. Schulz R. Intracellular targets of matrix metalloproteinase-2 in cardiac disease: rationale and therapeutic approaches. *Annu Rev Pharmacol Toxicol*. 2007; 47: 211-242.
4. Cauwe B, Opdenakker G. Intracellular substrate cleavage: a novel dimension in the biochemistry, biology and pathology of matrix metalloproteinases. *Crit Rev Biochem Mol Biol*. 2010; 45: 351-423.
5. Hadler-Olsen E, Fadnes B, Sylte I, Uhlin-Hansen L, Winberg JO. Regulation of matrix metalloproteinase activity in health and disease. *FEBS J*. 2011; 278: 28-45.
6. Hidalgo M, Eckhardt SG. Development of matrix metalloproteinase inhibitors in cancer therapy. *J Natl Cancer Inst*. 2001; 93: 178-193.
7. Parks WC, Wilson CL, Lopez-Boado YS. Matrix metalloproteinases as modulators of inflammation and innate immunity. *Nat Rev Immunol*. 2004; 4: 617-629.
8. Blobel G. Protein targeting. *Biosci Rep*. 2000; 20: 303-344.
9. von Heijne G. Signal sequences. The limits of variation. *J Mol Biol*. 1985; 184: 99-105.

10. Shaffer KL, Sharma A, Snapp EL, Hegde RS. Regulation of protein compartmentalization expands the diversity of protein function. *Dev Cell*. 2005; 9: 545-554.
11. Ma J, Wollmann R, Lindquist S. Neurotoxicity and neurodegeneration when PrP accumulates in the cytosol. *Science*. 2002; 298: 1781-1785.
12. Huang Y, Liu XQ, Wyss-Coray T, Brecht WJ, Sanan DA, Mahley RW. Apolipoprotein E fragments present in Alzheimer's disease brains induce neurofibrillary tangle-like intracellular inclusions in neurons. *Proc Natl Acad Sci U S A*. 2001; 98: 8838-8843.
13. Hegde RS, Bernstein HD. The surprising complexity of signal sequences. *Trends Biochem Sci*. 2006; 31: 563-571.
14. Levine CG, Mitra D, Sharma A, Smith CL, Hegde RS. The efficiency of protein compartmentalization into the secretory pathway. *Mol Biol Cell*. 2005; 16: 279-291.
15. Morgunova E, Tuuttila A, Bergmann U, Isupov M, Lindqvist Y, Schneider G, Tryggvason K. Structure of human pro-matrix metalloproteinase-2: activation mechanism revealed. *Science*. 1999; 284: 1667-1670.
16. Sternlicht MD, Werb Z. How matrix metalloproteinases regulate cell behavior. *Annu Rev Cell Dev Biol*. 2001; 17: 463-516.
17. Bergman MR, Cheng S, Honbo N, Piacentini L, Karliner JS, Lovett DH. A functional activating protein 1 (AP-1) site regulates matrix metalloproteinase 2 (MMP-2) transcription by cardiac cells through interactions with JunB-Fra1 and JunB-FosB heterodimers. *Biochem J*. 2003; 369: 485-496.

18. Alfonso-Jaume MA, Bergman MR, Mahimkar R, Cheng S, Jin ZQ, Karliner JS, Lovett DH. Cardiac ischemia-reperfusion injury induces matrix metalloproteinase-2 expression through the AP-1 components FosB and JunB. *Am J Physiol Heart Circ Physiol.* 2006; 291: H1838-46.
19. Jones CB, Sane DC, Herrington DM. Matrix metalloproteinases: a review of their structure and role in acute coronary syndrome. *Cardiovasc Res.* 2003; 59: 812-823.
20. Galis ZS, Muszynski M, Sukhova GK, Simon-Morrissey E, Libby P. Enhanced expression of vascular matrix metalloproteinases induced in vitro by cytokines and in regions of human atherosclerotic lesions. *Ann N Y Acad Sci.* 1995; 748: 501-507.
21. Siwik DA, Chang DL, Colucci WS. Interleukin-1beta and tumor necrosis factor-alpha decrease collagen synthesis and increase matrix metalloproteinase activity in cardiac fibroblasts in vitro. *Circ Res.* 2000; 86: 1259-1265.
22. Feinberg MW, Jain MK, Werner F, Sibinga NE, Wiesel P, Wang H, Topper JN, Perrella MA, Lee ME. Transforming growth factor-beta 1 inhibits cytokine-mediated induction of human metalloelastase in macrophages. *J Biol Chem.* 2000; 275: 25766-25773.
23. Uzui H, Harpf A, Liu M, Doherty TM, Shukla A, Chai NN, Tripathi PV, Jovinge S, Wilkin DJ, Asotra K, Shah PK, Rajavashisth TB. Increased expression of membrane type 3-matrix metalloproteinase in human atherosclerotic plaque: role of activated macrophages and inflammatory cytokines. *Circulation.* 2002; 106: 3024-3030.
24. Luchtefeld M, Grote K, Grothusen C, Bley S, Bandlow N, Selle T, Struber M, Haverich A, Bavendiek U, Drexler H, Schieffer B. Angiotensin II induces MMP-2 in a p47phox-dependent manner. *Biochem Biophys Res Commun.* 2005; 328: 183-188.

25. Ben-Yosef Y, Lahat N, Shapiro S, Bitterman H, Miller A. Regulation of endothelial matrix metalloproteinase-2 by hypoxia/reoxygenation. *Circ Res.* 2002; 90: 784-791.
26. Hoskins AA, Gelles J, Moore MJ. New insights into the spliceosome by single molecule fluorescence microscopy. *Curr Opin Chem Biol.* 2011; 15: 864-870.
27. Nilsen TW, Graveley BR. Expansion of the eukaryotic proteome by alternative splicing. *Nature.* 2010; 463: 457-463.
28. Tardif G, Dupuis M, Reboul P, Geng CS, Pelletier JP, Ranger P, Martel-Pelletier J. Identification and differential expression of human collagenase-3 mRNA species derived from internal deletion, alternative splicing, and different polyadenylation and transcription initiation sites. *Osteoarthritis Cartilage.* 2003; 11: 524-537.
29. Matsumoto S, Katoh M, Saito S, Watanabe T, Masuho Y. Identification of soluble type of membrane-type matrix metalloproteinase-3 formed by alternatively spliced mRNA. *Biochim Biophys Acta.* 1997; 1354: 159-170.
30. Ross HH, Fillmore HL. Identification of a novel human MT5-MMP transcript variant in multipotent NT2 cells. *FEBS Lett.* 2007; 581: 5923-5928.
31. Illman SA, Keski-Oja J, Parks WC, Lohi J. The mouse matrix metalloproteinase, epilysin (MMP-28), is alternatively spliced and processed by a furin-like proprotein convertase. *Biochem J.* 2003; 375: 191-197.
32. Hu SI, Klein M, Carozza M, Rediske J, Peppard J, Qi JS. Identification of a splice variant of neutrophil collagenase (MMP-8). *FEBS Lett.* 1999; 443: 8-10.

33. Delany AM, Jeffrey JJ, Rydziel S, Canalis E. Cortisol increases interstitial collagenase expression in osteoblasts by post-transcriptional mechanisms. *J Biol Chem.* 1995; 270: 26607-26612.
34. Vincenti MP. The matrix metalloproteinase (MMP) and tissue inhibitor of metalloproteinase (TIMP) genes. Transcriptional and posttranscriptional regulation, signal transduction and cell-type-specific expression. *Methods Mol Biol.* 2001; 151: 121-148.
35. Limaye AM, Desai KV, Chavalmane AK, Kondaiah P. Regulation of mRNAs encoding MMP-9 and MMP-2, and their inhibitors TIMP-1 and TIMP-2 by androgens in the rat ventral prostate. *Mol Cell Endocrinol.* 2008; 294: 10-18.
36. Matsumoto S, Katoh M, Saito S, Watanabe T, Masuho Y. Identification of soluble type of membrane-type matrix metalloproteinase-3 formed by alternatively spliced mRNA. *Biochim Biophys Acta.* 1997; 1354: 159-170.
37. Ali MA, Schulz R. Activation of MMP-2 as a key event in oxidative stress injury to the heart. *Front Biosci.* 2009; 14: 699-716.
38. Okamoto T, Akaike T, Sawa T, Miyamoto Y, van der Vliet A, Maeda H. Activation of matrix metalloproteinases by peroxynitrite-induced protein S-glutathiolation via disulfide S-oxide formation. *J Biol Chem.* 2001; 276: 29596-29602.
39. Gu Z, Kaul M, Yan B, Kridel SJ, Cui J, Strongin A, Smith JW, Liddington RC, Lipton SA. S-nitrosylation of matrix metalloproteinases: signaling pathway to neuronal cell death. *Science.* 2002; 297: 1186-1190.

40. Sariahmetoglu M, Crawford BD, Leon H, Sawicka J, Li L, Ballermann BJ, Holmes C, Berthiaume LG, Holt A, Sawicki G, Schulz R. Regulation of matrix metalloproteinase-2 (MMP-2) activity by phosphorylation. *FASEB J.* 2007; 21: 2486-2495.
41. Strongin AY, Collier I, Bannikov G, Marmer BL, Grant GA, Goldberg GI. Mechanism of cell surface activation of 72-kDa type IV collagenase. Isolation of the activated form of the membrane metalloprotease. *J Biol Chem.* 1995; 270: 5331-5338.
42. Sato H, Kinoshita T, Takino T, Nakayama K, Seiki M. Activation of a recombinant membrane type 1-matrix metalloproteinase (MT1-MMP) by furin and its interaction with tissue inhibitor of metalloproteinases (TIMP)-2. *FEBS Lett.* 1996; 393: 101-104.
43. Pei D, Weiss SJ. Furin-dependent intracellular activation of the human stromelysin-3 zymogen. *Nature.* 1995; 375: 244-247.
44. Okamoto T, Akaike T, Nagano T, Miyajima S, Suga M, Ando M, Ichimori K, Maeda H. Activation of human neutrophil procollagenase by nitrogen dioxide and peroxynitrite: a novel mechanism for procollagenase activation involving nitric oxide. *Arch Biochem Biophys.* 1997; 342: 261-274.
45. Fratelli M, Demol H, Puype M, Casagrande S, Eberini I, Salmona M, Bonetto V, Mengozzi M, Duffieux F, Miclet E, Bachi A, Vandekerckhove J, Gianazza E, Ghezzi P. Identification by redox proteomics of glutathionylated proteins in oxidatively stressed human T lymphocytes. *Proc Natl Acad Sci U S A.* 2002; 99: 3505-3510.
46. Huang KP, Huang FL. Glutathionylation of proteins by glutathione disulfide S-oxide. *Biochem Pharmacol.* 2002; 64: 1049-1056.

47. Owens MW, Milligan SA, Jourd'heuil D, Grisham MB. Effects of reactive metabolites of oxygen and nitrogen on gelatinase A activity. *Am J Physiol.* 1997; 273: L445-50.
48. Rajagopalan S, Meng XP, Ramasamy S, Harrison DG, Galis ZS. Reactive oxygen species produced by macrophage-derived foam cells regulate the activity of vascular matrix metalloproteinases in vitro. Implications for atherosclerotic plaque stability. *J Clin Invest.* 1996; 98: 2572-2579.
49. Viappiani S, Nicolescu AC, Holt A, Sawicki G, Crawford BD, Leon H, van Mulligen T, Schulz R. Activation and modulation of 72kDa matrix metalloproteinase-2 by peroxynitrite and glutathione. *Biochem Pharmacol.* 2009; 77: 826-834.
50. Finkel T. Signal transduction by reactive oxygen species in non-phagocytic cells. *J Leukoc Biol.* 1999; 65: 337-340.
51. Nyalendo C, Michaud M, Beaulieu E, Roghi C, Murphy G, Gingras D, Beliveau R. Src-dependent phosphorylation of membrane type I matrix metalloproteinase on cytoplasmic tyrosine 573: role in endothelial and tumor cell migration. *J Biol Chem.* 2007; 282: 15690-15699.
52. Williams KC, Coppolino MG. Phosphorylation of membrane-type 1-matrix metalloproteinase (MT1-MMP) and its vesicle-associated membrane protein 7 (VAMP7)-dependent trafficking facilitate cell invasion and migration. *J Biol Chem.* 2011; .
53. Brooks PC, Stromblad S, Sanders LC, von Schalscha TL, Aimes RT, Stetler-Stevenson WG, Quigley JP, Cheresh DA. Localization of matrix metalloproteinase MMP-2 to the surface of invasive cells by interaction with integrin alpha v beta 3. *Cell.* 1996; 85: 683-693.

54. Yu Q, Stamenkovic I. Cell surface-localized matrix metalloproteinase-9 proteolytically activates TGF-beta and promotes tumor invasion and angiogenesis. *Genes Dev.* 2000; 14: 163-176.
55. Yu WH, Woessner JF, Jr. Heparan sulfate proteoglycans as extracellular docking molecules for matrilysin (matrix metalloproteinase 7). *J Biol Chem.* 2000; 275: 4183-4191.
56. Wang W, Schulze CJ, Suarez-Pinzon WL, Dyck JR, Sawicki G, Schulz R. Intracellular action of matrix metalloproteinase-2 accounts for acute myocardial ischemia and reperfusion injury. *Circulation.* 2002; 106: 1543-1549.
57. Sawicki G, Leon H, Sawicka J, Sariahmetoglu M, Schulze CJ, Scott PG, Szczesna-Cordary D, Schulz R. Degradation of myosin light chain in isolated rat hearts subjected to ischemia-reperfusion injury: a new intracellular target for matrix metalloproteinase-2. *Circulation.* 2005; 112: 544-552.
58. Kwan JA, Schulze CJ, Wang W, Leon H, Sariahmetoglu M, Sung M, Sawicka J, Sims DE, Sawicki G, Schulz R. Matrix metalloproteinase-2 (MMP-2) is present in the nucleus of cardiac myocytes and is capable of cleaving poly (ADP-ribose) polymerase (PARP) in vitro. *FASEB J.* 2004; 18: 690-692.
59. Aldonyte R, Brantly M, Block E, Patel J, Zhang J. Nuclear localization of active matrix metalloproteinase-2 in cigarette smoke-exposed apoptotic endothelial cells. *Exp Lung Res.* 2009; 35: 59-75.
60. Puyraimond A, Fridman R, Lemesle M, Arbeille B, Menashi S. MMP-2 colocalizes with caveolae on the surface of endothelial cells. *Exp Cell Res.* 2001; 262: 28-36.

61. Chow AK, Cena J, El-Yazbi AF, Crawford BD, Holt A, Cho WJ, Daniel EE, Schulz R. Caveolin-1 inhibits matrix metalloproteinase-2 activity in the heart. *J Mol Cell Cardiol.* 2007; 42: 896-901.
62. Gratton JP, Bernatchez P, Sessa WC. Caveolae and caveolins in the cardiovascular system. *Circ Res.* 2004; 94: 1408-1417.
63. Feron O, Balligand JL. Caveolins and the regulation of endothelial nitric oxide synthase in the heart. *Cardiovasc Res.* 2006; 69: 788-797.
64. Atkinson SJ, English JL, Holway N, Murphy G. Cellular cholesterol regulates MT1 MMP dependent activation of MMP 2 via MEK-1 in HT1080 fibrosarcoma cells. *FEBS Lett.* 2004; 566: 65-70.
65. Fiucci G, Ravid D, Reich R, Liscovitch M. Caveolin-1 inhibits anchorage-independent growth, anoikis and invasiveness in MCF-7 human breast cancer cells. *Oncogene.* 2002; 21: 2365-2375.
66. Smart EJ, Ying YS, Conrad PA, Anderson RG. Caveolin moves from caveolae to the Golgi apparatus in response to cholesterol oxidation. *J Cell Biol.* 1994; 127: 1185-1197.
67. Fielding CJ, Bist A, Fielding PE. Caveolin mRNA levels are up-regulated by free cholesterol and down-regulated by oxysterols in fibroblast monolayers. *Proc Natl Acad Sci U S A.* 1997; 94: 3753-3758.
68. Parat MO, Stachowicz RZ, Fox PL. Oxidative stress inhibits caveolin-1 palmitoylation and trafficking in endothelial cells. *Biochem J.* 2002; 361: 681-688.
69. Baker AH, Edwards DR, Murphy G. Metalloproteinase inhibitors: biological actions and therapeutic opportunities. *J Cell Sci.* 2002; 115: 3719-3727.

70. Brew K, Dinakarbandian D, Nagase H. Tissue inhibitors of metalloproteinases: evolution, structure and function. *Biochim Biophys Acta*. 2000; 1477: 267-283.
71. Nuttall RK, Sampieri CL, Pennington CJ, Gill SE, Schultz GA, Edwards DR. Expression analysis of the entire MMP and TIMP gene families during mouse tissue development. *FEBS Lett*. 2004; 563: 129-134.
72. Greene J, Wang M, Liu YE, Raymond LA, Rosen C, Shi YE. Molecular cloning and characterization of human tissue inhibitor of metalloproteinase 4. *J Biol Chem*. 1996; 271: 30375-30380.
73. Schulze CJ, Wang W, Suarez-Pinzon WL, Sawicka J, Sawicki G, Schulz R. Imbalance between tissue inhibitor of metalloproteinase-4 and matrix metalloproteinases during acute myocardial [correction of myoectardial] ischemia-reperfusion injury. *Circulation*. 2003; 107: 2487-2492.
74. Pavloff N, Staskus PW, Kishnani NS, Hawkes SP. A new inhibitor of metalloproteinases from chicken: ChIMP-3. A third member of the TIMP family. *J Biol Chem*. 1992; 267: 17321-17326.
75. Fedak PW, Smookler DS, Kassiri Z, Ohno N, Leco KJ, Verma S, Mickle DA, Watson KL, Hojilla CV, Cruz W, Weisel RD, Li RK, Khokha R. TIMP-3 deficiency leads to dilated cardiomyopathy. *Circulation*. 2004; 110: 2401-2409.
76. Gasson JC, Bersch N, Golde DW. Characterization of purified human erythroid-potentiating activity. *Prog Clin Biol Res*. 1985; 184: 95-104.
77. Stetler-Stevenson WG, Bersch N, Golde DW. Tissue inhibitor of metalloproteinase-2 (TIMP-2) has erythroid-potentiating activity. *FEBS Lett*. 1992; 296: 231-234.

78. Qi JH, Ebrahim Q, Moore N, Murphy G, Claesson-Welsh L, Bond M, Baker A, Anand-Apte B. A novel function for tissue inhibitor of metalloproteinases-3 (TIMP3): inhibition of angiogenesis by blockage of VEGF binding to VEGF receptor-2. *Nat Med.* 2003; 9: 407-415.
79. Linask KK, Han M, Cai DH, Brauer PR, Maisastry SM. Cardiac morphogenesis: matrix metalloproteinase coordination of cellular mechanisms underlying heart tube formation and directionality of looping. *Dev Dyn.* 2005; 233: 739-753.
80. Ratajska A, Cleutjens JP. Embryogenesis of the rat heart: the expression of collagenases. *Basic Res Cardiol.* 2002; 97: 189-197.
81. Cai W, Vosschulte R, Afsah-Hedjri A, Koltai S, Kocsis E, Scholz D, Kostin S, Schaper W, Schaper J. Altered balance between extracellular proteolysis and antiproteolysis is associated with adaptive coronary arteriogenesis. *J Mol Cell Cardiol.* 2000; 32: 997-1011.
82. Alexander SM, Jackson KJ, Bushnell KM, McGuire PG. Spatial and temporal expression of the 72-kDa type IV collagenase (MMP-2) correlates with development and differentiation of valves in the embryonic avian heart. *Dev Dyn.* 1997; 209: 261-268.
83. Enciso JM, Gratzinger D, Camenisch TD, Canosa S, Pinter E, Madri JA. Elevated glucose inhibits VEGF-A-mediated endocardial cushion formation: modulation by PECAM-1 and MMP-2. *J Cell Biol.* 2003; 160: 605-615.
84. Zhang J, Bai S, Zhang X, Nagase H, Sarras MP, Jr. The expression of gelatinase A (MMP-2) is required for normal development of zebrafish embryos. *Dev Genes Evol.* 2003; 213: 456-463.

85. Itoh T, Ikeda T, Gomi H, Nakao S, Suzuki T, Itohara S. Unaltered secretion of beta-amyloid precursor protein in gelatinase A (matrix metalloproteinase 2)-deficient mice. *J Biol Chem.* 1997; 272: 22389-22392.
86. Cheng XW, Kuzuya M, Nakamura K, Maeda K, Tsuzuki M, Kim W, Sasaki T, Liu Z, Inoue N, Kondo T, Jin H, Numaguchi Y, Okumura K, Yokota M, Iguchi A, Murohara T. Mechanisms underlying the impairment of ischemia-induced neovascularization in matrix metalloproteinase 2-deficient mice. *Circ Res.* 2007; 100: 904-913.
87. Yasmin W, Strynadka KD, Schulz R. Generation of peroxynitrite contributes to ischemia-reperfusion injury in isolated rat hearts. *Cardiovasc Res.* 1997; 33: 422-432.
88. Yellon DM, Hausenloy DJ. Myocardial reperfusion injury. *N Engl J Med.* 2007; 357: 1121-1135.
89. Frears ER, Zhang Z, Blake DR, O'Connell JP, Winyard PG. Inactivation of tissue inhibitor of metalloproteinase-1 by peroxynitrite. *FEBS Lett.* 1996; 381: 21-24.
90. Donnini S, Monti M, Roncone R, Morbidelli L, Rocchigiani M, Oliviero S, Casella L, Giachetti A, Schulz R, Ziche M. Peroxynitrite inactivates human-tissue inhibitor of metalloproteinase-4. *FEBS Lett.* 2008; 582: 1135-1140.
91. Cheung PY, Sawicki G, Wozniak M, Wang W, Radomski MW, Schulz R. Matrix metalloproteinase-2 contributes to ischemia-reperfusion injury in the heart. *Circulation.* 2000; 101: 1833-1839.
92. Prasan AM, McCarron HC, White MY, McLennan SV, Tchen AS, Hambly BD, Jeremy RW. Duration of ischaemia determines matrix metalloproteinase-2 activation in the reperfused rabbit heart. *Proteomics.* 2002; 2: 1204-1210.

93. Inokubo Y, Hanada H, Ishizaka H, Fukushi T, Kamada T, Okumura K. Plasma levels of matrix metalloproteinase-9 and tissue inhibitor of metalloproteinase-1 are increased in the coronary circulation in patients with acute coronary syndrome. *Am Heart J.* 2001; 141: 211-217.
94. Lalu MM, Pasini E, Schulze CJ, Ferrari-Vivaldi M, Ferrari-Vivaldi G, Bachetti T, Schulz R. Ischaemia-reperfusion injury activates matrix metalloproteinases in the human heart. *Eur Heart J.* 2005; 26: 27-35.
95. Wang W, Sawicki G, Schulz R. Peroxynitrite-induced myocardial injury is mediated through matrix metalloproteinase-2. *Cardiovasc Res.* 2002; 53: 165-174.
96. Leon H, Baczko I, Sawicki G, Light PE, Schulz R. Inhibition of matrix metalloproteinases prevents peroxynitrite-induced contractile dysfunction in the isolated cardiac myocyte. *Br J Pharmacol.* 2008; 153: 676-683.
97. Mukherjee R, Mingoia JT, Bruce JA, Austin JS, Stroud RE, Escobar GP, McClister DM, Jr, Allen CM, Alfonso-Jaume MA, Fini ME, Lovett DH, Spinale FG. Selective spatiotemporal induction of matrix metalloproteinase-2 and matrix metalloproteinase-9 transcription after myocardial infarction. *Am J Physiol Heart Circ Physiol.* 2006; 291: H2216-28.
98. Wang GY, Bergman MR, Nguyen AP, Turcato S, Swigart PM, Rodrigo MC, Simpson PC, Karliner JS, Lovett DH, Baker AJ. Cardiac transgenic matrix metalloproteinase-2 expression directly induces impaired contractility. *Cardiovasc Res.* 2006; 69: 688-696.
99. Bergman MR, Teerlink JR, Mahimkar R, Li L, Zhu BQ, Nguyen A, Dahi S, Karliner JS, Lovett DH. Cardiac matrix metalloproteinase-2 expression independently induces

marked ventricular remodeling and systolic dysfunction. *Am J Physiol Heart Circ Physiol.* 2007; 292: H1847-60.

100. Zhou HZ, Ma X, Gray MO, Zhu BQ, Nguyen AP, Baker AJ, Simonis U, Cecchini G, Lovett DH, Karliner JS. Transgenic MMP-2 expression induces latent cardiac mitochondrial dysfunction. *Biochem Biophys Res Commun.* 2007; 358: 189-195.

101. Brenner DA, O'Hara M, Angel P, Chojkier M, Karin M. Prolonged activation of jun and collagenase genes by tumour necrosis factor-alpha. *Nature.* 1989; 337: 661-663.

102. Mountain DJ, Singh M, Menon B, Singh K. Interleukin-1beta increases expression and activity of matrix metalloproteinase-2 in cardiac microvascular endothelial cells: role of PKCalpha/beta1 and MAPKs. *Am J Physiol Cell Physiol.* 2007; 292: C867-75.

103. Kearney MT, Cotton JM, Richardson PJ, Shah AM. Viral myocarditis and dilated cardiomyopathy: mechanisms, manifestations, and management. *Postgrad Med J.* 2001; 77: 4-10.

104. Cheung C, Luo H, Yanagawa B, Leong HS, Samarasekera D, Lai JC, Suarez A, Zhang J, McManus BM. Matrix metalloproteinases and tissue inhibitors of metalloproteinases in coxsackievirus-induced myocarditis. *Cardiovasc Pathol.* 2006; 15: 63-74.

105. Heymans S, Pauschinger M, De Palma A, Kallwellis-Opara A, Rutschow S, Swinnen M, Vanhoutte D, Gao F, Torpai R, Baker AH, Padalko E, Neyts J, Schultheiss HP, Van de Werf F, Carmeliet P, Pinto YM. Inhibition of urokinase-type plasminogen activator or matrix metalloproteinases prevents cardiac injury and dysfunction during viral myocarditis. *Circulation.* 2006; 114: 565-573.

106. Westermann D, Savvatis K, Lindner D, Zietsch C, Becher PM, Hammer E, Heimesaat MM, Bereswill S, Volker U, Escher F, Riad A, Plendl J, Klingel K, Poller W, Schultheiss HP, Tschöpe C. Reduced Degradation of the Chemokine MCP-3 by Matrix Metalloproteinase-2 Exacerbates Myocardial Inflammation in Experimental Viral Cardiomyopathy. *Circulation*. 2011; 124: 2082-2093.
107. Gao CQ, Sawicki G, Suarez-Pinzon WL, Csont T, Wozniak M, Ferdinandy P, Schulz R. Matrix metalloproteinase-2 mediates cytokine-induced myocardial contractile dysfunction. *Cardiovasc Res*. 2003; 57: 426-433.
108. Gottlieb RA, Bursleson KO, Kloner RA, Babior BM, Engler RL. Reperfusion injury induces apoptosis in rabbit cardiomyocytes. *J Clin Invest*. 1994; 94: 1621-1628.
109. Olivetti G, Quaini F, Sala R, Lagrasta C, Corradi D, Bonacina E, Gambert SR, Cigola E, Anversa P. Acute myocardial infarction in humans is associated with activation of programmed myocyte cell death in the surviving portion of the heart. *J Mol Cell Cardiol*. 1996; 28: 2005-2016.
110. Menon B, Singh M, Singh K. Matrix metalloproteinases mediate beta-adrenergic receptor-stimulated apoptosis in adult rat ventricular myocytes. *Am J Physiol Cell Physiol*. 2005; 289: C168-76.
111. Menon B, Singh M, Ross RS, Johnson JN, Singh K. beta-Adrenergic receptor-stimulated apoptosis in adult cardiac myocytes involves MMP-2-mediated disruption of beta1 integrin signaling and mitochondrial pathway. *Am J Physiol Cell Physiol*. 2006; 290: C254-61.

112. Menon B, Johnson JN, Ross RS, Singh M, Singh K. Glycogen synthase kinase-3beta plays a pro-apoptotic role in beta-adrenergic receptor-stimulated apoptosis in adult rat ventricular myocytes: Role of beta1 integrins. *J Mol Cell Cardiol.* 2007; 42: 653-661.
113. Kandasamy AD, Schulz R. Glycogen synthase kinase-3beta is activated by matrix metalloproteinase-2 mediated proteolysis in cardiomyoblasts. *Cardiovasc Res.* 2009; 83: 698-706.
114. Shen J, O'Brien D, Xu Y. Matrix metalloproteinase-2 contributes to tumor necrosis factor alpha induced apoptosis in cultured rat cardiac myocytes. *Biochem Biophys Res Commun.* 2006; 347: 1011-1020.
115. Shapiro S, Khodalev O, Bitterman H, Auslender R, Lahat N. Different activation forms of MMP-2 oppositely affect the fate of endothelial cells. *Am J Physiol Cell Physiol.* 2010; 298: C942-51.
116. Yarbrough WM, Mukherjee R, Stroud RE, Meyer EC, Escobar GP, Sample JA, Hendrick JW, Mingoia JT, Spinale FG. Caspase inhibition modulates left ventricular remodeling following myocardial infarction through cellular and extracellular mechanisms. *J Cardiovasc Pharmacol.* 2010; 55: 408-416.
117. Wainwright CL. Matrix metalloproteinases, oxidative stress and the acute response to acute myocardial ischaemia and reperfusion. *Curr Opin Pharmacol.* 2004; 4: 132-138.
118. Brauer PR. MMPs--role in cardiovascular development and disease. *Front Biosci.* 2006; 11: 447-478.
119. Rouet-Benzineb, P. Perennec, J. Delcourt, A. Franco-Montoya, M.L. Dreyfus, P. Frisdal, E. Hart, A. Crozatir, B. Lafuma, C. Cardiac gelatinase expression and

involvement in human dilated cardiomyopathy.[Abstract]. *Circulation*. 1998; 98 (Suppl I): 626.

120. Ali MA, Cho WJ, Hudson B, Kassiri Z, Granzier H, Schulz R. Titin is a target of matrix metalloproteinase-2: implications in myocardial ischemia/reperfusion injury. *Circulation*. 2010; 122: 2039-2047.

121. Hein S, Scheffold T, Schaper J. Ischemia induces early changes to cytoskeletal and contractile proteins in diseased human myocardium. *J Thorac Cardiovasc Surg*. 1995; 110: 89-98.

122. Matsumura Y, Saeki E, Inoue M, Hori M, Kamada T, Kusuoka H. Inhomogeneous disappearance of myofilament-related cytoskeletal proteins in stunned myocardium of guinea pig. *Circ Res*. 1996; 79: 447-454.

123. Van Eyk JE, Powers F, Law W, Larue C, Hodges RS, Solaro RJ. Breakdown and release of myofilament proteins during ischemia and ischemia/reperfusion in rat hearts: identification of degradation products and effects on the pCa-force relation. *Circ Res*. 1998; 82: 261-271.

124. Coker ML, Doscher MA, Thomas CV, Galis ZS, Spinale FG. Matrix metalloproteinase synthesis and expression in isolated LV myocyte preparations. *Am J Physiol*. 1999; 277: H777-87.

125. Sung MM, Schulz CG, Wang W, Sawicki G, Bautista-Lopez NL, Schulz R. Matrix metalloproteinase-2 degrades the cytoskeletal protein alpha-actinin in peroxynitrite mediated myocardial injury. *J Mol Cell Cardiol*. 2007; 43: 429-436.

126. Yang Y, Candelario-Jalil E, Thompson JF, Cuadrado E, Estrada EY, Rosell A, Montaner J, Rosenberg GA. Increased intranuclear matrix metalloproteinase activity in neurons interferes with oxidative DNA repair in focal cerebral ischemia. *J Neurochem.* 2010; 112: 134-149.
127. Si-Tayeb K, Monvoisin A, Mazzocco C, Lepreux S, Decossas M, Cubel G, Taras D, Blanc JF, Robinson DR, Rosenbaum J. Matrix metalloproteinase 3 is present in the cell nucleus and is involved in apoptosis. *Am J Pathol.* 2006; 169: 1390-1401.
128. Jackson DA, Cook PR. The structural basis of nuclear function. *Int Rev Cytol.* 1995; 162A: 125-149.
129. Martelli AM, Bareggi R, Bortul R, Grill V, Narducci P, Zweyer M. The nuclear matrix and apoptosis. *Histochem Cell Biol.* 1997; 108: 1-10.
130. Georgi AB, Stukenberg PT, Kirschner MW. Timing of events in mitosis. *Curr Biol.* 2002; 12: 105-114.
131. Owen CA, Campbell EJ. Neutrophil proteinases and matrix degradation. The cell biology of pericellular proteolysis. *Semin Cell Biol.* 1995; 6: 367-376.
132. Moshal KS, Tipparaju SM, Vacek TP, Kumar M, Singh M, Frank IE, Patibandla PK, Tyagi N, Rai J, Metreveli N, Rodriguez WE, Tseng MT, Tyagi SC. Mitochondrial matrix metalloproteinase activation decreases myocyte contractility in hyperhomocysteinemia. *Am J Physiol Heart Circ Physiol.* 2008; 295: H890-7.
133. Limb GA, Matter K, Murphy G, Cambrey AD, Bishop PN, Morris GE, Khaw PT. Matrix metalloproteinase-1 associates with intracellular organelles and confers resistance to lamin A/C degradation during apoptosis. *Am J Pathol.* 2005; 166: 1555-1563.

134. Zimmet JM, Hare JM. Nitroso-redox interactions in the cardiovascular system. *Circulation*. 2006; 114: 1531-1544.
135. McCord JM, Fridovich I. The reduction of cytochrome c by milk xanthine oxidase. *J Biol Chem*. 1968; 243: 5753-5760.
136. Berry CE, Hare JM. Xanthine oxidoreductase and cardiovascular disease: molecular mechanisms and pathophysiological implications. *J Physiol*. 2004; 555: 589-606.
137. Berge RK, Aarsland A. Correlation between the cellular level of long-chain acyl-CoA, peroxisomal beta-oxidation, and palmitoyl-CoA hydrolase activity in rat liver. Are the two enzyme systems regulated by a substrate-induced mechanism? *Biochim Biophys Acta*. 1985; 837: 141-151.
138. Valko M, Leibfritz D, Moncol J, Cronin MT, Mazur M, Telser J. Free radicals and antioxidants in normal physiological functions and human disease. *Int J Biochem Cell Biol*. 2007; 39: 44-84.
139. Michel T, Feron O. Nitric oxide synthases: which, where, how, and why? *J Clin Invest*. 1997; 100: 2146-2152.
140. Pacher P, Beckman JS, Liaudet L. Nitric oxide and peroxynitrite in health and disease. *Physiol Rev*. 2007; 87: 315-424.
141. Pastor N, Weinstein H, Jamison E, Brenowitz M. A detailed interpretation of OH radical footprints in a TBP-DNA complex reveals the role of dynamics in the mechanism of sequence-specific binding. *J Mol Biol*. 2000; 304: 55-68.

142. Sawa T, Akaike T, Maeda H. Tyrosine nitration by peroxynitrite formed from nitric oxide and superoxide generated by xanthine oxidase. *J Biol Chem.* 2000; 275: 32467-32474.
143. Radi R. Nitric oxide, oxidants, and protein tyrosine nitration. *Proc Natl Acad Sci U S A.* 2004; 101: 4003-4008.
144. Adachi T, Weisbrod RM, Pimentel DR, Ying J, Sharov VS, Schoneich C, Cohen RA. S-Glutathiolation by peroxynitrite activates SERCA during arterial relaxation by nitric oxide. *Nat Med.* 2004; 10: 1200-1207.
145. Weiss SJ, Peppin G, Ortiz X, Ragsdale C, Test ST. Oxidative autoactivation of latent collagenase by human neutrophils. *Science.* 1985; 227: 747-749.
146. Hare JM, Stamler JS. NO/redox disequilibrium in the failing heart and cardiovascular system. *J Clin Invest.* 2005; 115: 509-517.
147. Little SA, de Haen C. Effects of hydrogen peroxide on basal and hormone-stimulated lipolysis in perfused rat fat cells in relation to the mechanism of action of insulin. *J Biol Chem.* 1980; 255: 10888-10895.
148. May JM, de Haen C. Insulin-stimulated intracellular hydrogen peroxide production in rat epididymal fat cells. *J Biol Chem.* 1979; 254: 2214-2220.

CHAPTER 2

Mechanism of cytosolic targeting of matrix metalloproteinase-2

A version of this chapter is published in:

Ali MA, Chow A, Kandasamy A, Fan X, West L, Crawford B, Simmen T, Schulz R.
Mechanisms of cytosolic targeting of matrix metalloproteinase-2. *Journal of Cellular
Physiology* in press.

2.1: Introduction

MMP-2 is widely considered to be a secreted, zinc-dependent protease that primarily targets extracellular matrix proteins. However, an increasing number of studies shows that MMP-2 can also cleave cytosolic substrates and thereby modulate diverse cell functions including cardiomyocyte contractility, proliferation, apoptosis and transcription¹⁻³. For example, upon oxidative stress injury in the heart, MMP-2 proteolyzes cytosolic targets including TnI^{4, 5}, α -actinin⁶ and MLC-1⁷. Cleavage of these and other substrates by MMP-2 results in acute myocardial contractile dysfunction, underscoring the importance of a portion of MMP-2 that is not entering the secretory pathway.

The cytosolic enzymatic activity of MMP-2 is consistent with multiple demonstrations that MMP-2 itself is localized to the cardiac sarcomere^{4, 5}. Moreover, MMP-2 activity has been detected on mitochondria⁴ and nuclei⁸. Evidence for all of these localizations has been provided by immunogold electron microscopy, confocal microscopy, immunoprecipitation experiments and zymographic analysis (see¹ for review). Surprisingly however, to date no biological mechanism has been described that could account for this unusual intracellular and extracellular distribution. Yet, MMP-2 is a known substrate for cytosol-associated post-translational modifications including phosphorylation⁹ and glutathiolation¹⁰, which alter its enzymatic activity. Together with the ever-increasing number of known intracellular substrates, these post-translational modifications suggest that a significant portion of MMP-2 fails to enter the secretory pathway and instead remains in the cytosol.

MMP-2 possesses a signal sequence which allows its entry into the endoplasmic reticulum (ER) lumen for secretion ¹¹. Here we examined whether the presence and efficiency of the MMP-2 signal sequence could account for these intracellular moieties of MMP-2 that are critical for its biological functions in the heart and other tissues. The recognition of signal sequence at the ER can determine protein secretion efficiencies and subcellular localizations ¹²⁻¹⁴. For instance, BiP and ERp44 (ER resident chaperone proteins) were shown to have signal sequences that allow for their efficient translocation into the ER ^{15, 16}. Therefore, we hypothesized that the signal sequence efficiency of canonical MMP-2 could determine its unusual partitioning between the cytosol and the secretory pathway. Additionally, we scanned cDNA databases for the presence of different transcript variants of MMP-2, which could also account for its inefficient import into the ER, since such variants are known for several other MMPs, e.g. MMP-16 ¹⁷. Indeed, we were able to identify a splice variant MMP-2 that entirely lacks the canonical MMP-2 signal sequence. Together, our findings show that it is a combination of the MMP-2 signal sequence efficiency, as well as its splicing that dictate its distribution between the cytosol and the secretory pathway.

2.2: Materials and Methods

This investigation conforms to the *Guide to the Care and Use of Experimental Animals* published by the Canadian Council on Animal Care, and was approved by the respective Institutional Animal Care and Use Committee.

2.2.1: Quantitative RT-PCR

For comparative quantification of splice variant MMP-2 and canonical MMP-2 expression in human cardiomyocytes, we obtained neonatal and adult human

cardiomyocyte cDNA from ScienCell Research Laboratories. Briefly, purified human cardiomyocytes isolated from neonatal or adult hearts were pooled and total RNA were extracted. The total RNA were reverse transcribed into first strand cDNA using Applied Biosystems' High-Capacity cDNA Reverse Transcription kits with RNase Inhibitor. The cDNA quality was determined by the A_{260}/A_{280} ratio using a Beckman Coulter DU 800 spectrophotometer. qPCR amplification was done with each cDNA at empirically determined optimal concentrations of forward and reverse primers and a FAM-labeled TaqMan probe using a TaqMan Fast Universal PCR Master kit. Primers and probes were specifically designed on the first exon where the different sequences were located for splice variant or canonical MMP-2. The primers and probes used in this study were designed as follows:

Splice-variant-MMP2-forward primer:

(5'-GAATGAAGCACAGCAGGTCTCA-3'),

Splice-variant-MMP2-reverse primer:

(5'-CAAACCAGGCACCTCCATCT-3'),

Splice-variant-MMP2-Probe:

(5'FAM-CCTCATCTT/ZEN/ACCCAGCCCCCACTC-IABkFQ-3'),

Canonical-MMP2-forward primer:

(5'-GGCTGCCCTCCCTTGTTT-3'),

Canonical-MMP2-reverse primer:

(5'-TGGCAATCCCTTTGTATGTTTAAA-3'),

Canonical-MMP2-Probe:

(5'-FAM-CATCCAGAC/ZEN/TTCCTCAGGCGGTGG-IABkFQ-3'),

GAPDH-forward primer:

(5'-GAAGGTGAAGGTCGGAGTCA-3'),

GAPDH-reverse primer:

(5'-GAAGATGGTGATGGGATTTC-3'),

GAPDH-Probe:

(5'-FAM-CAAGCTTC/ZEN/CCGTTCTCAGCC-IABkFQ-3').

Cycling conditions were as follows: initial denaturation at 95°C for 20 sec, followed by 40 cycles at 95°C for 1 sec, then 60°C for 30 sec using a CFX96 real-time PCR system (Bio-Rad). Triplicate reactions were performed for all samples and the relative quantification of splice variant MMP-2 mRNA expression levels was calculated by the comparative C_T method.

2.2.2: Construction of expression vectors harbouring different MMP-2 variants or mutants

The canonical-, splice variant-, BiP- and ERp44-MMP-2 sequences were amplified from full length human MMP-2 cDNA (Invitrogen) by *high fidelity* PCR using specific primers (Sigma) listed in Table 2.1. PCR products were subcloned into pcDNA3 (Invitrogen) between the EcoRI and XhoI restriction sites. The constructs were expressed as C-terminal hemagglutinin (HA)-tagged chimeras. The N-terminus HA-tagged (right after the signal sequence) MMP-2-BiP was amplified by PCR from human BiP cDNA

(Invitrogen) and subcloned into pcDNA3 between the KpnI and XhoI restriction sites. All constructs were verified by DNA sequencing (Molecular Biology Facility, Department of Biological Sciences, University of Alberta). Figure 2.1 shows the schematic diagram of all chimeras made for this study.

2.2.3: Cell culture, transfection and subcellular fractionation

HeLa and HEK 293 cells were cultured as described¹⁸. For transient transfection, the pcDNA3 constructs (and empty vector for control) were transfected into HeLa or HEK 293 cells using Lipofectamine 2000 (Invitrogen) by following the manufacturer's instructions. After 24 h, cells were transferred to serum-free medium (Opti-MEM, Gibco®) and conditioned media and cells were collected 24 h later. The cytosolic and membrane fractions were prepared using a Qproteome Cell Compartment Kit (Qiagen). In brief, cells were trypsinized by adding 500 µl trypsin (0.25%, Gibco®) for 5 min at 37°C and the cell suspension was collected using 2 ml DMEM medium. The cells were pelleted down by centrifugation (500 xg for 10 min) and by sequential addition of different extraction buffers to a cell pellet, proteins in the different cellular compartments can be selectively isolated. Extraction Buffer CE1 is added to cells and selectively disrupts the plasma membrane without solubilizing it, resulting in the isolation of cytosolic proteins in the supernatant (cytosolic fraction). Compartmentalized organelles such as ER, Golgi apparatus, secretory vesicles, mitochondria and nuclei remain intact and are pelleted by centrifugation (1000 xg, 10 min, 4°C). The pellet is then resuspended in Extraction Buffer CE2, which solubilizes all organelle membranes except the nuclear membrane. After solubilization, the sample is centrifuged (6000 xg, 10 min, 4°C) and this supernatant contains proteins from the lumen of organelles, e.g. ER and secretory vesicles (membrane fraction).

To determine the intracellular proportion of endogenous MMP-2 in HEK 293 cells versus that of the expressed canonical or splice variant MMP-2, cells, either non-transfected control (for endogenous MMP-2) or transfected with pcDNA3 expressing canonical or splice variant MMP-2, were used. After 24 h, cells were transferred into serum-free medium and conditioned media and cell lysates were collected at different time intervals (0, 1, 2, 4 and 8 h). The secreted MMP-2 in the media was precipitated by adding 4 volumes of -20°C acetone and incubating for 1 h at -20°C. The pellet was centrifuged for 10 min at 15,000 x g and the supernatant was carefully decanted in order to not dislodge the protein pellet which was then dried by allowing the acetone to evaporate at room temperature for 10-15 min. Over drying of the pellet was avoided. The pellet was dissolved in 200 µl of 2X sample buffer (100 mM Tris-HCl, 10% glycerol, 3% SDS, 4 mg% bromophenol blue) and boiled for 5 min and the corresponding cell lysates were prepared by sonication using 200 µl 2X sample buffer. The same proportions from both the media and the cell lysates were loaded and examined using 10% SDS-PAGE. Secreted MMP-2 (in media) in comparison to intracellular MMP-2 (in cell lysates) were blotted using either anti-MMP-2 (for endogenous MMP-2) or anti-HA (for canonical and splice variant MMP-2). See Table 2.2 for details of the primary antibodies used in this study.

2.2.4: MG-132 or bafilomycin A1 treatment

To assess whether splice variant MMP-2 is more susceptible to intracellular degradation than canonical MMP-2, HEK 293 cells expressing canonical or splice variant MMP-2 were treated with 10 µM MG-132 (proteasome inhibitor) or 100 nM bafilomycin A1 (lysosome inhibitor) for 4 h according to Oberdorf et al.¹⁹ or Ge et al.,²⁰ respectively. The cells were lysed in RIPA buffer (Sigma-Aldrich, St Louis, MO) and cell lysates were

centrifuged at 12,000 g for 5 min to discard cell debris. 10 µg total proteins were loaded onto 10% SDS-PAGE and the expressed MMP-2 level was detected using anti-HA in non-treated control, MG-132 or bafilomycin A1 treated cells. Actin was used as a loading control and HA/actin ratios were used for quantification.

2.2.5: Protein assay

Protein concentration was assessed by the bicinchoninic acid method using bovine serum albumin as a reference standard.

2.2.6: Immunocytochemistry and confocal microscopy

Cells were washed with phosphate-buffered saline containing 1 mM CaCl₂ and 0.5 mM MgCl₂ (PBS²⁺) and fixed with 3% paraformaldehyde for 20 min. After washing with PBS²⁺, cells were permeabilized for 1 min with 0.1% Triton X-100, 0.2% bovine serum albumin in PBS²⁺. Cells were then incubated with primary antibodies (1:100 dilution) and secondary antibodies conjugated to either AlexaFluor 488 or 596 (Invitrogen) (1:2000 dilution) in PBS²⁺, 0.2% bovine serum albumin for 1 h each, interrupted with three washes using PBS²⁺. After the final wash cells were mounted in ProLong Antifade (Invitrogen). Images were obtained with a spinning disc confocal microscope (Olympus).

2.2.7: Western blotting and band quantification

Conditioned media or cell fractions were electrophoresed by 10% SDS-PAGE under reducing conditions. Samples were electroblotted onto PVDF membranes (Bio-Rad Laboratories) and probed with the corresponding antibodies (Table 2.2). After washing, PVDF membranes were probed with appropriate peroxidase-conjugated secondary antibodies, washed, and then protein bands were developed using the ECL detection kit

(GE Healthcare UK Limited, Buckinghamshire, UK) according to the manufacturer's instructions.

For quantification of MMP-2 levels in cytosolic vs. membrane fractions, equal percentage from each fraction was loaded onto SDS-PAGE. MMP-2 bands were developed as described above and scanned using a calibrated densitometer GS-800 (Biorad, Mississauga, ON) and the band intensities were analyzed by densitometric analysis using the ImageJ software program (NIH). Total MMP-2 was calculated as a sum of band intensities in both cytosolic and membrane fractions. The %MMP-2 in each fraction was calculated relative to total MMP-2 in both fractions.

2.2.8: Neonatal rat cardiomyocytes

Neonatal cardiomyocytes from 1- to 2-day-old Sprague–Dawley rats were isolated and cultured²¹ with modifications. Hearts from the rat pups were removed and the ventricles were minced and digested with collagenase II (0.10% w/v, Worthington, Lakewood, NJ), trypsin (0.05% w/v, Worthington) and DNase I (0.025% w/v, Worthington) in phosphate buffered saline at 37 °C for 20 min. After digestion the tissue was centrifuged at 114 x g for 1 min at 4 °C in 20 ml of DMEM F12 media (Sigma) containing 20% fetal bovine serum (Invitrogen), and 50 µg/ml gentamicin. The supernatant was discarded and the pellet was subsequently added to DNase/collagenase/trypsin buffer for further digestion at 37°C for 20 min. After a second digestion, the tissue was centrifuged at 114 x g for 1 min at 4°C and subjected to a third digestion. After this all the supernatant fractions were pooled and centrifuged at 300 x g for 7 min at 4°C. The resulting pellet was resuspended in 10 ml of plating media (DMEM F12 media containing 5% fetal bovine serum, 10% horse serum, 50 µg/ml gentamicin) and the cell suspension was filtered through a cell strainer (BD Biosciences) and

preplated for 60-90 min at 37°C to remove fibroblasts. The cells were added to 35 mm Primaria dishes (Falcon) at a density of $1.8\text{--}2.0 \times 10^6$ cells/dish.

2.2.9: Lentiviral vector production and transduction of cardiomyocytes

Lentiviral EF-1 vectors were produced from four expression plasmids bearing canonical-, splice variant-, BiP-, or ERp44-MMP-2. The HindIII and XbaI fragments digested from expression vectors harbouring different MMP-2 variants or mutants were blunted using T4 DNA polymerase (Fermentas). Purified DNA fragments were inserted into the PmeI site of the lentiviral expression plasmid pWPI. The sequence of the resulting plasmids were verified for the positioning our gene of interest downstream of the human EF1- α promoter and upstream of the EMCV IRES as well as enhanced green fluorescent protein (eGFP) reporter gene. An EMCV IRES element connected the inserts with eGFP assured co-transcription of the eGFP marker and our gene of interest. Four lentiviral constructs harbouring MMP-2 variants and mutants were denoted pEF1-canonical MMP2-GFP, pEF1-splice variant MMP2-GFP, pEF1-BiP-MMP2-GFP and pEF1-ERp44-MMP2-GFP respectively. To package lentiviral vectors, 293T cells were co-transfected with one of the expression plasmids, packaging plasmid pDelta 8.74 and vesicular stomatitis virus envelope expression plasmid pMD2G using the calcium phosphate method. Lentiviral EF-1 vectors were produced from four expression plasmids bearing canonical-, splice variant-, BiP-, or ERp44-MMP-2. Vector containing supernatants were harvested 72 h after transfection and filtered through 0.22 μm pore size cellulose acetate filters. The viral supernatants were serially diluted and titrated onto 293T cells. Concentration by ultracentrifugation yielded titers of up to 5×10^8 transducing units per ml. Lentiviral stock was either used immediately or stored at -80°C .

For transduction of cardiomyocytes, 1×10^6 neonatal cardiomyocytes were incubated overnight with 5×10^6 transduction units of lentiviral vector in the presence of 6 $\mu\text{g/ml}$ polybrene (Invitrogen). Supernatant was replaced with fresh media and cells were harvested 72 h after for subsequent assays.

2.2.10: Hypoxia-reoxygenation protocol

Neonatal cardiomyocytes transduced with lentiviral vectors for either canonical or splice variant MMP-2 were cultured in DMEM F12 media containing 5% fetal bovine serum, 10% horse serum, 50 $\mu\text{g/ml}$ gentamicin and incubated in a hypoxic chamber (82% N_2 , 18% CO_2 , $< 0.5\%$ O_2) at 37°C for 24 h. The cells were reoxygenated for 4 h at 37°C in ambient atmosphere (containing 5% CO_2) and replacing the hypoxic medium with fresh medium. Control cells (normoxia) were cultured for 28 h at 37°C in ambient atmosphere containing 5% CO_2 with one replacement of media 4 h before the end of the experiment. Where indicated, 10 μM ARP-100 (a selective MMP-2 inhibitor, Calbiochem) was added 1 h before the induction of hypoxia. Alternatively, the expression of MMP-2 was knocked down by transducing cardiomyocytes with a lentiviral vector harboring microRNA-adapted MMP-2 silencing shRNA (shRNA_{mir}) (V2LMM_21212, Open Biosystems) 24 h prior to hypoxia.

2.2.11: Statistical analysis

Results are expressed as mean \pm SEM for n individual experiments. As appropriate, Student's t -test or one-way ANOVA followed by Tukey's post-hoc test were used to analyze differences between groups. Differences were considered significant at $p < 0.05$.

2.3: Results

2.3.1: Presence of MMP-2 in the cytosol and distribution MMP-2 splicing variants

MMP-2 is a protease thought to enter the secretory pathway due to the presence of a 29 amino acid signal sequence at its N-terminus (Table 2.3). However, MMP-2 also resides outside the secretory pathway on thin myofilaments of cardiomyocytes⁴. These conflicting observations suggest that the targeting of MMP-2 to the secretory pathway might be incomplete or that alternative forms of MMP-2 exist that do not target to the secretory pathway. With the present study, we tested both possibilities. To do so, we first examined the localization of endogenous MMP-2 in HEK 293 cells by western blot, which can be easily transfected and could thus serve as a model system to examine MMP-2 targeting. Indeed, in non-transfected cells we were able to detect approximately 40% of endogenous MMP-2 in the cytosolic fraction and 60% in the membrane fraction (containing ER, Golgi and secretory vesicle membranes) of these cells (Figure 2.2). Subcellular fractionation procedure was validated with antibodies against GAPDH (cytosolic marker), calnexin (ER marker) and VAMP-3 (secretory vesicles marker). As shown in Figure 2.2 GAPDH was mainly detected in the cytosolic fraction, whereas the vast majority of calnexin and VAMP-3 were detected in the membrane fraction verifying fractions purity. These results also showed that HEK 293 cells can be used to study MMP-2 targeting.

Splicing can give rise to alternatively targeted protein variants. In the case of MMP-2 and, given a precedent of other MMP splice variants, we hypothesized that alternative splicing could give rise to intracellular MMP-2. We tested this hypothesis with

in silico searches for alternative transcripts of MMP-2. Our expressed sequence tag database searches identified a clone (“DB059054, FLJ project”) of MMP-2 (Figure 2.3A) which has an alternate first exon and gives rise to an N-terminally-truncated translation product lacking the first 50 amino acids containing the signal sequence of canonical MMP-2 (splice variant MMP-2). Using primers and TaqMan[®] probes specific for canonical and splice variant MMP-2, qRT-PCR analysis determined that this splice variant is present in both neonatal and adult human cardiomyocyte cDNA at 9% and 13% of the level of canonical MMP-2, respectively (Figure 2.3B). While these amounts are significant, they are still not close to the actual amounts of MMP-2 protein observed in the cytosol of HEK 293 cells. Therefore, our results suggested that the cytosolic targeting of MMP-2 could be achieved by additional mechanisms.

To further investigate this question, we next compared the intracellular targeting of canonical and splice variant MMP-2. To do so, we transfected canonical and splice variant MMP-2 constructs tagged with hemagglutinin (HA)-epitope at their C-termini into HEK 293 cells and examined their partitioning to the secretory pathway. As shown by immunoblotting, canonical MMP-2 was secreted into the medium, whereas splice variant MMP-2 was not, providing that HEK 293 cells were expressing canonical or splice variant MMP-2 to a similar level (Figure 2.3C). Furthermore, canonical MMP-2 was associated with ER, Golgi and secretory vesicle membranes, suggesting its proper targeting to the secretory pathway. However, consistent with the idea that splice variant MMP-2 only partially explains cytosolic MMP-2, a substantial fraction of canonical MMP-2 was also found in the cytosol (Figure 2.3D). Interestingly, titration of expression levels did not affect the proportion of canonical MMP-2 mistargeted to the cytosol (Figure 2.4), suggesting that our observation did not stem from excessive protein expression. Figure 2.5 shows that both canonical and splice variant MMP-2 were

subjected to a similarly low degree of intracellular degradation via either lysosomal (canonical MMP-2) or proteasomal (splice variant MMP-2) pathways. As expected, splice variant MMP-2 that lacks the signal sequence was mostly cytosolic (Figure 2.3D). However, this protein still showed residual membrane association. We hypothesized that the membrane-associated portion of splice variant MMP-2 could localize to the cytosolic face of cellular membranes, as it is not secreted. We tested this by digesting homogenates from HEK 293 cells expressing either canonical or splice variant MMP-2 with proteinase K, a broad spectrum protease unable to penetrate membrane-bound organelles. Unlike canonical MMP-2, proteinase K-treated homogenates showed complete proteolysis of splice variant MMP-2 in a similar manner to β -COP, the cytosolic coatomer protein (Figure 2.6). Thus, canonical MMP-2 targets to both the secretory pathway and the cytosol, whereas splice variant MMP-2 targets exclusively to the cytosol.

To further determine the proportion of MMP-2 that is intracellular in comparison to the secreted portion, we compared the amount of MMP-2 secreted in the media vs. intracellular MMP-2 in HEK 293 cell lysates at different time intervals. We found that for both endogenous MMP-2 (in non-transfected controls) and canonical MMP-2 (in cells transfected with HA-tagged canonical MMP-2 construct), there was a time-dependent increase in the secreted MMP-2 whereas the intracellular MMP-2 constituted a considerable proportion of the total MMP-2. On the other hand, splice variant MMP-2 (in cells transfected with HA-tagged splice variant MMP-2 construct) was exclusively intracellular (Figure 2.7).

2.3.2: Strength of the MMP-2 signal sequence

Our results so far suggested that canonical MMP-2, the predominant transcript in cardiomyocytes, generates the bulk of cytosolic MMP-2 in HEK 293 cells and

cardiomyocytes. This observation could be based on the inefficient recognition of its signal sequence at the ER. The MMP-2 signal sequence consists of a long basic N-domain of a net charge equal to +1 and a relatively short hydrophobic core (Table 2.3). Since signal sequence characteristics can determine a protein's sub-cellular partitioning^{14, 22}, we investigated this hypothesis with a site-directed mutagenesis approach. We designed two chimeric proteins, in which the signal sequence of MMP-2 was replaced by the signal sequence of BiP (BiP-MMP-2) or ERp44 (ERp44-MMP-2) (Figure 2.8A), two proteins that efficiently target to the ER^{15, 16}. The signal sequence of ERp44 is similar to that of MMP-2 in length, but more hydrophobic. We compared the targeting of these chimeras and found that, indeed, the BiP- and ERp44-MMP-2 chimeras were more efficiently targeted to membranes (Figure 2.8B). This improved targeting to the membrane fraction was not due to different expression levels (Figure 2.8C). Therefore, in comparison to canonical MMP-2, both BiP- and ERp44-MMP-2 chimeras are more efficiently targeted to the secretory pathway due to the nature of their signal sequence.

To further elucidate the MMP-2 signal sequence efficiency, we generated a chimeric construct in which BiP bears the MMP-2 signal sequence (MMP-2-BiP chimera, see Figure 2.9A) and transfected this into HEK 293 cells. Consistent with the different targeting qualities of the MMP-2 and BiP signal sequence, the MMP-2-BiP chimera was evenly distributed amongst both cytosolic and membrane fractions, whereas native BiP was mainly detected in the membrane fraction (Figure 2.9B). The efficiency of the MMP-2 signal sequence is therefore necessary and sufficient to reproduce the distribution of transfected and endogenous MMP-2 between the secretory pathway and the cytosol.

To corroborate our results by immunofluorescence, we examined the localization of transfected canonical, splice variant, and BiP-MMP-2 constructs in HeLa cells, a well-known model system for immunofluorescence microscopy. In these cells, BiP-MMP-2 showed more extensive co-localization with protein disulfide isomerase, an ER marker, compared to canonical MMP-2. In contrast, splice variant MMP-2 did not co-localize with the ER suggesting poor targeting to the secretory pathway (Figure 2.10). Together our data again suggest that the MMP-2 signal sequence is inefficient in its ER targeting abilities.

2.3.3: MMP-2 targeting determines troponin I cleavage in neonatal cardiomyocytes

Our experiments thus far had relied on protein expression in HEK 293 or HeLa cells, which could result in cell-specific mistargeting. To test this possibility, we extended our studies into cardiomyocytes, where MMP-2 had previously been found on sarcomeric myofilaments^{4, 7}. Canonical-, splice variant-, BiP- and ERp44-MMP-2 cDNAs were subcloned into lentiviral vectors in order to transduce neonatal rat cardiomyocytes. As in HEK293 cells, canonical MMP-2 was detectable in both cytosolic and membrane fractions of the cardiomyocytes, while both BiP- and ERp44-MMP-2 chimeras were membrane-associated. In contrast, the majority of splice variant MMP-2 was cytosolic (Figure 2.11). Therefore, our observations in cardiomyocytes reproduce those made in HEK 293 cells perfectly and exclude a cell-type specific explanation for our findings.

Cytosolic localization of MMP-2 could result in severe consequences through aberrant or dysregulated cleavage of its substrates, but could also determine the extent of proteolysis of physiological and pathological substrates. Therefore, we next examined how the subcellular distribution of secretory and cytosolic MMP-2 affects its function. To do so, we took advantage of canonical MMP-2, which shows a distribution resembling

endogenous MMP-2 and splice variant MMP-2, which is restricted to the cytosol. Figure 2.12 shows that neonatal cardiomyocytes over-expressing either canonical or splice variant MMP-2 have similar expression levels, which are approximately 6-7 times the level of endogenous MMP-2 in non-transduced control cells. As a model substrate, we chose TnI that is found in cardiomyocytes. Here, an increase in oxidative stress during I/R injury activates MMP-2, which then proteolyzes specific intracellular targets including TnI to contribute to the acute loss in contractile function ⁴. Thus, TnI cleavage during cell stress can serve as a readout of cytosolic MMP-2 activity in cardiomyocytes. We transduced neonatal rat cardiomyocytes with either canonical or splice variant MMP-2 and subjected them to hypoxia-reoxygenation injury, a model of oxidative stress. Cells expressing splice variant MMP-2 showed indeed more cleavage of TnI upon hypoxia-reoxygenation compared to cardiomyocytes expressing the same levels of canonical MMP-2 (Figure 2.13). To show that cleavage of TnI was MMP-2 dependent, we performed additional experiments to study the effects of a selective MMP-2 inhibitor, ARP-100, or MMP-2 shRNAmir mediated gene silencing, on TnI degradation. Our data showed that TnI cleavage in neonatal cardiomyocytes expressing splice variant-MMP-2 and subjected to hypoxia/reoxygenation was prevented by either ARP-100 treatment or MMP-2 silencing shRNAmir. These observations further strengthen our notion that TnI cleavage in hypoxia/reoxygenation is MMP-2 dependent (Figure 2.14).

Therefore, our findings indicate that MMP-2 signal sequence recognition and/or splice variant production determine the extent of TnI proteolysis in an injury model of cardiomyocytes.

2.4: Discussion

Previous research by us and other laboratories have demonstrated the abundance of intracellular MMP-2 substrates outside the secretory pathway (see ^{1, 3} for reviews), despite the presence of a signal sequence in canonical MMP-2. We report here for the first time a set of two mechanisms that explain these findings. Firstly, we demonstrate that a splice variant of MMP-2 lacking a secretory signal sequence is expressed in human cardiomyocytes. Secondly, we show that the signal sequence of canonical MMP-2 does not restrict it to the secretory pathway in HEK 293 and HeLa cells as well as cardiomyocytes. Moreover, we demonstrate that the pool of MMP-2 that is excluded from the ER has significant biological and pathological roles. Such a cytosolic pool of MMP-2 could be particularly relevant in cardiomyocytes, which contain sarcomeres, a known prominent localization of MMP-2 ^{1, 4, 7}. In neonatal cardiomyocytes exposed to oxidative stress from hypoxia and reoxygenation injury, the level of degradation of a known cardiac MMP-2 substrate, TnI, is higher when the intracellular pool of MMP-2 was increased with a form of MMP-2 that resides exclusively in the cytosol. Given that the mRNA levels for splice variant MMP-2 are inferior to the relative amounts of MMP-2 found in the cytosol, our findings suggest that the low targeting efficiency of canonical MMP-2 to the secretory pathway is the predominant mechanism that gives rise to cytosolic MMP-2, at least in cardiomyocytes. Our results have therefore identified two previously unknown mechanisms that explain the described localizations and enzymatic activities of MMP-2 outside the secretory pathway of cardiomyocytes and other cell types.

To further determine how canonical MMP-2 contributes to this cytosolic pool, we designed BiP-MMP-2 and ERp44-MMP-2 mutants in which the MMP-2 signal sequence

was replaced with those from BiP or ERp44, respectively. Both BiP and ERp44 are ER-resident chaperone proteins that play a crucial role in assuring proper protein folding in the ER lumen ²³. We speculate that their signal sequences are under more stringent selective pressure to allow for adequate translocation into ER, even at high expression levels induced by cellular stress. Indeed, consistent with this possibility, BiP- and ERp44-MMP-2 chimeras reduced the cytosolic levels of MMP-2 in HEK 293 and neonatal cardiomyocytes in comparison to canonical MMP-2. It is worth noting that the signal sequence of BiP was previously analyzed in HeLa cells and was found to be as efficient as that of prolactin, which also possesses a very efficient signal sequence ¹⁵. Despite the fact that canonical BiP is minimally detectable in the cytosolic fraction as reported previously ¹⁵ and as seen in this study, the MMP-2-BiP chimera, in which the signal sequence of BiP is replaced with that of MMP-2, significantly increased the level of BiP residing in the cytosol. Therefore, this construct further confirms that the MMP-2 signal sequence is weak in its ER targeting ability, and because of this, a substantial proportion of canonical MMP-2 resides in the cytosol.

Our findings are consistent with previous observations that physiologically relevant quantities of signal sequence containing proteins can reside and function in the cytosol and that the diverse targeting of such proteins depends substantially on the nature of the signal sequence ^{14, 22, 24, 25}. For example, calreticulin is one such protein, originally thought to be an ER-only targeted protein, whose signal sequence generates both ER-associated and cytosolic populations. However, some controversy remains concerning the exact mechanism by which calreticulin is found in the cytosol ²⁶. Shaffer *et al.* (2005) showed that the dual distribution of calreticulin is explained by its slightly inefficient ER-targeting signal sequence, resulting in a detectable cytosolic population. Moreover, modifying calreticulin to have a more efficient signal sequence (from prolactin)

significantly increased the proportion of protein targeted to the ER¹⁴. Prion protein, a cell surface protein implicated in neurodegeneration, is another example of signal sequence inefficiency. It is targeted to the ER by virtue of its signal sequence, however, a small proportion is not translocated into the ER and remains cytosolic. It is the cytosolic moiety of prion protein that results in pathogenic forms, thus causing neurodegenerative disorders¹³. Interestingly, replacing the prion protein signal sequence with a more efficient signal sequence decreased the level of cytosolic prion protein and increased the survival of cultured cells expressing this protein²⁷. Expression of prion protein lacking the ER-targeting signal sequence in the brains of transgenic mice causes severe neurodegeneration¹³. Therefore, inefficiency of the ER-targeting signal sequence is one mechanism exploited by the cell to regulate the subcellular distribution of signal sequence containing proteins. Other examples of mislocalization of secretory pathway proteins in various pathologies are known^{12, 13, 28, 29}. For example, the normally secreted apolipoprotein E has been suggested to interact with neurofilament Tau in the cytosol to induce neurofibrillary tangles in Alzheimer's disease¹².

In cardiomyocytes, MMP-2 has discrete intracellular localizations including the thin and thick myofilaments^{4, 7}, the cytoskeleton^{6, 30}, nucleus⁸, mitochondria⁴ and caveolae³¹. It is worth noting that 72-kD MMP-2 can be activated directly by peroxynitrite, an important mediator of hypoxia/reoxygenation injury³², via S-glutathiolation of the propeptide domain¹⁰. Our results demonstrate that neonatal rat cardiomyocytes expressing splice variant MMP-2 lacking the signal sequence show more TnI cleavage upon hypoxia-reoxygenation injury. Moreover, TnI cleavage, in neonatal cardiomyocytes expressing splice variant-MMP-2 and subjected to hypoxia/reoxygenation, is prevented by either ARP-100 (a selective MMP-2 inhibitor) or MMP-2 silencing shRNAmir, indicating that TnI cleavage is MMP-2 dependent. These

observations are consistent with the MMP-2 mediated loss of TnI in rat hearts subjected to I/R injury ⁴ and the reduced contractile function and TnI levels in the heart in transgenic mice with myocardial specific expression of a constitutively active, MMP-2 mutant ⁵. In our hypoxia/reoxygenation experiments there was a small increase in TnI cleavage in cardiomyocytes expressing canonical MMP-2 as well. Presumably, this trend in TnI cleavage could be due, at least in part, to the amount of transfected canonical MMP-2 sorted to the cytosol. Our data, though, do not completely rule out additional properties that may distinguish splice variant MMP-2 from canonical MMP-2. Our results suggest that the level of cytosolically-targeted MMP-2 determines the extent of this proteolytic activity. Therefore, our findings demonstrate that the subcellular targeting of MMP-2 is a crucial component to its biological actions in cardiomyocytes subjected to enhanced oxidative stress. Future studies will have to determine how the extent of MMP-2 splicing or signal sequence recognition may be altered depending on cellular stress or other unusual conditions.

In summary, a weak signal sequence in canonical MMP-2 and a splice variant of MMP-2 provide two novel mechanisms how intracellular MMP-2 activity could contribute to cardiac contractile dysfunction in myocardial oxidative stress injury ¹. Given the similar distribution of endogenous and transfected canonical MMP-2, the MMP-2 targeting pattern is mostly based on its signal sequence in the cellular systems that we have analyzed. Likewise, the mechanisms for MMP-2 we describe here suggest that other MMPs may be subjected to similar “fuzzy” targeting, as demonstrated by the cleavage of estrogen receptor- β by MMP-26 in the cytosol ³³, the proteolytic cleavage of cytosolic huntingtin by MMP-10 ³⁴, or the partial nuclear localization of MMP-3 ³⁵. Thus, our results provide a set of mechanisms that give rise to intracellular MMP-2 and highlight

the gaining importance of intracellular MMPs activity in the gamut of their multiple biological effects ^{1,3}.

Figure 2.1: Schematic diagram of chimeric proteins used in the study.

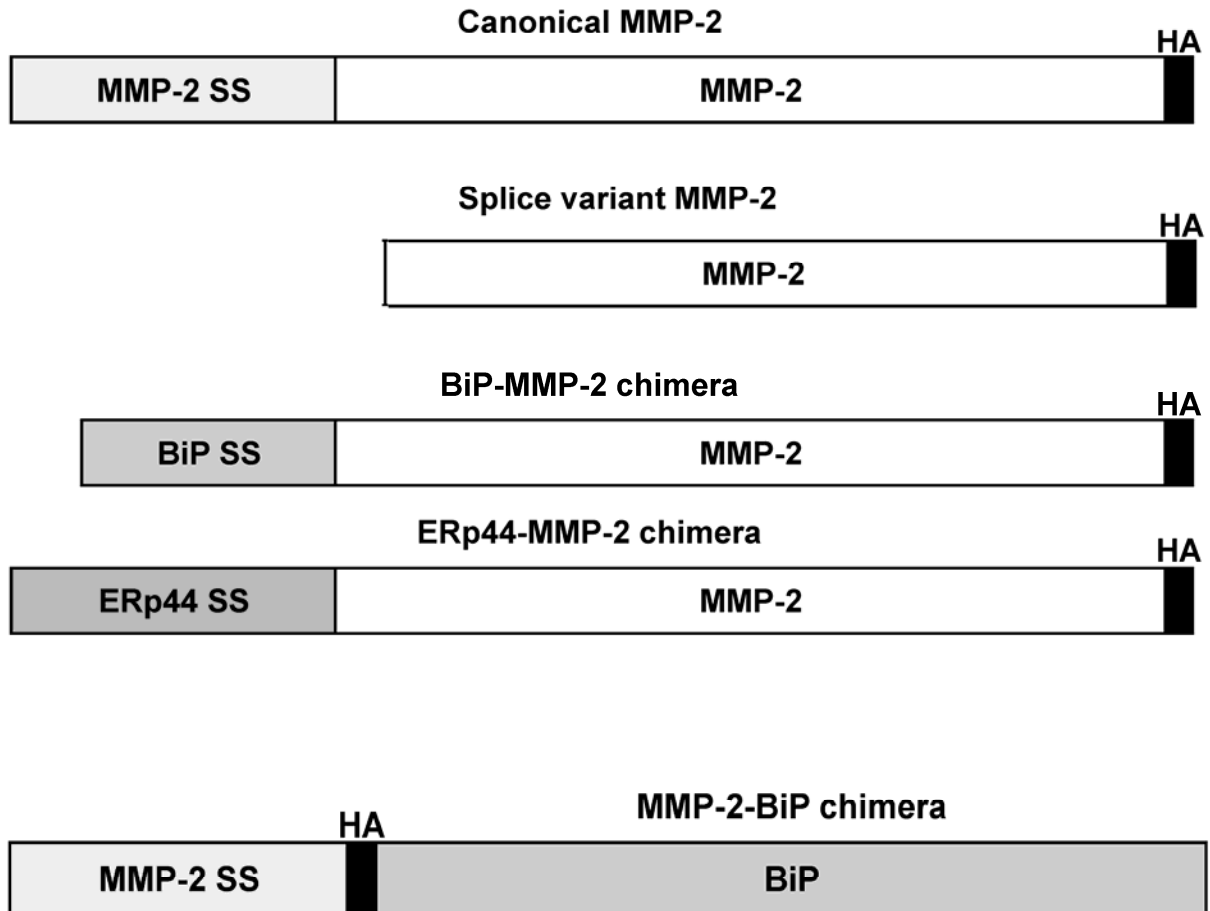


Figure 2.2: Subcellular distribution of endogenous MMP-2 in HEK 293 cells.

Upper: Western blot using anti-MMP-2 shows that endogenous MMP-2 resides in both cytosolic (Cyto) and membrane (Memb) fractions of HEK 293 cells. Fraction purity was validated with antibodies against GAPDH (cytosolic marker), calnexin (ER marker) and VAMP-3 (secretory vesicles marker). Lower: Quantification of endogenous MMP-2 distribution in cytosolic and membrane fractions. * $p < 0.05$ (unpaired t-test), $n = 4$. Experiments done by M. A. Ali.

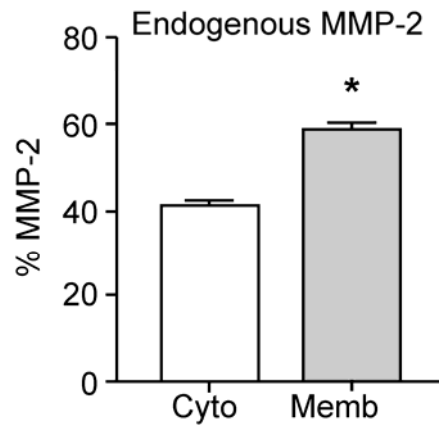
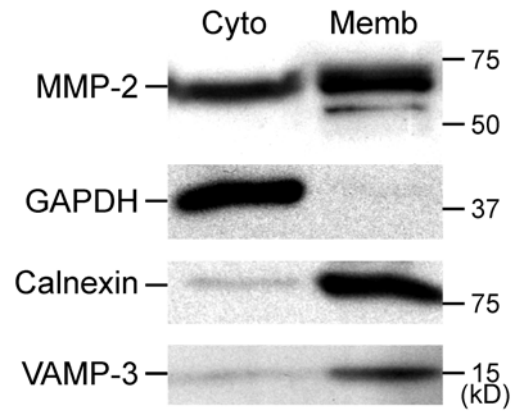


Figure 2.3: Canonical and splice variant MMP-2.

A) Alignment of the primary sequences of canonical MMP-2 and splice variant MMP-2 (DB059054 clone). The signal sequence of MMP-2 is underlined. Splice variant MMP-2 lacks the first N-terminal 50 amino acids including the SS. B) qRT-PCR data show that the expression level of splice variant MMP-2 in neonatal and adult human cardiomyocytes is 9% and 13% relative to canonical MMP-2 expression, respectively. n=3. C) Upper: Western blot using anti-HA in HEK 293 cells transfected with canonical or splice variant MMP-2 shows that canonical MMP-2 is secreted into the conditioned media whereas splice variant MMP-2 is not. Each lane contains 50 μ l conditioned media. Lower: Cell lysates (10 μ g total protein) show similar expression level of canonical and splice variant MMP-2. D) Upper: Subcellular distribution of canonical and splice variant MMP-2 in transfected HEK 293 cells using anti-HA in cytosolic (Cyto) and membrane (Memb) fractions. Fraction purity was validated with antibodies against GAPDH (cytosolic marker), calnexin (ER marker) and VAMP-3 (secretory vesicles marker). Lower: Quantification of MMP-2 distribution in cytosolic and membrane fractions. MMP-2, whether canonical or splice variant, is found in both fractions, however, the latter is more abundant in the cytosolic fraction. *p<0.05 (unpaired t-test), n=3 for each experiment. Experiments done by M. A. Ali and X. Fan.

A. Canonical MMP-2

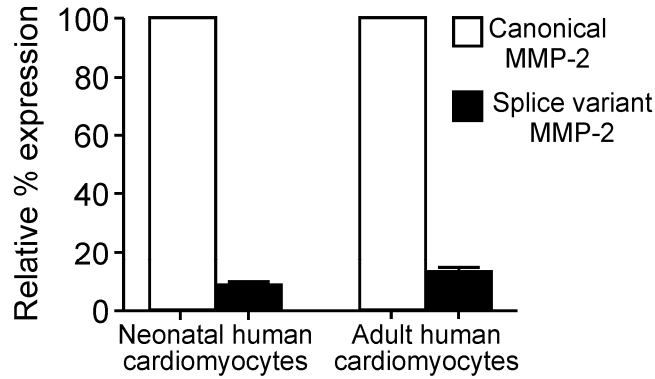
52

MEALMARGALTGPLRALCLLGCLLSHAAAAPSPIIKFPGDVAPKTDKELAVQYLNTF.....

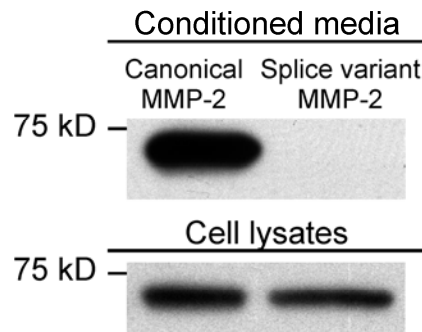
Splice variant MMP-2

MQYLNTF.....

B.



C.



D.

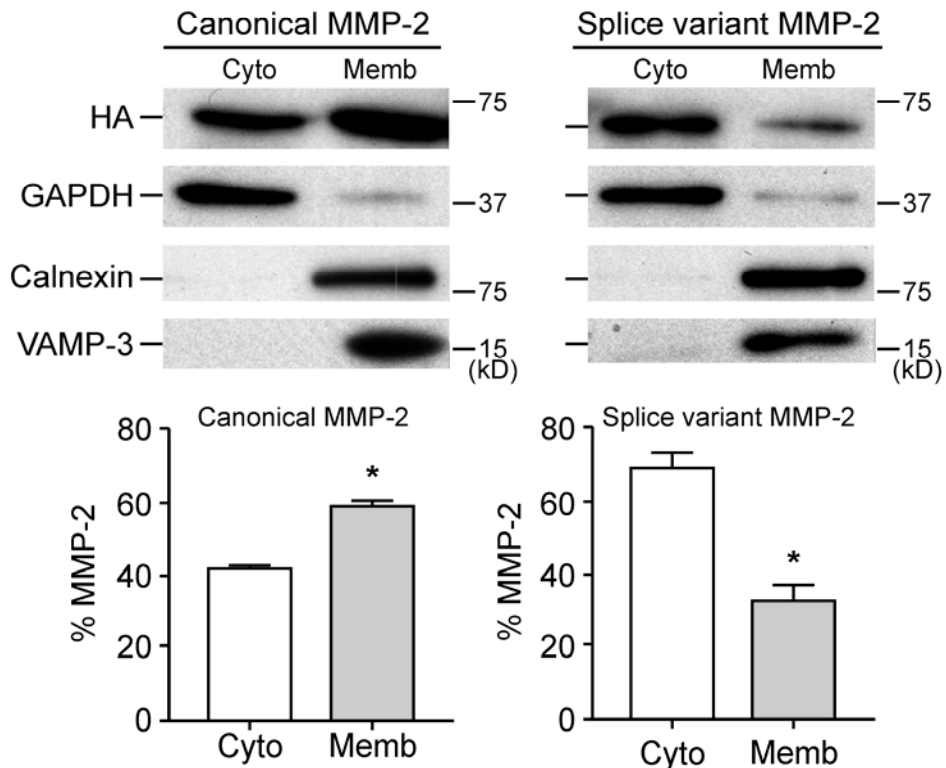


Figure 2.4: Titration of expression levels of HA-tagged canonical MMP-2.

Western blot using anti-HA in cytosolic and membrane fractions of HEK 293 cells transfected with increasing amount of plasmid (0.2 μ g-2.0 μ g DNA for 24 h) as indicated shows that different expression levels do not affect the amount of canonical MMP-2 mistargeted to the cytosol. Experiments done by M. A. Ali.

Amount of Plasmid transfected

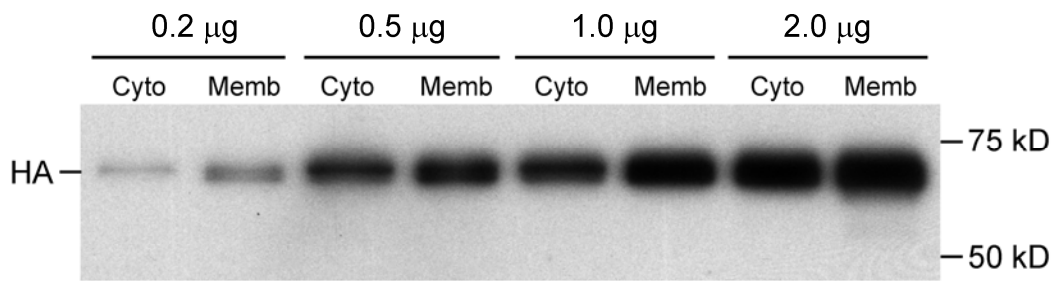


Figure 2.5: Effect of proteasomal inhibition (using MG132) or lysosomal inhibition (using bafilomycin A1) on the level of canonical and splice variant MMP-2 in HEK 293 cells.

A) anti-HA blots show the level of either canonical or splice variant MMP-2 in cell lysates from non-transfected HEK 293 cells (Control) vs. MG132 treated cells (MG132) or bafilomycin A1 treated cells (Baf. A1). Actin is used as a loading control. B) Quantification of HA/Actin ratios in non-transfected HEK 293 cells vs. MG132 or bafilomycin A1 treated cells for canonical MMP-2 (left panel) or splice variant MMP-2 (right panel). $p > 0.05$, One-way ANOVA followed by Tukey's post-hoc test, $n=3$ experiments. Experiments done by M. A. Ali.

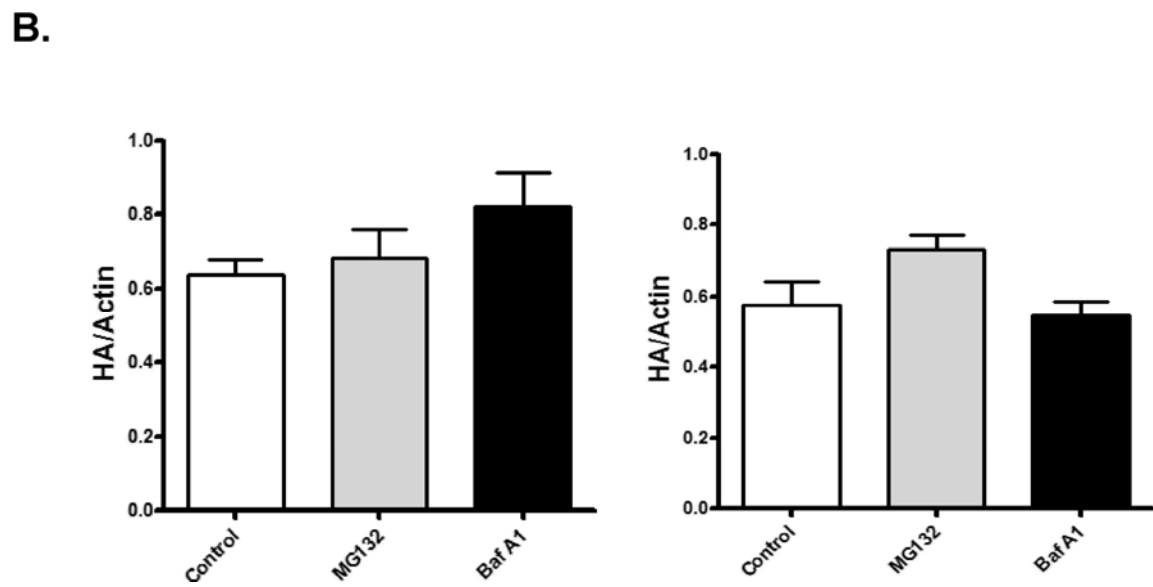
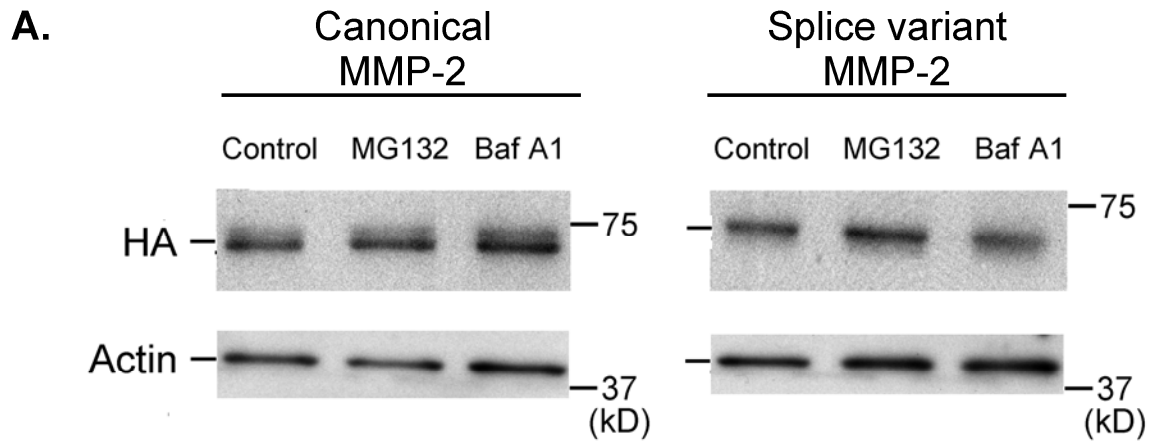


Figure 2.6: Proteolysis of splice variant MMP-2 by proteinase K.

Anti-HA western blots for canonical and splice variant MMP-2 in HEK 293 cell homogenates without (control) or with proteinase K treatment (+PK). Canonical MMP-2 resists proteolysis by proteinase K, similar to protein disulfide isomerase (PDI) control. Splice variant MMP-2 is completely proteolyzed by proteinase K similar to β -COP control. Molecular weight markers are indicated. The experiment was repeated twice with similar results. Experiments done by M. A. Ali.

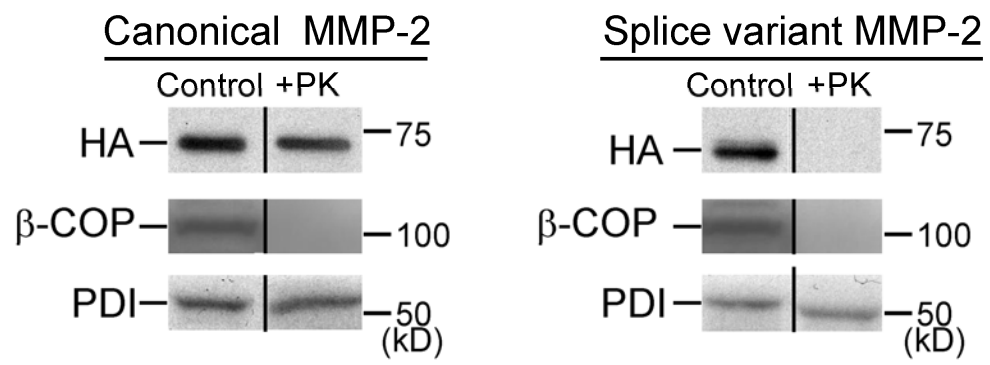


Figure 2.7: Assaying secreted vs. intracellular MMP-2.

A) Western blot using anti-MMP-2 showing the time course of changes in endogenous MMP-2 in non-transfected HEK 293 cells secreted into the media (left) or in the corresponding cell lysates (right). MW, molecular weight marker which corresponds to 75-kD. B) Western blot using anti-HA showing the time course of changes in MMP-2 in transfected HEK 293 cells expressing canonical HA-tagged MMP-2. The amount of HA-tagged MMP-2 in the media (left) or corresponding cell lysates (right) are shown. C) Western blot using anti-HA showing the time course of changes in MMP-2 in transfected HEK 293 cells expressing splice variant HA-tagged MMP-2. The amount of HA-tagged MMP-2 in the media (left) or corresponding cell lysates (right) are shown. Note that splice variant MMP-2 is exclusively intracellular. Actin serves as loading control in all cell lysate experiments. Experiments done by M. A. Ali.

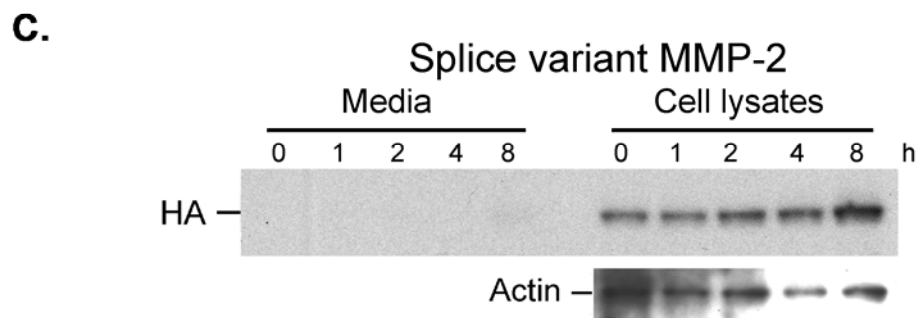
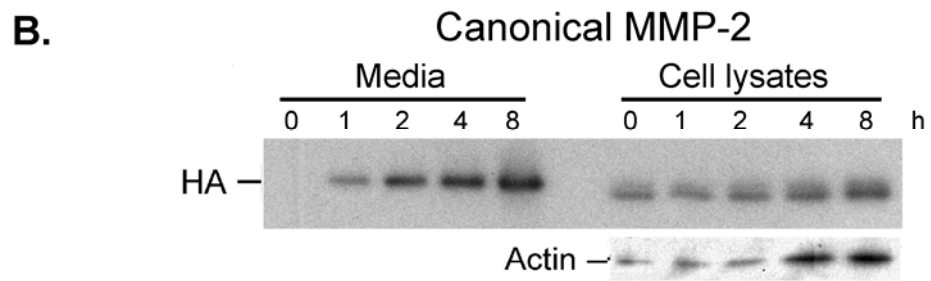
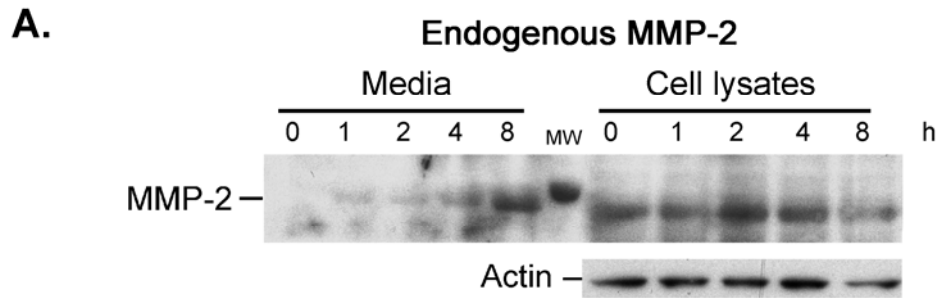


Figure 2.8: Comparison of signal sequence efficiencies of MMP-2 chimeras.

A) Schematic diagram showing canonical MMP-2 and the BiP- and ERp44-MMP-2 chimeras. SS, signal sequence; HA, hemagglutinin tag. B) Western blots showing MMP-2 in cytosolic and membrane fractions of HEK 293 cells expressing canonical-, BiP- or ERP-44-MMP-2. * $p < 0.05$ (unpaired t-test), $n=3$ for each experiment. Fraction purity validated with GAPDH, calnexin and VAMP-3 antibodies as per Fig. 2.2. C) Western blot using anti-HA in HEK 293 cell lysates showing similar expression levels among all MMP-2 constructs. Molecular weight markers are indicated. Experiments done by M. A. Ali and A. K. Chow.

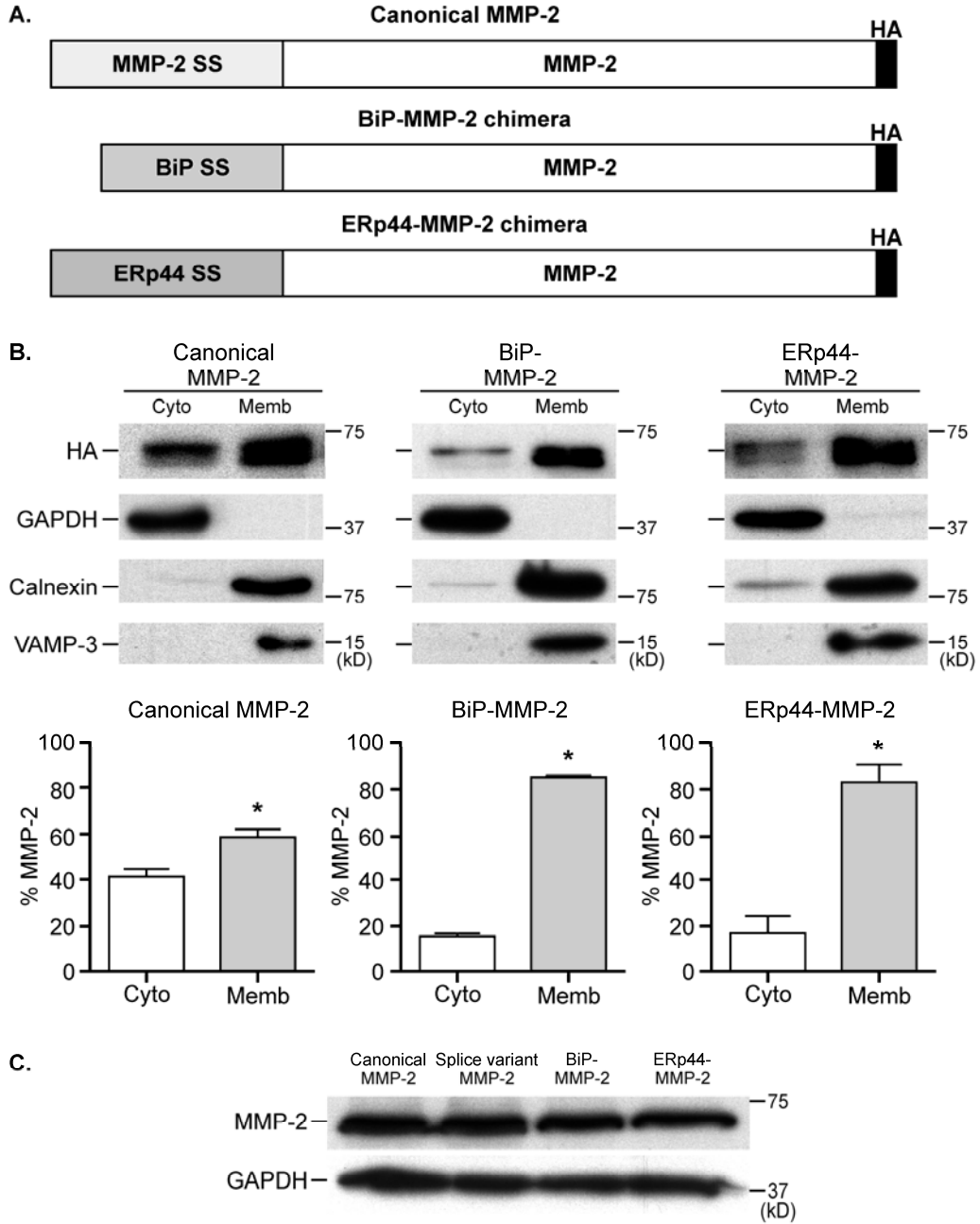


Figure 2.9: MMP-2 signal sequence reduces targeting of BiP to the endoplasmic reticulum.

A) Schematic diagram of the MMP-2-BiP chimera. SS, signal sequence; HA, hemagglutinin tag. B) Western blots show the abundance of canonical BiP or MMP-2-BiP chimera in cytosolic and membrane fractions of HEK 293 cells. Canonical BiP mainly resides in the membrane fraction, while the MMP-2-BiP chimera is equally distributed between the cytosolic and membrane fractions. * $p < 0.05$ (unpaired t-test), $n = 3$ for each experiment. Experiments done by M. A. Ali and A. K. Chow.

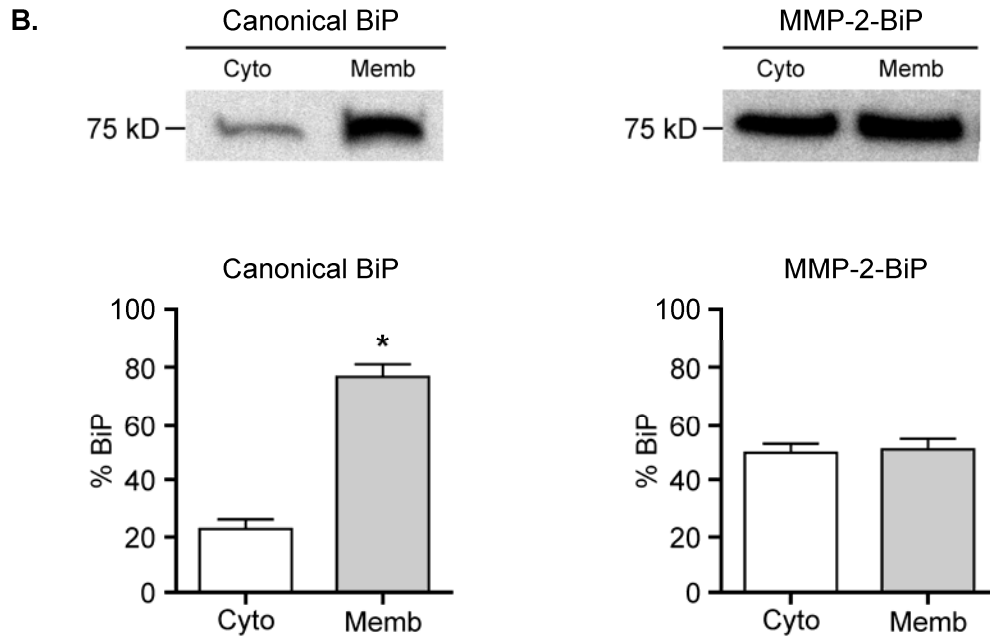
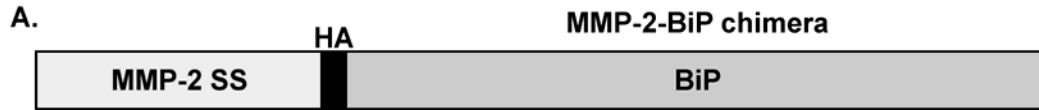


Figure 2.10: ER localization of MMP-2 chimeras.

Immunocytochemistry-confocal microscopy images of HeLa cells expressing canonical-, splice variant- or BiP-MMP-2. Protein disulphide isomerase (PDI) was used as an ER marker (red), HA-tagged MMP-2 (green) and the yellow colour in the merged images shows the co-localization of MMP-2 to the ER. BiP-MMP-2 shows stronger localization to the ER in comparison with canonical MMP-2. Splice variant MMP-2 does not localize to the ER but instead shows cytosolic and nuclear staining. The nuclear presence of MMP-2 has been previously reported by our group ⁸. Insets show a magnified area as indicated by the white frames. Scale bar indicates 16 μm . Experiments done by M. A. Ali.

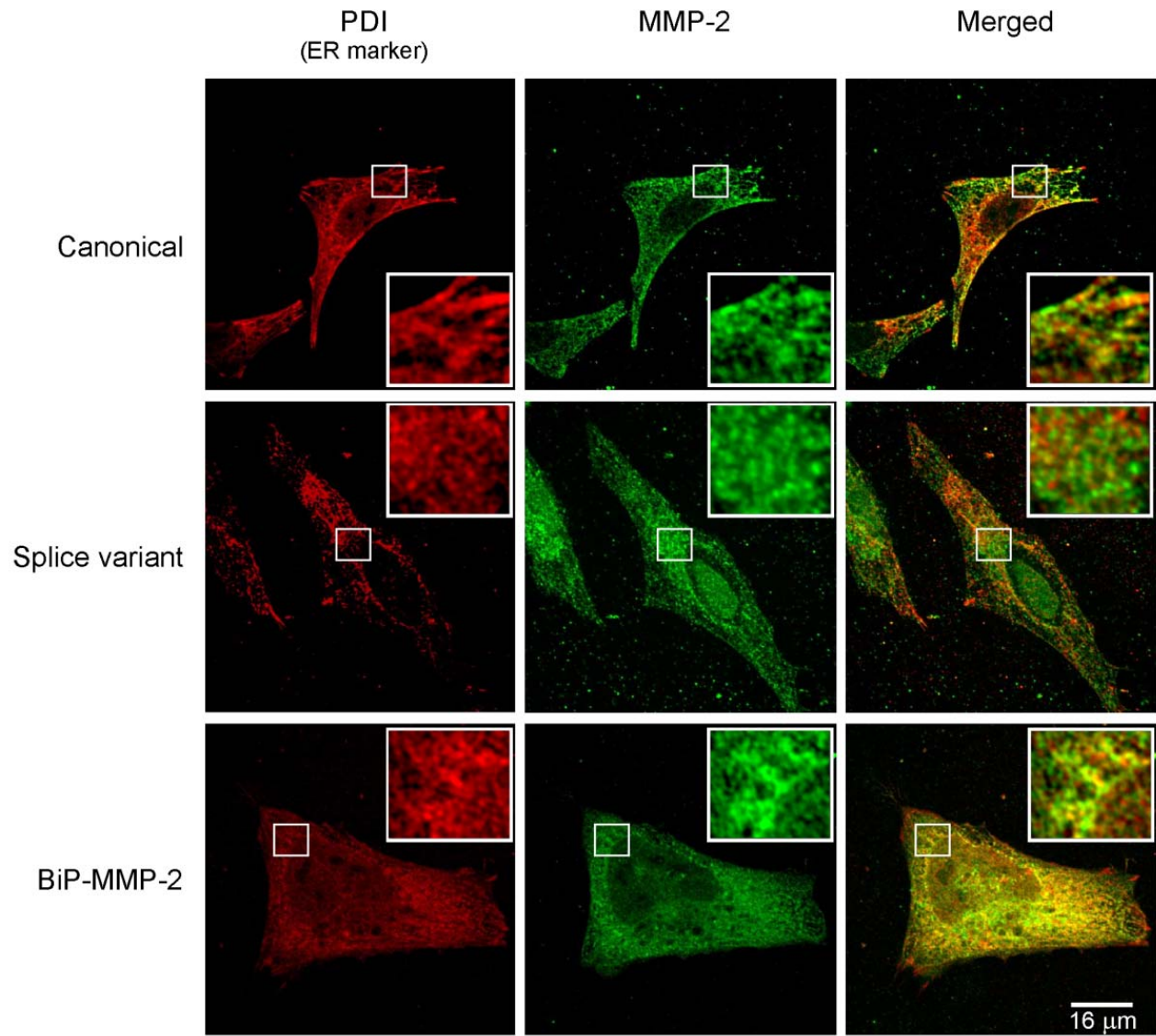


Figure 2.11: Differential distributions of MMP-2 chimeras in cardiomyocytes.

MMP-2 in the cytosolic and membrane fractions of neonatal rat cardiomyocytes transduced with lentiviral vectors encoding for canonical-, splice variant-, BiP- or ERp44-MMP-2 chimeras. Canonical MMP-2 is primarily found in the membrane fraction whereas at least 40% remains cytosolic. Splice variant-MMP-2 is predominantly localized to the cytosolic fraction whereas BiP-MMP-2 and ERp-44-MMP-2 are found mainly in the membrane fraction. * $p < 0.05$ (unpaired t-test), $n=3$ for each experiment. Fraction purity validated with GAPDH, calnexin and VAMP-3 antibodies as per Fig. 2.2. Molecular weight markers are indicated. Experiments done by M. A. Ali and A. D. Kandasamy.

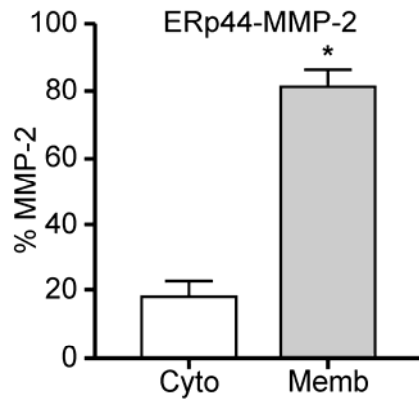
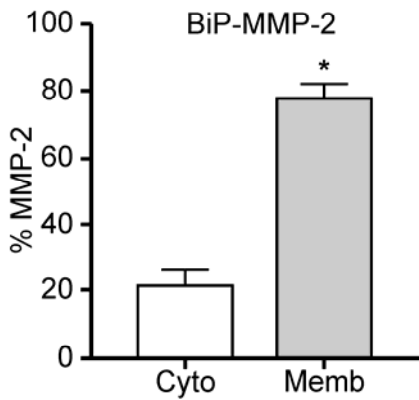
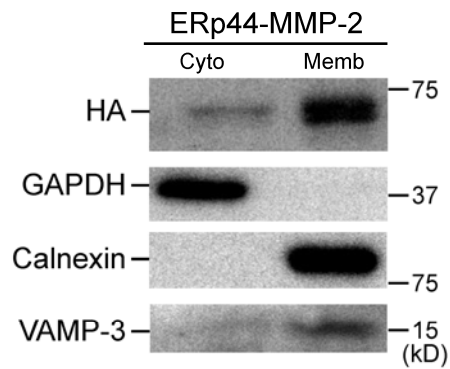
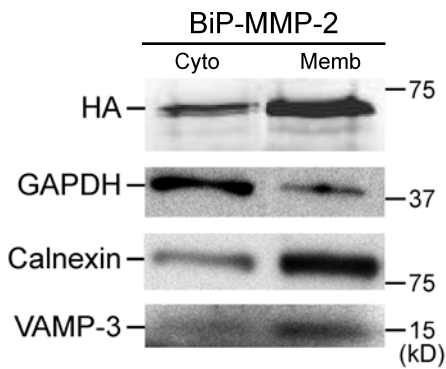
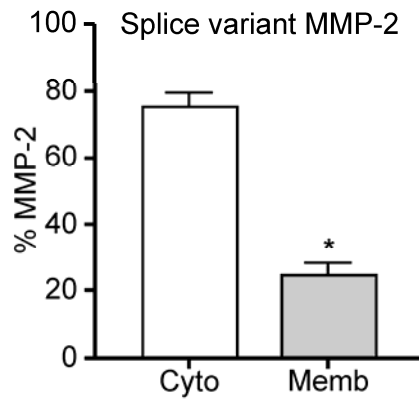
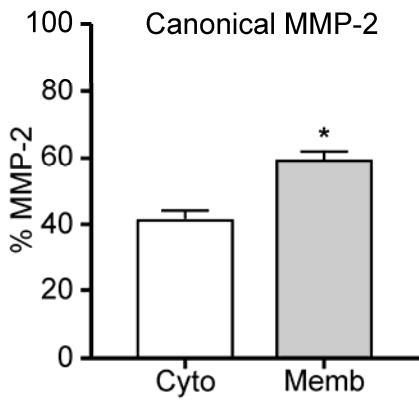
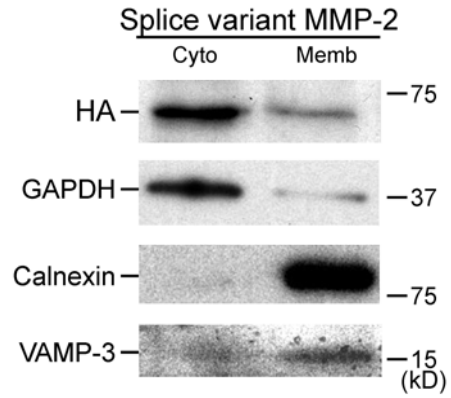
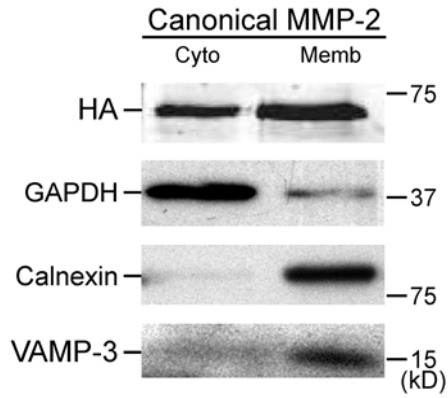


Figure 2.12: Relative expression levels of endogenous MMP-2 to expressed canonical or splice variant MMP-2 in cardiomyocytes.

Upper, Anti-MMP-2 western blot shows the level of endogenous MMP-2 in non-transduced cardiomyocytes (NT) relative to MMP-2 level in cardiomyocytes expressing canonical MMP-2 (Can.) or splice variant MMP-2 (SV.). Lower, Fold increase of MMP-2 level in cardiomyocytes expressing canonical MMP-2 (Can.) or splice variant MMP-2 (SV.) in comparison to non-transduced control (NT). * $p < 0.05$, One-way ANOVA followed by Tukey's post-hoc test, $n=3$ experiments. Experiments done by M. A. Ali.

Neonatal cardiomyocytes

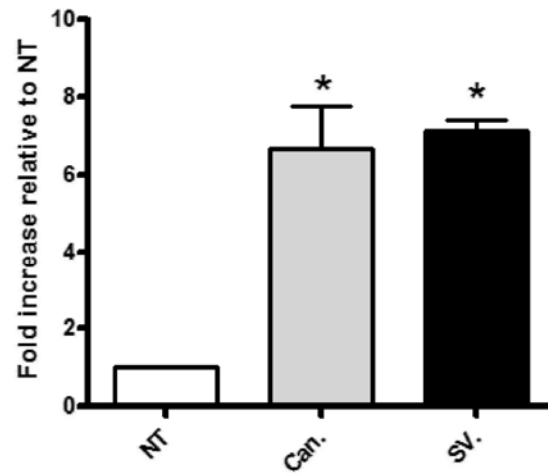
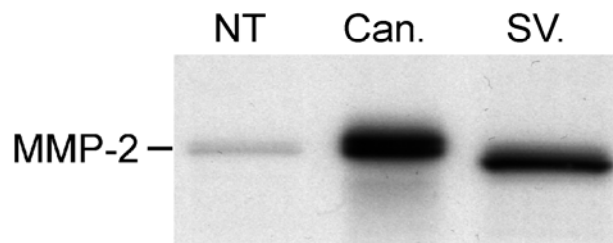


Figure 2.13: Splice variant MMP-2 increases intracellular substrate cleavage during cell stress.

A) Assessment of troponin I (TnI) cleavage by western blot, an intracellular MMP-2 target, in lentivirus-transduced neonatal cardiomyocytes expressing either canonical- or splice variant-MMP-2 and then exposed to either 28 h normoxia (Normoxia) or 24 h hypoxia followed by 4 h reoxygenation (Hypoxia/reox.). HA immunoblots of cell homogenates show the expression level of the corresponding MMP-2. Actin serves as a loading control. B) Quantification of cleaved TnI/actin ratios, * $p < 0.05$ vs. normoxia (unpaired t-test), $n=3$. Molecular weight markers are indicated. Experiments done by M. A. Ali and A. D. Kandasamy.

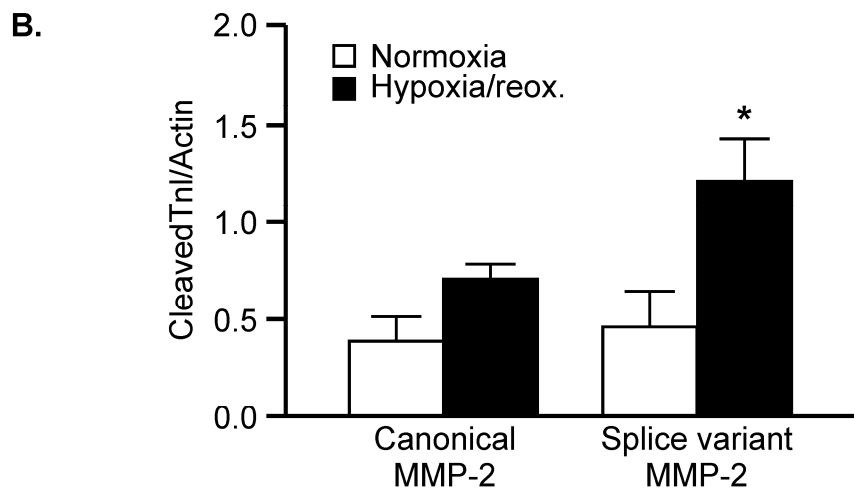
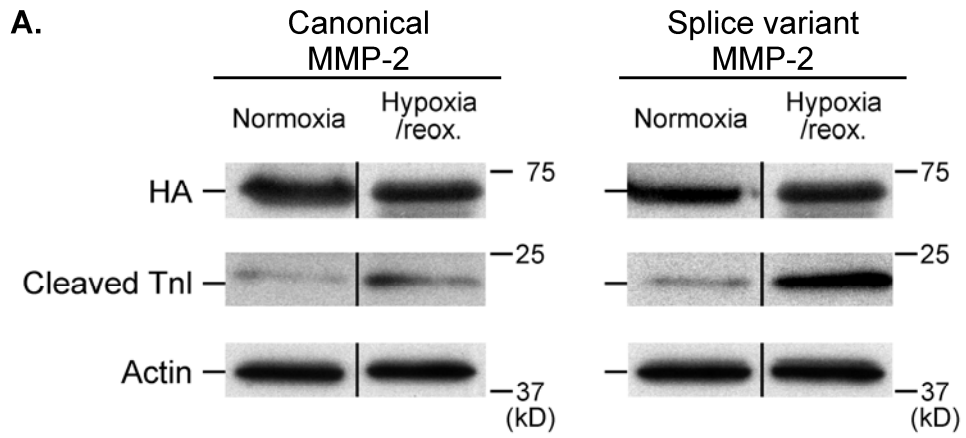


Figure 2.14: Troponin I (TnI) cleavage is reduced by either pharmacologic or biologic inhibition of MMP-2.

TnI cleavage in neonatal cardiomyocytes expressing splice variant-MMP-2 and then exposed to 28 h normoxia (Normoxia), 24 h hypoxia followed by 4 h reoxygenation either without (Hypoxia/reox.), or with ARP-100 treatment (Hypoxia/reox. + ARP-100), or with lentiviral MMP-2 silencing shRNAmir transduction (Hypoxia/reox. + MMP-2 shRNAmir). HA immunoblots of cell homogenates show the expression level of splice variant MMP-2 for the corresponding treatments. The experiment was repeated twice with similar results. Actin serves as a loading control. Experiments done by M. A. Ali and X. Fan.

Splice variant MMP-2

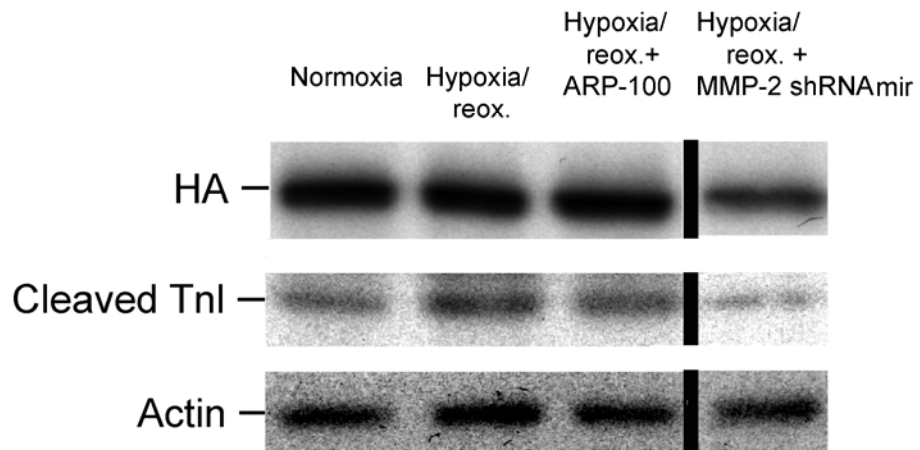


Table 2.1: The PCR primers used for the indicated chimeras.

Sequence	Forward Primers	Reverse Primers
Canonical MMP-2	ATATGAATTCGCCGGCGCCATGGAG GCGCTAATGGCCCGGGGC	ATATCTCGAGTCAGGCGTAGTC GGGGACGTCGTAGGGGTAGAA GCAGCCTAGCCAGTCGGATTTG ATGCTTCC
Splice variant MMP-2	ATATGAATTCGCCGGCGCCATGCAAT ACCTGAACACCTTCTATGGCTG	ATATCTCGAGTCAGGCGTAGTC GGGGACGTCGTAGGGGTAGAA GCAGCCTAGCCAGTCGGATTTG ATCGTTCC
BiP-MMP-2: Overlap Extension PCR	1.CGCGATGCTGCTGCTGCTCAGCGC GGCGCGGGCCGCGCCGTCGCCAT CATCAAGTTCCC 2.ATATGAATTCGCTGGCAAGATGAA GCTCTCCCTGGTGGCCGCGATGCTG CTGCTGCTCAGCGC	ATATCTCGAGTCAGGCGTAGTC GGGGACGTCGTAGGGGTAGAA GCAGCCTAGCCAGTCGGATTTG ATGCTTCC
ERp44-MMP-2: Overlap Extension PCR	1.TCCTGGTAACTTGGGTTTTACTCC TGTAACAACCTGCGCCGTCGCCATC ATCAAGTTCCC 2.CCTATCCTTACCCGACCTCAGATG CTCCCTTCTGCTCCTGGTAACTTGGG TTTTAC 3.ATATGAATTCGTTACCATGCATCCT GCCGTCTTCTATCCTTACCCGACCT CAGAT	ATATCTCGAGTCAGGCGTAGTC GGGGACGTCGTAGGGGTAGAA GCAGCCTAGCCAGTCGGATTTG ATGCTTCC
MMP-2-BiP: Overlap Extension PCR	1.GAGCCACGCCGCGCCTTCTACCC CTACGACGTCCCCGACTACGCCGAG GAGGAGGACAAGAAGGACGTG 2.CGCTCACGGGTCCCCTGAGGGCG CTCTGTCTCCTGGGCTGCCTGCTGA GCCACGCCGCTTCTACC 3.ATATGGTACCGCCGGCGCCATGGA GGCGCTAATGGCCCGGGGCGCGCT CACGGGTCCCCTGAGGGCG	ATATCTCGAGCTACAACCTCATCT TTTTCTGCTGTATC

Table 2.2: Primary antibodies used in the study.

Antibody	Host	Source	Dilution used
anti-MMP-2	Mouse-monoclonal	Calbiochem	1:1000 WB
anti-GAPDH	Rabbit-polyclonal	Cell Signaling	1:5000 WB
anti-calnexin	Rabbit-polyclonal	Stressgen	1:3000 WB
anti-VAMP-3	Goat-polyclonal	Santa Cruz Biotech.	1:1000 WB
anti-HA	Mouse-monoclonal	Covance	1:2500 WB 1:100 IF
anti- β -COP	Mouse-monoclonal	GeneTex	1:1000 WB
anti-PDI	Rabbit-polyclonal	Pierce	1:1000 WB 1:100 IF
anti-TnI	Mouse-monoclonal	Nanogen	1:1000 WB
anti-actin	Rabbit-polyclonal	Santa Cruz Biotech.	1:5000 WB
anti-BiP	Mouse-monoclonal	BD Biosciences	1:1000 WB

WB, Western blotting; IF, Immunofluorescence.

Table 2.3: Comparison of signal sequences.

Protein	Signal Sequence	Length	Charge
BiP	M<u>KLSLVAAMLLLL</u>SAARA	18, <u>11</u>	+1
ERp44	MHPAVFLSLPDL<u>RCLLLLVTWVFTP</u>VTT	29, <u>11</u>	0
MMP2 can.	MEALMARGALTG<u>PLRALC</u>LLG<u>CLL</u>SHAAA	29, <u>9</u>	+1
MMP7	M<u>RLTVLCAV</u>CLLP<u>GS</u>LA	18, <u>11</u>	+1
MMP8	M<u>FSLKTL</u>P<u>FLLL</u>H<u>VQ</u>ISKA	20, <u>9</u>	+1
MMP9	M<u>SLWQPL</u>V<u>L</u>LL<u>V</u>L<u>G</u>CCF	19, <u>8</u>	0
MMP14	M<u>SPAPR</u>PP<u>RC</u>LL<u>L</u>PL<u>LL</u>T<u>L</u>GTALA	23, <u>11</u>	+2

Alignment of selected human protein signal sequences with the signal sequence of canonical (can.) human MMP-2. The hydrophobic domain is underlined. On the right, we list the amino acid length of the various signal sequences (total and hydrophobic core is underlined) and the charge of the N-terminal charged portion. Bona fide ER-targeted proteins (BiP and ERp44) have varying lengths of signal sequences that can reach the length of MMP-2. Interestingly, the hydrophobic core of the MMP-2 signal sequence is unusually short and marked by cysteine residues.

2.5: References

1. Schulz R. Intracellular targets of matrix metalloproteinase-2 in cardiac disease: rationale and therapeutic approaches. *Annu Rev Pharmacol Toxicol.* 2007; 47: 211-242.
2. Butler GS, Overall CM. Proteomic identification of multitasking proteins in unexpected locations complicates drug targeting. *Nat Rev Drug Discov.* 2009; 8: 935-948.
3. Cauwe B, Opdenakker G. Intracellular substrate cleavage: a novel dimension in the biochemistry, biology and pathology of matrix metalloproteinases. *Crit Rev Biochem Mol Biol.* 2010; 45: 351-423.
4. Wang W, Schulze CJ, Suarez-Pinzon WL, Dyck JR, Sawicki G, Schulz R. Intracellular action of matrix metalloproteinase-2 accounts for acute myocardial ischemia and reperfusion injury. *Circulation.* 2002; 106: 1543-1549.
5. Bergman MR, Teerlink JR, Mahimkar R, Li L, Zhu BQ, Nguyen A, Dahi S, Karliner JS, Lovett DH. Cardiac matrix metalloproteinase-2 expression independently induces marked ventricular remodeling and systolic dysfunction. *Am J Physiol Heart Circ Physiol.* 2007; 292: H1847-60.
6. Sung MM, Schulz CG, Wang W, Sawicki G, Bautista-Lopez NL, Schulz R. Matrix metalloproteinase-2 degrades the cytoskeletal protein alpha-actinin in peroxynitrite mediated myocardial injury. *J Mol Cell Cardiol.* 2007; 43: 429-436.
7. Sawicki G, Leon H, Sawicka J, Sariahmetoglu M, Schulze CJ, Scott PG, Szczesna-Cordary D, Schulz R. Degradation of myosin light chain in isolated rat hearts subjected to

- ischemia-reperfusion injury: a new intracellular target for matrix metalloproteinase-2. *Circulation*. 2005; 112: 544-552.
8. Kwan JA, Schulze CJ, Wang W, Leon H, Sariahmetoglu M, Sung M, Sawicka J, Sims DE, Sawicki G, Schulz R. Matrix metalloproteinase-2 (MMP-2) is present in the nucleus of cardiac myocytes and is capable of cleaving poly (ADP-ribose) polymerase (PARP) in vitro. *FASEB J*. 2004; 18: 690-692.
 9. Sariahmetoglu M, Crawford BD, Leon H, Sawicka J, Li L, Ballermann BJ, Holmes C, Berthiaume LG, Holt A, Sawicki G, Schulz R. Regulation of matrix metalloproteinase-2 (MMP-2) activity by phosphorylation. *FASEB J*. 2007; 21: 2486-2495.
 10. Viappiani S, Nicolescu AC, Holt A, Sawicki G, Crawford BD, Leon H, van Mulligen T, Schulz R. Activation and modulation of 72kDa matrix metalloproteinase-2 by peroxynitrite and glutathione. *Biochem Pharmacol*. 2009; 77: 826-834.
 11. Massova I, Kotra LP, Fridman R, Mobashery S. Matrix metalloproteinases: structures, evolution, and diversification. *FASEB J*. 1998; 12: 1075-1095.
 12. Huang Y, Liu XQ, Wyss-Coray T, Brecht WJ, Sanan DA, Mahley RW. Apolipoprotein E fragments present in Alzheimer's disease brains induce neurofibrillary tangle-like intracellular inclusions in neurons. *Proc Natl Acad Sci U S A*. 2001; 98: 8838-8843.
 13. Ma J, Wollmann R, Lindquist S. Neurotoxicity and neurodegeneration when PrP accumulates in the cytosol. *Science*. 2002; 298: 1781-1785.
 14. Shaffer KL, Sharma A, Snapp EL, Hegde RS. Regulation of protein compartmentalization expands the diversity of protein function. *Dev Cell*. 2005; 9: 545-554.

15. Kang SW, Rane NS, Kim SJ, Garrison JL, Taunton J, Hegde RS. Substrate-specific translocational attenuation during ER stress defines a pre-emptive quality control pathway. *Cell*. 2006; 127: 999-1013.
16. Anelli T, Alessio M, Mezghrani A, Simmen T, Talamo F, Bachi A, Sitia R. ERp44, a novel endoplasmic reticulum folding assistant of the thioredoxin family. *EMBO J*. 2002; 21: 835-844.
17. Matsumoto S, Katoh M, Saito S, Watanabe T, Masuho Y. Identification of soluble type of membrane-type matrix metalloproteinase-3 formed by alternatively spliced mRNA. *Biochim Biophys Acta*. 1997; 1354: 159-170.
18. Gilady SY, Bui M, Lynes EM, Benson MD, Watts R, Vance JE, Simmen T. Ero1alpha requires oxidizing and normoxic conditions to localize to the mitochondria-associated membrane (MAM). *Cell Stress Chaperones*. 2010; 15: 619-629.
19. Oberdorf J, Carlson EJ, Skach WR. Uncoupling proteasome peptidase and ATPase activities results in cytosolic release of an ER polytopic protein. *J Cell Sci*. 2006; 119: 303-313.
20. Ge W, Guo R, Ren J. AMP-dependent kinase and autophagic flux are involved in aldehyde dehydrogenase-2-induced protection against cardiac toxicity of ethanol. *Free Radic Biol Med*. 2011; 51: 1736-1748.
21. Karnabi E, Qu Y, Mancarella S, Yue Y, Wadgaonkar R, Boutjdir M. Silencing of Cav1.2 gene in neonatal cardiomyocytes by lentiviral delivered shRNA. *Biochem Biophys Res Commun*. 2009; 384: 409-414.
22. Hegde RS, Bernstein HD. The surprising complexity of signal sequences. *Trends Biochem Sci*. 2006; 31: 563-571.

23. Simmen T, Lynes EM, Gesson K, Thomas G. Oxidative protein folding in the endoplasmic reticulum: tight links to the mitochondria-associated membrane (MAM). *Biochim Biophys Acta*. 2010; 1798: 1465-1473.
24. Levine CG, Mitra D, Sharma A, Smith CL, Hegde RS. The efficiency of protein compartmentalization into the secretory pathway. *Mol Biol Cell*. 2005; 16: 279-291.
25. Hegde RS, Kang SW. The concept of translocational regulation. *J Cell Biol*. 2008; 182: 225-232.
26. Coppolino MG, Dedhar S. Calreticulin. *Int J Biochem Cell Biol*. 1998; 30: 553-558.
27. Rane NS, Yonkovich JL, Hegde RS. Protection from cytosolic prion protein toxicity by modulation of protein translocation. *EMBO J*. 2004; 23: 4550-4559.
28. Yoon GS, Lee H, Jung Y, Yu E, Moon HB, Song K, Lee I. Nuclear matrix of calreticulin in hepatocellular carcinoma. *Cancer Res*. 2000; 60: 1117-1120.
29. Brunagel G, Shah U, Schoen RE, Getzenberg RH. Identification of calreticulin as a nuclear matrix protein associated with human colon cancer. *J Cell Biochem*. 2003; 89: 238-243.
30. Coker ML, Doscher MA, Thomas CV, Galis ZS, Spinale FG. Matrix metalloproteinase synthesis and expression in isolated LV myocyte preparations. *Am J Physiol*. 1999; 277: H777-87.
31. Chow AK, Cena J, El-Yazbi AF, Crawford BD, Holt A, Cho WJ, Daniel EE, Schulz R. Caveolin-1 inhibits matrix metalloproteinase-2 activity in the heart. *J Mol Cell Cardiol*. 2007; 42: 896-901.
32. Zenebe WJ, Nazarewicz RR, Parihar MS, Ghafourifar P. Hypoxia/reoxygenation of isolated rat heart mitochondria causes cytochrome c release and oxidative stress; evidence for involvement of mitochondrial nitric oxide synthase. *J Mol Cell Cardiol*. 2007; 43: 411-419.

33. Strongin AY. Mislocalization and unconventional functions of cellular MMPs in cancer. *Cancer Metastasis Rev.* 2006; 25: 87-98.
34. Miller JP, Holcomb J, Al-Ramahi I, de Haro M, Gafni J, Zhang N, Kim E, Sanhueza M, Torcassi C, Kwak S, Botas J, Hughes RE, Ellerby LM. Matrix metalloproteinases are modifiers of huntingtin proteolysis and toxicity in Huntington's disease. *Neuron.* 2010; 67: 199-212.
35. Si-Tayeb K, Monvoisin A, Mazzocco C, Lepreux S, Decossas M, Cubel G, Taras D, Blanc JF, Robinson DR, Rosenbaum J. Matrix metalloproteinase 3 is present in the cell nucleus and is involved in apoptosis. *Am J Pathol.* 2006; 169: 1390-1401.

CHAPTER 3

Hydrogen peroxide-induced necrotic cell death in cardiomyocytes is independent of matrix metalloproteinase-2

3.1: Introduction

MMPs are zinc-dependent endopeptidases best known to be involved in the proteolysis of extracellular matrix proteins. A variety of cells including cardiomyocytes synthesize MMPs in a zymogen form which can be activated by either proteolytic cleavage¹ or oxidative stress^{2,3}. Generally MMPs contribute to long-term remodelling processes such as embryogenesis, tumor cell invasion, and wound healing⁴. However, evidence is accumulating which shows that MMPs (in particular MMP-2) can also have rapid effects in regulating diverse cellular functions independent of extracellular matrix degradation (for reviews see^{5,6}).

Recently, the involvement of MMP-2 in oxidative stress-induced cell death pathways has been suggested⁷⁻⁹. Aldonyte et al. (2009) showed that cigarette smoke exposure causes nuclear localization and activation of MMP-2 in pulmonary artery endothelial cells. Interestingly, this increased nuclear MMP-2 activity was associated with subsequent apoptotic events⁸. Neuronal apoptosis, induced by ischemic injury to rat brains, was associated with increased nuclear MMP-2 activity and treatment of rats with a broad-spectrum MMP inhibitor significantly attenuated apoptosis in ischemic brain cells⁹. Moreover, MMP-2 activation has been shown to contribute to tumor necrosis factor alpha-induced apoptosis in cardiomyocytes. Inhibiting MMP activity with 10 μ M GM-6001 prior to tumor necrosis factor alpha insult decreased myocardial cell death as seen by reduced TUNEL-positive myocytes, DNA fragmentation, Bax expression and caspase-3 activity⁷. The mechanisms, however, implicating MMP-2 in oxidative stress-induced myocardial cell death are still poorly understood.

In addition to the well established role of reactive oxygen species generation in cardiomyocyte death^{10,11}, reactive oxygen species can also activate key transcription factors which can regulate MMPs expression^{12,13}. For instance, several *in vivo* and *in*

vitro studies have demonstrated a direct relationship between the generation of reactive oxygen species and MMP-2 expression level and/or activity¹⁴⁻¹⁶. In isolated mouse hearts, oxidative stress induced by I/R injury enhances MMP-2 expression via the AP-1 components FosB and JunB¹⁷. Using an *in vivo* model of myocardial infarction in mice, the generation of reactive oxygen species in hearts was accompanied by an increase in MMP-2 activity whereas the reactive oxygen species scavenger (dimethylthiourea) decreased its activity¹⁶. Kameda *et al.* (2003) demonstrated a positive correlation between a specific marker of oxidative stress (8-iso-PGF2 alpha) and relative levels of MMP-2 in the pericardial fluid of patients with coronary artery disease¹⁸.

Hydrogen peroxide is a relatively stable reactive oxygen species that is widely used to trigger cell death in various cell culture models. However, there is a controversy about the mode of cell death induced by hydrogen peroxide in cardiomyocytes. Apoptosis is defined as a pattern of programmed cell death marked by cell shrinkage, chromatin condensation and fragmentation of the cell into membrane-bound bodies without loss of plasma membrane integrity. By contrast, necrosis typically begins with cell swelling and disruption of the plasma membrane and other organelle membranes. While some studies report that hydrogen peroxide exposure (10-200 μ M) induces apoptosis in neonatal cardiomyocytes¹⁹⁻²², others have shown that similar concentrations of hydrogen peroxide induce cell death with ultrastructural changes typical of necrosis, which was not accompanied by caspase-3 cleavage or activation^{23, 24}. Moreover, Goto *et al.* (2009)²⁴ found that hydrogen peroxide-induced cell death does not satisfy the typical morphological criteria of apoptosis in cardiomyocytes.

We therefore sought to investigate the concentration- and time-dependent effects of hydrogen peroxide on MMP-2 expression and activity as well as the mode(s) of the induced cell death in neonatal rat cardiomyocytes. We hypothesized that hydrogen

peroxide-induced cell death is mediated, at least in part, via an increase in MMP-2 level/activity that may be prevented by pharmacological inhibition of MMPs.

3.2: Materials and Methods

3.2.1: Neonatal rat cardiomyocytes culture

All experiments were performed according to the recommendations given by the Guide to the Care and Use of Experimental Animals published by the Canadian Council on Animal Care and institutional guidelines for the care and use of animals.

Neonatal cardiomyocytes from 1- to 2-day-old Sprague–Dawley rats were isolated and cultured²⁵ with modifications. Hearts from the rat pups were removed and the ventricles were minced and digested with collagenase II (0.10% w/v, Worthington), trypsin (0.05% w/v, Worthington) and DNase I (0.025% w/v, Worthington) in phosphate buffered saline at 37 °C for 20 min. After digestion the tissue was centrifuged at 114 x g for 1 min at 4 °C in 20 ml of DMEM F12 media (Sigma) containing 20% fetal bovine serum (Invitrogen), and 50 µg/ml gentamicin. The supernatant was discarded and the pellet was subsequently added to DNase/collagenase/trypsin buffer for further digestion at 37°C for 20 min. After a second digestion, the tissue was centrifuged at 114 x g for 1 min at 4°C and subjected to a third digestion. After this all the supernatant fractions were pooled and centrifuged at 300 x g for 7 min at 4°C. The resulting pellet was resuspended in 10 ml of plating media (DMEM F12 media containing 5% fetal bovine serum, 10% horse serum, 50 µg/ml gentamicin) and the cell suspension was filtered through a cell strainer (BD Biosciences) and preplated for 60-90 min at 37°C to remove fibroblasts. The cells were added to 35 mm Primaria dishes (Falcon) at a density of 1.8–2.0 x 10⁶ cells/dish and maintained in DMEM/F12 medium containing 10% FBS. Twenty four

hours prior to experiments, the maintenance medium was replaced with serum free DMEM/F12 medium with 1% penicillin/streptomycin.

3.2.2: Hydrogen peroxide and MMP inhibitor treatments

For the induction of cell death, cardiomyocytes were exposed to hydrogen peroxide (30% ACS, Fischer Scientific) at different concentrations (50, 100, 200, 300, or 500 μ M) for the following time periods (0.5, 1, 2, 4, 8, 16, or 24 h). Where indicated, MMP inhibitors GM-6001 (10 μ M), ONO-4817 (10 μ M) or vehicle (DMSO) were added 1 h prior to hydrogen peroxide treatment. The concentration of DMSO during cell incubation did not exceed 0.01% v/v.

3.2.3: Lactate dehydrogenase leakage assay

Loss of plasma membrane integrity (cell necrosis) was assessed by measurement of the release of lactate dehydrogenase into the culture media. Lactate dehydrogenase activity was measured using a cytotoxicity detection kit (CytoTox-ONE, Promega Corporation, Madison, WI). In brief, at the specific time points, 50 μ l of culture medium was transferred to a black fluorescence plate and incubated for 10 min with 50 μ l of CytoTox-ONE™ reagent, followed by 20 μ l of stop solution. Fluorescence was measured at 560 nm excitation and 590 nm emission²⁶.

3.2.4: Western blotting

Cultured cells were washed twice with ice-cold phosphate-buffered saline and harvested in RIPA buffer (Pierce Biotechnology, Rockford, IL) including a protease inhibitor cocktail (P8340, Sigma) and Halt® phosphatase inhibitor cocktail (Pierce Biotechnology, Rockford, IL) and lysed gently, shaking the plates for 5 min at 4°C. Cell debris was removed by centrifuging the cell lysate at 14,000 g for 5 min at 4°C. The supernatant (cell lysate) was used for further analysis.

Protein concentration was measured using bicinchoninic acid protein assay reagent (Sigma). Equal protein samples (20 µg) of the cell lysates were electrophoresed on 10% or 12% SDS-PAGE under reducing conditions and the separated proteins were then transferred onto PVDF membranes. The membranes were blocked with 5% skim milk in Tris-buffered saline (10 mM Tris HCl, 150 mM NaCl, pH 7.5) containing 0.05% Tween-20 and then incubated at 4°C overnight with primary antibodies raised against MMP-2, caspase-3 (cleaved or full length) or PARP-1 (cleaved or full length). After washing, the blots were coupled with the peroxidase-conjugated secondary antibodies, washed, and then developed using the ECL detection kit (GE Healthcare UK Limited, Buckinghamshire, UK) according to the manufacturer's instructions. The membranes were stripped using Restore[®] western blot stripping buffer (Thermoscientific, Rockford, IL) and re-probed for α -actin. The intensity of protein bands was quantified densitometrically, and the value was estimated relative to that for α -actin which was used as a protein loading control.

3.2.5: Gelatin zymography

Cell lysate (10 µg protein/lane) was applied to 8% polyacrylamide gel copolymerized with 2 mg/ml of gelatin. After electrophoresis, gels were washed 3 times for 20 min each with 2.5% Triton X-100 to remove SDS. Then gels were rinsed with incubation buffer containing 50 mM Tris HCl (pH 7.6), 5 mM CaCl₂, 150 mM NaCl, and 0.05% w/v NaN₃ and incubated with the same incubation buffer at 37°C overnight. Conditioned media from HT1080 cells was used as standard for MMP-2. The gels were stained in 2% Coomassie brilliant blue G-250, 25% methanol and 10% acetic acid for 2 h and then destained for 1 h in 2% methanol / 4% acetic acid (v/v). Zymograms were scanned using a calibrated densitometer GS 800 (Biorad, Mississauga, ON) and the band

intensities were analyzed by densitometric analysis using the ImageJ software program (NIH).

3.2.6: Caspase-3 activity assay

Enzymatic reactions using cell lysates were carried out in a buffer containing 50 µg of protein, 25 mM HEPES (pH 7.4), 5 mM EDTA, 2 mM dithiothreitol, 10 µM digitonin and 50 µM acetyl-Asp-Glu-Val-Asp-aminotrifluoromethylcoumarin (DEVD-AFC, Enzo Life Sciences, Plymouth Meeting, USA) and the reaction mixtures were incubated at 37°C for 30 min. The fluorescence signal from liberated AFC was measured at 400/505 nm using a microplate fluorescence reader²⁷.

3.2.7: Statistical analysis

Results are expressed as mean ± S.E.M. for $n = 3$ experiments done using independent cell isolations. The statistical significance of differences between the mean values was analyzed by ANOVA followed by Dunnett's post-hoc test. Differences were considered significant at $p < 0.05$.

3.3: Results

3.3.1: Hydrogen peroxide treatment increases MMP-2 level and activity in neonatal cardiomyocytes

Neonatal rat cardiomyocytes were treated with hydrogen peroxide (50-500 µM) for different time intervals (0.5, 1, 2, 4, 8, 16 and 24 h). The MMP-2 response of the cardiomyocytes to hydrogen peroxide was dependent upon its concentration. At ≤ 100 µM hydrogen peroxide, there was either a modest or statistically insignificant increase in MMP-2 level and activity in a time-dependent manner (data not shown, $n=3$). However,

treatment with 200 μ M hydrogen peroxide showed a prominent effect on MMP-2 level/activity. Figure 3.1A shows that 200 μ M hydrogen peroxide stimulated a time-dependent increase in MMP-2 protein level which was significant at ≥ 8 h whereas the increase in MMP-2 gelatinolytic activity was significant at ≥ 4 h in comparison to the control (Figure 3.1B). Increasing hydrogen peroxide concentration beyond 200 μ M (300 and 500 μ M) did not significantly increase MMP-2 level or activity over controls (data not shown, n=3). Parallel time controls (without hydrogen peroxide treatment) did not show any significant changes in MMP-2 level or activity at the selected time intervals (data not shown, n=3).

3.3.2: Hydrogen peroxide induces necrotic but not apoptotic cell death in neonatal cardiomyocytes

Lactate dehydrogenase release is a sensitive measure of a damaged plasma membrane indicating necrotic cell death. Hydrogen peroxide (≤ 100 μ M) resulted in time-dependent increase in lactate dehydrogenase activity released into culture media that reached statistical significant at ≥ 8 h (data not shown). Figure 3.2A shows that 200 μ M hydrogen peroxide caused a significant increase in lactate dehydrogenase activity in the culture media at ≥ 2 h of treatment in comparison to control. However, hydrogen peroxide did not cause significant cleavage of the full length caspase-3 into its active, cleaved form at any of the selected time intervals (Figure 3.2B). Caspase-3 activity was not changed from basal levels by hydrogen peroxide (200 μ M, 4 h, n=3, data not shown). In contrast, hydrogen peroxide induced PARP-1 cleavage mainly into a 50 kD fragment as shown in Figure 3.2C, indicative of necrotic cell death²⁸⁻³⁰.

3.3.3: MMP inhibitors do not prevent increased MMP-2 level induced by hydrogen peroxide

We next determined the effect of MMP inhibitors (GM-6001 or ONO-4817) on the hydrogen peroxide-induced elevation in MMP-2 level and necrotic cell death. Figure 3.3 shows that 4 h treatment of cardiomyocytes with 200 μ M hydrogen peroxide significantly increased MMP-2 levels, yet neither GM-6001 nor ONO-4817 diminished this effect.

3.3.4: MMP inhibitors do not prevent hydrogen peroxide-induced necrotic cell death

Figure 3.4A shows that lactate dehydrogenase release induced by hydrogen peroxide (200 μ M, 4 h) was not prevented by GM-6001 or ONO-4817. Likewise, cleavage of PARP-1 mainly into its 50 kD fragment was not diminished by either GM-6001 or ONO-4817 (Figure 3.4B).

3.4: Discussion

Here, we demonstrated that hydrogen peroxide causes an increase in MMP-2 level and gelatinolytic activity in neonatal rat cardiomyocytes with the most prominent effect seen at 200 μ M. Additionally, hydrogen peroxide at this concentration induces necrotic rather than apoptotic cell death in cardiomyocytes as investigated between 0.5 to 24 h exposure times. However, pharmacological inhibition of MMP activity using two unique MMP inhibitors of different chemical classes did not prevent cardiomyocyte necrosis caused by hydrogen peroxide.

The effect of hydrogen peroxide on MMP-2 level/activity in neonatal cardiomyocytes observed here is in agreement with previous reports which utilized endothelial cells³¹, fibroblasts¹⁵ or H9c2 cardiomyoblasts³². Siwik et al.¹⁵ showed that MMP-2 activity is increased in both neonatal and adult cardiac fibroblasts by either hydrogen peroxide (5.0 μ M) or a superoxide generating system. However, they neither investigated the mode of cell death nor the effects or functional consequences of MMPs inhibition in their cell culture model.

It was shown that reactive oxygen species generation mediated by I/R injury can induce transcriptional upregulation of MMP-2 in the heart and this effect is via a mechanism involving nuclear localization and binding of AP-1 transcription factor complex to the intrinsic MMP-2 promoter¹⁷. Interestingly, treating neonatal cardiomyocytes with hydrogen peroxide was shown to induce Jun kinase activity in a concentration-dependent manner with a maximal effect seen at 200 μ M²², a concentration we show here which best augments MMP-2 levels and activity. Ispanovic and Haas (2006) reported that Jun kinase increases MMP-2 mRNA levels in endothelial cells³³.

Our study was also designed to investigate the mode of cell death (apoptosis vs. necrosis) in cardiomyocytes in response to hydrogen peroxide. We demonstrated that 200 μ M hydrogen peroxide induced cardiomyocyte necrosis but not apoptosis. Our findings are in contrast to previous studies which showed that similar concentrations of hydrogen peroxide induced apoptosis in cardiomyocytes, however, in most of the previous studies DNA laddering, TUNEL assay or annexin V staining were used to identify apoptotic cell death¹⁹⁻²¹. It is noteworthy that DNA laddering, TUNEL assay and annexin V staining are not highly specific to apoptosis and may also detect necrotic cells³⁴⁻³⁷. We however

showed that necrotic cell death is efficiently stimulated in cardiomyocytes as shown by the release of lactate dehydrogenase (a sensitive measure of plasma membrane integrity) and by the necrotic cleavage of PARP-1. Apoptotic cell death as measured by caspase-3 cleavage or its activity, or apoptotic PARP-1 cleavage to its 89 kD fragment (examples of biochemical hallmarks of apoptosis) did not occur. On the other hand, our present study is in agreement with two recent reports showing that necrosis, rather than apoptosis, is the main mode of cell death in hydrogen peroxide treated cardiomyocytes^{23,24}.

PARP-1 is a 113 kD nuclear enzyme that modifies other nuclear proteins by poly ADP-ribosylation in response to DNA damage³⁸. It has been considered that cleavage of PARP-1 into a 89 kD fragment by caspase-3 or -7 is a useful hallmark of apoptotic cell death^{39,40}. On the contrary, during necrosis, PARP-1 has been found to be cleaved into a major 50 kD fragment and a minor 89 kD fragment²⁸⁻³⁰. Moreover, this necrotic cleavage of PARP-1 is caused at least in part by lysosomal proteases (cathepsins B and G) which are released during necrosis³⁰. Interestingly, our results demonstrate that PARP-1 is cleaved primarily into a 50 kD fragment during hydrogen peroxide exposure, which further support that the primary mode of cell death is necrosis and not apoptosis.

We showed that hydrogen peroxide exposure caused necrotic death which was associated with increased MMP-2 level and activity in cardiomyocytes. This led us to hypothesize that necrotic cell death following hydrogen peroxide is at least partially mediated by MMP-2 activity. We used a concentration of GM-6001 which was previously shown to inhibit MMP-2 activity and protected against tumor necrosis factor alpha-induced cell death in cardiomyocytes⁷. Since the K_i values of GM-6001 (0.5 nM) and ONO-4817 (0.7 nM) for MMP-2 are comparable, we used the same concentration (10 μ M) of either compound. In contrast to GM-6001, ONO-4817 shows greater selectivity

towards MMP-2 and MMP-9 compared to other MMPs ⁴¹. Both GM-6001 and ONO-4817 did not affect the ability of hydrogen peroxide to increase MMP-2 level which suggests that these compounds do not interfere with the signalling pathway elicited by reactive oxygen species to induce MMP-2 expression. However, neither GM-6001 nor ONO-4817 showed protection against hydrogen peroxide-induced necrotic death in cardiomyocytes under our conditions. Likewise, a previous study showed that calpain-1 and cathepsin D inhibitors did not reduce 200 μ M hydrogen peroxide-induced cardiomyocyte necrosis suggesting other classes of proteases may be involved in mediating necrotic cell death ²³. Despite the fact that calpains and cathepsins proteases have been implicated as key mediators of necrosis ⁴², we and others reveal some complexity of the role played by proteases in necrosis. Our study, however, does not exclude the possibility that inhibiting these classes of proteases together (MMPs, calpains and cathepsins) may prove to be more effective in preventing necrotic cell death in cardiomyocytes.

In conclusion, the present study shows that 200 μ M hydrogen peroxide causes a time-dependent increase in MMP-2 protein level and activity in neonatal cardiomyocytes. Hydrogen peroxide is also found to induce primarily necrosis, but not apoptosis, in an MMP-independent manner. The release of lactate dehydrogenase in the absence of caspase-3 cleavage or activation, and the necrotic signature of PARP-1 cleavage are three lines of evidence which support this notion. Our results caution against the use of hydrogen peroxide to trigger apoptosis in neonatal cardiomyocytes. Thus, there is still a need for further investigations to unravel the exact role of proteases in mediating necrotic death following oxidative stress.

Figure 3.1: Hydrogen peroxide increases MMP-2 protein level and activity in neonatal cardiomyocytes.

A. Upper panel: Representative western blot shows the effect of 200 μ M hydrogen peroxide on MMP-2 and α -actin levels in cell lysates of neonatal cardiomyocytes following 30 min up to 24 h exposure. Lower panel: Quantitative analysis of MMP-2 level normalized to actin in cardiomyocytes treated with 200 μ M hydrogen peroxide at the indicated time intervals. (n= 3, * p < 0.05 vs. zero time, ANOVA followed by Dunnett's pos-hoc test). B. Upper panel: Representative gelatin zymogram shows the effect of 200 μ M hydrogen peroxide on MMP-2 activity in neonatal cardiomyocytes from 30 min up to 24 h after the exposure. Lower panel: Quantitative analysis of MMP-2 activity as fold increase vs. zero time in cardiomyocytes treated with 200 μ M hydrogen peroxide at the indicated time intervals. (n= 3, * p < 0.05, ** p < 0.01 vs. zero time, ANOVA followed by Dunnett's pos-hoc test). Experiments done by M. A. Ali and A. D. Kandasamy.

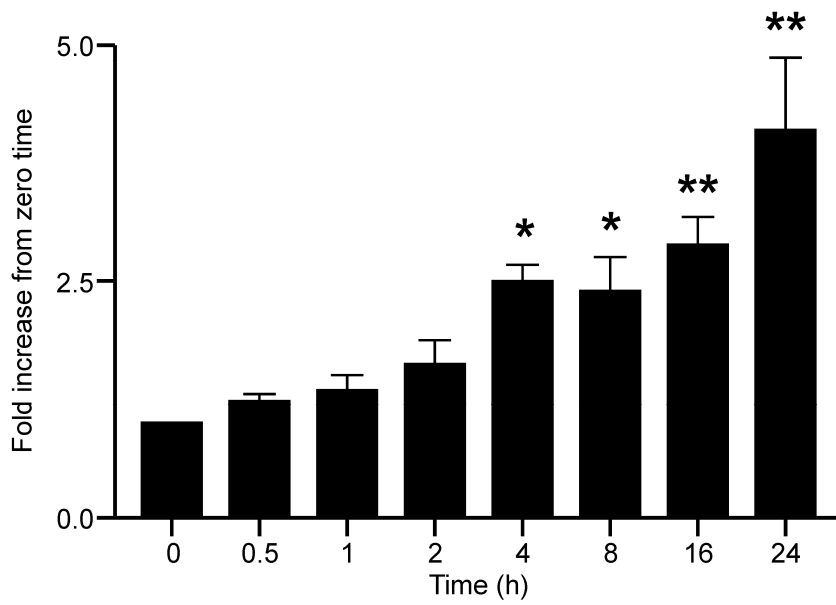
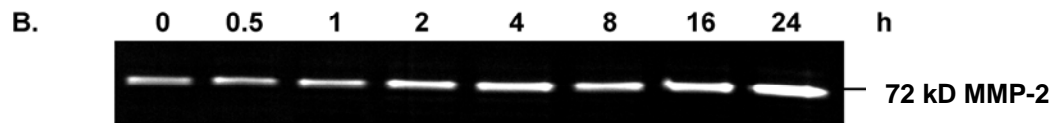
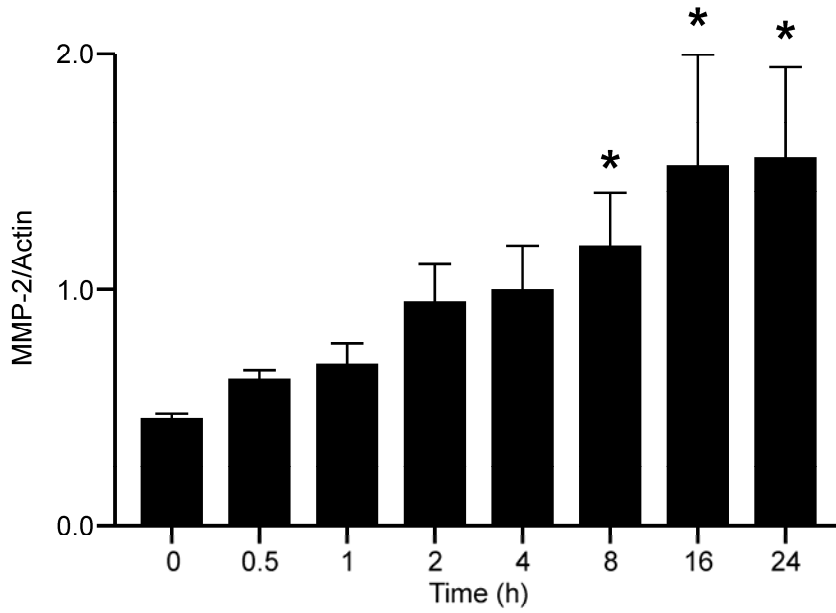
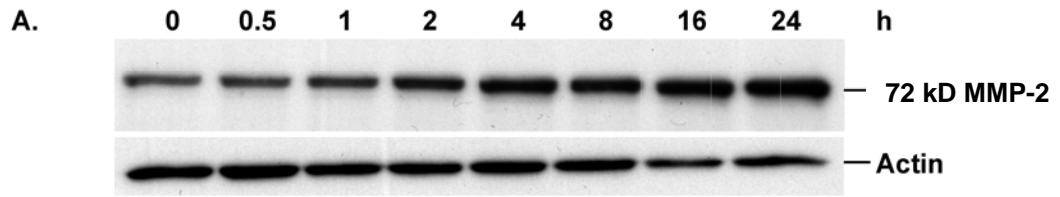


Figure 3.2: Hydrogen peroxide induces necrotic but not apoptotic cell death in neonatal cardiomyocytes.

A. Treating cardiomyocytes with 200 μ M hydrogen peroxide causes release of lactate dehydrogenase into the culture medium in a time-dependent manner. (n= 3, * p < 0.05 vs. zero time, ANOVA followed by Dunnett's pos-hoc test). B. Western blot from a representative experiment in cell lysates shows that hydrogen peroxide treatment does not efficiently cleave caspase-3 into a 17 kD fragment in cardiomyocytes up to 24 h after the exposure. C. Western blot shows that PARP-1 is cleaved in hydrogen peroxide-treated cardiomyocytes into a major fragment of 50 kD (indicative of necrosis) and a minor 89 kD fragment (indicative of apoptosis) (The blots are representative of three independent experiments with similar results). Experiments done by M. A. Ali and A. D. Kandasamy.

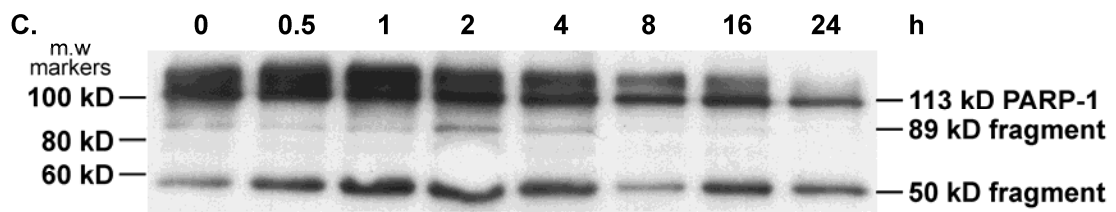
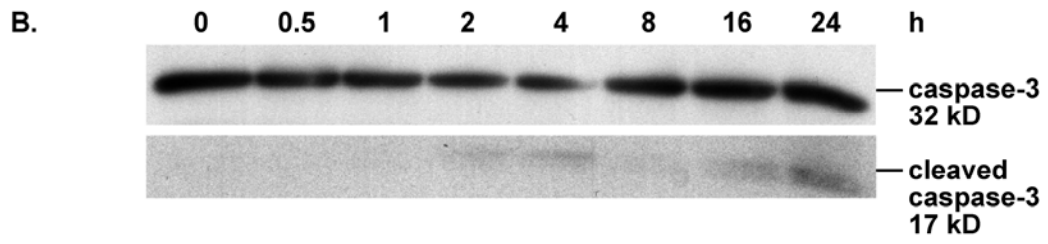
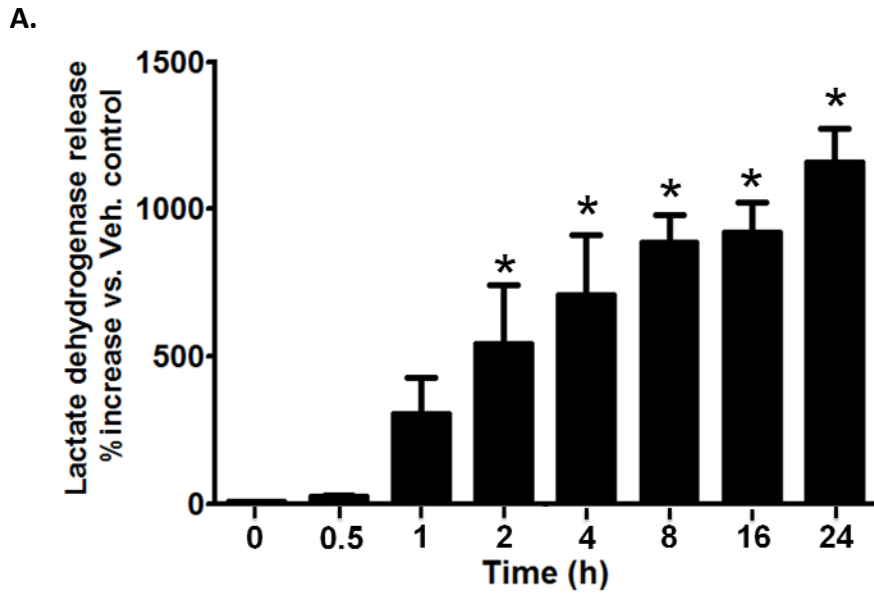


Figure 3.3: Effect of MMP inhibitors on hydrogen peroxide-induced MMP-2 elevation.

Upper panel: Representative western blot of cell lysates showing that MMP inhibitors (GM-6001 or ONO-4817, 10 μ M each) do not affect the increase in MMP-2 level induced by 200 μ M hydrogen peroxide exposure for 4 h. Lower panel: Quantitative analysis of MMP-2/actin ratios in cell lysates from cardiomyocytes treated with 200 μ M hydrogen peroxide for 4 h with or without GM-6001 or ONO-4817. (n= 3, * p < 0.05 vs. control, ANOVA followed by Dunnett's post-hoc test). DMSO was used as a vehicle control. Experiments done by M. A. Ali and A. D. Kandasamy.

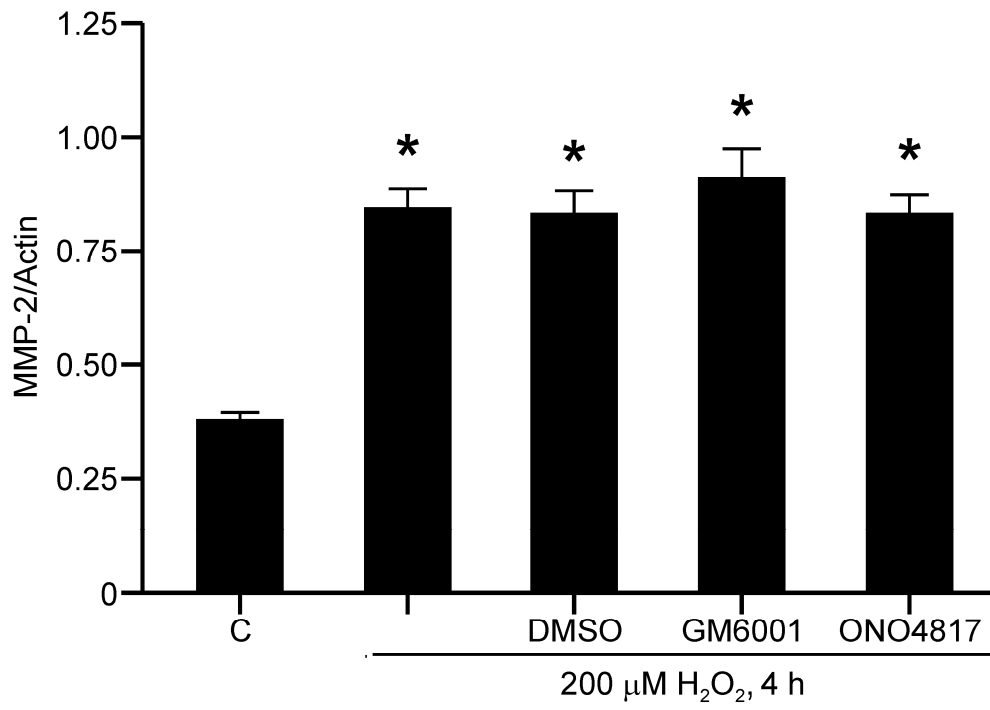
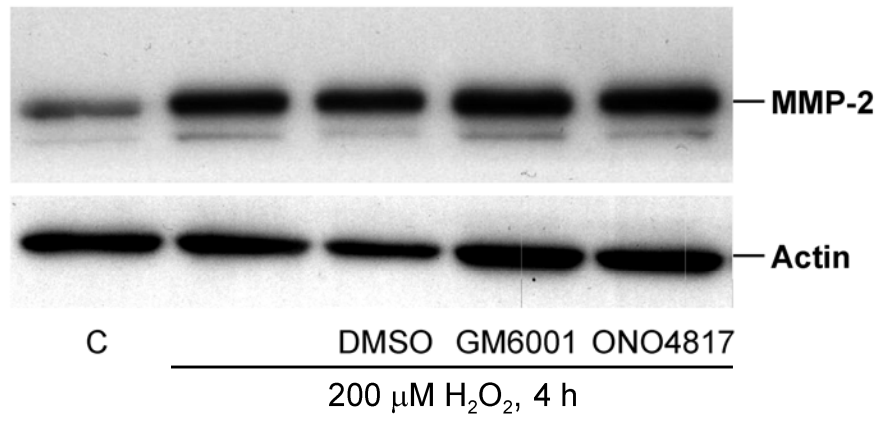
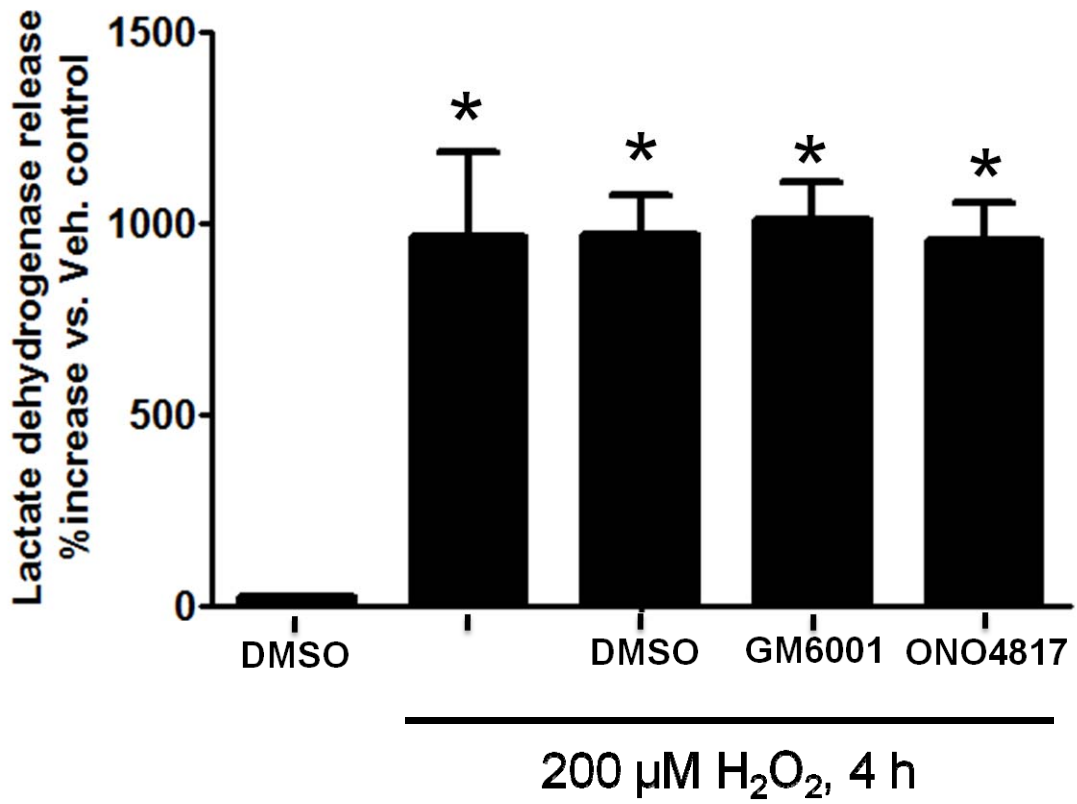


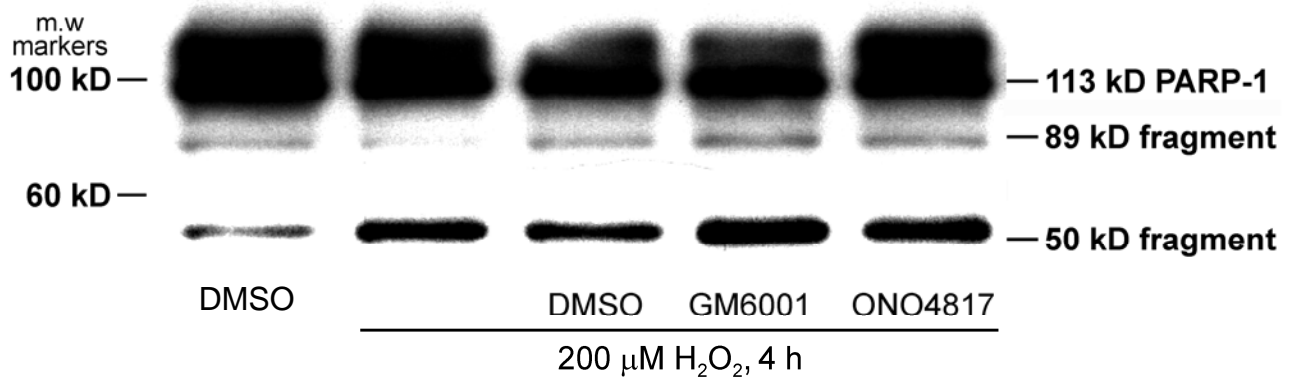
Figure 3.4: MMP inhibitors do not protect against hydrogen peroxide-induced necrosis in cardiomyocytes.

A. Hydrogen peroxide (200 μ M) causes a significant release of lactate dehydrogenase into the culture medium which is not affected by GM-6001 or ONO-4817 treatment. (n= 3, * p < 0.05 vs. control, ANOVA followed by Dunnett's post-hoc test). B. Western blot of cell lysates shows that PARP-1 is cleaved into a 50 kD fragment (indicative of necrosis) by hydrogen peroxide, an effect which is not diminished with MMP inhibitors. DMSO was used as a vehicle control. (The blot is representative of three independent experiments which showed similar results). Experiments done by M. A. Ali and A. D. Kandasamy.

A.



B.



3.5: Referneces

1. Cao J, Sato H, Takino T, Seiki M. The C-terminal region of membrane type matrix metalloproteinase is a functional transmembrane domain required for pro-gelatinase A activation. *J Biol Chem.* 1995; 270: 801-805.
2. Okamoto T, Akaike T, Sawa T, Miyamoto Y, van der Vliet A, Maeda H. Activation of matrix metalloproteinases by peroxynitrite-induced protein S-glutathiolation via disulfide S-oxide formation. *J Biol Chem.* 2001; 276: 29596-29602.
3. Viappiani S, Nicolescu AC, Holt A, Sawicki G, Crawford BD, Leon H, van Mulligen T, Schulz R. Activation and modulation of 72kDa matrix metalloproteinase-2 by peroxynitrite and glutathione. *Biochem Pharmacol.* 2009; 77: 826-834.
4. Woessner JF, Jr. Matrix metalloproteinases and their inhibitors in connective tissue remodeling. *FASEB J.* 1991; 5: 2145-2154.
5. McCawley LJ, Matrisian LM. Matrix metalloproteinases: they're not just for matrix anymore! *Curr Opin Cell Biol.* 2001; 13: 534-540.
6. Schulz R. Intracellular targets of matrix metalloproteinase-2 in cardiac disease: rationale and therapeutic approaches. *Annu Rev Pharmacol Toxicol.* 2007; 47: 211-242.
7. Shen J, O'Brien D, Xu Y. Matrix metalloproteinase-2 contributes to tumor necrosis factor alpha induced apoptosis in cultured rat cardiac myocytes. *Biochem Biophys Res Commun.* 2006; 347: 1011-1020.

8. Aldonyte R, Brantly M, Block E, Patel J, Zhang J. Nuclear localization of active matrix metalloproteinase-2 in cigarette smoke-exposed apoptotic endothelial cells. *Exp Lung Res.* 2009; 35: 59-75.
9. Yang Y, Candelario-Jalil E, Thompson JF, Cuadrado E, Estrada EY, Rosell A, Montaner J, Rosenberg GA. Increased intranuclear matrix metalloproteinase activity in neurons interferes with oxidative DNA repair in focal cerebral ischemia. *J Neurochem.* 2010; 112: 134-149.
10. Maulik N, Yoshida T, Das DK. Oxidative stress developed during the reperfusion of ischemic myocardium induces apoptosis. *Free Radic Biol Med.* 1998; 24: 869-875.
11. von Harsdorf R, Li PF, Dietz R. Signaling pathways in reactive oxygen species-induced cardiomyocyte apoptosis. *Circulation.* 1999; 99: 2934-2941.
12. Giordano FJ. Oxygen, oxidative stress, hypoxia, and heart failure. *J Clin Invest.* 2005; 115: 500-508.
13. Siwik DA, Colucci WS. Regulation of matrix metalloproteinases by cytokines and reactive oxygen/nitrogen species in the myocardium. *Heart Fail Rev.* 2004; 9: 43-51.
14. Galli A, Svegliati-Baroni G, Ceni E, Milani S, Ridolfi F, Salzano R, Tarocchi M, Grappone C, Pellegrini G, Benedetti A, Surrenti C, Casini A. Oxidative stress stimulates proliferation and invasiveness of hepatic stellate cells via a MMP2-mediated mechanism. *Hepatology.* 2005; 41: 1074-1084.
15. Siwik DA, Pagano PJ, Colucci WS. Oxidative stress regulates collagen synthesis and matrix metalloproteinase activity in cardiac fibroblasts. *Am J Physiol Cell Physiol.* 2001; 280: C53-60.

16. Kinugawa S, Tsutsui H, Hayashidani S, Ide T, Suematsu N, Satoh S, Utsumi H, Takeshita A. Treatment with dimethylthiourea prevents left ventricular remodeling and failure after experimental myocardial infarction in mice: role of oxidative stress. *Circ Res.* 2000; 87: 392-398.
17. Alfonso-Jaume MA, Bergman MR, Mahimkar R, Cheng S, Jin ZQ, Karliner JS, Lovett DH. Cardiac ischemia-reperfusion injury induces matrix metalloproteinase-2 expression through the AP-1 components FosB and JunB. *Am J Physiol Heart Circ Physiol.* 2006; 291: H1838-46.
18. Kameda K, Matsunaga T, Abe N, Hanada H, Ishizaka H, Ono H, Saitoh M, Fukui K, Fukuda I, Osanai T, Okumura K. Correlation of oxidative stress with activity of matrix metalloproteinase in patients with coronary artery disease. Possible role for left ventricular remodelling. *Eur Heart J.* 2003; 24: 2180-2185.
19. Kakita T, Hasegawa K, Iwai-Kanai E, Adachi S, Morimoto T, Wada H, Kawamura T, Yanazume T, Sasayama S. Calcineurin pathway is required for endothelin-1-mediated protection against oxidant stress-induced apoptosis in cardiac myocytes. *Circ Res.* 2001; 88: 1239-1246.
20. Iwai-Kanai E, Hasegawa K, Adachi S, Fujita M, Akao M, Kawamura T, Kita T. Effects of endothelin-1 on mitochondrial function during the protection against myocardial cell apoptosis. *Biochem Biophys Res Commun.* 2003; 305: 898-903.
21. Long X, Goldenthal MJ, Wu GM, Marin-Garcia J. Mitochondrial Ca²⁺ flux and respiratory enzyme activity decline are early events in cardiomyocyte response to H₂O₂. *J Mol Cell Cardiol.* 2004; 37: 63-70.

22. Tran TH, Andreka P, Rodrigues CO, Webster KA, Bishopric NH. Jun kinase delays caspase-9 activation by interaction with the apoptosome. *J Biol Chem.* 2007; 282: 20340-20350.
23. Casey TM, Arthur PG, Bogoyevitch MA. Necrotic death without mitochondrial dysfunction-delayed death of cardiac myocytes following oxidative stress. *Biochim Biophys Acta.* 2007; 1773: 342-351.
24. Goto K, Takemura G, Maruyama R, Nakagawa M, Tsujimoto A, Kanamori H, Li L, Kawamura I, Kawaguchi T, Takeyama T, Fujiwara H, Minatoguchi S. Unique mode of cell death in freshly isolated adult rat ventricular cardiomyocytes exposed to hydrogen peroxide. *Med Mol Morphol.* 2009; 42: 92-101.
25. Karnabi E, Qu Y, Mancarella S, Yue Y, Wadgaonkar R, Boutjdir M. Silencing of Cav1.2 gene in neonatal cardiomyocytes by lentiviral delivered shRNA. *Biochem Biophys Res Commun.* 2009; 384: 409-414.
26. El-Andaloussi S, Jarver P, Johansson HJ, Langel U. Cargo-dependent cytotoxicity and delivery efficacy of cell-penetrating peptides: a comparative study. *Biochem J.* 2007; 407: 285-292.
27. Xiang J, Chao DT, Korsmeyer SJ. BAX-induced cell death may not require interleukin 1 beta-converting enzyme-like proteases. *Proc Natl Acad Sci U S A.* 1996; 93: 14559-14563.
28. Shah GM, Shah RG, Poirier GG. Different cleavage pattern for poly(ADP-ribose) polymerase during necrosis and apoptosis in HL-60 cells. *Biochem Biophys Res Commun.* 1996; 229: 838-844.

29. Casiano CA, Ochs RL, Tan EM. Distinct cleavage products of nuclear proteins in apoptosis and necrosis revealed by autoantibody probes. *Cell Death Differ.* 1998; 5: 183-190.
30. Gobeil S, Boucher CC, Nadeau D, Poirier GG. Characterization of the necrotic cleavage of poly(ADP-ribose) polymerase (PARP-1): implication of lysosomal proteases. *Cell Death Differ.* 2001; 8: 588-594.
31. Belkhir A, Richards C, Whaley M, McQueen SA, Orr FW. Increased expression of activated matrix metalloproteinase-2 by human endothelial cells after sublethal H₂O₂ exposure. *Lab Invest.* 1997; 77: 533-539.
32. Kandasamy AD, Schulz R. Glycogen synthase kinase-3beta is activated by matrix metalloproteinase-2 mediated proteolysis in cardiomyoblasts. *Cardiovasc Res.* 2009; 83: 698-706.
33. Ispanovic E, Haas TL. JNK and PI3K differentially regulate MMP-2 and MT1-MMP mRNA and protein in response to actin cytoskeleton reorganization in endothelial cells. *Am J Physiol Cell Physiol.* 2006; 291: C579-88.
34. Collins RJ, Harmon BV, Gobe GC, Kerr JF. Internucleosomal DNA cleavage should not be the sole criterion for identifying apoptosis. *Int J Radiat Biol.* 1992; 61: 451-453.
35. Grasl-Kraupp B, Ruttkay-Nedecky B, Koudelka H, Bukowska K, Bursch W, Schulte-Hermann R. In situ detection of fragmented DNA (TUNEL assay) fails to discriminate among apoptosis, necrosis, and autolytic cell death: a cautionary note. *Hepatology.* 1995; 21: 1465-1468.

36. Dong Z, Saikumar P, Weinberg JM, Venkatachalam MA. Internucleosomal DNA cleavage triggered by plasma membrane damage during necrotic cell death. Involvement of serine but not cysteine proteases. *Am J Pathol.* 1997; 151: 1205-1213.
37. Lecoecur H, Prevost MC, Gougeon ML. Oncosis is associated with exposure of phosphatidylserine residues on the outside layer of the plasma membrane: a reconsideration of the specificity of the annexin V/propidium iodide assay. *Cytometry.* 2001; 44: 65-72.
38. D'Amours D, Desnoyers S, D'Silva I, Poirier GG. Poly(ADP-ribosyl)ation reactions in the regulation of nuclear functions. *Biochem J.* 1999; 342 (Pt 2): 249-268.
39. Kaufmann SH, Desnoyers S, Ottaviano Y, Davidson NE, Poirier GG. Specific proteolytic cleavage of poly(ADP-ribose) polymerase: an early marker of chemotherapy-induced apoptosis. *Cancer Res.* 1993; 53: 3976-3985.
40. Lazebnik YA, Kaufmann SH, Desnoyers S, Poirier GG, Earnshaw WC. Cleavage of poly(ADP-ribose) polymerase by a proteinase with properties like ICE. *Nature.* 1994; 371: 346-347.
41. Yamada A, Uegaki A, Nakamura T, Ogawa K. ONO-4817, an orally active matrix metalloproteinase inhibitor, prevents lipopolysaccharide-induced proteoglycan release from the joint cartilage in guinea pigs. *Inflamm Res.* 2000; 49: 144-146.
42. Syntichaki P, Tavernarakis N. The biochemistry of neuronal necrosis: rogue biology? *Nat Rev Neurosci.* 2003; 4: 672-684.

CHAPTER 4

Calpain inhibitors exhibit matrix metalloproteinase-2 inhibitory activity

A version of this chapter is published in:

Ali MA, Stepanko A, Fan X, Holt A, Schulz R. Calpain inhibitors exhibit matrix metalloproteinase-2 inhibitory activity. *Biochemical & Biophysical Research Communications* 2012 in press.

4.1: Introduction

MMP-2 is a member of the metzincin endopeptidase family that is capable of degrading proteins which make up the extracellular matrix. It was recognized, from their first description in amphibian metamorphosis ¹, that MMPs play an active role in remodeling the extracellular matrix accompanying both physiological and pathological processes, such as embryogenesis, wound healing, uterine involution, bone resorption, metastasis, arthritis, and heart failure ². Although most research has focused on the extracellular role of MMPs over long term pathophysiological processes, it has more recently been recognized that MMPs also act on non-extracellular matrix substrates both outside ³ and inside ^{4,5} the cell.

Many studies have shown that the activity of MMP-2 is enhanced in several cardiovascular diseases, including myocardial I/R injury ^{4, 6-8}. MMP-2 is expressed in the heart at substantial levels and its activity is increased upon oxidative stress injury ^{6, 7, 9}. It is well known that oxidative stress is an important mediator of acute myocardial contractile failure which occurs during I/R injury ¹⁰ and involves an overproduction of reactive oxygen species, particularly ONOO⁻ ^{11, 12}. ONOO⁻ by its turn activates intracellular MMP-2 via covalent modification of the critical cysteine residue in the propeptide domain ¹³. Indeed, this intracellular activity of MMP-2 is responsible for the proteolysis of specific sarcomeric and cytoskeletal proteins including TnI ¹⁴, MLC-1 ¹⁵, α -actinin ¹⁶ and titin ⁸ resulting in acute myocardial contractile dysfunction.

Calcium overload is another important mediator of I/R injury ¹⁰. During the early phase of reperfusion, there is an abrupt increase in intracellular calcium that induces

myocardial contractile dysfunction by various mechanisms, one of which may occur through the activation of calpains, calcium-dependant cytosolic proteases. Calpains are a family of non-lysosomal cysteine proteases that consists of several isoforms. The most characterized isoforms are calpain-1 (μ -calpain), calpain-2 (m-calpain) and calpain-3 (p94 calpain). The terms μ -calpain and m-calpain indicate the required calcium concentration (micromolar range for μ -calpain and millimolar range for m-calpain) for in vitro activity. Calpain-1 and -2 are heterodimers consisting of a large (82 kD) catalytic subunit and a small (28 kD) regulatory subunit. Calpain-1 and -2 are considered ubiquitous calpains expressed nearly in all tissues, whereas calpain-3 is tissue specific expressed mainly in skeletal muscles¹⁷. Calpains participate in various cellular processes including cytoskeletal remodelling, signal transduction and cell death¹⁸. Calpain-1, in particular, has been implicated in the pathogenesis of myocardial stunning injury¹⁹, under similar conditions where MMP-2 is activated^{6, 8, 14}. For example, it was suggested that calpain-1 proteolyzes cardiac TnI²⁰ and its activation seems to play an important role in myocardial I/R injury, in a similar manner to the role played by MMP-2.

Apparently, there may be an overlap in the substrates and/or biological actions of MMP-2 and calpains in various cellular pathways²¹. It may be that MMP-2 targets a similar subset of proteins as calpains, or that calpains have been misidentified as the proteases responsible for some intracellular proteolytic activity. Notably, much of the evidence of substrate degradation by calpains in the heart rests on the use of pharmacological inhibitors²²⁻²⁴. Interestingly, myocardial-specific over-expression of calpain-1 in transgenic mice showed no evidence of TnI degradation in the heart²⁵ whereas TnI levels were reduced in hearts from transgenic mice with myocardial-specific over-expression of constitutively active MMP-2²⁶. These observations led us to hypothesize that the beneficial effects of calpain inhibitors may also involve direct

inhibition of MMP-2 activity. Thus, we investigated the effect of four chemically distinct calpain inhibitors (calpain inhibitor III (aka MDL-28170), ALLN, ALLM and PD-150606) on the activity of MMP-2 and compared the inhibitory potencies of these compounds with that of a selective MMP inhibitor (ONO-4817).

4.2: Materials and methods

All reagents were of analytical grade and unless otherwise specified were purchased from Sigma-Aldrich (Oakville, ON). Human recombinant MMP-2 catalytic domain and OmniMMP[®] fluorogenic peptide substrate were obtained from Biomol (Plymouth Meeting, PA); calpain inhibitor III, ALLN, ALLM, PD-150606 and human erythrocytes calpain-1 from Calbiochem (San Diego, CA). ONO-4817 was a kind gift from Ono Pharmaceutical (Osaka, Japan).

The calpain inhibitors, calpain inhibitor III, ALLM, ALLN and PD-150606, have the following K_i values against calpain-1; 8 nM, 0.12 μ M, 0.2 μ M and 0.21 μ M, respectively (see manufacturer's data sheets). The K_i value of the MMP inhibitor, ONO-4817, for MMP-2 is 0.73 nM²⁷. K_i is the inhibition constant for an inhibitor that indicates its binding affinity to the enzyme, whereas IC_{50} indicates the concentration of the inhibitor required to decrease enzyme activity by 50%. IC_{50} values for an inhibitor are valid only for the particular assay performed while K_i is a constant.

4.2.1: Gelatin zymography

Gelatinolytic activity of 72 kD MMP-2 (from HT1080 cell conditioned culture media) by zymography was performed as previously described²⁸ with some modifications. Briefly, multiple 10 μ l aliquots of HT1080 media were electrophoresed on an 8% polyacrylamide gel containing 2 mg/ml gelatin for 90 min (125 V, ambient

temperature). After washing with Triton X-100 (2.5% v/v, 3 × 20 min), the gels were cut into individual vertical lanes representing individual aliquots. Each strip of electrophoresed proteins was incubated separately overnight at 37 °C in 10 ml zymography buffer (50 mM Tris-HCl, 150mM NaCl, 5 mM CaCl₂, pH 7.6) in the absence or presence of different calpain inhibitors: calpain inhibitor III, ALLN, ALLM or PD-150606 (100 μM each). For comparison other gel strips were incubated in the absence or presence of the MMP inhibitor ONO-4817 (K_i in the nanomolar range for MMP-2 and almost no inhibitory activity up to 100 μM against several other proteases of different classes including calpains ²⁷). Gels were stained with 0.05% Coomassie blue and subsequently destained. Gelatinolytic activities were detected as transparent bands against the blue-stained background.

4.2.2: TnI degradation assay

Two micrograms of recombinant human TnI (a kind gift from Dr. James Potter, University of Miami) were incubated with either human recombinant MMP-2 catalytic domain (10 ng, Biomol) in 50 mM Tris-HCl buffer (5 mM CaCl₂, 150 mM NaCl, pH 7.4) or calpain-1 (0.66 unit) in 20 mM Tris-HCl (0.15 mM CaCl₂, 25 mM NaCl, 10 mM DTT, pH 7.5) at 37°C for 30 or 60 minutes. In additional experiments MMP-2 or calpain-1 were incubated with the indicated calpain inhibitors (20 or 100 μM) or the MMP inhibitor ONO-4817 (20 or 100 μM) for 15 minutes at 37°C before adding TnI. The reaction mixtures (total volume 40 μL) were analyzed by 12% SDS-PAGE under reducing conditions and visualized by the Coomassie blue staining method. Band densities were measured using a densitometer (GS-800, BioRad) and ImageJ software. The ratio of cleaved to full-length TnI was calculated for each lane and presented as a percentage change from the DMSO vehicle control.

4.2.3: OmniMMP kinetic assay

The hydrolysis of OmniMMP[®] fluorogenic substrate (25 μ M, prepared in 0.4% v/v DMSO) by MMP-2 catalytic domain (0.5 nM in reaction buffer 50 mM Tris, pH 7.6, 10 mM CaCl₂, 0.05% Brij-35, 10 μ M ZnSO₄) was measured in the presence of calpain inhibitor III, ALLN, ALLM or PD-150606 or the selective MMP inhibitor (ONO-4817) at 37°C using a plate reader-based protocol²⁸. Assays were made in a total volume of 120 μ l in black polystyrene half-area plates (Corning, NY) and contained MMP-2 (60 μ l in 2X reaction buffer) and substrate (60 μ l) or DMSO vehicle (the final concentration of which did not exceed 0.16% v/v). Fluorescence associated with the (7-methoxycoumarin-4-yl)acetyl-tagged cleavage product was measured every 30 s for 1 h (λ_{ex} 328 nm, λ_{em} 393 nm) in a SPECTRAmax Gemini XPS (Molecular Devices, Sunnyvale, CA) fluorescence plate reader. The rate of product formation in each well was determined through linear regression of the experimental data ($r^2 > 0.98$) using SOFTmax Pro 4.8 software (Molecular Devices, Sunnyvale, CA). The experimental rates in the presence of inhibitors were normalized to the rates of the vehicle control. All experiments were performed with five replicates and the inhibitor concentrations required to produce 50% inhibition of enzyme activity (IC₅₀) were determined using non-linear curve fitting of data (GraphPad Prism version 5.0, San Diego, CA).

4.3: Results

4.3.1: Calpain inhibitors, but not ONO-4817, inhibit calpain-1-induced TnI cleavage

Figure 4.1 illustrates the chemical structures of calpain inhibitors used in the study in comparison with the MMP inhibitor, ONO-4817. Figure 4.2 shows that TnI was

completely proteolyzed to a ~ 15 kD product when incubated with calpain-1 (37°C, 60 min). As expected, all calpain inhibitors (100 µM) tested in this study abolished calpain-1-induced TnI degradation. In contrast, the same concentration of ONO-4817 did not show any calpain inhibitory activity, verifying its selectivity towards MMPs (Figure 4.2).

4.3.2: Calpain inhibitors decrease the gelatinolytic activity of MMP-2

Initially we screened the MMP-2 inhibitory effects of calpain inhibitors, in comparison with the specific MMP inhibitor ONO-4817 (Figure 4.1), using gelatin zymography. Used as a positive control, ONO-4817 (100 µM) showed complete inhibition of MMP-2 gelatinolytic activity (Figure 4.3). 72 kD MMP-2 activity was also significantly reduced by several of the calpain inhibitors (100 µM, each) including calpain inhibitor III (39%), ALLN (67%) or PD-150606 (84%) as compared to DMSO vehicle control as shown in Figure 4.3. In marked contrast, ALLM did not inhibit MMP-2 gelatinolytic activity.

4.3.3: Inhibition of MMP-2 catalytic activity by calpain inhibitors

As we have previously shown, TnI is also highly susceptible to proteolysis by MMP-2¹⁴. MMP-2 induced TnI degradation was then used as another mean to further test the inhibitory effects of calpain inhibitors on MMP-2 catalytic activity. The catalytic domain of MMP-2 cleaved TnI into a major 22 kD cleavage fragment when incubated for only 20 min at 37°C (Figure 4.4A). The ratio of cleaved to full length TnI was used as a measure of MMP-2 catalytic activity and was considered 100% in the absence of any inhibitors (DMSO vehicle control). ONO-4817 (20 µM) significantly inhibited MMP-2 activity by 97% in comparison to DMSO vehicle control (Figure 4.4). MMP-2 catalytic activity was significantly reduced by ALLN (43%) or PD-150606 (80%). In contrast,

calpain inhibitor III or ALLM did not significantly inhibit MMP-2 activity. All calpain inhibitors were tested at 20 μ M.

4.3.4: Determination of IC₅₀ of calpain and MMP inhibitors on MMP-2 activity using OmniMMP assay

We then analyzed the MMP-2 inhibitory effects of calpain inhibitors, versus the selective MMP inhibitor ONO-4817, using the OmniMMP kinetic assay. ONO-4817 and the calpain inhibitors blocked MMP-2 activity in a concentration-dependent manner with the following rank order of IC₅₀ values: ONO-4817 <<< PD-150606 < ALLN < calpain inhibitor III <<< ALLM (Figure 4.5). The IC₅₀ values of ONO-4817, PD-150606 and ALLN were 0.00025 μ M, 9.3 μ M and 21.9 μ M respectively. It is worth noting that this IC₅₀ value of ONO-4817 was measured using the 40 kD MMP-2 catalytic domain while the K_i value listed above is for active 64 kD MMP-2²⁷.

We could only estimate that the IC₅₀ value of calpain inhibitor III was between 50-100 μ M whereas ALLM was devoid of MMP-2 inhibitory activity.

4.4: Discussion

This study demonstrates that certain commonly employed calpain inhibitors (calpain inhibitor III, ALLN and PD-150606) possess significant additional pharmacological properties in their ability to also inhibit the enzymatic activity of MMP-2. In fact two calpain inhibitors (PD-150606 and ALLN, IC₅₀ = 9.3 μ M and 21.9 μ M, respectively) have similar potencies as MMP-2 inhibitors comparable to that of the widely used matrix metalloprotease inhibitors (doxycycline, minocycline and o-

phenanthroline)²⁸. These data suggest that the biological effects of some calpain inhibitors may include inhibition of MMP-2 activity.

Among the calpain inhibitors tested in the current study, PD-150606 was the most potent MMP-2 inhibitor. In its action as a calpain inhibitor, PD-150606 does not bind to the active cysteine site of the calpain as do other calpain inhibitors, but targets the calcium binding domain of the small regulatory subunit²⁹. It is worth noting that MMP-2 has a calcium binding subdomain within its catalytic domain and that calcium ions stabilize MMP-2 structure³⁰. The potential interaction of PD-150606 with the calcium binding site of MMP-2 provides an explanation of its marked inhibitory effect on MMP-2 activity. On the other hand carboxylate and thiol groups, both present in the PD-150606 structure (Figure 4.1), are reported to bind zinc ions³¹. Thus, PD-150606 may also chelate the catalytic zinc which is crucial for MMP-2 activity. Although hydroxamate compounds (e.g. ONO-4817, Fig. 1) are much stronger MMP inhibitors than carboxylate compounds, it was suggested that within acidic pH (as seen in inflammatory and ischemic conditions) carboxylates may become more potent MMP inhibitors than they are at neutral pH³¹. Apart from specific chelation of the catalytic zinc, recently designed MMP inhibitors bind the S₁' pocket and interact with amino acid residues (e.g. T, Y, F, and M) in the specificity loop, thereby interfering with enzyme activity³². PD-150606 contains an electron-rich aromatic ring that establishes electronic interaction with similar residues (Y, F and M) within the hydrophobic pocket on domain VI of the calpain small subunit²⁹. Such interaction may result in the observed MMP-2 inhibitory effect of PD-150606.

The cardio-³³, renal-³⁴ or neuro-^{35,36} protective effects of PD-150606 against I/R injury were previously shown when the compound was used in a concentration range of 25-100 μM . Although the IC₅₀ of PD-150606 against calpain-1 is around 0.2 μM ³⁵, the

protective effect was observed within a range of concentrations (25-100 μM) that exceed its IC_{50} on MMP-2. It is now well understood that MMP-2 plays an important role in mediating I/R injury in the heart ⁷, kidney ³⁷ or brain ³⁸. The protective effect of ALLN in various models of I/R injury has been shown to occur at concentrations (20-100 μM) ³⁹⁻⁴¹ that interfere with MMP-2 activity. Interestingly, a recent study shows that although both ALLM and ALLN at 25 μM inhibit in vitro calpain activity to a similar extent, whereas only ALLN protected against myocardial contractile dysfunction in rat hearts subjected to I/R injury ⁴¹. We previously observed that 50 μM ONO-4817, a selective MMP inhibitor that does not interfere with calpain activity up to 100 μM as seen here, functionally protected hearts against myocardial I/R injury ⁸ as have other MMP inhibitors o-phenanthroline, doxycycline or a neutralizing MMP-2 antibody ⁶. Together, these observations strongly suggest that the protective effect of ALLN in myocardial I/R injury ⁴¹ was likely due to its ability to inhibit MMP-2 activity. However, it is interesting to speculate what a combined approach to inhibit both MMP-2 and calpains, may achieve, in comparison to targeting one or the other protease independently.

In conclusion, the MMP-2 inhibitory effect demonstrated by some calpain inhibitors shown here may represent an alternative approach for designing more selective MMP inhibitors. Furthermore, our work suggests that the interpretation of biological results obtained using some calpain inhibitors must include possible effects mediated by the inhibition of MMP-2 activity, which is found in almost all cell types.

Figure 4.1: Chemical structures of the calpain inhibitors in comparison with the selective MMP inhibitor ONO-4817.

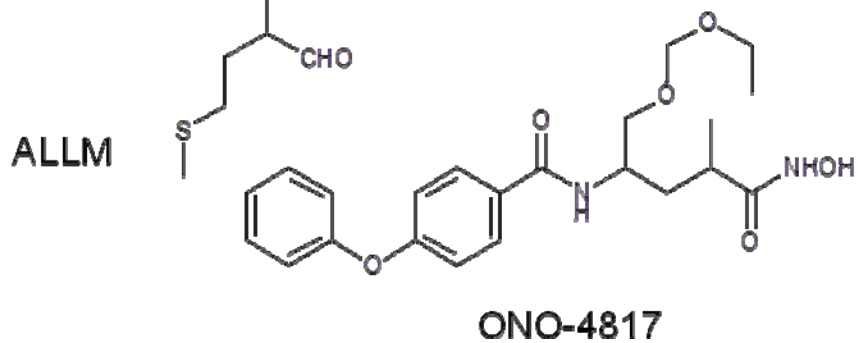
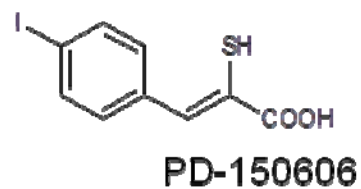
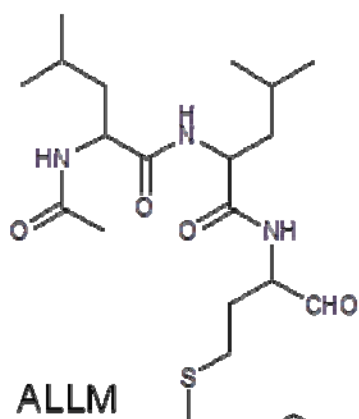
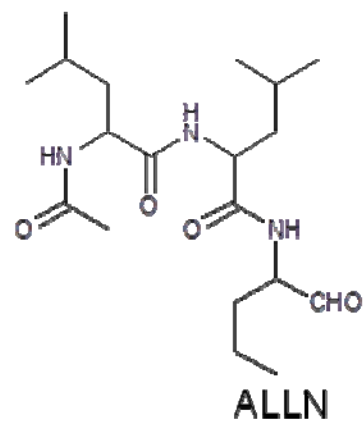
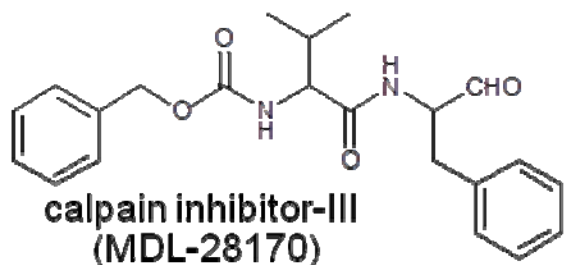


Figure 4.2: Calpain inhibitors, but not the selective MMP inhibitor ONO-4817, inhibit calpain-1 activity.

Coomassie blue stained SDS-PAGE gel following incubation of TnI with calpain-1 at 37°C for 60 min. TnI is completely degraded by calpain-1 to a \approx 15 kD product. DMSO is the vehicle control. Calpain inhibitors (calpain inhibitor III, ALLN, ALLM or PD-150606, 100 μ M each) efficiently inhibit calpain-1 activity whereas the selective MMP inhibitor ONO-4817 (100 μ M), does not inhibit calpain-1. MW, molecular weight markers. Experiments done by M. A. Ali.

Calpain-1

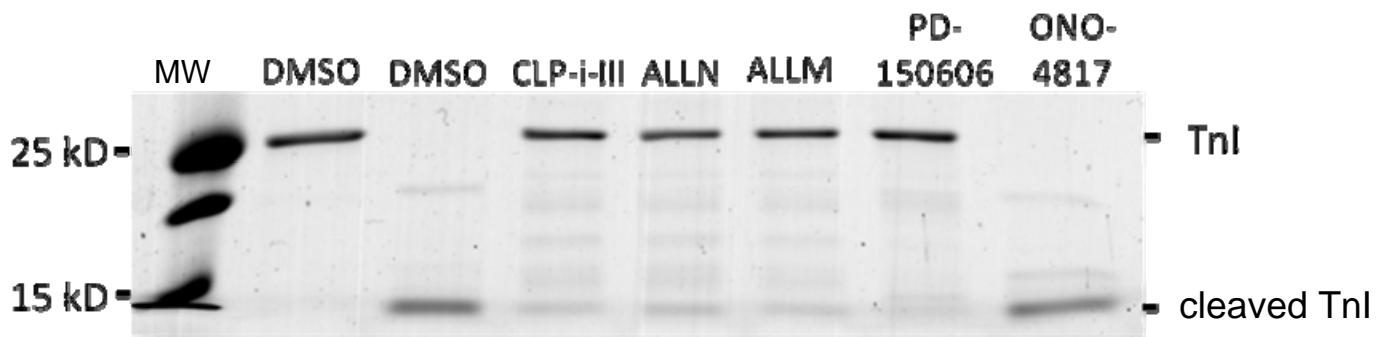


Figure 4.3: Calpain inhibitors inhibit MMP-2 gelatinolytic activity.

A) Representative gelatin zymograms of 72 kD MMP-2 incubated at 37°C overnight with calpain inhibitors (calpain inhibitor III, ALLN, ALLM or PD-150606, 100 µM each) or selective MMP inhibitor (ONO-4817, 100 µM). DMSO is the vehicle control. B) Quantitative analysis of MMP-2 gelatinolytic activity (% of DMSO control) in the presence of calpain inhibitors or selective MMP inhibitor ONO-4817. One-way ANOVA followed by Dunnett's multiple comparison post hoc test, n=3, * p < 0.05. Experiments done by M. A. Ali and A. Stepanko.

A



B

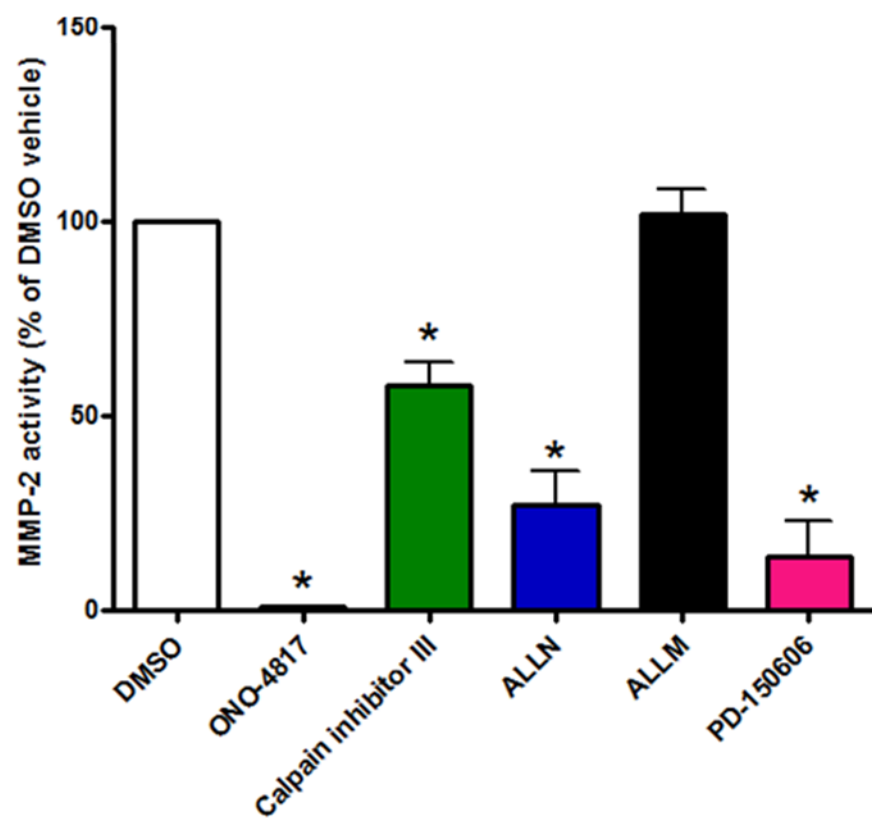
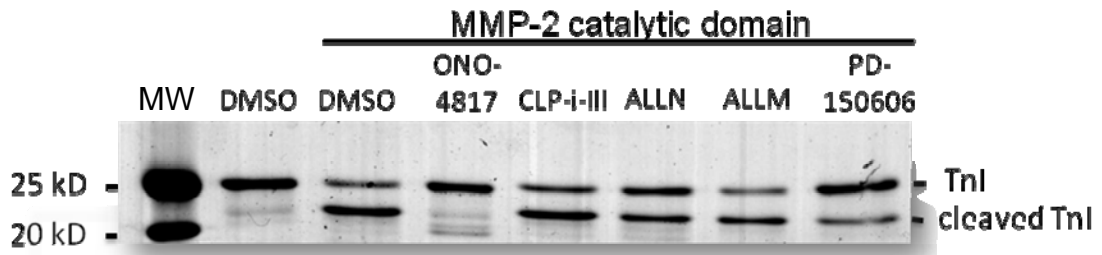


Figure 4.4: Some calpain inhibitors exhibit MMP-2 inhibitory activity as assessed by TnI degradation assay.

A) Coomassie blue stained SDS-PAGE shows that MMP-2 also efficiently cleaves TnI in vitro however, to a ~ 22 kD product. This cleavage of TnI is significantly inhibited by the calpain inhibitors (ALLN and PD-150606). ONO-4817 (selective MMP inhibitor) was used as positive control. DMSO is a vehicle control. B) Quantitative analysis of MMP-2 induced cleavage of TnI expressed as the ratio of cleaved TnI: full length TnI (as a % of DMSO control) in the presence of calpain inhibitors (calpain inhibitor III, ALLN, ALLM or PD-150606) or the selective MMP inhibitor (ONO-4817). All inhibitors were tested at 20 μ M. MW, molecular weight markers. One-way ANOVA followed by Dunnett's multiple comparison post hoc test, n=3, * p < 0.05. Experiments done by M. A. Ali and A. Stepanko.

A



B

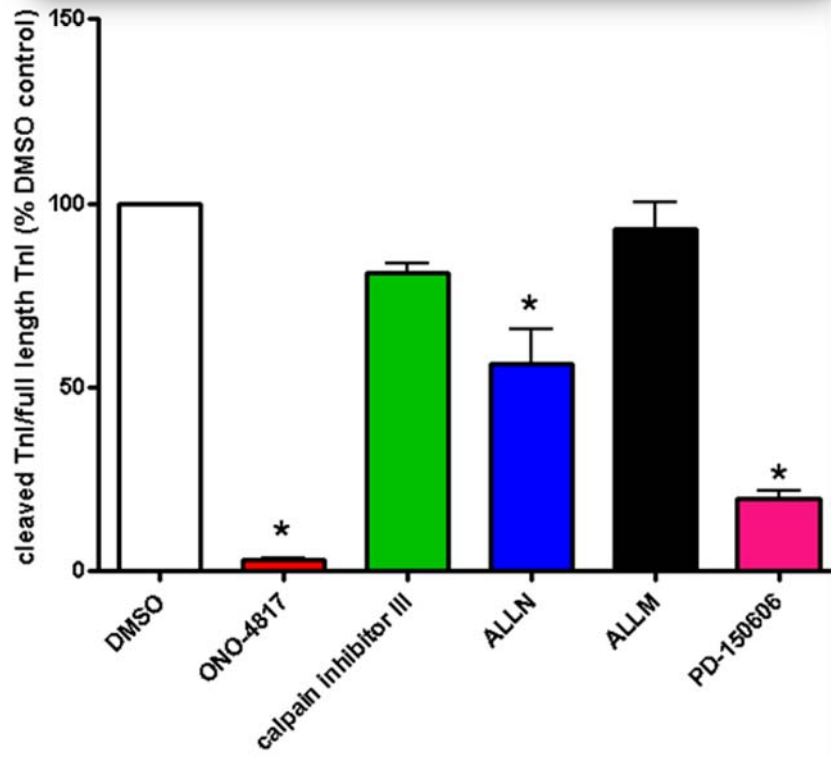
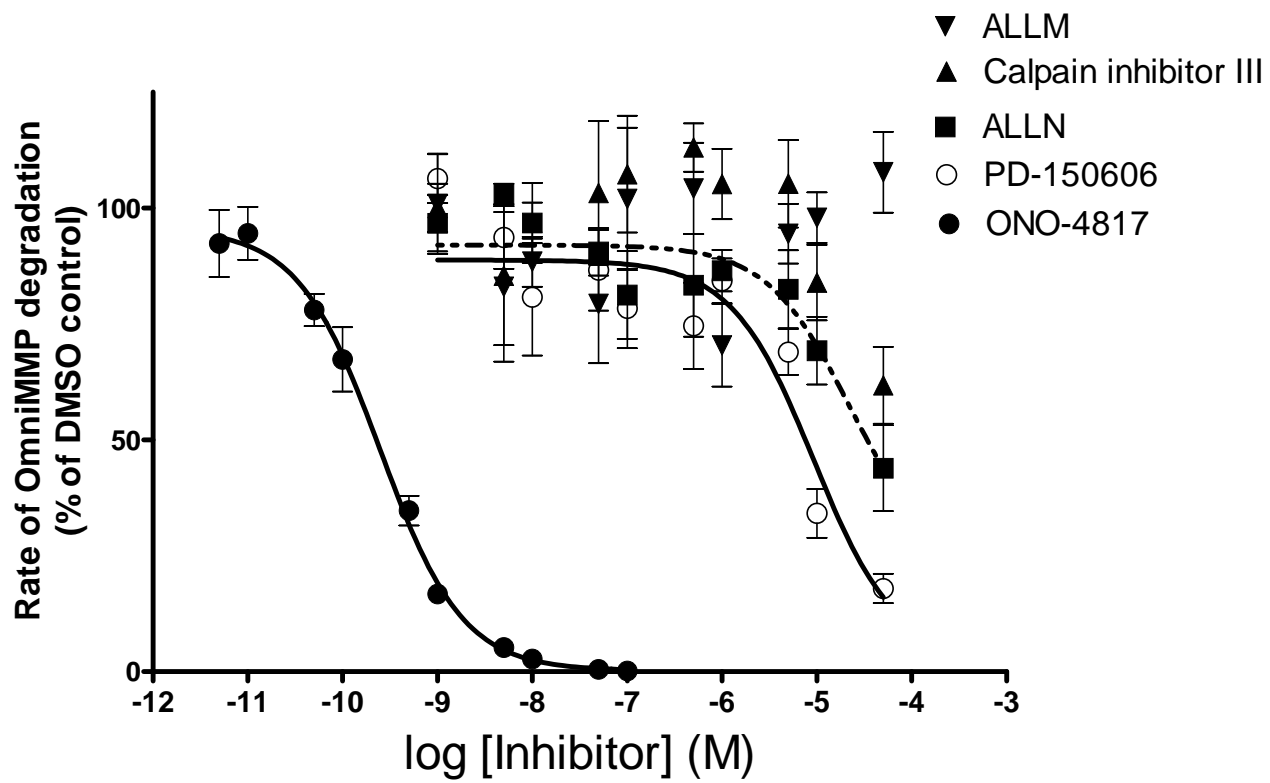


Figure 4.5: Concentration-dependent inhibitory effects of calpain inhibitors and a selective MMP inhibitor (ONO-4817) on MMP-2 activity as measured by fluorogenic substrate (OmniMMP) kinetic assay.

Calpain or MMP inhibitors were incubated with 0.5 nM MMP-2 catalytic domain and 25 μ M OmniMMP fluorogenic substrate at 37°C in 50 mM Tris buffer, pH 7.6, containing 10 mM CaCl₂ and 10 μ M ZnSO₄. Data represent means \pm SEM of five replicate determinations and were fitted to sigmoidal curves. Experiments done by M. A. Ali and A. Stepanko.



4.5: References

1. Gross J, Lapiere CM. Collagenolytic activity in amphibian tissues: a tissue culture assay. *Proc Natl Acad Sci U S A*. 1962; 48: 1014-1022.
2. Rodriguez D, Morrison CJ, Overall CM. Matrix metalloproteinases: what do they not do? New substrates and biological roles identified by murine models and proteomics. *Biochim Biophys Acta*. 2010; 1803: 39-54.
3. McCawley LJ, Matrisian LM. Matrix metalloproteinases: they're not just for matrix anymore! *Curr Opin Cell Biol*. 2001; 13: 534-540.
4. Schulz R. Intracellular targets of matrix metalloproteinase-2 in cardiac disease: rationale and therapeutic approaches. *Annu Rev Pharmacol Toxicol*. 2007; 47: 211-242.
5. Cauwe B, Opdenakker G. Intracellular substrate cleavage: a novel dimension in the biochemistry, biology and pathology of matrix metalloproteinases. *Crit Rev Biochem Mol Biol*. 2010; 45: 351-423.
6. Cheung PY, Sawicki G, Wozniak M, Wang W, Radomski MW, Schulz R. Matrix metalloproteinase-2 contributes to ischemia-reperfusion injury in the heart. *Circulation*. 2000; 101: 1833-1839.
7. Lalu MM, Pasini E, Schulze CJ, Ferrari-Vivaldi M, Ferrari-Vivaldi G, Bachetti T, Schulz R. Ischaemia-reperfusion injury activates matrix metalloproteinases in the human heart. *Eur Heart J*. 2005; 26: 27-35.
8. Ali MA, Cho WJ, Hudson B, Kassiri Z, Granzier H, Schulz R. Titin is a target of matrix metalloproteinase-2: implications in myocardial ischemia/reperfusion injury. *Circulation*. 2010; 122: 2039-2047.

9. Spinale FG. Myocardial matrix remodeling and the matrix metalloproteinases: influence on cardiac form and function. *Physiol Rev.* 2007; 87: 1285-1342.
10. Yellon DM, Hausenloy DJ. Myocardial reperfusion injury. *N Engl J Med.* 2007; 357: 1121-1135.
11. Yasmin W, Strynadka KD, Schulz R. Generation of peroxynitrite contributes to ischemia-reperfusion injury in isolated rat hearts. *Cardiovasc Res.* 1997; 33: 422-432.
12. Pacher P, Schulz R, Liaudet L, Szabo C. Nitrosative stress and pharmacological modulation of heart failure. *Trends Pharmacol Sci.* 2005; 26: 302-310.
13. Viappiani S, Nicolescu AC, Holt A, Sawicki G, Crawford BD, Leon H, van Mulligen T, Schulz R. Activation and modulation of 72kDa matrix metalloproteinase-2 by peroxynitrite and glutathione. *Biochem Pharmacol.* 2009; 77: 826-834.
14. Wang W, Schulze CJ, Suarez-Pinzon WL, Dyck JR, Sawicki G, Schulz R. Intracellular action of matrix metalloproteinase-2 accounts for acute myocardial ischemia and reperfusion injury. *Circulation.* 2002; 106: 1543-1549.
15. Sawicki G, Leon H, Sawicka J, Sariahmetoglu M, Schulze CJ, Scott PG, Szczesna-Cordary D, Schulz R. Degradation of myosin light chain in isolated rat hearts subjected to ischemia-reperfusion injury: a new intracellular target for matrix metalloproteinase-2. *Circulation.* 2005; 112: 544-552.
16. Sung MM, Schulz CG, Wang W, Sawicki G, Bautista-Lopez NL, Schulz R. Matrix metalloproteinase-2 degrades the cytoskeletal protein alpha-actinin in peroxynitrite mediated myocardial injury. *J Mol Cell Cardiol.* 2007; 43: 429-436.

17. Suzuki K, Hata S, Kawabata Y, Sorimachi H. Structure, activation, and biology of calpain. *Diabetes*. 2004; 53 Suppl 1: S12-8.
18. Huang Y, Wang KK. The calpain family and human disease. *Trends Mol Med*. 2001; 7: 355-362.
19. Gao WD, Liu Y, Mellgren R, Marban E. Intrinsic myofilament alterations underlying the decreased contractility of stunned myocardium. A consequence of Ca²⁺-dependent proteolysis? *Circ Res*. 1996; 78: 455-465.
20. McDonough JL, Arrell DK, Van Eyk JE. Troponin I degradation and covalent complex formation accompanies myocardial ischemia/reperfusion injury. *Circ Res*. 1999; 84: 9-20.
21. Kandasamy AD, Chow AK, Ali MA, Schulz R. Matrix metalloproteinase-2 and myocardial oxidative stress injury: beyond the matrix. *Cardiovasc Res*. 2010; 85: 413-423.
22. Iwamoto H, Miura T, Okamura T, Shirakawa K, Iwatate M, Kawamura S, Tatsuno H, Ikeda Y, Matsuzaki M. Calpain inhibitor-1 reduces infarct size and DNA fragmentation of myocardium in ischemic/reperfused rat heart. *J Cardiovasc Pharmacol*. 1999; 33: 580-586.
23. Khalil PN, Neuhof C, Huss R, Pollhammer M, Khalil MN, Neuhof H, Fritz H, Siebeck M. Calpain inhibition reduces infarct size and improves global hemodynamics and left ventricular contractility in a porcine myocardial ischemia/reperfusion model. *Eur J Pharmacol*. 2005; 528: 124-131.

24. Mani SK, Balasubramanian S, Zavadzkas JA, Jeffords LB, Rivers WT, Zile MR, Mukherjee R, Spinale FG, Kuppaswamy D. Calpain inhibition preserves myocardial structure and function following myocardial infarction. *Am J Physiol Heart Circ Physiol*. 2009; 297: H1744-51.
25. Galvez AS, Diwan A, Odley AM, Hahn HS, Osinska H, Melendez JG, Robbins J, Lynch RA, Marreez Y, Dorn GW, 2nd. Cardiomyocyte degeneration with calpain deficiency reveals a critical role in protein homeostasis. *Circ Res*. 2007; 100: 1071-1078.
26. Bergman MR, Teerlink JR, Mahimkar R, Li L, Zhu BQ, Nguyen A, Dahi S, Karliner JS, Lovett DH. Cardiac matrix metalloproteinase-2 expression independently induces marked ventricular remodeling and systolic dysfunction. *Am J Physiol Heart Circ Physiol*. 2007; 292: H1847-60.
27. Yamada A, Uegaki A, Nakamura T, Ogawa K. ONO-4817, an orally active matrix metalloproteinase inhibitor, prevents lipopolysaccharide-induced proteoglycan release from the joint cartilage in guinea pigs. *Inflamm Res*. 2000; 49: 144-146.
28. Nicolescu AC, Holt A, Kandasamy AD, Pacher P, Schulz R. Inhibition of matrix metalloproteinase-2 by PARP inhibitors. *Biochem Biophys Res Commun*. 2009; 387: 646-650.
29. Lin GD, Chattopadhyay D, Maki M, Wang KK, Carson M, Jin L, Yuen PW, Takano E, Hatanaka M, DeLucas LJ, Narayana SV. Crystal structure of calcium bound domain VI of calpain at 1.9 Å resolution and its role in enzyme assembly, regulation, and inhibitor binding. *Nat Struct Biol*. 1997; 4: 539-547.
30. Massova I, Kotra LP, Fridman R, Mobashery S. Matrix metalloproteinases: structures, evolution, and diversification. *FASEB J*. 1998; 12: 1075-1095.

31. Hu J, Van den Steen PE, Sang QX, Opdenakker G. Matrix metalloproteinase inhibitors as therapy for inflammatory and vascular diseases. *Nat Rev Drug Discov.* 2007; 6: 480-498.
32. Johnson AR, Pavlovsky AG, Ortwine DF, Prior F, Man CF, Bornemeier DA, Banotai CA, Mueller WT, McConnell P, Yan C, Baragi V, Lesch C, Roark WH, Wilson M, Datta K, Guzman R, Han HK, Dyer RD. Discovery and characterization of a novel inhibitor of matrix metalloprotease-13 that reduces cartilage damage in vivo without joint fibroplasia side effects. *J Biol Chem.* 2007; 282: 27781-27791.
33. Shan D, Marchase RB, Chatham JC. Overexpression of TRPC3 increases apoptosis but not necrosis in response to ischemia-reperfusion in adult mouse cardiomyocytes. *Am J Physiol Cell Physiol.* 2008; 294: C833-41.
34. Liu X, Rainey JJ, Harriman JF, Schnellmann RG. Calpains mediate acute renal cell death: role of autolysis and translocation. *Am J Physiol Renal Physiol.* 2001; 281: F728-38.
35. Wang KK, Nath R, Posner A, Raser KJ, Buroker-Kilgore M, Hajimohammadreza I, Probert AW, Jr, Marcoux FW, Ye Q, Takano E, Hatanaka M, Maki M, Caner H, Collins JL, Fergus A, Lee KS, Lunney EA, Hays SJ, Yuen P. An alpha-mercaptoacrylic acid derivative is a selective nonpeptide cell-permeable calpain inhibitor and is neuroprotective. *Proc Natl Acad Sci U S A.* 1996; 93: 6687-6692.
36. Farkas B, Tantos A, Schlett K, Vilagi I, Friedrich P. Ischemia-induced increase in long-term potentiation is warded off by specific calpain inhibitor PD150606. *Brain Res.* 2004; 1024: 150-158.

37. Kunugi S, Shimizu A, Kuwahara N, Du X, Takahashi M, Terasaki Y, Fujita E, Mii A, Nagasaka S, Akimoto T, Masuda Y, Fukuda Y. Inhibition of matrix metalloproteinases reduces ischemia-reperfusion acute kidney injury. *Lab Invest.* 2011; 91: 170-180.
38. Yang Y, Candelario-Jalil E, Thompson JF, Cuadrado E, Estrada EY, Rosell A, Montaner J, Rosenberg GA. Increased intranuclear matrix metalloproteinase activity in neurons interferes with oxidative DNA repair in focal cerebral ischemia. *J Neurochem.* 2010; 112: 134-149.
39. Collard CD, Agah A, Stahl GL. Complement activation following reoxygenation of hypoxic human endothelial cells: role of intracellular reactive oxygen species, NF-kappaB and new protein synthesis. *Immunopharmacology.* 1998; 39: 39-50.
40. Ohno H, Uemura K, Shintani-Ishida K, Nakamura M, Inomata M, Yoshida K. Ischemia promotes calpain-mediated degradation of p120-catenin in SH-SY5Y cells. *Biochem Biophys Res Commun.* 2007; 353: 547-552.
41. Gilchrist JS, Cook T, Abrenica B, Rashidkhani B, Pierce GN. Extensive autolytic fragmentation of membranous versus cytosolic calpain following myocardial ischemia-reperfusion. *Can J Physiol Pharmacol.* 2010; 88: 584-594.

CHAPTER 5

Titin is a target of matrix metalloproteinase-2: implications in myocardial ischemia/reperfusion injury

A version of this chapter has been published in:

Ali MA, Cho W, Hudson B, Kassiri Z, Granzier H, Schulz R. Titin is a target of matrix metalloproteinase-2: implications of myocardial ischemia/reperfusion injury. *Circulation* 2010; 122:2039-2047.

5.1: Introduction

MMP-2 is a zinc-dependent protease that is best known for its ability to degrade the extracellular matrix in both physiological and pathological conditions. MMP-2 is synthesized as a zymogen by a variety of cells including cardiac myocytes and is activated either by proteases¹ (such as by action of MMP-14) or by post-translational modifications to the full length enzyme stimulated by enhanced oxidative stress. For example, ONOO⁻, which is generated in early reperfusion following ischemia², directly activates several MMPs³ including MMP-2⁴ via a non-proteolytic mechanism involving the *S*-glutathiolation of a critical propeptide cysteine in its autoinhibitory domain.

MMPs are best recognized for their role in tissue remodeling by proteolyzing various components of the extracellular matrix in both health and disease, i.e. in angiogenesis, embryogenesis, wound healing⁵, atherosclerosis⁶, aortic aneurysm⁷ and myocardial infarction⁸. More recent studies, however, show that MMP-2 is involved in several acute biological processes independent of its actions on extracellular matrix proteins. This includes platelet activation⁹, regulation of vascular tone¹⁰ and myocardial stunning injury immediately after reperfusion of the ischemic heart¹¹. Indeed, several reports indicate that MMP-2 does not exclusively degrade extracellular matrix components^{12,13}.

In normal cardiac myocytes MMP-2 is found in discrete subcellular compartments including the thin and thick myofilaments of the cardiac sarcomere^{14,15}, the cytoskeleton^{16,17}, nuclei¹⁸, mitochondria¹⁴ and caveolae¹⁹ (for review see²⁰). MMP-2 is activated in rat hearts subjected to myocardial oxidative stress injury and is

responsible for the degradation of specific sarcomeric and cytoskeletal proteins including TnI^{14,21}, MLC-1¹⁵ and α -actinin¹⁷. Inhibition of MMPs activity reduced both the loss of contractile function as well as the degradation of these substrates, to which MMP-2 was co-localized. Furthermore, transgenic mice with myocardial specific expression of a mutant, constitutively active MMP-2, in the absence of additional injury, show significantly impaired cardiac contractile function, disrupted sarcomeres, profound myofilament lysis, breakdown of Z-band registration and reduced TnI level²².

Titin, the largest known mammalian protein (3,000-4,000 kD), forms an intrasarcomeric elastic filament that is thought to serve as a framework for the ordered assembly of other myofilament proteins²³. In mammalian hearts, titin is mainly expressed in two isoforms, the smaller and stiffer N2B and the larger and more compliant N2BA isoforms²⁴. Hearts from adult small mammals (such as rats, mice and rabbits) express predominantly N2B titin, whereas large mammals including humans co-express N2B and N2BA titins at an approximate 1:1 ratio²⁵. In the sarcomere the titin molecule spans the distance from the Z-disc to the M-line region (half the length of the sarcomere). Moreover, the I-band region of titin is comprised of distinct elastic segments that allows titin to behave as a molecular spring, contributing to the passive tension of myofibrils and maintaining the structural and functional stability of the sarcomere. Titin is an important determinant of both systolic and diastolic function and the Frank-Starling mechanism of the heart²⁶. Although loss and/or disorganization of titin in ischemic and failing human hearts has been reported^{27,28}, the mechanism of titin degradation has not been extensively studied in hearts subjected to I/R injury. Since MMP-2 is localized to sarcomeric and cytoskeletal proteins and is activated in myocardial I/R injury, we address here whether MMP-2 targets titin to contribute to the pathogenesis of myocardial I/R injury.

5.2: Materials and Methods

5.2.1: Titin isolation and purification

Titin was prepared as described previously^{29, 30}. Briefly, myofibrils were prepared from chilled fresh rabbit longissimus dorsi muscle by homogenisation in 3 volumes of 50 mM KCl, 5 mM EGTA, 1 mM NaHCO₃ and 5 µM E64 (Sigma); (pH 7.0, 4°C). This was followed by three cycles of centrifugation (2000 g) and resuspension in buffer without E64 inhibitor. After the fourth spin the myofibrils were resuspended and extracted on ice for 5 min with stirring in 2 volumes of 0.9 M KCl, 2 mM MgCl₂, 10 mM imidazole, 2 mM EGTA, 1 mM phenylmethylsulfonylfluoride, 10 µg/ml trypsin inhibitor, 0.5 mM dithiothreitol, 5 µM E64; pH 7.0. The extract was clarified at 20,000 g for 30 min, diluted three times with water (final ionic strength ~0.2 mol/L) and after 1 h for precipitation, myosin was removed by spinning for 30 min at 20,000 g. The supernatant was diluted five times more (final ionic strength 0.05 mol/L), left for 40 min, and then spun at 11,000 g for 30 min. The crude titin pellet was resuspended in 0.6 M KCl, 30 mM potassium phosphate (pH 7.0), clarified for 30 min at 25,000 g, and then chromatographed in this buffer in a 90 cm × 1 cm Sepharose CL2B column maintained at 1°C. On occasion the titin at this stage was also passed through a Q-Sepharose column as described by Nave et al.³¹ The purification was monitored by SDS-polyacrylamide electrophoresis in gradient slab gels (4% to 15%). Samples for these were dissociated at 56°C for 20 min in SDS/urea, as described by Fritz et al.³².

5.2.2: Skinned cardiomyocyte isolation

Skinned cardiomyocytes were isolated as described previously³³. Briefly, mice were anesthetized via isoflurane inhalation, sacrificed via cervical dislocation, and the

heart was rapidly (< 90 seconds) cannulated via the aorta. The heart was then perfused for 4 min with perfusion buffer (113 NaCl, 4.7 KCl, 0.6 Na₂HPO₄, 1.2 MgSO₄, 12 NaHCO₃, 10 KHCO₃, 10 HEPES, and 30 taurine, all in mM) and then switched to digestion buffer (perfusion buffer plus 0.148 mg/ml Liberase blendzyme 2 (Roche Applied Science, IN, USA), 0.13 mg/ml of trypsin, 12.5 μM CaCl₂) for 8-10 min. When the heart was flaccid, digestion was halted and the heart was placed in myocyte stopping buffer 1 (perfusion buffer plus 0.04 ml bovine calf serum (BCS)/ml buffer and 5 μM CaCl₂). The left ventricle was cut into small pieces, triturated several times with a transfer pipet, filtered through a 300 μm nylon mesh filter and the filtered cells were gravity pelleted. We added 10 ml of myocyte stopping buffer 2 (perfusion buffer plus 0.05 ml BCS/ml buffer and 12.5 μM CaCl₂) and then skinned the cells in 1X relaxing solution (N,N-Bis(2-hydroxyethyl)-2-aminoethanesulfonate 40 mM, EGTA 10 mM, MgCl₂ 6.56 mM, ATP 5.88 mM, dithiothreitol 1 mM, potassium propionate 46.35 mM, creatine phosphate 15 mM, pH 7.0) (chemicals from Sigma-Aldrich, MO, USA) with 1% Triton-X-100 (Pierce, IL, USA) for 6 min and then quickly washed in 1X relaxing solution without Triton-X-100. Finally, skinned cells were stored in 50% glycerol/50% relaxing solution at -20°C.

5.2.3: In silico analysis

According to Turk *et al.*³⁴ and Chen *et al.*³⁵ three MMP-2 cleavage motifs were chosen. These are PVS↓LRS, PVG↓LLA and L/ISR↓LTA with MMP-2 cleavage site indicated by the arrow. These consensus sequences were shown to be optimal MMP-2 cleavage motifs and, importantly, they showed high selectivity towards MMP-2 in comparison to other MMPs including MMP-1, MMP-3, MMP-7, MMP-9 and MMP-14³⁴. These consensus sequences were aligned vs. N2B mouse and human titin

and the result was restricted to the top 20 with more than 60% homology using the SIM Alignment tool for protein sequence.

5.2.4: Cleavage of native titin in skinned cardiomyocytes

Skinned cardiomyocytes were incubated with human recombinant MMP-2 catalytic domain (Enzo Life Sciences, 4-120 nM) with or without MMP inhibitors (10 μ M *o*-phenanthroline or ONO-4817) at 37°C for 60 min. This concentration of *o*-phenanthroline inhibits MMP-2 activity under similar in vitro conditions³⁶. The samples were denatured with 2X urea sample buffer (8 M urea, 2 M thiourea, 3% SDS, 75 mM dithiothreitol, 0.03% bromophenol blue, and 0.05 M Tris-HCl, pH 6.8) at 100°C for 3 min, and the proteins were electrophoresed by 1% SDS-agarose and stained with Coomassie brilliant blue.

5.2.5: In vitro degradation of titin

Two micrograms of rabbit longissimus dorsi titin were incubated with human recombinant 64 kDa MMP-2 (Calbiochem, 500:1, 50:1 and 5:1, titin:MMP-2 molar ratios) in 50 mM Tris-HCl buffer (5 mM CaCl₂ and 150 mM NaCl) at 37°C for 60 min. In additional experiments, MMP-2 was preincubated with either of the MMP inhibitors GM-6001 (100 nM) or ONO-4817 (10 μ M) for 15 min at 37°C before adding to titin. This concentration of GM-6001 was previously shown to inhibit the exogenously added MMP-2 activity under similar in vitro conditions^{34, 36}. The reaction mixtures were denatured with 2X urea sample buffer (8 M urea, 2 M thiourea, 3% SDS, 75 mM dithiothreitol, 0.03% bromophenol blue, and 0.05 M Tris-HCl; pH 6.8) at 100°C for 3 min, and the proteins were separated by 2% SDS-PAGE strengthened with 0.5% agarose³⁷. Protein bands were visualized with silver stain (Invitrogen kit).

5.2.6: Isolated working rat heart- ex vivo model of I/R

Male Sprague–Dawley rats (300–350 g) were anesthetized with sodium pentobarbital (60 mg/kg, ip). Hearts were isolated and paced at 300 beats per minute during perfusion at 37°C as working hearts³⁸ with 100 ml recirculating Krebs–Henseleit solution containing 118 mM NaCl, 4.7 mM KCl, 1.2 mM KH₂PO₄, 1.2 mM MgSO₄, 25 mM NaHCO₃, 11 mM glucose, 100 µU/ml insulin, 2.5 mM Ca²⁺, 0.5 mM EDTA and 0.1% bovine serum albumin; continuously gassed with 95% O₂/5% CO₂ (pH 7.4). The perfusate enters the left atrium at a hydrostatic preload pressure of 9.5 mmHg and the left ventricle ejects it against a hydrostatic afterload of 70 mmHg. Cardiac work (cardiac output x peak systolic pressure) was used as an index of mechanical function. After 25 min of equilibration, hearts were either aerobically perfused for 85 min (Control, *n*=6) or subjected to 25 min global, no-flow ischemia followed by 60 min aerobic reperfusion without (I/R, *n*=7) or with 50 µM ONO-4817 (I/R + ONO-4817, *n*=8). ONO-4817, a selective MMP inhibitor (K_i in the nanomolar range for MMP-2 and almost no inhibitory activity up to 100 µM against several other proteases of different classes³⁹), was added to the perfusion buffer 10 min before the induction of ischemia. All hearts were perfused for a total of 110 min. At the end of perfusion the ventricles were rapidly frozen in liquid nitrogen and processed for titin analysis in ventricular extracts as described below.

Additional series of hearts (Control *n*=5, I/R *n*=5, and I/R + ONO-4817 *n*=4) were perfused and processed for titin immunohistochemistry and confocal microscopy analysis for assessment of titin immunostaining.

Another six hearts were briefly perfused for 10 min at 37°C with Krebs–Henseleit buffer at a constant hydrostatic pressure of 70 mmHg to clear them of blood,

followed by processing for immunohistochemistry as described below to investigate the co-localization of titin and MMP-2 in the left ventricle.

This investigation conforms to the *Guide to the Care and Use of Experimental Animals* published by the Canadian Council on Animal Care.

5.2.7: In vivo model of I/R

I/R was induced in vivo by modifying a previously described protocol⁴⁰. Briefly, MMP-2 knockout and age-matched wild type male C57BL/6 mice were anaesthetized with isoflurane, intubated and kept on a heating pad to maintain body temperature at 37°C. The heart was exposed and the left anterior descending coronary artery was temporarily ligated with a 7-0 silk suture, with a piece of 4-0 silk placed between the left anterior descending coronary artery and the 7-0 silk. After 30 min of left anterior descending coronary artery occlusion, reperfusion was initiated by releasing the ligature and removing the 4-0 silk. The loosened suture was left in place to help identify the ischemic area of the left ventricle. After 30 min of reperfusion, the hearts were excised, the ischemic and non-ischemic regions of the left ventricle were dissected out under a magnifying glass and flash frozen in liquid nitrogen for titin analysis.

5.2.8: Analysis of titin by gel electrophoresis

Titin was analyzed in ventricular extracts using 1% vertical SDS-agarose gel electrophoresis as previously described⁴¹. Briefly, the frozen ventricles were pulverized under liquid nitrogen and homogenized in urea sample buffer (8 M urea, 2 M thiourea, 3% SDS, 75 mM dithiothreitol, 0.05 M Tris-HCl, 0.03% bromophenol blue, 25% glycerol and 10 µM leupeptin, 10 µM E64 and 0.5 mM phenylmethylsulfonylfluoride, pH adjusted to 6.8) (20:1 v/w buffer to tissue ratio). Samples were thoroughly vortexed and

then heated at 60°C for 10 min. The samples were again vortexed and subsequently centrifuged (12,000g for 5 min) at 4°C. The supernatant was removed and stored at -80°C until use. The integrated optical density of T1 titin (full-length titin), T2 titin (degradation product) and myosin heavy chain (MHC) were determined as a function of the volume of the solubilized protein sample that was loaded (a range of volumes was loaded onto each gel). The slope of the linear range of the relation between integrated optical density and loaded volume was obtained for each protein. The total titin (T1+T2):MHC and titin's degradation product T2:MHC ratios were calculated as the slope of titin (either T1 + T2 or T2 alone) divided by the slope of MHC.

5.2.9: Immunohistochemistry and confocal microscopy

5.2.9.1 Co-localization of titin and MMP-2

Rat hearts perfused aerobically for 10 min to flush them of blood or left ventricular tissue from the explanted heart of a heart transplant patient (procured with the help of Dr. Costas Schulze, Division of Cardiac Surgery, University of Alberta Hospitals) were fixed with 4% paraformaldehyde in 0.1 M sodium phosphate buffer (pH 7.4) and cryoprotected with 30% sucrose in 0.1 M sodium phosphate buffer. The cryoprotected hearts were cryosectioned into 6 µm thick sections which were attached to glass slides coated with poly-L-lysine (Cat. No. 63410, Electron Microscopy Sciences, Hatfield, PA, USA) and dried at room temperature. The dried cryosections were rinsed twice (5 min each) in 0.5% Triton-X 100 in phosphate buffered saline (PBS, pH 7.4) and rinsed once in PBS for 5 min. Double immunolabeling was accomplished by sequential staining of each primary antibody (mouse anti-MMP-2 IgG, 1:200 final dilution, Cat. No. 3308, Chemicon International; mouse anti-titin T12 IgG, 1:10 final dilution; rabbit anti-titin M8 IgG, 1:200 final dilution, both titin antibodies provided by Dr. Elisabeth Ehler, King's

College London, UK) for 16 h. The T12 antibody labels titin near the Z disc region of titin and the M8 antibody recognizes an epitope at the M line region of titin. Therefore, T12 and M8 antibodies were used to address the proximity of MMP-2 localization to either the N-terminus or C-terminus regions of titin, respectively. Secondary antibodies conjugated with fluorescent dyes (Cy3-donkey anti-mouse IgG, 1:25 final dilution, Cat. No. 715-165-151, Jackson ImmunoResearch Laboratories; Alexa488-donkey anti-rabbit IgG, 1:50 final dilution, Cat. No. A-21206, Invitrogen) were applied for 2 h. During incubation with any of the antibodies, 2% normal donkey serum was added. A solution of 10 μ M DRAQ5 (Biostatus Ltd., Leicestershire, UK) was applied to stain nuclei. To determine specificity of immunolabeling, primary or secondary antibodies were omitted.

The immunolabeled cryosections were observed by confocal microscopy (LSM 510, Carl Zeiss Co., Jena, Germany). Cy3 (red) was scanned with a helium/neon green laser (543 nm) with a band pass 565 - 615 nm filter (565 - 615 nm excitation). Alexa488 (green) was captured using an argon laser (488 nm) with band pass 500 - 530 filter (500 - 530 nm excitation). DRAQ5 (blue) for nuclei was obtained with a helium/neon red laser (633 nm) with a long pass 650 nm filter. All confocal images were exported as TIFF files without any modifications by LSM 510 Image.

5.2.9.2 Titin 9D10 immunostaining

At the end of the 110 min working heart perfusion protocol some Control, I/R or I/R + ONO-4817 hearts were fixed and cryoprotected as described above. The cryoprotected hearts were cryosectioned and dried at room temperature. The dried cryosections were rinsed and titin immunolabeling was accomplished using 9D10 antibody (mouse anti-titin 9D10 IgM, 1:100, developed by Dr. Marion Greaser and available at the Development Studies Hybridoma Bank at the University of Iowa). 9D10

antibody is raised against the proline-glutamate-valine-lysine (PEVK) domain in the spring region of titin and is used to measure titin immunostaining in Control, I/R and I/R + ONO-4817 groups. Secondary antibody conjugated with fluorescent dyes (Alexa488-goat anti-mouse IgM, 1:40, Cat. No. 20142, Invitrogen) were applied. DRAQ5 was applied to stain nuclei. To determine specificity of immunolabeling, primary or secondary antibodies were omitted. The immunolabeled cryosections were observed by confocal microscopy for Alexa488 and DRAQ5 as above.

5.2.9.3. Three dimensional surface rendered image construction

Z-stack images obtained from the LSM 510 were reconstructed to three dimensional images and surface rendered using the Inside 4D module of AxioVison software (Version 4.6, Carl Zeiss Co., Jena, Germany). The same configuration of the Inside 4D module was applied to all images.

5.2.10: Overlay assay to determine MMP-2 binding to titin

Skinned muscle fibers, stored in relaxing solution (40 mM (N,N-Bis(2-hydroxyethyl)-2-aminoethanesulfonate pH 7.0, 10 mM EGTA, 6.56 mM MgCl₂, 5.88 mM ATP, 1 mM dithiothreitol, 46.35 mM potassium propionate and 15 mM creatine phosphate) for 24 h post-dissection, were incubated with 0.75 ug/ml of trypsin from bovine pancreas (Sigma, T9201) in relaxing solution for 10 min at room temperature. The fibers were solubilized with a glass pestle, in solubilization buffer (750 µl of 8 M urea, 2 M thiourea, 3% SDS, 50 mM Tris-HCL pH 6.8, 0.03% bromphenol blue, 250 µl of 50% glycerol with leupeptin, E-64, and phenylmethylsulfonylfluoride, and 23 mg of dithiothreitol), heated for 5 min at 65°C and centrifuged 11,000 g for 10 min to remove the particulate fraction. The proteins of the samples were separated by electrophoresis on 1% agarose gel SDS-PAGE and run with Fairbank's buffer (50 mM Tris-HCl pH 7.5, 384

mM glycine, 0.1% SDS, 10 mM 2-mercaptoethanol) for 3 h and 20 min at 15 mA. Then the proteins were transferred to a PVDF (Millipore) membrane, 2 h and 30 min at 1.33 mA/cm², and stained with Ponceau S to visualize the protein bands.

The overlay assay was performed using the transferred membrane as described previously⁴² followed by western blot. Briefly, membranes were blocked in blocking buffer (Odyssey, 927-40000) for 1 h followed by a 4 h incubation with recombinant MMP-2 (active human; EMD, PF023), 100 nM in 10 ml blocking buffer (1.3µl/20 ml). Both steps were performed at room temperature on a gentle rocker. Following incubation, the blot was washed 3 X 5 min with 10 ml of blocking buffer and then incubated with primary antibody (MMP-2 (1:250), Millipore; MAB3308, mouse monoclonal, 2 mg/ml). Following overnight incubation with the primary antibody in blocking solution (0.05% Tween-20) membranes were washed with 0.1% Tween-20 in phosphate-buffered saline, subjected to secondary antibodies labeled with IR dyes (Goat anti mouse 1:20,000. 800 green) for 1 h, and washed again with 0.1% Tween-20 in phosphate-buffered saline. Membranes were scanned using a Li-Cor Odyssey infrared imager at 700 nm and 800 nm.

5.2.11: Statistical analysis

Results are expressed as mean ± S.E.M. for *n* hearts. As appropriate, one-way ANOVA or repeated measures two-way ANOVA followed by Tukey's post hoc test were used. Differences were considered significant at $p < 0.05$.

5.3: Results

5.3.1: Co-localization of MMP-2 and titin near the Z disc region of the cardiac sarcomere

We first investigated whether MMP-2 is localized to titin in the cardiac sarcomere. In this regard, we used and validated two different anti-titin antibodies which target specific epitopes (Figure 5.1A). The T12 antibody labels titin near the Z disc region of titin and the M8 antibody recognizes an epitope at the M line region of titin. Images obtained by immunohistochemistry followed by confocal microscopy showed that T12-immunoreactivity distributes near Z-lines and M8-immunoreactivity is alternatively distributed at M-lines without overlapping (Figure 5.1B). Images obtained using anti-MMP-2 and anti-titin T12 in left ventricle sections from 10 min aerobically perfused rat hearts showed clear co-localization of MMP-2 to the Z disc region of titin (Figure 5.2). When using anti-titin M8, we observed a weaker localization of MMP-2 to this region of titin (Figure 5.2). These data suggest that MMP-2 localizes mainly near the Z-disc region of the sarcomere, with a secondary and weaker localization near the M-line portion in the titin molecule.

5.3.2: MMP-2 binds and cleaves titin in a concentration-dependent manner

In silico mapping of MMP-2 cleavage sites in both human and mouse N2B titin revealed multiple putative sites in both I-band and A-band titin regions, including near the Z-line terminus of titin. These sites show more than 60% homology to the three MMP-2 cleavage motifs (Figure 5.3). Moreover, human recombinant MMP-2 was able to bind to titin prepared from skinned muscle fibers as shown by the overlay assay method (Figure 5.4). Next we tested the susceptibility of purified titin to proteolytic degradation

by MMP-2 in vitro. Incubation of titin with MMP-2 (60 min, 37°C) at increasing MMP-2:titin molar ratios (1:500, 1:50 and 1:5) caused titin degradation in a concentration-dependent manner (Figure 5.5A). Inhibition of MMP-2 activity with GM-6001 or ONO-4817 prevented titin cleavage by MMP-2 (Figure 5.5B). To determine whether MMP-2 directly cleaves cardiac titin in situ, we incubated skinned mouse cardiomyocytes with increasing concentration of MMP-2 (60 min, 37°C). This resulted in concentration-dependent cleavage of cardiac titin (T1) as shown by the increased level of the degradation product of titin (T2) with increasing MMP-2 concentration (Figure 5.6A). Inhibition of MMP-2 activity with *o*-phenanthroline or ONO-4817 prevented titin cleavage by MMP-2 (Figure 5.6B).

5.3.3: Effect of ONO-4817 on functional recovery of I/R hearts

Isolated working rat hearts were perfused for 110 min under one of three conditions: (1) aerobic perfusion (Control); (2) 25 min of global, no-flow ischemia and 60 min of aerobic reperfusion (I/R); or (3) I/R in the presence of a selective MMP inhibitor, ONO-4817 (I/R + ONO-4817, Figure 5.7A). Control hearts showed no significant loss of mechanical function over 110 min of aerobic perfusion (Figure 5.7). I/R hearts showed markedly reduced recovery of mechanical function during reperfusion in comparison with control hearts (Figure 5.7B). The recovery of cardiac work during reperfusion was significantly improved following MMP inhibition with ONO-4817 compared to the I/R group (Figure 5.7B).

5.3.4: Myocardial I/R causes titin cleavage, an effect diminished by an MMP inhibitor

To investigate whether MMP-2 can cleave titin in the intact heart under pathophysiological conditions, titin content was assessed using 1% vertical SDS-agarose gels in ventricular extracts prepared from the Control, I/R or I/R + ONO-4817 hearts. Ventricular extracts from control hearts revealed a titin band at ~3000 kD (Figure 5.8A). I/R caused a significant increase in T2 band density, an effect abolished in the I/R + ONO-4817 hearts (Figure 5.8A). Quantification of total titin/MHC ratio showed that I/R did not significantly change this ratio as compared to control hearts (Figure 5.8B) whereas T2/MHC ratio significantly increased in I/R hearts. ONO-4817 abolished the I/R-induced increase in the T2/MHC ratio (Figure 5.8C). These observations were further confirmed by immunohistochemistry experiments using the anti-titin 9D10 antibody, raised against the PEVK domain in the spring region of titin. Titin immunostaining was significantly reduced by I/R whereas ONO-4817 treatment preserved titin immunostaining to a level comparable to control (Figure 5.8D).

5.3.5: Titin degradation is reduced in hearts from MMP-2 knockout mice subjected to I/R injury in vivo

We next determined whether genetic ablation of MMP-2 could influence titin degradation in cardiac muscle. Mouse hearts subjected in vivo to left anterior descending coronary artery ligation for 30 min followed by 30 min reperfusion exhibited titin degradation which was significantly less in MMP-2 knockout hearts than in wild type control hearts (Figure 5.9).

5.3.6: MMP-2 localizes near the Z-disc region of titin in the human heart

Immunostaining of sections prepared from the left ventricle of an explanted heart from a patient undergoing heart transplantation showed co-localization of MMP-2 and titin mainly near the Z-disc, with a weaker co-localization at the M-line. In comparison to the rat heart, MMP-2 immunostaining in the human heart was more diffuse yet still showed a sarcomeric staining pattern (Figure 5.10).

5.4: Discussion

In this study we demonstrated that the giant sarcomeric protein, titin, is a target of the proteolytic activity of MMP-2 in the setting of acute myocardial I/R injury. Immunohistochemical analysis shows that MMP-2 clearly co-localizes with titin near the Z-disc region of the sarcomere in both rat and human hearts. We established that under *in vitro* conditions MMP-2 is able to bind to and cleave titin in a concentration-dependent manner. The proteolytic action of MMP-2 is blocked by the selective MMP inhibitors, GM-6001 and ONO-4817, verifying that the cleavage is indeed due to MMP activity. ONO-4817 not only improves the functional recovery after I/R in isolated rat hearts but also prevents the significant increase in the titin degradation product T2 caused by I/R injury, indicating that titin degradation is reduced when MMP activity is inhibited. Furthermore, hearts from MMP-2 knockout mice subjected to *in vivo* I/R injury show less titin degradation in comparison to wild type controls. Titin proteolysis has been observed in various human heart diseases associated with increased myocardial oxidative stress including dilated cardiomyopathy, the terminally failing heart and Chagas' cardiomyopathy^{27, 28, 43}, however the protease(s) responsible for this was not identified.

MMPs are best known as proteases responsible for the degradation and remodeling of extracellular matrix proteins in both physiological and pathological conditions, including various cardiac pathologies. However, the discovery of the intracellular localization^{14, 16, 18, 22} and functions of MMP-2 to proteolyze TnI^{14, 22} MLC-1¹⁵ and α -actinin¹⁷ during myocardial oxidative stress injury challenged the canonical notion of extracellular-only actions of this enzyme. In previous studies we showed that ONOO⁻ biosynthesis in I/R rat hearts peaks within the first minute of reperfusion² and the peak in MMP-2 activity follows at 2 to 5 minutes of reperfusion¹¹. Infusion of ONOO⁻ into isolated perfused rat hearts⁴⁴ or isolated cardiomyocytes⁴⁵ caused a time- and concentration-dependent contractile dysfunction which was abrogated with MMP inhibitors. *In vitro*, ONOO⁻ was shown to directly activate MMP-2 via a non-proteolytic mechanism involving S-glutathiolation of the propeptide cysteine sulphhydryl group⁴. Indeed, this intracellular activity of MMP-2 upon I/R injury caused proteolytic degradation of specific sarcomeric (TnI¹⁴ and MLC-1¹⁵) and cytoskeletal (α -actinin¹⁷) proteins which are susceptible to its proteolytic activity.

MMP-2 is localized within the cardiac sarcomere including near to the Z-discs¹⁴⁻¹⁶. These previous observations are supplemented by the current data showing clear co-localization of MMP-2 near the Z disc region of titin using the T12 clone in rat (Figure 5.2) and human (Figure 5.10) hearts. Several studies show that titin interacts with α -actinin at the Z-disc of the sarcomere and this interaction plays a crucial role in Z-disc assembly and sarcomeric integrity⁴⁶⁻⁴⁸. Interestingly, MMP-2 was found to not only co-localize with α -actinin in the Z-disc of cardiac sarcomeres^{16, 17} but also degrades it following ONOO⁻ infusion into isolated rat hearts¹⁷. The M8 titin antibody (raised against the M-line region of titin) shows a weaker localization of MMP-2 to this region of

titin. Although our data do not rule out the possible localization of MMP-2 also to other region(s) of titin, they do suggest that a main MMP-2 anchoring site is at/near the Z-disc of the sarcomere.

Titin is the third myofilament (in addition to thick and thin myofilaments) of the sarcomere that plays an important role in sarcomere integrity and cardiac muscle contraction ²³. Any alterations in its structure could severely affect the contractile performance of the heart. The increase in T2 titin and the decrease in titin immunostaining after I/R injury observed here (Figure 5.8) was associated with poor cardiac mechanical recovery during reperfusion (Figure 5.7). These effects are likely at least in part due to titin degradation by MMP-2, given the co-localization of MMP-2 with titin near the Z-disc of cardiac sarcomeres, the susceptibility of titin to degradation by MMP-2 and the reduction in I/R-induced titin degradation in hearts from MMP-2 knockout mice or in rat hearts where MMP activity was selectively blocked with ONO-4817. A significant increase in MMP-2 activity was seen in the heart after experimental *Trypanosoma cruzi* infection (the parasite responsible for Chagas' disease) and mortality was markedly reduced upon treatment with an MMP inhibitor, suggesting a role of MMP-2 in mediating the acute Chagas' cardiomyopathy ⁴⁹. Putative titin degradation products were detected in the plasma of patients with Chagas' disease ⁴³, further supporting a role of MMP-2 in titin degradation. Moreover, myocardial infarction is associated with a significant right shift in the left ventricle pressure-volume relation (an observation which is consistent with titin degradation in the heart) and the broad spectrum MMP inhibitor PD-166793 was shown to protect against this shift ⁵⁰. Although cardiac mechanical function at the end of perfusion is inversely related with T2/MHC ratios in hearts (Figures 5.7B and 5.8C), caution is needed in relating this effect exclusively to titin degradation. As mentioned above, other sarcomeric/cytoskeletal

proteins including TnI, MLC-1 and α -actinin are also susceptible to degradation by MMP-2 under conditions of myocardial oxidative stress injury. However, our work clearly suggests that titin proteolysis is an important factor that negatively impacts myocardial contractility upon I/R injury.

Titin content in rat ventricles was investigated here by SDS-agarose gel electrophoresis or immunofluorescence staining against titin epitopes at the PEVK domain. Our electrophoresis results showed the approximate 60% elevation in the T2/MHC ratio in the I/R group in comparison with aerobic control hearts. Immunofluorescence data also showed a reduction of titin immunostaining in I/R group using the 9D10 antibody. In addition to degradation, post-translational modifications of titin may have occurred upon I/R that led to diminished binding of titin antibodies to the specific epitopes. Post-translational modifications of many cardiac myofilament/cytoskeletal proteins during I/R, including actin⁵¹ and MLC-1⁵², have been reported in previous studies.

Our study does not rule out the possible action of other proteases in titin degradation. Calpains are most likely involved in sarcomeric protein degradation after ischemic episodes more severe than that observed in our model⁵³. Indeed, calpain was shown to be able to cleave titin only after 24 h doxorubicin treatment of rat cardiomyocytes⁵⁴. The ubiquitin-proteasome system is another proteolytic pathway that may be involved in titin degradation. Increased proteasome activities have been reported in various models of I/R injury⁵⁵⁻⁵⁷. Moreover, the E3 ubiquitin-ligase MURF1 is known to be associated with the M-line region of titin⁵⁸ and ubiquitinates titin in yeast two-hybrid screens⁵⁹. In a rat heart failure model, both a loss of titin⁶⁰ and an increase in MMP-2 gene expression⁶¹ were observed in diaphragm muscle. However, in our short-

term experiments we did not observe a significant loss in intact titin upon I/R injury. We speculate that MMP-2 activation results not only in titin cleavage but it may also trigger a cascade of proteolytic events leading to titin loss several hours after reperfusion.

In conclusion, the present results indicate that MMP-2 cleaves titin during either *ex vivo* or *in vivo* I/R injury. Furthermore, MMP-2 inactivation by pharmacologic or genetic approaches protects against titin degradation. Our previous findings of TnI¹⁴, MLC-1¹⁵ and α -actinin¹⁷ cleavage by MMP-2, in addition to our current results with titin, suggest that MMP-2 plays a crucial role in the pathogenesis of acute I/R injury at the level of the sarcomere and cytoskeleton. Whether MMP-2 causes contractile protein alterations in other cardiac pathologies needs further investigation. Pharmacological inhibition of MMP activity could represent a useful strategy for the prevention and/or treatment of myocardial I/R injury.

Figure 5.1 A, Schematic representation of titin (N2B isoform) showing T12 and M8 epitopes near the Z-disc and at the M-line regions, respectively. B, Three dimensional rendered images of T12 and M8 epitopes of titin in sarcomeres of the left ventricular myocardium in aerobic normal control. *a-c* show frontal views of distributions of T12 (red) and M8 (green). *d-f* show clipping views of distributions of T12 (red) and M8 (green). Nuclei are blue in all images. Experiments done by M. A. Ali and W. Cho.

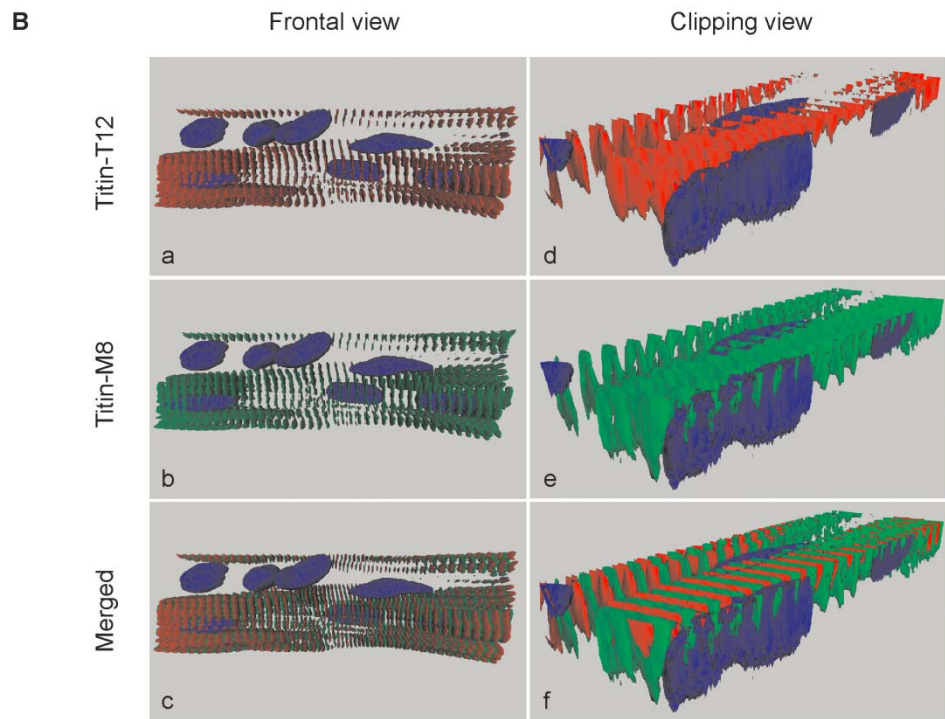


Figure 5.2 Co-localization of MMP-2 and titin at the Z disc region of the left ventricular cardiac sarcomere in 10 min aerobically perfused rat hearts (longitudinal sections). MMP-2 shows better co-localization with T12 than M8 epitope of titin in the sarcomere of left ventricular myocardium. MMP-2-immunoreactivity reveals at Z-lines with high density as well as M-lines with low density. T12 epitope reveals at only Z-lines and M8 epitope reveals at only M-lines. *a-c* shows that high density of MMP-2 (green) co-localizes (yellow) with T12 epitope (red) at the Z-lines. *d-f* shows that low density of MMP-2 (red) co-localizes (yellow) with M8 epitope (green) at M-lines. Scale bar is 5 μm for all images except for the enlarged portion of *c* illustrating the Z- and M-lines. Experiments done W. Cho and M. A. Ali.

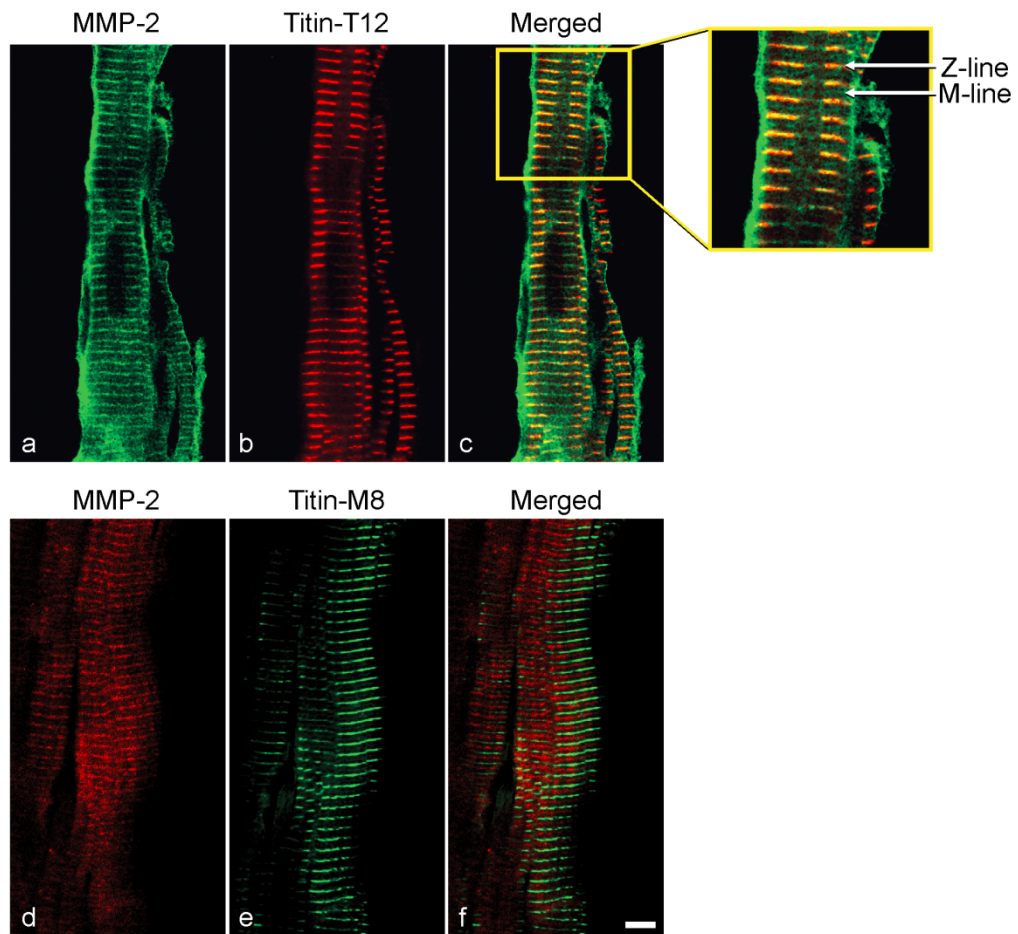


Figure 5.3 Possible MMP-2 cleavage sites within mouse and human N2B titin. A, Titin schematic indicating putative MMP-2 cleavage sites (*). Possible cleavage sites are located in both the I-band including near the Z-disc and the A-band of titin. Panel B lists the putative MMP-2 cleavage sites in mouse and human titin shown in A; data are based from three consensus cleavage motifs: PVS↓LRS, PVG↓LLA, and L/ISR↓LTA. Number correlates with the initial amino acid that is in parenthesis listed in the left column. Experiments done by M. A. Ali and B. Hudson.

Figure 5.4 MMP-2 binds to titin in vitro. A, Coomassie blue stain following electrophoretic separation of proteins from skinned muscle fibers treated for 10 min with trypsin, in order to increase T1 degradation to T2, and used for overlay/WB analysis seen in B. B, Overlay assay showing MMP-2 binding to both T1 and T2. C, Quantification of the overlay/WB analysis T1. $p < 0.001$ (One-way ANOVA, $n = 3$), MHC (myosin heavy chain). Experiments done by B. Hudson.

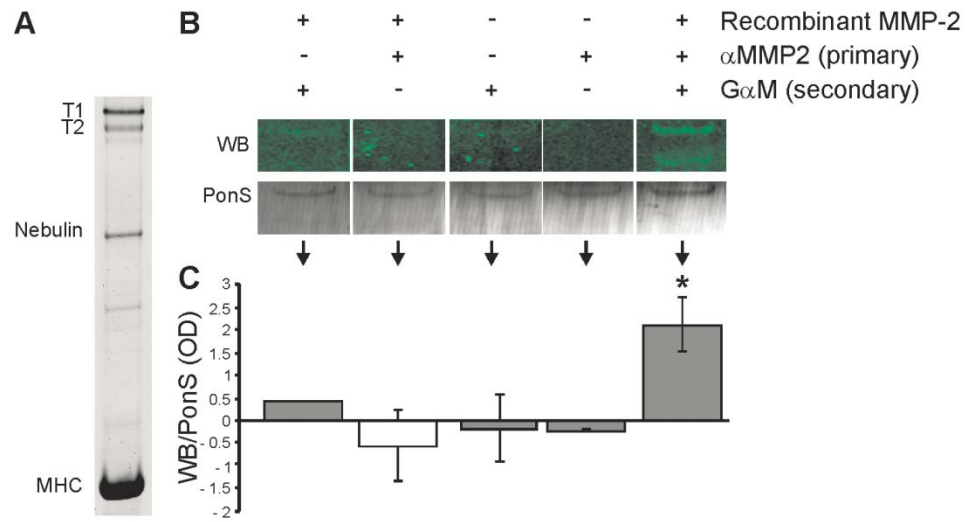


Figure 5.5 In vitro degradation (60 min, 37°C) of rabbit longissimus dorsi titin by MMP-2. A, MMP-2 cleaved titin in a concentration-dependent manner (1:500, 1:50 and 1:5 MMP-2:titin molar ratios). B, The cleavage of titin by MMP-2 was prevented by inhibiting the activity of MMP-2 with GM-6001 (100 nM) or ONO-4817 (10 µM). Experiments done by M. A. Ali and B. Hudson.

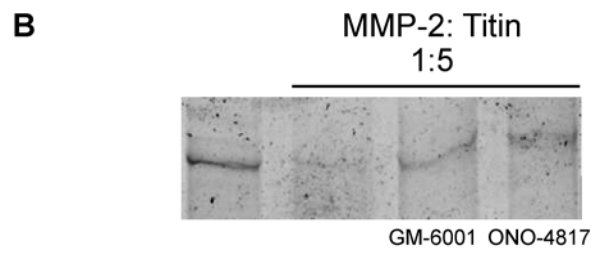
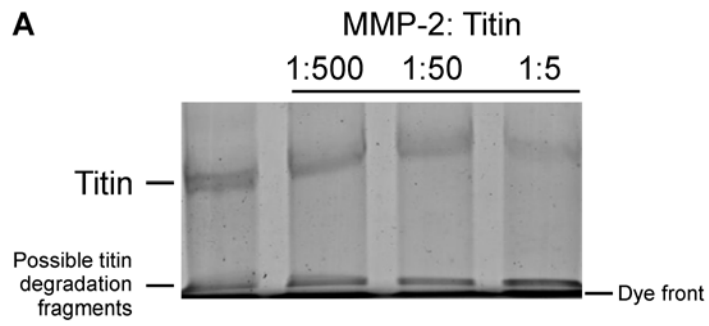


Figure 5.6 In vitro incubation (60 min, 37°C) of skinned cardiomyocytes with MMP-2. A, MMP-2 cleaved cardiac titin in a concentration-dependent manner (4-120 nM). B, The cleavage of titin by MMP-2 was prevented by inhibiting the activity of MMP-2 with 10 µM MMP inhibitors *o*-phenanthroline (*o*-ph) or ONO-4817. T1, full-length titin; T2, titin degradation product. The figure is a representative of three experiments with similar results. Experiments done by M. A. Ali and B. Hudson.

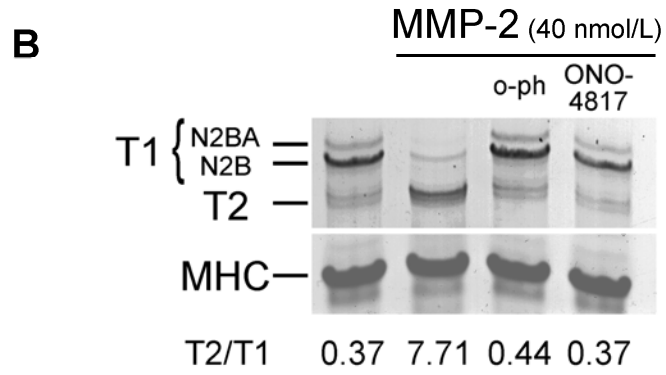
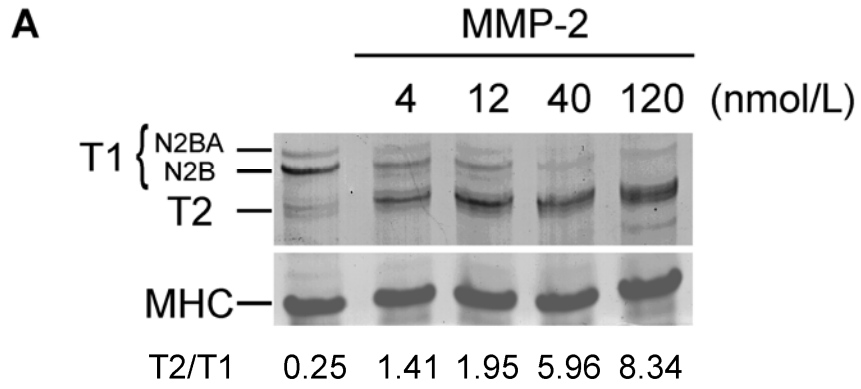


Figure 5.7 Mechanical recovery of isolated perfused working rat hearts subjected to 25 min global, no-flow ischemia followed by 60 min reperfusion without (I/R) or with 50 $\mu\text{mol/L}$ ONO-4817 (I/R + ONO-4817) in comparison with aerobically perfused control hearts. A, Schematic representation of the perfusion protocols for Control (n=6), I/R (n=7) and I/R + ONO-4817 (n=8) groups. B, Time course of changes in cardiac work of isolated working rat hearts. ** $p < 0.001$, * $p < 0.05$ versus corresponding values of I/R group (Two-way ANOVA). Experiments done by M. A. Ali.

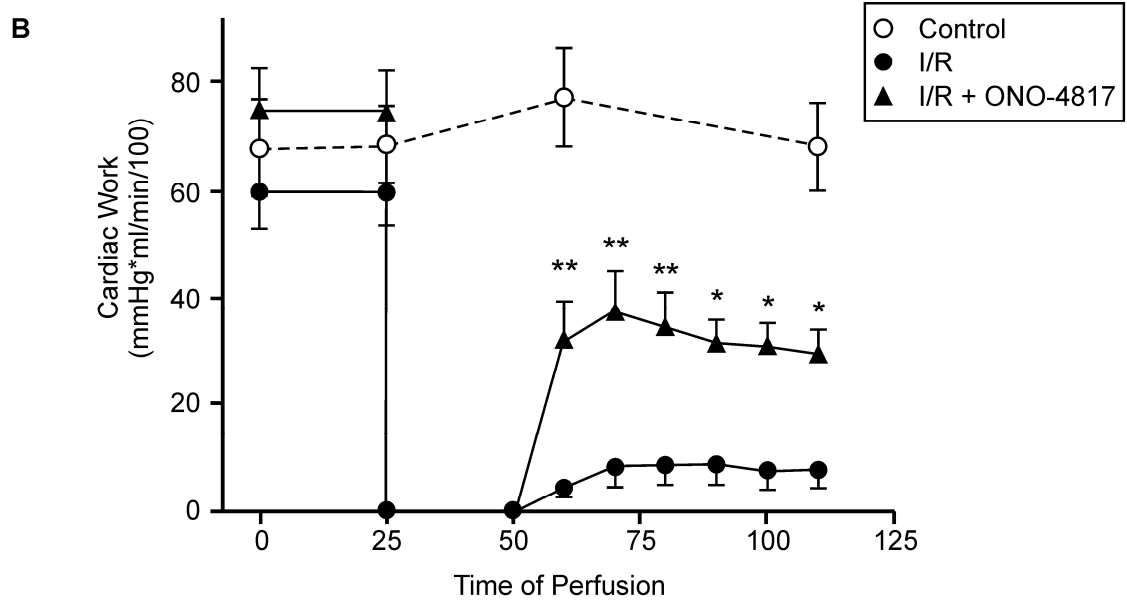
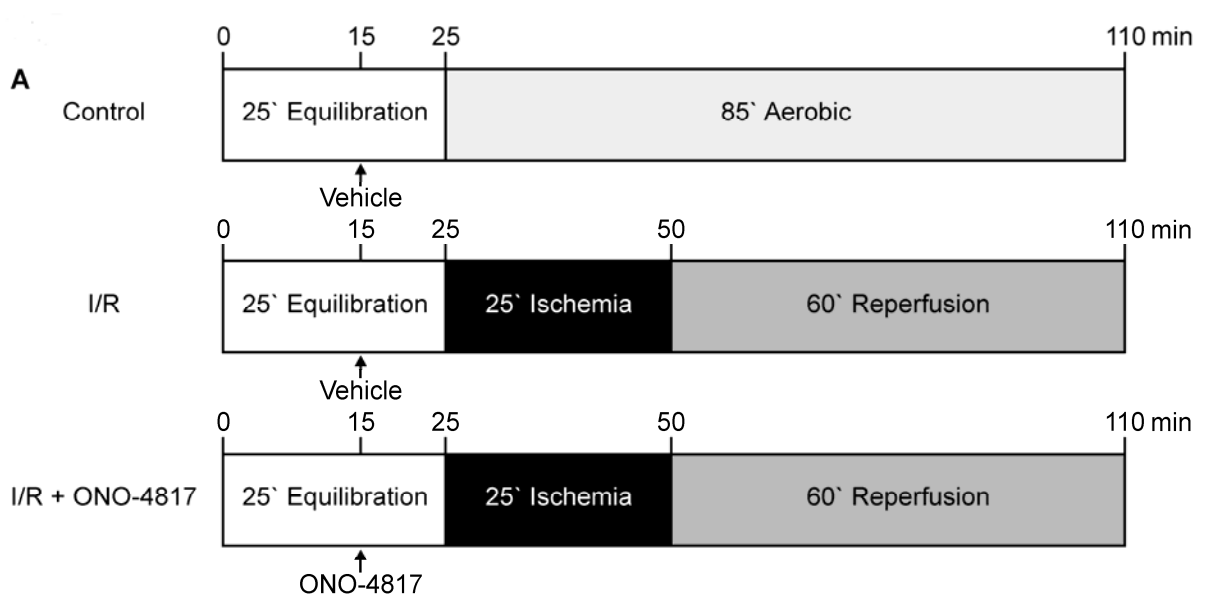


Figure 5.8 Titin degradation in ischemic-reperfused rat hearts. A, Representative SDS-agarose gel for analysis of titin in ventricular extracts. Titin (T1) and titin degradation product (T2) in ventricular homogenates from control, I/R and I/R + ONO-4817 hearts analyzed using a 1% vertical SDS-agarose gel. MHC (myosin heavy chain). BLV (bovine left ventricle) was used as a standard and shows N2BA and N2B isoforms of titin; note that the majority of rat heart titin is the N2B isoform. Each lane is an extract from individually perfused hearts. B, Ratio of total titin (T1 + T2) to MHC content (n=6 in each group). C, Ratio of T2 titin to MHC content (n=6 in each group). * $p < 0.05$ versus control (One-way ANOVA, Tukey's post hoc test). D, Representative left ventricular cryosections immunostained against titin epitope 9D10. Titin immunostaining using the 9D10 antibody (raised against the proline-glutamate-valine-lysine, PEVK, domain) was decreased in I/R hearts compared to control, whereas staining intensity was comparable between I/R + ONO-4817 and control hearts. Scale bar is 10 μm for all images. Images are representative of at least four individual hearts investigated under each condition. Experiments done by M. A. Ali, B. Hudson and W. Cho.

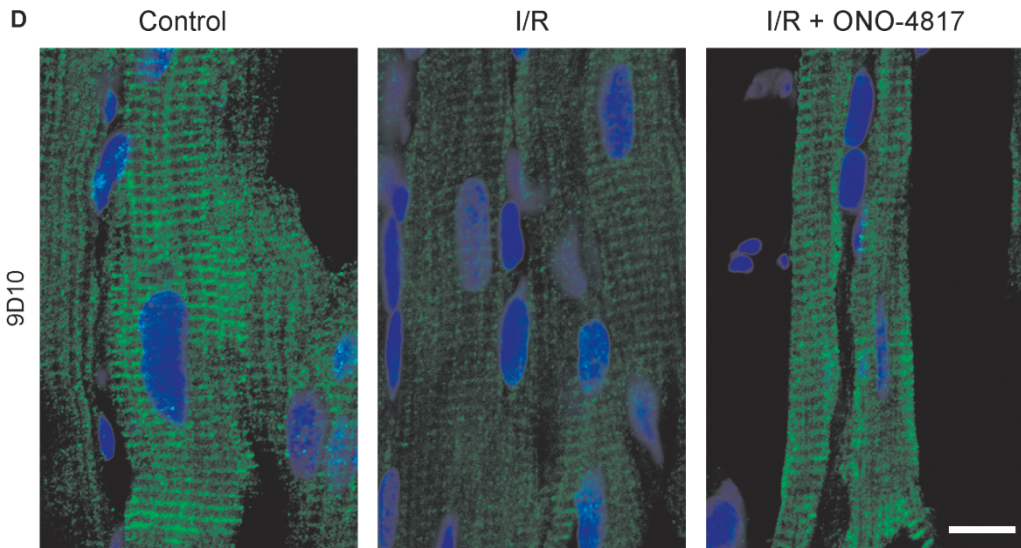
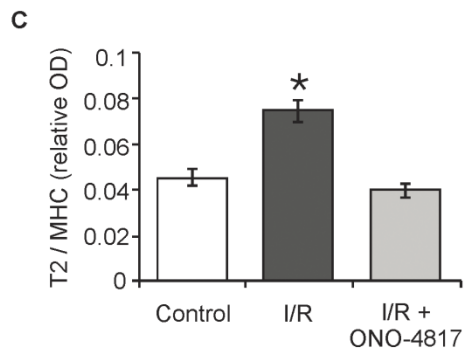
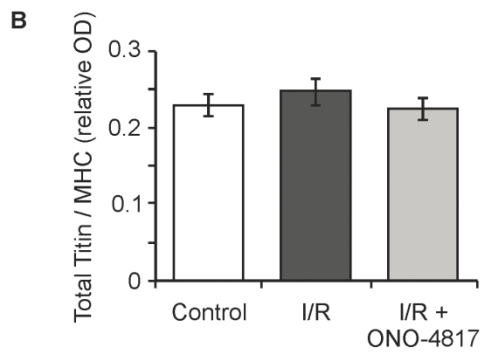
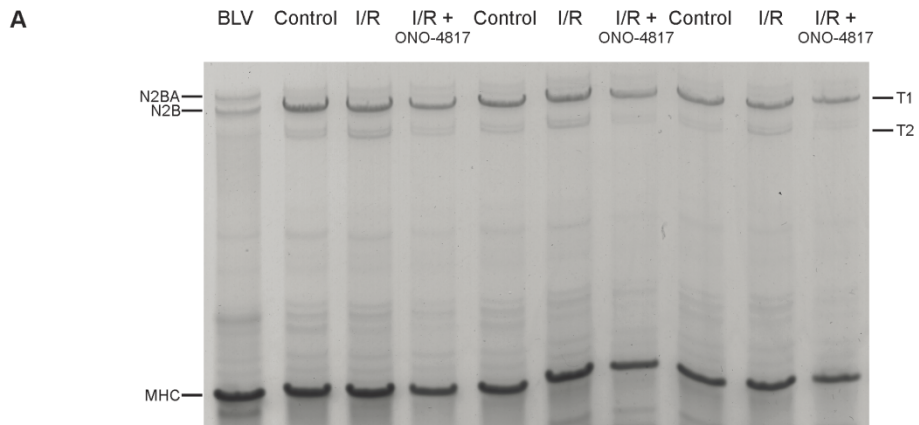


Figure 5.9 Titin degradation in MMP-2 knockout and wild type mouse hearts subjected to I/R in vivo. A, Representative 1% vertical SDS-agarose gel shows titin isoforms (N2BA and N2B) and titin degradation product T2 in left ventricle from Sham or in ischemic regions from I/R groups in either wild type or MMP-2 knockout mice. B, Quantification of T2 titin to total titin ratios (n=6 in each group). *p < 0.01 versus Sham control (One-way ANOVA, Tukey's post hoc test). WT (wild type), KO (MMP-2 knockout). Experiments done by Z. Kassiri and B. Hudson.

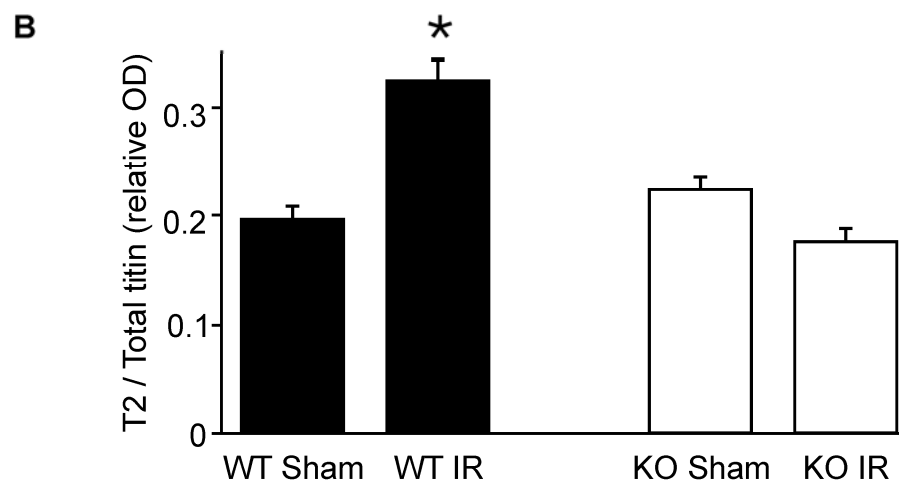
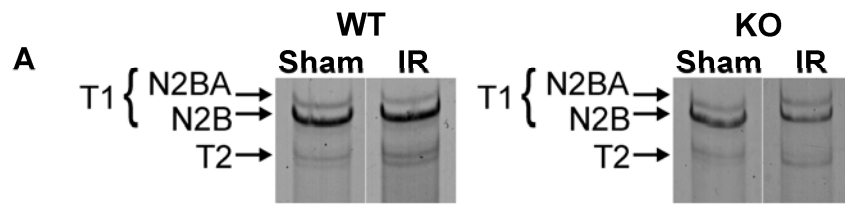
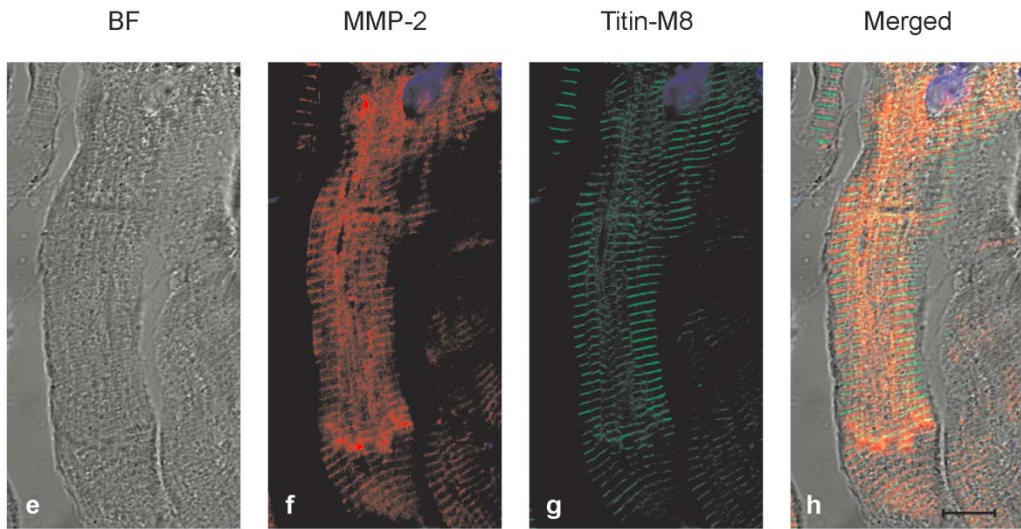
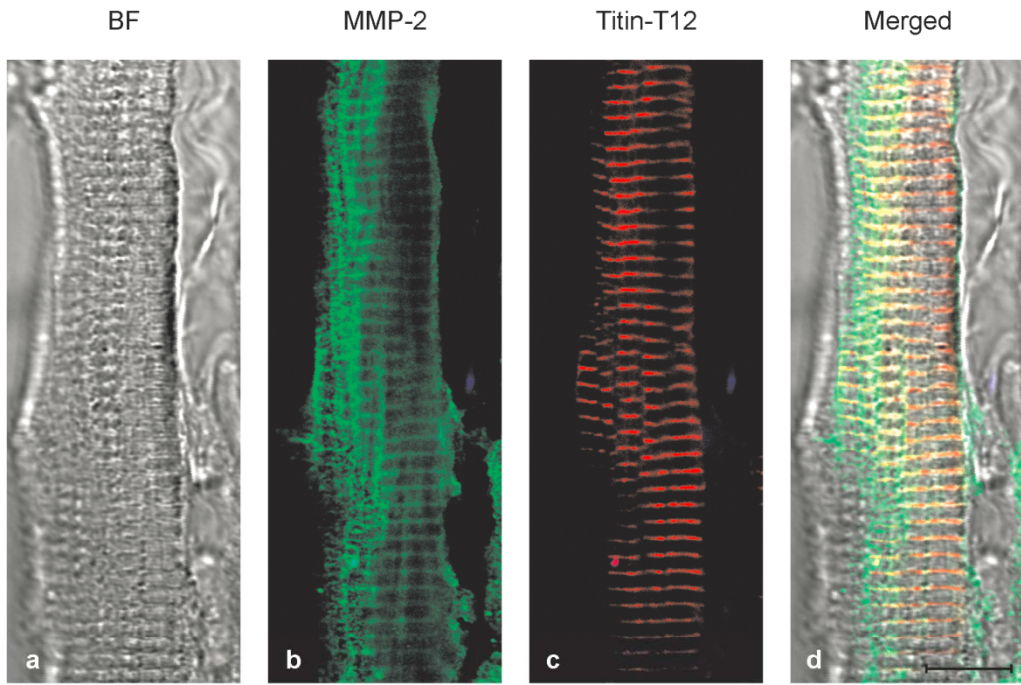


Figure 5.10 Co-localization of MMP-2 and titin near the Z-disc in diseased human heart.

Left ventricle sections were used from the explanted failing heart from a patient receiving a heart transplant. **a-d** shows that high density of MMP-2 (green) co-localizes (yellow) with T12 epitope (red) at the Z-lines. **e-h** shows that low density of MMP-2 (red) co-localizes (yellow) with M8 epitope (green) at M-lines. BF (bright field images). Scale bar is 10 μ m. Experiments done by M. A. Ali and W. Cho.



5.5: References

1. Birkedal-Hansen H. Proteolytic remodeling of extracellular matrix. *Curr Opin Cell Biol.* 1995; 7: 728-735.
2. Yasmin W, Strynadka KD, Schulz R. Generation of peroxynitrite contributes to ischemia-reperfusion injury in isolated rat hearts. *Cardiovasc Res.* 1997; 33: 422-432.
3. Okamoto T, Akaike T, Sawa T, Miyamoto Y, van der Vliet A, Maeda H. Activation of matrix metalloproteinases by peroxynitrite-induced protein S-glutathiolation via disulfide S-oxide formation. *J Biol Chem.* 2001; 276: 29596-29602.
4. Viappiani S, Nicolescu AC, Holt A, Sawicki G, Crawford BD, Leon H, van Mulligen T, Schulz R. Activation and modulation of 72kDa matrix metalloproteinase-2 by peroxynitrite and glutathione. *Biochem Pharmacol.* 2009; 77: 826-834.
5. Woessner JF,Jr. Matrix metalloproteinases and their inhibitors in connective tissue remodeling. *FASEB J.* 1991; 5: 2145-2154.
6. Newby AC, Southgate KM, Davies M. Extracellular matrix degrading metalloproteinases in the pathogenesis of arteriosclerosis. *Basic Res Cardiol.* 1994; 89 Suppl 1: 59-70.
7. Thompson RW, Parks WC. Role of matrix metalloproteinases in abdominal aortic aneurysms. *Ann N Y Acad Sci.* 1996; 800: 157-174.
8. Creemers EE, Cleutjens JP, Smits JF, Daemen MJ. Matrix metalloproteinase inhibition after myocardial infarction: a new approach to prevent heart failure? *Circ Res.* 2001; 89: 201-210.

9. Sawicki G, Salas E, Murat J, Miszta-Lane H, Radomski MW. Release of gelatinase A during platelet activation mediates aggregation. *Nature*. 1997; 386: 616-619.
10. Fernandez-Patron C, Radomski MW, Davidge ST. Vascular matrix metalloproteinase-2 cleaves big endothelin-1 yielding a novel vasoconstrictor. *Circ Res*. 1999; 85: 906-911.
11. Cheung PY, Sawicki G, Wozniak M, Wang W, Radomski MW, Schulz R. Matrix metalloproteinase-2 contributes to ischemia-reperfusion injury in the heart. *Circulation*. 2000; 101: 1833-1839.
12. McCawley LJ, Matrisian LM. Matrix metalloproteinases: they're not just for matrix anymore! *Curr Opin Cell Biol*. 2001; 13: 534-540.
13. Doucet A, Overall CM. Protease proteomics: revealing protease in vivo functions using systems biology approaches. *Mol Aspects Med*. 2008; 29: 339-358.
14. Wang W, Schulze CJ, Suarez-Pinzon WL, Dyck JR, Sawicki G, Schulz R. Intracellular action of matrix metalloproteinase-2 accounts for acute myocardial ischemia and reperfusion injury. *Circulation*. 2002; 106: 1543-1549.
15. Sawicki G, Leon H, Sawicka J, Sariahmetoglu M, Schulze CJ, Scott PG, Szczesna-Cordary D, Schulz R. Degradation of myosin light chain in isolated rat hearts subjected to ischemia-reperfusion injury: a new intracellular target for matrix metalloproteinase-2. *Circulation*. 2005; 112: 544-552.
16. Coker ML, Doscher MA, Thomas CV, Galis ZS, Spinale FG. Matrix metalloproteinase synthesis and expression in isolated LV myocyte preparations. *Am J Physiol*. 1999; 277: H777-87.

17. Sung MM, Schulz CG, Wang W, Sawicki G, Bautista-Lopez NL, Schulz R. Matrix metalloproteinase-2 degrades the cytoskeletal protein alpha-actinin in peroxynitrite mediated myocardial injury. *J Mol Cell Cardiol.* 2007; 43: 429-436.
18. Kwan JA, Schulze CJ, Wang W, Leon H, Sariahmetoglu M, Sung M, Sawicka J, Sims DE, Sawicki G, Schulz R. Matrix metalloproteinase-2 (MMP-2) is present in the nucleus of cardiac myocytes and is capable of cleaving poly (ADP-ribose) polymerase (PARP) in vitro. *FASEB J.* 2004; 18: 690-692.
19. Chow AK, Cena J, El-Yazbi AF, Crawford BD, Holt A, Cho WJ, Daniel EE, Schulz R. Caveolin-1 inhibits matrix metalloproteinase-2 activity in the heart. *J Mol Cell Cardiol.* 2007; 42: 896-901.
20. Schulz R. Intracellular targets of matrix metalloproteinase-2 in cardiac disease: rationale and therapeutic approaches. *Annu Rev Pharmacol Toxicol.* 2007; 47: 211-242.
21. Gao CQ, Sawicki G, Suarez-Pinzon WL, Csont T, Wozniak M, Ferdinandy P, Schulz R. Matrix metalloproteinase-2 mediates cytokine-induced myocardial contractile dysfunction. *Cardiovasc Res.* 2003; 57: 426-433.
22. Bergman MR, Teerlink JR, Mahimkar R, Li L, Zhu BQ, Nguyen A, Dahi S, Karliner JS, Lovett DH. Cardiac matrix metalloproteinase-2 expression independently induces marked ventricular remodeling and systolic dysfunction. *Am J Physiol Heart Circ Physiol.* 2007; 292: H1847-60.
23. Granzier HL, Labeit S. The giant protein titin: a major player in myocardial mechanics, signaling, and disease. *Circ Res.* 2004; 94: 284-295.

24. Freiburg A, Trombitas K, Hell W, Cazorla O, Fougerousse F, Centner T, Kolmerer B, Witt C, Beckmann JS, Gregorio CC, Granzier H, Labeit S. Series of exon-skipping events in the elastic spring region of titin as the structural basis for myofibrillar elastic diversity. *Circ Res.* 2000; 86: 1114-1121.
25. Cazorla O, Freiburg A, Helmes M, Centner T, McNabb M, Wu Y, Trombitas K, Labeit S, Granzier H. Differential expression of cardiac titin isoforms and modulation of cellular stiffness. *Circ Res.* 2000; 86: 59-67.
26. Fukuda N, Granzier HL, Ishiwata S, Kurihara S. Physiological functions of the giant elastic protein titin in mammalian striated muscle. *J Physiol Sci.* 2008; 58: 151-159.
27. Hein S, Scholz D, Fujitani N, Rennollet H, Brand T, Friedl A, Schaper J. Altered expression of titin and contractile proteins in failing human myocardium. *J Mol Cell Cardiol.* 1994; 26: 1291-1306.
28. Morano I, Hadicke K, Grom S, Koch A, Schwinger RH, Bohm M, Bartel S, Erdmann E, Krause EG. Titin, myosin light chains and C-protein in the developing and failing human heart. *J Mol Cell Cardiol.* 1994; 26: 361-368.
29. Kellermayer MS, Granzier HL. Calcium-dependent inhibition of in vitro thin-filament motility by native titin. *FEBS Lett.* 1996; 380: 281-286.
30. Soteriou A, Gamage M, Trinick J. A survey of interactions made by the giant protein titin. *J Cell Sci.* 1993; 104 (Pt 1): 119-123.
31. Nave R, Furst D, Vinkemeier U, Weber K. Purification and physical properties of nematode mini-titins and their relation to twitchin. *J Cell Sci.* 1991; 98 (Pt 4): 491-496.

32. Fritz JD, Swartz DR, Greaser ML. Factors affecting polyacrylamide gel electrophoresis and electroblotting of high-molecular-weight myofibrillar proteins. *Anal Biochem.* 1989; 180: 205-210.
33. O'Connell TD, Rodrigo MC, Simpson PC. Isolation and culture of adult mouse cardiac myocytes. *Methods Mol Biol.* 2007; 357: 271-296.
34. Turk BE, Huang LL, Piro ET, Cantley LC. Determination of protease cleavage site motifs using mixture-based oriented peptide libraries. *Nat Biotechnol.* 2001; 19: 661-667.
35. Chen EI, Kridel SJ, Howard EW, Li W, Godzik A, Smith JW. A unique substrate recognition profile for matrix metalloproteinase-2. *J Biol Chem.* 2002; 277: 4485-4491.
36. Nicolescu AC, Holt A, Kandasamy AD, Pacher P, Schulz R. Inhibition of matrix metalloproteinase-2 by PARP inhibitors. *Biochem Biophys Res Commun.* 2009; 387: 646-650.
37. Tatsumi R, Hattori A. Detection of giant myofibrillar proteins connectin and nebulin by electrophoresis in 2% polyacrylamide slab gels strengthened with agarose. *Anal Biochem.* 1995; 224: 28-31.
38. Schulz R, Panas DL, Catena R, Moncada S, Olley PM, Lopaschuk GD. The role of nitric oxide in cardiac depression induced by interleukin-1 beta and tumour necrosis factor-alpha. *Br J Pharmacol.* 1995; 114: 27-34.
39. Yamada A, Uegaki A, Nakamura T, Ogawa K. ONO-4817, an orally active matrix metalloproteinase inhibitor, prevents lipopolysaccharide-induced proteoglycan release from the joint cartilage in guinea pigs. *Inflamm Res.* 2000; 49: 144-146.

40. Kandalam V, Basu R, Abraham T, Wang X, Soloway PD, Jaworski DM, Oudit GY, Kassiri Z. TIMP2 deficiency accelerates adverse post-myocardial infarction remodeling because of enhanced MT1-MMP activity despite lack of MMP2 activation. *Circ Res.* 2010; 106: 796-808.
41. Warren CM, Krzesinski PR, Greaser ML. Vertical agarose gel electrophoresis and electroblotting of high-molecular-weight proteins. *Electrophoresis.* 2003; 24: 1695-1702.
42. Ku NO, Fu H, Omary MB. Raf-1 activation disrupts its binding to keratins during cell stress. *J Cell Biol.* 2004; 166: 479-485.
43. Dhiman M, Nakayasu ES, Madaiah YH, Reynolds BK, Wen JJ, Almeida IC, Garg NJ. Enhanced nitrosative stress during *Trypanosoma cruzi* infection causes nitrotyrosine modification of host proteins: implications in Chagas' disease. *Am J Pathol.* 2008; 173: 728-740.
44. Wang W, Sawicki G, Schulz R. Peroxynitrite-induced myocardial injury is mediated through matrix metalloproteinase-2. *Cardiovasc Res.* 2002; 53: 165-174.
45. Leon H, Baczko I, Sawicki G, Light PE, Schulz R. Inhibition of matrix metalloproteinases prevents peroxynitrite-induced contractile dysfunction in the isolated cardiac myocyte. *Br J Pharmacol.* 2008; 153: 676-683.
46. Young P, Ferguson C, Banuelos S, Gautel M. Molecular structure of the sarcomeric Z-disk: two types of titin interactions lead to an asymmetrical sorting of alpha-actinin. *EMBO J.* 1998; 17: 1614-1624.

47. Atkinson RA, Joseph C, Dal Piaz F, Birolo L, Stier G, Pucci P, Pastore A. Binding of alpha-actinin to titin: implications for Z-disk assembly. *Biochemistry*. 2000; 39: 5255-5264.
48. Gregorio CC, Trombitas K, Centner T, Kolmerer B, Stier G, Kunke K, Suzuki K, Obermayr F, Herrmann B, Granzier H, Sorimachi H, Labeit S. The NH2 terminus of titin spans the Z-disc: its interaction with a novel 19-kD ligand (T-cap) is required for sarcomeric integrity. *J Cell Biol*. 1998; 143: 1013-1027.
49. Gutierrez FR, Lalu MM, Mariano FS, Milanezi CM, Cena J, Gerlach RF, Santos JE, Torres-Duenas D, Cunha FQ, Schulz R, Silva JS. Increased activities of cardiac matrix metalloproteinases matrix metalloproteinase (MMP)-2 and MMP-9 are associated with mortality during the acute phase of experimental *Trypanosoma cruzi* infection. *J Infect Dis*. 2008; 197: 1468-1476.
50. Ikonomidis JS, Hendrick JW, Parkhurst AM, Herron AR, Escobar PG, Dowdy KB, Stroud RE, Hapke E, Zile MR, Spinale FG. Accelerated LV remodeling after myocardial infarction in TIMP-1-deficient mice: effects of exogenous MMP inhibition. *Am J Physiol Heart Circ Physiol*. 2005; 288: H149-58.
51. Eaton P, Byers HL, Leeds N, Ward MA, Shattock MJ. Detection, quantitation, purification, and identification of cardiac proteins S-thiolated during ischemia and reperfusion. *J Biol Chem*. 2002; 277: 9806-9811.
52. Doroszko A, Polewicz D, Sawicka J, Richardson JS, Cheung PY, Sawicki G. Cardiac dysfunction in an animal model of neonatal asphyxia is associated with increased degradation of MLC1 by MMP-2. *Basic Res Cardiol*. 2009; 104: 669-679.

53. Bolli R, Marban E. Molecular and cellular mechanisms of myocardial stunning. *Physiol Rev.* 1999; 79: 609-634.
54. Lim CC, Zuppinger C, Guo X, Kuster GM, Helmes M, Eppenberger HM, Suter TM, Liao R, Sawyer DB. Anthracyclines induce calpain-dependent titin proteolysis and necrosis in cardiomyocytes. *J Biol Chem.* 2004; 279: 8290-8299.
55. Kukan M. Emerging roles of proteasomes in ischemia-reperfusion injury of organs. *J Physiol Pharmacol.* 2004; 55: 3-15.
56. Stansfield WE, Moss NC, Willis MS, Tang R, Selzman CH. Proteasome inhibition attenuates infarct size and preserves cardiac function in a murine model of myocardial ischemia-reperfusion injury. *Ann Thorac Surg.* 2007; 84: 120-125.
57. Zolk O, Schenke C, Sarikas A. The ubiquitin-proteasome system: focus on the heart. *Cardiovasc Res.* 2006; 70: 410-421.
58. Centner T, Yano J, Kimura E, McElhinny AS, Pelin K, Witt CC, Bang ML, Trombitas K, Granzier H, Gregorio CC, Sorimachi H, Labeit S. Identification of muscle specific ring finger proteins as potential regulators of the titin kinase domain. *J Mol Biol.* 2001; 306: 717-726.
59. Witt SH, Granzier H, Witt CC, Labeit S. MURF-1 and MURF-2 target a specific subset of myofibrillar proteins redundantly: towards understanding MURF-dependent muscle ubiquitination. *J Mol Biol.* 2005; 350: 713-722.
60. van Hees HW, Ottenheijm CA, Granzier HL, Dekhuijzen PN, Heunks LM. Heart failure decreases passive tension generation of rat diaphragm fibers. *Int J Cardiol.* 2010; 141: 275-283.

61. Carvalho RF, Dariolli R, Justulin Junior LA, Sugizaki MM, Politi Okoshi M, Cicogna AC, Felisbino SL, Dal Pai-Silva M. Heart failure alters matrix metalloproteinase gene expression and activity in rat skeletal muscle. *Int J Exp Pathol.* 2006; 87: 437-443.

CHAPTER 6

CONCLUSIONS

6.1: Conclusions

Coronary heart diseases are the leading cause of mortality and morbidity in Canada. Heart attacks (acute myocardial infarction) occur due to reduced coronary blood flow, thus the supply of oxygen and nutrients to the affected part of the heart is compromised (ischemic heart), as well as the removal of metabolic wastes. After an acute myocardial infarction, early restoration of blood supply to the ischemic heart (myocardial reperfusion) is, not surprisingly, the most effective rescue strategy for reducing infarct size and improving clinical outcome in patients. Myocardial reperfusion can be attained either pharmacologically (with thrombolytics), surgically (coronary artery bypass grafting) or by a minimally invasive approach (percutaneous coronary intervention). Surprisingly, myocardial reperfusion can cause further injury, termed I/R injury, which paradoxically reduces the beneficial effect of reperfusion therapy. I/R injury can arguably explain why despite successful reperfusion, the mortality rate and the incidence of heart failure after an acute myocardial infarction approach 10% and 25%, respectively¹. This necessitates development of strategies to ameliorate I/R injury which will have a great impact in improving clinical outcomes in acute myocardial infarction.

Though important inroads have been achieved in studying myocardial I/R injury, its exact mechanism(s) has not been fully elucidated. Furthermore, pharmacological agents used clinically to amend I/R injury are almost lacking.

In 2000, the Schulz lab published a key study implicating the proteolytic activity of MMP-2 in I/R injury of the heart and suggested the use of MMP inhibitors as a novel pharmacological therapy in reperfusion injury². Despite its well-known role in extracellular matrix remodelling following an infarct, this study underscored that MMP-2 role in I/R injury goes beyond its role in remodelling, and in a rapid time frame of

minutes as opposed to hours or days. MMP-2 activity was shown to be a causative factor, in part, in the acute myocardial contractile dysfunction seen early during reperfusion after ischemia, otherwise known as stunning injury. Although substrates of MMP-2 that could explain this effect were lacking in this study, evidence was provided excluding extracellular matrix degradation/remodelling. This further motivated rigorous research in the lab in order to identify potential novel substrates of MMP-2 in the heart which are proteolyzed as a result of acute I/R injury. Two years later, TnI, a protein in the thin myofilaments which regulates actin-myosin interaction, was discovered as a novel target of MMP-2 in myocardial I/R injury ³. To the surprise of many, in particular to MMP researchers, this substrate is an intracellular rather than an extracellular protein which challenged the paradigm of the actions of MMP-2 at that time. The fact that MMPs were first described as secreted proteases which bear a secretory signal sequence at their N-termini, and the lack of molecular mechanism(s) to explain the intracellular localizations of MMP-2 which the Schulz laboratory subsequently discovered, created some resistance within the research community to further investigate the novel intracellular biology of MMP-2.

In this thesis I provided at least two mechanisms by which MMP-2 can reside intracellularly. First, a splice variant of MMP-2 which lacks the secretory signal sequence is expressed in both neonatal and adult human cardiomyocytes which makes it exclusively present in the cytosol. In addition, the signal sequence of canonical MMP-2 is inefficient and does not restrict it only to the secretory pathway, resulting in a considerable portion of canonical MMP-2 which also resides in the cytosol. Given that the splice variant mRNA is expressed at only ~10% of that of canonical MMP-2 in cardiomyocytes, it appears that canonical MMP-2 which is inefficiently targeted for secretion and thus remains in the cytosol, is likely the major intracellular moiety of

MMP-2. Moreover, in neonatal cardiomyocytes exposed to oxidative stress injury, the degradation of a known cardiac MMP-2 substrate, TnI, was particularly enhanced when the intracellular pool of MMP-2 was increased by increasing the expression of the splice variant MMP-2. Therefore, the work in Chapter 2 will bridge a large gap in our knowledge as it demonstrates how MMP-2 comes to reside within the cell. Accordingly, it should stimulate hosts of researchers to considerably broaden their horizons as to where MMP-2, and likely also other MMPs, can have biological actions, not only outside the cell. Likewise, Chapter 2 added another piece of puzzle to explain why despite the 50 years of research providing evidence for the role of MMPs in various pathologies including atherosclerosis, osteoarthritis and cancer (to name a few), the clinical use of MMP inhibitors in such diseases (with the exception of a sub-antimicrobial dose formulation of doxycycline in chronic periodontitis (Periostat®) and rosacea (Oracea®)) seems still in its infancy.

MMP-2 is suggested to play a role in cell death induced by oxidative stress injury in various cell types including cardiomyocytes⁴⁻⁶. However, the mechanism(s) and/or the substrate(s) targeted by MMP-2 to induce cell death were missing in these studies. The aim of Chapter 3 was to further investigate the possible role of MMP-2 in cell death especially in cardiomyocytes. In light of the findings of Chapter 2, I hypothesized that MMP-2 targets intracellular rather than extracellular substrates to effect cell death. Treating neonatal cardiomyocytes with hydrogen peroxide led to elevated MMP-2 level and activity in a time-dependent manner with maximal effects seen within 4 h when using 200 μ M. Hydrogen peroxide caused necrotic cell death by disrupting the plasmalemma as evidenced by the release of lactate dehydrogenase into the culture medium in a concentration- and time-dependant manner as well as by the necrotic signature of PARP-1 cleavage. The absence of both caspase-3 cleavage/activation and apoptotic cleavage of

PARP-1 illustrated the weak contribution of apoptosis in hydrogen peroxide-induced cardiomyocyte death. Despite previous studies using hydrogen peroxide to stimulate cardiomyocyte apoptosis (e.g. see ⁷), that hydrogen peroxide is, in our hands, too strong a stimulus and promotes necrosis over apoptosis. However, I found that pretreatment with selective MMP inhibitors (GM-6001 or ONO-4817) did not protect against hydrogen peroxide-induced necrosis. Chapter 3 concluded that hydrogen peroxide increases the level and activity of MMP-2 and induces necrotic cell death in cardiomyocytes, yet, the later effect is independent of MMP-2 activity. This work cautions against the use of hydrogen peroxide to trigger apoptosis in neonatal cardiomyocytes. Thus, there is still a need for further investigations to unravel the exact role of MMPs or other proteases in mediating cell death following oxidative stress.

It has been found during myocardial I/R injury MMP-2 proteolyzes specific sarcomeric proteins, some of these are also known to be cleaved by a cytosolic Ca²⁺-dependent protease, calpain-1. Cleavage of these sarcomeric proteins rapidly impairs cardiac contractile function. Despite the lack of evidence showing clear co-localization of calpain to these sarcomeric proteins in cardiomyocytes, some calpain inhibitors were shown to significantly improve the recovery of myocardial contractile function, in a similar manner to MMP-2 inhibitors. In Chapter 4, I demonstrated that the protective effects of some calpain inhibitors may be due in part to their ability to inhibit MMP-2 activity. I tested four calpain inhibitors (calpain inhibitor III, ALLM, ALLN, and PD-150606) for their ability to inhibit MMP-2 in comparison to the selective MMP inhibitor ONO-4817. At 100 μM, all calpain inhibitors except ALLM showed significant inhibition of MMP-2 gelatinolytic activity. On the other hand, ONO-4817 did not inhibit calpain-1 activity in a concentration up to 100 μM. When assessed using the TnI degradation assay, both ALLN and PD-150606, but not ALLM or calpain inhibitor III (all at 20 μM),

significantly inhibited MMP-2 catalytic activity. Using the OmniMMP substrate kinetic assay, I determined the IC₅₀ values of PD-150606 and ALLN to be 9.3 μM and 21.9 μM, respectively (compared to 0.00025 μM for ONO-4817). These experiments showed that the calpain inhibitors PD-150606 and ALLN have significant additional pharmacological activity as MMP-2 inhibitors. This chapter suggests that the protective effects of some calpain inhibitors previously observed during I/R injury of the heart (and likely also in our injury models in other tissues and organs) may be due to their ability to inhibit MMP activity. Also, I showed that the selective MMP inhibitor ONO-4817 is devoid of any calpain-1 inhibitory activity.

As mentioned above, previous studies from the lab reported that MMP-2 is localized to the cardiac sarcomere and upon activation in I/R injury proteolyzes specific myofilament proteins including TnI, MLC-1 and α-actinin. In the light of these studies, Chapter 5 determined that titin is another important sarcomeric substrate for MMP-2 and its degradation during I/R contributes to cardiac contractile dysfunction. Titin is the largest mammalian (~3000-4000 kD) and myofilament protein which also acts as a molecular spring, contributing to the passive tension of myofibrils and maintaining the structural and functional stability of the cardiac sarcomere. Titin is a crucial determinant of both systolic and diastolic function and the Frank-Starling mechanism of the heart. Loss of titin in ischemic hearts has been reported^{8,9}, however, the protease(s) responsible for titin degradation was a missing piece of knowledge in those studies.

I used immunohistochemistry and confocal microscopy in rat and human hearts and showed the discrete co-localization between MMP-2 and titin in the Z-disc region of titin and that MMP-2 is mainly localized to titin near the Z-disc of the cardiac sarcomere. Both purified titin and titin in skinned cardiomyocytes were proteolyzed when incubated

with MMP-2 in a concentration-dependent manner and this was prevented by MMP inhibitors. Isolated rat hearts subjected to I/R injury showed cleavage of titin in ventricular extracts by gel electrophoresis which was confirmed by reduced titin immunostaining in tissue sections. Inhibition of MMP activity with ONO-4817 prevented I/R-induced titin degradation and improved the recovery of myocardial contractile function. Titin degradation was also reduced in hearts from MMP-2 knockout mice subjected to I/R in vivo, compared to wild type controls. That chapter, therefore, shows that MMP-2 plays an important role in titin homeostasis, which directly affects the contractile function of the heart at the sarcomeric level. Moreover, that study highlights an interesting link between the two components responsible for myocardial stiffness: the extracellular matrix (also known to be degraded by MMPs including MMP-2) and titin filaments inside the cardiomyocyte. The remodeling of both components may now be deemed a characteristic of many heart diseases with detrimental effects on cardiac contractile function.

Figure 6.1 depicts the new findings in this thesis regarding the mechanisms of cytosolic targeting of MMP-2 and its cardiac sarcomeric protein substrates in the context of previous observations of MMP-2 post-translational modification.

6.2: Limitations

In general, there are some limitations to the experimental approaches which were taken that should be acknowledged and considered in future studies and in order to prevent over- or misinterpretation of the data.

In Chapter 2, in order to assess the differential subcellular localization of canonical and splice-variant MMP-2, chimeric proteins which are tagged with

hemagglutinin at the C-terminus were expressed in cultured cells instead of the native protein sequence. However, the tag enabled me to readily differentiate between the expressed and endogenous MMP-2 in cells. Also, although the expression levels of MMP-2 protein from all different constructs were similar, this level is still higher than that seen for the endogenous MMP-2 under normal physiological conditions. To quantify the amount of MMP-2 which resides in the cytosolic and membrane fractions, I performed subcellular fractionation followed by western blotting. However, the use of secondary antibodies and the ECL detection methods to amplify the signal to detectable levels render the western blotting technique a semi-quantitative method rather than a fully quantitative one. Additionally, post-translation modifications of MMP-2 may affect the primary antibody affinity in an unpredictable manner. This is relevant in this study especially since post-translation modifications of MMP-2 in the cytosol^{10,11} are predicted to be different than MMP-2 which is processed in the ER and Golgi system¹². I showed that around 40% of the intracellular canonical MMP-2 escaped the secretory pathway and remained in the cytosol. However, the study does not totally exclude the possibility whether this canonical MMP-2 found in the cytosol entered the ER secretory pathway and routed back into the cytosol by some unknown mechanism.

In Chapter 3, I demonstrated that apoptosis contributed minimally to hydrogen peroxide induced cardiomyocyte death. This conclusion was drawn due to the absence of caspase-3 cleavage and/or activation in this cell death model under my experimental conditions. However, it is worth mentioning that apoptosis can also occur in a caspase-independent pathway that was not investigated here. Also, MMP inhibitors did not mitigate necrotic cell death in cardiomyocytes. Although, this indicates that hydrogen peroxide-induced necrosis occurs in an MMP-2 independent manner in cardiomyocytes, it does not totally exclude the possible role of MMP-2 in other types of cell death

including apoptosis or autophagy. MMP-2 activity was shown to significantly increase with 200 μ M hydrogen peroxide treatment in a time-dependent manner as assessed by gelatin zymography technique. This technique is highly sensitive and reproducible, however, several limitations can be accounted to it. More importantly, the non-reducing condition of the gel activates latent MMPs as well as dissociates MMPs from their protein inhibitor complexes (eg. TIMPs, caveolin-1¹³, etc) during electrophoresis. This means that the increase in MMP-2 gelatinolytic activity in the cell lysate does not always mean an increase in the net MMP-2 activity within the cell. Therefore one should supplement assays of MMPs activity by zymography using other techniques such as substrate degradation assays including specific synthetic peptides. It is worth noting that a research is currently ongoing in the Schulz lab in order to develop FRET-based protease biosensors¹⁴ specific for MMP-2 which will allow us to assess intracellular MMP activity in a real-time manner.

In Chapter 4, the 40 kD catalytic domain of MMP-2 which lacks the C-terminus hemopexin domain was used in in vitro degradation and OmniMMP kinetic assays. Providing that the hemopexin domain can bind to other proteins or substrates altering MMP activity, the above mentioned assays may need to be demonstrated using 64 kD MMP-2 which bears the hemopexin domain as well as 72 kD MMP-2 activated by peroxynitrite¹¹. The MMP-2 inhibitory effect of calpain inhibitors was assessed only using in vitro assays and is yet to be shown using an in vivo model. However, the in vitro assays are simple, effective and economical tools to use prior to initiating more resource-intensive and time consuming in vivo experiments.

In Chapter 5, the use of isolated perfused working rat hearts has many advantages. It is a well-established simplified model that has been in use for almost 50

years as a tool to study cardiac mechanical function. This experimental model allows us to concomitantly measure myocardial contractile function as well as various metabolic parameters under physiological conditions of preload and afterload. However it also comes with its own limitations. The perfusion of isolated hearts with crystalloid buffers mimic but do not replace all the components of blood or *in vivo* experimental models. Likewise, the absence of neurohormonal regulation in isolated hearts brings difference to what may be observed *in vivo*. Therefore, extrapolation of these results to pathological events that occur *in vivo* must be done with caution. Also, operator skill plays a significant role in the use of this technique. Use of the isolated working heart model requires fine motor skills and keen eyesight. In addition to this is the necessity to work rapidly in order to prevent the nearly instantaneous deterioration or ischemic preconditioning of the heart especially at the onset of the procedure, thus, inter-operator variability is considerable.

Immunohistochemistry has the advantage as it is able to detect the localization of proteins, however, like other techniques that rely heavily on antibodies, the interpretation of immunohistochemical results is reliant on the specificity and avidity of primary and secondary antibodies that are used. Non-specific binding of an antibody could easily lead to misinterpretation of results. Additionally, immunohistochemistry is not readily quantifiable and thus is difficult to compare the levels of proteins between samples. In fact, interpretation of immunohistochemistry results can be highly dependent on the field of view that is chosen and therefore a large sample of tissue slices is required. Finally, despite that less titin degradation was seen in MMP-2 knockout mice exposed to *in vivo* I/R injury compared to wild type controls, functional data from these mice are lacking.

6.3: Future directions

My thesis presents exciting results which open an avenue for future studies not only in the area of cardiovascular research but also in the general field of MMP biology. However, caution should be taken in how these data are extrapolated to the human population.

The finding that a transcript variant of MMP-2 is present in human cardiomyocytes leads me to consider future studies in order to clarify its exact role in both cellular physiology and pathology. The abundance of this splice variant of MMP-2 needs to be investigated in other types of cells and tissues. Although my data shows that the level of MMP-2 transcript variant is around 10% of that of the canonical transcript, it is also tempting to study the effect of various pathophysiological conditions on MMP-2 transcript splicing and protein expression. My thesis suggests that the secretory signal sequence of MMP-2 is inefficient in targeting to the secretory pathway, however, future directions may determine the exact domain of the signal sequence which is responsible for this effect.

The results of my studies exclude the role of MMP-2 in hydrogen peroxide induced cardiomyocyte necrosis, but still suggest that MMP-2 may have a role in other types of cell death (apoptosis, autophagy...) and this needs further investigation. In an in vitro preliminary study, I showed that MMP-2 cleaves and activates the pro-apoptotic factor, Bid, which induces cytochrome c release from isolated mitochondria preparation (see Appendix). MMP inhibitors were shown to improve the recovery of contractile function in isolated perfused hearts after I/R injury or ONOO⁻ infusion^{2, 3, 15, 16} and protected heart function in diabetic cardiomyopathy¹⁷ or in endotoxin induced cardiac dysfunction^{18, 19}. On the other hand, hydrogen peroxide induced cardiac contractile

dysfunction in isolated rat hearts was not improved by inhibiting MMPs ²⁰. In an interesting similarity, my data also showed that MMP inhibitors did not prevent hydrogen peroxide induced cardiomyocyte death. Accordingly, these results suggest that the magnitude and pathophysiological consequences of MMP-2 activation after oxidative stress challenge are different depending on the reactive oxygen/nitrogen species used. However, future studies directly comparing the differential effects of different reactive oxygen/nitrogen species on MMP-2 activity may address this question.

Finding another novel intracellular target for MMP-2 during I/R such as titin is very exciting and it provides an insight into the pathophysiological role of MMP-2 in the heart. This finding also opens the opportunity to explore whether the same event occurs in the human heart subjected to oxidative stress injury such as during coronary artery bypass grafting surgery, pharmacological (using thrombolytics) or interventional (percutaneous coronary intervention) reperfusion. In addition, it underlines the need to evaluate the possible beneficial role of MMP inhibitors on heart function in clinical trials of patients who undergo coronary artery bypass grafting surgery or interventional reperfusion. For instance, it will be interesting to explore whether MMP inhibitors in the cardioplegic solution might bring beneficial effects such as the reduction of I/R injury.

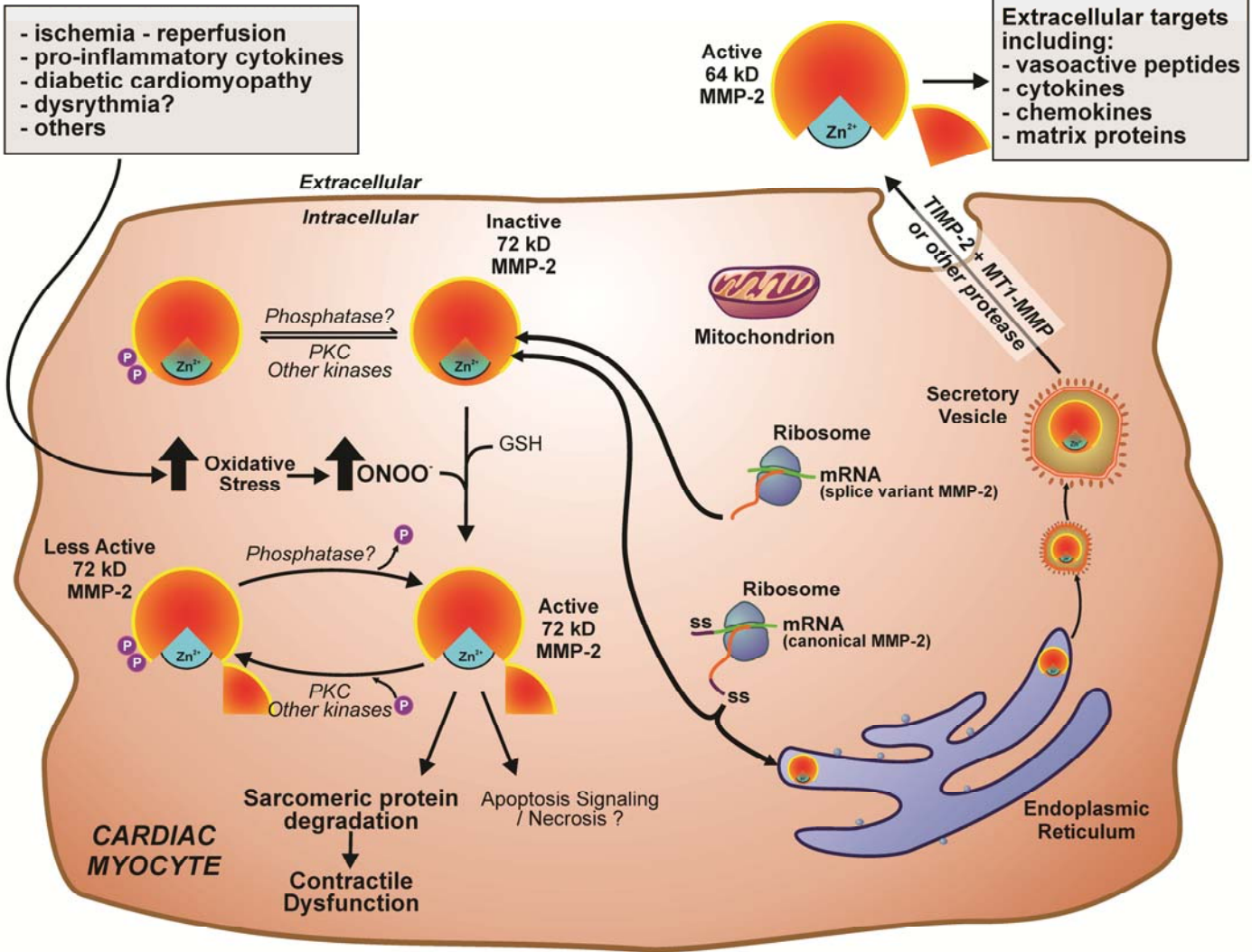
Finally, the observation that MMP-2 is co-localized to titin in human and rat hearts suggests a possible physiological role of MMP-2 in normal titin turnover. The latter is a crucial physiological process involved in sarcomerogenesis and sarcomere disassembly, both which actively occur during embryonic cardiac cell division ²¹.

6.4: Final words:

In light of studies of my thesis, it has been shown that activation of MMP-2 which has a unique subcellular distribution in cardiomyocytes could be one of the earliest pathophysiological events triggered downstream of enhanced oxidative stress. Despite most research to date has focused on the extracellular actions of MMPs, much more recent evidence suggests that MMP-2, and other MMPs, can also degrade specific protein targets inside the cell. Future studies will likely reveal other novel intra- and extra-cellular targets of MMP-2 which will aid our understanding of the pathology underlying myocardial injury caused by enhanced oxidative stress. Finally, MMP inhibitors, including one selective for MMP-2, should be rigorously tested as a possible therapeutic strategy to prevent or treat oxidative stress injury of the heart and other organs

Figure 6.1: Cytosolic targeting and post-translational modifications of MMP-2 in the cardiac myocyte.

MMP-2 is targeted to the cytosol via at least two mechanisms. First, there exists a splice variant of MMP-2 in cardiomyocytes that lack the secretory signal sequence. Secondly, the inefficient signal sequence of the canonical MMP-2 results in its targeting both to the endoplasmic reticulum lumen for secretion and to the cytosol. The 72 kD form of MMP-2 can be activated extracellularly by MT1-MMP in the presence of TIMP-2, or by other proteases (e.g. plasminogen) via cleavage of its propeptide domain to yield 64 kD MMP-2 which acts on targets outside the cell. 72 kD MMP-2 can also be activated intracellularly by S-glutathiolation when exposed to peroxynitrite (as caused by I/R injury, pro-inflammatory cytokines, etc.) in the presence of cellular glutathione without losing the propeptide domain. This activated 72 kD MMP-2 can target and proteolyze specific sarcomeric proteins causing myocardial contractile dysfunction as seen in I/R injury. MMP-2 is also a phosphoprotein with several identified phosphorylation sites and whose activity is further modulated by its phosphorylation status. The kinases and phosphatases involved in its regulation in vivo are yet to be discovered. GSH, glutathione; ONOO⁻, peroxynitrite; PKC, protein kinase C; SS, signal sequence.



6.4: References

1. Yellon DM, Hausenloy DJ. Myocardial reperfusion injury. *N Engl J Med.* 2007; 357: 1121-1135.
2. Cheung PY, Sawicki G, Wozniak M, Wang W, Radomski MW, Schulz R. Matrix metalloproteinase-2 contributes to ischemia-reperfusion injury in the heart. *Circulation.* 2000; 101: 1833-1839.
3. Wang W, Schulze CJ, Suarez-Pinzon WL, Dyck JR, Sawicki G, Schulz R. Intracellular action of matrix metalloproteinase-2 accounts for acute myocardial ischemia and reperfusion injury. *Circulation.* 2002; 106: 1543-1549.
4. Shen J, O'Brien D, Xu Y. Matrix metalloproteinase-2 contributes to tumor necrosis factor alpha induced apoptosis in cultured rat cardiac myocytes. *Biochem Biophys Res Commun.* 2006; 347: 1011-1020.
5. Aldonyte R, Brantly M, Block E, Patel J, Zhang J. Nuclear localization of active matrix metalloproteinase-2 in cigarette smoke-exposed apoptotic endothelial cells. *Exp Lung Res.* 2009; 35: 59-75.
6. Yang Y, Candelario-Jalil E, Thompson JF, Cuadrado E, Estrada EY, Rosell A, Montaner J, Rosenberg GA. Increased intranuclear matrix metalloproteinase activity in neurons interferes with oxidative DNA repair in focal cerebral ischemia. *J Neurochem.* 2010; 112: 134-149.
7. Tran TH, Andreka P, Rodrigues CO, Webster KA, Bishopric NH. Jun kinase delays caspase-9 activation by interaction with the apoptosome. *J Biol Chem.* 2007; 282: 20340-20350.

8. Hein S, Scholz D, Fujitani N, Rennollet H, Brand T, Friedl A, Schaper J. Altered expression of titin and contractile proteins in failing human myocardium. *J Mol Cell Cardiol.* 1994; 26: 1291-1306.
9. Morano I, Hadicke K, Grom S, Koch A, Schwinger RH, Bohm M, Bartel S, Erdmann E, Krause EG. Titin, myosin light chains and C-protein in the developing and failing human heart. *J Mol Cell Cardiol.* 1994; 26: 361-368.
10. Sariahmetoglu M, Crawford BD, Leon H, Sawicka J, Li L, Ballermann BJ, Holmes C, Berthiaume LG, Holt A, Sawicki G, Schulz R. Regulation of matrix metalloproteinase-2 (MMP-2) activity by phosphorylation. *FASEB J.* 2007; 21: 2486-2495.
11. Viappiani S, Nicolescu AC, Holt A, Sawicki G, Crawford BD, Leon H, van Mulligen T, Schulz R. Activation and modulation of 72kDa matrix metalloproteinase-2 by peroxynitrite and glutathione. *Biochem Pharmacol.* 2009; 77: 826-834.
12. Braakman I, Balleid NJ. Protein folding and modification in the mammalian endoplasmic reticulum. *Annu Rev Biochem.* 2011; 80: 71-99.
13. Chow AK, Cena J, El-Yazbi AF, Crawford BD, Holt A, Cho WJ, Daniel EE, Schulz R. Caveolin-1 inhibits matrix metalloproteinase-2 activity in the heart. *J Mol Cell Cardiol.* 2007; 42: 896-901.
14. Ai HW, Hazelwood KL, Davidson MW, Campbell RE. Fluorescent protein FRET pairs for ratiometric imaging of dual biosensors. *Nat Methods.* 2008; 5: 401-403.
15. Wang W, Sawicki G, Schulz R. Peroxynitrite-induced myocardial injury is mediated through matrix metalloproteinase-2. *Cardiovasc Res.* 2002; 53: 165-174.

16. Ali MA, Cho WJ, Hudson B, Kassiri Z, Granzier H, Schulz R. Titin is a Target of Matrix Metalloproteinase-2. Implications in Myocardial Ischemia/Reperfusion Injury. *Circulation*. 2010; 122: 2039-2047.
17. Yaras N, Sariahmetoglu M, Bilginoglu A, Aydemir-Koksoy A, Onay-Besikci A, Turan B, Schulz R. Protective action of doxycycline against diabetic cardiomyopathy in rats. *Br J Pharmacol*. 2008; 155: 1174-1184.
18. Gao CQ, Sawicki G, Suarez-Pinzon WL, Csont T, Wozniak M, Ferdinandy P, Schulz R. Matrix metalloproteinase-2 mediates cytokine-induced myocardial contractile dysfunction. *Cardiovasc Res*. 2003; 57: 426-433.
19. Lalu MM, Gao CQ, Schulz R. Matrix metalloproteinase inhibitors attenuate endotoxemia induced cardiac dysfunction: a potential role for MMP-9. *Mol Cell Biochem*. 2003; 251: 61-66.
20. Leon H, Bautista-Lopez N, Sawicka J, Schulz R. Hydrogen peroxide causes cardiac dysfunction independent from its effects on matrix metalloproteinase-2 activation. *Can J Physiol Pharmacol*. 2007; 85: 341-348.
21. Ahuja P, Perriard E, Perriard JC, Ehler E. Sequential myofibrillar breakdown accompanies mitotic division of mammalian cardiomyocytes. *J Cell Sci*. 2004; 117: 3295-3306.

APPENDIX

A.1: Introduction

During apoptosis, the mechanisms for cytochrome c release from the intermembrane space in mitochondria involve proteins of the Bcl-2 family. In the mitochondrial outer membrane, the proapoptotic functions of Bak and the related Bax protein depend at least in part on the presence of Bid, a cytosolic BH3-only protein of the Bcl-2 family. Proteolytic cleavage of full length Bid to the mitochondrially active, truncated form, t-Bid, is a feature of caspase-8-mediated apoptosis induced via death receptors ¹. In addition to caspase-8, granzyme B ² and calpain-1 ³ are also reported to cleave Bid. Consequently, t-Bid translocates to mitochondria, where it is involved in oligomerization of Bak and/or Bax leading to cytochrome c release and apoptosis.

In this preliminary study I sought to determine the susceptibility of Bid as a substrate of MMP-2 in vitro.

A.2: Methods

A.2.1: In vitro cleavage assays

Human recombinant Bid (~25 kD, Oncogene®) was incubated with human recombinant 64 kD MMP-2 (Calbiochem®) at different enzyme-substrate molar ratios at 37°C for 1 h in 50 mM Tris buffer (5 mM CaCl₂, 150 mM NaCl, pH 7.6). Upon completion of the incubation, the samples were heated for 5 min at 95 °C, electrophoresed on 10% SDS-polyacrylamide gels and immunoblotted following membrane transfer using mouse-monoclonal Bid antibody (abcam®). To demonstrate the specificity of MMP-mediated effects, certain incubations were performed in the presence of the MMP inhibitors (doxycycline, o-phenanthroline or TIMP-2). In parallel experiments calpain-1 (human erythrocytes, Calbiochem®) was incubated with Bid at

37°C for 1 h in 50 mM NaCl buffer (50 mM NaCl, 5 mM CaCl₂, 1 mM EDTA, 1 mM EGTA, and 5 mM β-mercaptoethanol, pH 7.4) for comparison purposes.

A.2.2: Cytochrome c release

Full length human recombinant Bid (50 ng) was incubated with either caspase-8 (12.5 U, human recombinant, Calbiochem®), 64 kD MMP-2 (15 ng) or calpain-1 (22.5 ng) at 37°C in a reaction buffer consisting of 300 mM sucrose, 20 mM MOPS, 1 mM EGTA, and 0.1% bovine serum albumin, pH 7.4 in the presence of 2 mM Ca²⁺. After 4 h incubation mitochondria (60 μg of protein) prepared from mouse liver using commercially available kit (Mitoiso1, Sigma) were added to the reaction mixture and further incubated for 1 h at 30 °C. Mitochondria were pelleted by centrifugation at 16,000 × *g* for 10 min at 4°C, and the supernatant and pellet were assessed by immunoblotting for cytochrome *c*. Two separate control samples were run for each assay in order to determine the total as well as spontaneous release of cytochrome *c* from treated and untreated mitochondria respectively³.

A.3: Results

A.3.1: MMP-2 cleaves full length Bid into a 15 kD fragment

Incubation of recombinant Bid with human recombinant 64 kD MMP-2 at 37°C with increasing MMP-2:Bid molar ratios caused Bid cleavage in a concentration-dependent manner into lower molecular weights fragments, the most prominent of which is the band which appeared ~15 kD (Figure A.1). For comparison purposes, calpain-1 was also incubated with recombinant Bid and found to cleave Bid into 19 and 15 kD fragments, in accordance with previous findings³. Inhibition of MMP-2 activity with

doxycycline, *o*-phenanthroline or TIMP-2 prevented the cleavage of Bid by MMP-2 (Figure A.2).

A.3.2: MMP-2-cleaved Bid induces cytochrome c release from isolated mitochondria.

When incubated with mouse liver mitochondria for 1 h at 30°C, MMP-2 cleaved Bid caused a marked release of cytochrome *c*, in a similar fashion to both caspase-8 and calpain-cleaved Bid (Figure A.3). MMP-2 or calpain-1 did not induce cytochrome *c* release *per se* when incubated with isolated mitochondria in the absence of Bid (data not shown).

A.4: Discussion

The mitochondrial cell death pathway is regulated by the pro- and anti-apoptotic Bcl-2 proteins. These proteins share up to four conserved Bcl-2 homology (BH) domains. Anti-apoptotic Bcl-2 proteins, such as Bcl-2 and Bcl-XL, contain all four subtypes of BH domains (BH1-4) and promote cell survival. The pro-apoptotic Bcl-2 proteins contain one or three BH domains and therefore are divided into two structurally distinctive subfamilies: (1) multidomain proteins such as Bax and Bak that share three BH regions (BH1-3), and (2) BH3-only domain proteins such as Bnip3, Nix/Bnip3L, Bad, Bid, Noxa, and Puma ⁴. Bid (BH3-interacting domain death agonist), a proapoptotic protein of the Bcl-2 family, is cleaved and thereby proteolytically activated by caspase-8. In the intrinsic/mitochondrial pathway stimuli are transmitted to the mitochondria via the BH3-only proteins (ie. Bid) which then translocate to the outer mitochondrial membrane ⁵. This causes the release of apoptogens such as cytochrome *c* and Smac/DIABLO.

Downstream from this the apoptosome is formed, leading to procaspase-9 activation, which then activates procaspase-3⁶. Bid is an important link between the extrinsic and intrinsic pathways. Its cleavage by caspase-8 to t-Bid which then via the mitochondria triggers the activation of Bax and Bad and the release of cytochrome c⁶. Bid can also be cleaved by calpain or a 'calpain like activity' in ischemic-reperfused rat hearts³. In this preliminary study I showed that Bid can be cleaved by MMP-2 and more importantly the resultant fragments have the capacity, similar to that of caspase-8 cleaved Bid, to stimulate cytochrome c release from isolated mitochondria. Since some studies demonstrated a possible involvement of MMP-2 in lung epithelial cell⁷ and cardiomyocyte⁸ apoptosis, yet, the exact mechanisms implicating MMP-2 in apoptosis are poorly understood. This preliminary study suggests a possible mechanism via Bid cleavage.

A.5: References

1. Gross A, Yin XM, Wang K, Wei MC, Jockel J, Milliman C, Erdjument-Bromage H, Tempst P, Korsmeyer SJ. Caspase cleaved BID targets mitochondria and is required for cytochrome c release, while BCL-XL prevents this release but not tumor necrosis factor-R1/Fas death. *J Biol Chem.* 1999; 274: 1156-1163.
2. Heibein JA, Goping IS, Barry M, Pinkoski MJ, Shore GC, Green DR, Bleackley RC. Granzyme B-mediated cytochrome c release is regulated by the Bcl-2 family members bid and Bax. *J Exp Med.* 2000; 192: 1391-1402.
3. Chen M, He H, Zhan S, Krajewski S, Reed JC, Gottlieb RA. Bid is cleaved by calpain to an active fragment in vitro and during myocardial ischemia/reperfusion. *J Biol Chem.* 2001; 276: 30724-30728.

4. Danial NN, Korsmeyer SJ. Cell death: critical control points. *Cell*. 2004; 116: 205-219.
5. Cook SA, Sugden PH, Clerk A. Regulation of bcl-2 family proteins during development and in response to oxidative stress in cardiac myocytes: association with changes in mitochondrial membrane potential. *Circ Res*. 1999; 85: 940-949.
6. Luo X, Budihardjo I, Zou H, Slaughter C, Wang X. Bid, a Bcl2 interacting protein, mediates cytochrome c release from mitochondria in response to activation of cell surface death receptors. *Cell*. 1998; 94: 481-490.
7. Aldonyte R, Brantly M, Block E, Patel J, Zhang J. Nuclear localization of active matrix metalloproteinase-2 in cigarette smoke-exposed apoptotic endothelial cells. *Exp Lung Res*. 2009; 35: 59-75.
8. Shen J, O'Brien D, Xu Y. Matrix metalloproteinase-2 contributes to tumor necrosis factor alpha induced apoptosis in cultured rat cardiac myocytes. *Biochem Biophys Res Commun*. 2006; 347: 1011-1020.

Figure A.1: In vitro cleavage of Bid by MMP-2

Immunoblot showing that MMP-2 cleaves 22 kD Bid into mainly a 15 kD fragment in a concentration-dependent manner. Bid was also cleaved, albeit to a lesser extent, with calpain-1. Molar ratios of enzyme to substrate are indicated (blot is representative of three independent experiments). Experiments done by M. A. Ali.

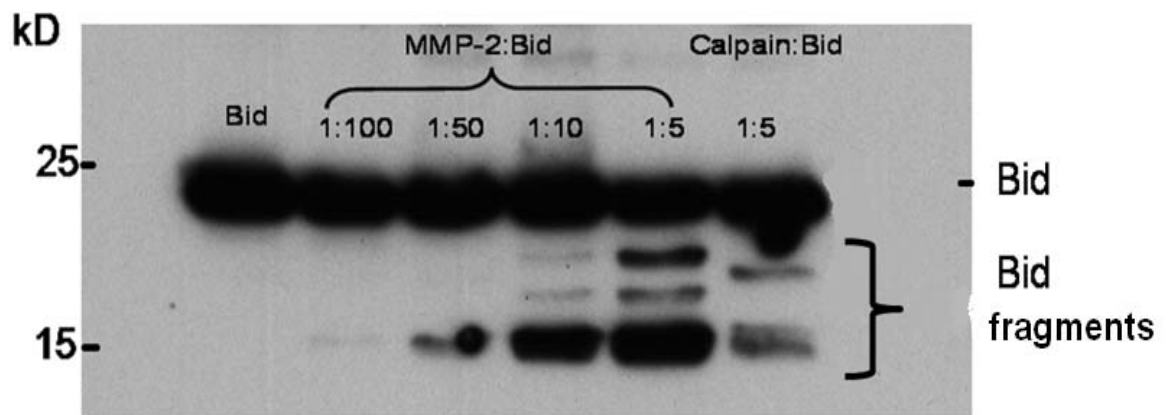


Figure A.2: MMP inhibitors prevent Bid cleavage by MMP-2

Bid cleavage by MMP-2 was prevented by inhibiting the activity of MMP-2 with MMP inhibitors doxycycline (Doxy, 100 μ M), o-phenanthroline (o-Phen, 100 μ M) or TIMP-2 (0.3 μ M). The blot is representative of three independent experiments done by M. A. Ali.

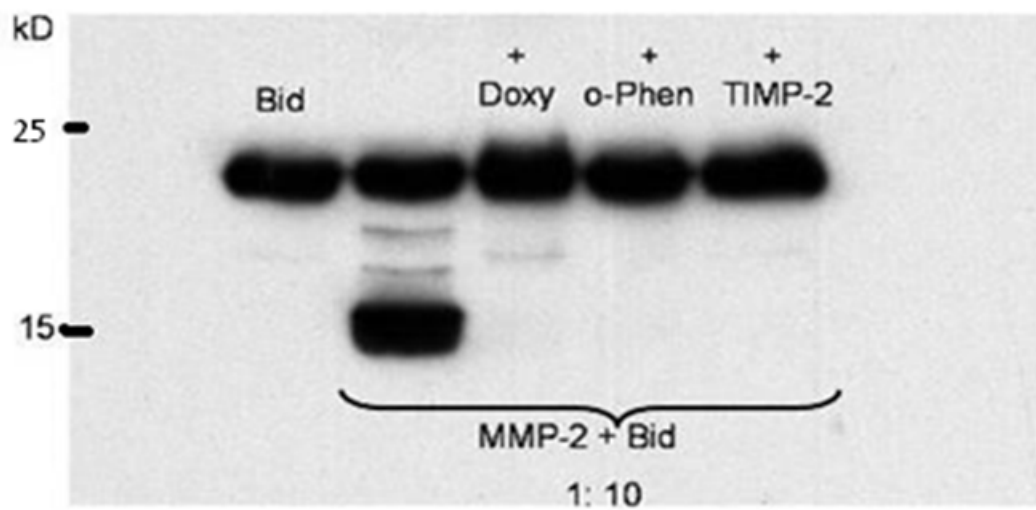


Figure A.3: MMP-2-cleaved Bid induces cytochrome c release from isolated mitochondria preparation.

Immunoblot for cytochrome c release from isolated mouse liver mitochondria exposed for 1 hr (30° C) to either full length Bid or Bid which had been cleaved by either caspase-8, MMP-2 or calpain-1. Spontaneous release of cytochrome c was negligible but was slightly enhanced by intact Bid and significantly enhanced by Bid fragments. (blot is representative of three independent experiments). Experiments done by M. A. Ali and C. Rosenfelt.

